

DISSERTATION (PhD-Thesis)

# **Development and Engineering Design of a Novel Exocentric Carbon-Ion Gantry for Cancer Therapy (The "Riesenrad" Gantry)**

ausgeführt zum Zwecke der Erlangung des akademischen Grades eines  
Doktors der technischen Wissenschaften

unter der Leitung von  
Univ. Prof. Dr.-Ing. Degenhard Sommer  
Institut für Hoch- und Industriebau (E 215)

eingereicht an der Technischen Universität Wien  
Fakultät für Bauingenieurwesen

ausgeführt am  
Europäischen Laboratorium für Teilchenphysik (CERN), Genf

von

**Dipl.-Ing. Stefan Reimoser**

Matrikelnummer: 9027828  
Email: stefan.reimoser@cern.ch

Genf, im Oktober 2000

Stefan Reimoser

## Deutsche Kurzfassung

In der heutigen Zeit kommt dem Kampf gegen Krebs im allgemeinen sowie der Strahlentherapie und ihrer Weiterentwicklung im besonderen ein enormer Stellenwert zu. Folgende Fakten mögen dies verdeutlichen:

- Jeder *dritte* (Europäer) wird im Laufe seines Lebens mit der Diagnose Krebs konfrontiert.
- Nur 45% der Betroffenen werden geheilt, wobei eine Strahlentherapie bei Zweidrittel dieser Patienten zur Anwendung kommt (sowohl als alleinige Form der Therapie als auch in Kombination mit einer operativen Tumorentfernung).

Von den derzeit 55% unheilbar kranken Krebspatienten muß immerhin noch ein Drittel - d.h. 18% aller Krebspatienten oder etwa 6% der Gesamtbevölkerung (!) - deshalb sterben, weil trotz des Einsatzes aller heute zur Verfügung stehenden Behandlungsformen die zum Zeitpunkt der Erstdiagnose noch *lokal begrenzte* Krebsgeschwulst nicht beherrschbar ist. Der Grund hierfür liegt in diesen Fällen meist an der *Nähe des Tumors zu kritischen Organen* bzw. seiner Radioresistenz. In der Folge kann die im Zuge einer Strahlentherapie applizierte Dosis nicht ausreichend hoch gewählt werden, ohne dabei gleichzeitig das angrenzende, gesunde Gewebe *nachhaltig* zu schädigen.

Eine wesentliche Verbesserung der Situation wird durch die Verwendung von Protonen- bzw. Ionenstrahlen erzielt. Diese - in der Strahlentherapie als Hadronen bezeichnete - Teilchen zeigen gegenüber den bisher eingesetzten Photonen eine „inverse“ Tiefendosisverteilung im Gewebe: Während das gesunde Gewebe im Eintrittskanal des Therapiestrahles einer relativ geringen Dosisbelastung ausgesetzt wird, steigt diese in einer, von der ursprünglichen Teilchenenergie abhängigen Eindringtiefe - im sogenannten „Bragg peak“ - massiv an, um knapp danach gegen null abzufallen. Im Falle von Kohlenstoffionen nimmt zudem die *biologische* Wirksamkeit im Bereich des „Bragg peak“ deutlich zu. Im Vergleich zur konventionellen Strahlentherapie gestattet die Bestrahlung mit Kohlenstoffionen somit in einmaliger Weise die Konzentration der therapeutischen Wirkung auf das tatsächliche Tumolvolumen bei gleichzeitiger maximaler Schonung des gesunden Gewebes. Diese Technologie wird bereits am Heavy Ion Medical Accelerator (HIMAC) in Japan sowie an der Gesellschaft für Schwerionenforschung (GSI) in Deutschland mit großem Erfolg eingesetzt, wobei Patienten mit einem horizontalen (GSI) bzw. einem horizontalen und vertikalen (HIMAC) Ionenstrahl behandelt werden.

Eine weitere Möglichkeit, die Konformität der Bestrahlung zu erhöhen, ergibt sich durch die Verwendung sogenannter (medizinischer) Gantries, die in der konventionellen Strahlentherapie bereits Stand der Technik sind. *Unter einer Gantry ist eine Konstruktion zu verstehen, die es erlaubt, den Therapiestrahle von (fast) jeder beliebigen Richtung des Raumes auf den Patienten zu lenken.* Letzterer ist hierbei - zumeist auf einem Patiententisch liegend - mit Hilfe einer individuellen Form oder Gesichtsmaske so weit wie möglich „immobilisiert“, um Organbewegungen während der Behandlung möglichst klein zu halten.

Die für die *klassische* Strahlentherapie benötigten Elektronbeschleuniger (Linearbeschleuniger) sind ausreichend kompakt, sodaß diese in ihrer *Gesamtheit* um den Patienten gedreht werden können. In einer *Protonengantry* hingegen muß der (meist horizontal) von einem vergleichsweise großen Teilchenbeschleuniger (Cyclotron oder Synchrotron) gelieferte Protonenstrahl mit Hilfe von Biegemagneten (Dipolen) ab- und anschließend auf den Patienten gelenkt werden. Diese Strahlführung muß sich in irgendeiner Form relativ zu dem auf einem Positionierungssystem (Tisch) liegenden Patienten bewegen bzw. rotieren lassen. Das Gewicht der Magnete, der erforderliche Bewegungsraum sowie die geforderte Präzision stellen bereits hohe Ansprüche an die Konstruktion einer solchen Gantry. Protonengantries für den täglichen Einsatz im Patientenbetrieb findet man heute in Loma Linda (3), Kashiwa (2) und in Boston (2). Sie alle folgen dem Prinzip einer *isozentrischen* Gantry, d.h. der Patient befindet sich nahe bei

der Achse, um die sich die schwere Gantrykonstruktion dreht. Eine Gantry, bei der sich sowohl der Patient als auch die Strahlführung exzentrisch zur Drehachse befinden, wurde am PSI (Schweiz) verwirklicht. In Japan und den USA sind zudem mehrere klinische Zentren mit weiteren Protonengantries in Bau.

Es erscheint wünschenswert, ähnliche Apparaturen auch in der vielversprechenden Ionentherapie einzusetzen. *Bis dato wurde jedoch noch keine Ionengantry errichtet.* Die Konkurrenzfähigkeit und somit auch der Erfolg der Ionentherapie werden wesentlich von der zu findenden *effektiven* Lösung für eine Ionengantry abhängen - und genau das ist auch das Ziel der vorliegenden Arbeit. Die Zunahme an Komplexität gegenüber Protonengantries basiert - vereinfacht gesprochen - auf der bei gleicher Einstrahltiefe *höheren Steifigkeit des Ionenstrahls*, die wiederum für einen etwa dreifach vergrößerten Radius eines entsprechenden Biegemagneten verantwortlich ist.

*Kapitel 1* setzt sich mit den Beweggründen für diese Arbeit auseinander und erläutert ihre Struktur. In *Kapitel 2* werden existierende Gantry- und andere Strahlführungssysteme in Hinblick auf ihre Anwendbarkeit für eine Kohlenstoff-Ionengantry untersucht. *Kapitel 3* gilt der Erarbeitung der *Planungsgrundlagen* - ein unentbehrlicher Schritt bei Projekten, die durch eine hohe Komplexität gekennzeichnet sind. Diese Programmfindung („*Programming*“) zielt auf folgende Fragen ab: „*Welche Prozesse werden in der Ionentherapie und der Gantry ablaufen?*“ sowie „*Wie kann man baulich diese Prozesse bestmöglich unterstützen?*“ Die Aufbereitung solcher Fragen garantiert einen nachvollziehbaren Entscheidungsprozeß, legt Systemzusammenhänge offen und führt bereits zu ersten Systementscheidungen - in unserem Fall zugunsten einer sogenannten „Riesenrad-Gantry“. Hierunter versteht man ein Gantrykonzept, bei dem der ankommende Strahl von einem 90°-Dipol radial nach außen auf einen *exzentrisch positionierten Patienten* gerichtet wird (exzentrische Gantry). Unterschiedliche Einstrahlwinkel werden durch die Rotation des Systems erzielt, wobei das „*Waagrecht-Halten*“ des liegenden Patienten eine zweite, parallele Drehachse um den Tumor - das „lokale“ Isozentrum - erfordert.

In *Kapitel 4* werden mehrere konstruktive Varianten einer derartigen Ionengantry entwickelt, wobei sich die Riesenrad-Gantry mit einer *mechanisch getrennten, teleskopierbaren* Patientenkabine als die technisch-wirtschaftlich effizienteste und vor allem in Belangen der Sicherheit zufriedenstellende Lösung herauskristallisiert. *Kapitel 5* widmet sich der detaillierten Ausarbeitung dieses Prinzips, insbesondere der

- Optimierung der Konstruktion zugunsten einer Minimierung der *elastischen* Deformationen (→ maximal etwa 0.1 mm bei 150 t Gesamtgewicht).
- Untersuchung der Auswirkungen dieser Deformationen auf die Präzision des Ionenstrahls beim Patienten (→ systematische Abweichung < 0.2 mm),
- Abschätzung der zu erwartenden *zufälligen* Abweichungen des Ionenstrahls beim Patienten ( $3\sigma < 1$  mm),
- Ausarbeitung eines integrierten Meß- und Steuerungskonzeptes, welches sicherstellt, daß über den gesamten Behandlungsprozeß hinweg der Ionenstrahl - mit einer bestimmten Genauigkeit - dort ankommt, wo er soll - nämlich im Tumor.

Der vorliegende Entwurf einer Riesenrad-Gantry für die Kohlenstoff-Ionentherapie ist ausreichend detailliert, um im Sinne eines *Technologietransfers* von der Industrie aufgegriffen und weiterentwickelt zu werden. *Kapitel 6* faßt hierzu den nunmehr definierten *Prozeß* der Behandlung unter Einsatz einer Riesenrad-Gantry zusammen und bietet einen Ausblick auf mögliche *alternative Szenarien*. Am Ende des Anhangs findet sich ein *Glossar*, das einige wichtige Fachbegriffe der verschiedenen Disziplinen, die bei diesem Projekt zusammengeführt werden müssen, für den Laien erläutert.

Die vorliegende Dissertation wurde initiiert und gefördert von Med-AUSTRON - das Projekt eines klinischen Zentrums zur Protonen- und Ionentherapie in Österreich. Darüber hinaus ergänzt diese Arbeit eine umfassenden Studie des Europäischen Laboratoriums für Teilchenphysik (CERN) zur Entwicklung eines neuartigen, speziell in Hinblick auf die Bedürfnisse der Ionentherapie optimierten Teilchenbeschleunigers - der „Proton-Ion

Medical Machine Study” (PIMMS). Der Abschlußbericht dieser Studie in Form einer CD-rom, die auch eine *Computeranimation der Riesenrad-Ionengantry* enthält, kann bei der Bibliothek des CERN bzw. dem Autor bezogen werden.

## English Summary

Mechanical structures capable of delivering a particle beam for cancer treatment from any direction to a patient are called medical gantries. Typically, a gantry rotates around the patient who is kept in a supine position ("rotating isocentric gantries"). In Europe, several currently proposed facilities for ion therapy plan the installation of an ion gantry equipped with a pencil-beam scanning system. Such a treatment system allows a superior optimisation of the dose-to-target conformity, but the active pencil-beam scanning increases the demands considerably on the beam transport accuracy. Usually, a sub-millimetre precision of the beam position at the patient (i.e. at the gantry isocentre) is required in order to treat tumours in the vicinity of critical organs, which is one of the main domains of ion therapy. So far, experience exists only for a *fixed* beam line using the pencil-beam scanning technique, which is installed at the Gesellschaft für Schwerionenforschung (GSI) in Darmstadt.

The use of gantries is state-of-the-art in conventional radiation therapy (photon therapy), where the necessary linear accelerator (electron LINAC) is light enough to be mounted directly on the gantry structure. Radiation therapy with heavy particles like protons or even heavier carbon ions requires a different approach, since the beam is delivered (horizontally) from a cyclotron or - obligatory in case of ion therapy - a synchrotron. The few existing proton gantries are *already* impressive structures of the order of 10 m diameter and 100 tons in weight. The increased magnetic beam rigidity of a carbon-ion beam (which is about three times higher than for a proton beam) yields structural difficulties for the design of the gantry. The obvious approach of "scaling" the construction principles of proton gantries to ion gantries seems doubtful concerning structural efficiency, cost and achievable precision. The objective of the present thesis is to develop a novel gantry concept leading to a viable and efficient design for a carbon-ion gantry.

*Chapter 1* is meant to give some background information on radiation therapy and on the promises of ion treatment. *Chapter 2* presents and summarises *existing* gantry systems (in particular for protons) and briefly describes the experimental facilities for ion treatment in order to form an idea in what direction the design of an ion gantry might point. *Chapter 3* is dedicated to the *definition* of the medical, beam-optical and mechanical constraints affecting the design of the ion gantry. The principal processes likely to take place inside the ion gantry are highlighted and the various technical systems and their interdependencies are investigated. As a result of these considerations it was decided to focus on the development of an *exocentric* gantry system for ion therapy, which was eventually named the "Riesenrad" gantry. In contrast to conventional isocentric gantries, the main 90°-bending magnet of the Riesenrad is placed *on* the axis of gantry rotation, hence minimising the moment of inertia of the mobile structure and maximising its rigidity. Several preliminary structural concepts for the Riesenrad gantry were generated, analysed and compared in *Chapter 4*. Finally, the variant featuring an independent telescopic cabin was chosen for further elaboration in a design phase (*Chapter 5*).

In the proposed variant, the bending magnet that sits on the axis and its counterweight (62 ton and 23 ton respectively) are supported by a central "cage" of about 40 t. This gantry yields a higher efficiency in terms of structural weight to supported load compared to any other possible variant. A patient cabin is smoothly moved towards the desired treatment position by a system that is *mechanically de-coupled* from the central cage. Any desired position (that corresponds to a particular gantry angle) is achieved by vertical translation and horizontal telescopic movement of the cabin. The *patient couch aligns itself automatically with respect to the exit face of the large bending magnet* by means of a photogrammetric system, hence the positioning accuracy of the patient cabin need only be moderate. Once the correct position of the patient towards the ion beam has been secured, the personnel leave the gantry hall and irradiation can start.

The sophisticated structural concept intrinsically compensates parts of the elastic deformations, which therefore will not exceed  $\pm 0.1$  mm along the beam line. This very high "rigidity" simplifies alignment procedures and improves operability of the system. The proposed concept is also suitable from the safety and flexibility points of view. A lift affords quick and *redundant* access to the patient and there is always a possibility of using the conventional staircase for a maximum of two floors vertical distance. Another advantage is the large floor area of the patient cabin that provides plenty of space around the patient, which is not true for other gantry concepts.

Special attention was paid to the assessment of the beam position accuracy at the gantry isocentre as a function of elastic deformations (systematic) and possible random errors such as temperature fluctuations. This kind of analysis was necessary to estimate realistically the achievable precision with this novel gantry system as well as to specify the required alignment tolerances for the beam transport elements of the gantry. In order to achieve a sub-millimetre treatment precision (defined in a way that the  $3\sigma$ -value of the beam position probability distribution at the tumour is lower than 1 mm) the *random* misalignment shifts of the beam transport elements have to be *lower* than 0.1 mm. This imposes tough constraints on the temperature stability inside the gantry hall as well as on the alignment concept and the beam position control system, which were also discussed in the present work.

The Riesenrad gantry forms an integrated concept considering the interdependent aspects of beam optics, structural design, surrounding architecture and organisation. The present document is meant to function as a basis for a successful transfer of the new technology to industry.

This thesis was initiated and supported by Med-AUSTRON - the project of a proton-ion cancer therapy facility in Austria. The work also complements a study for a dedicated medical accelerator - the Proton-Ion Medical Machine Study (PIMMS) - which was hosted by the European Laboratory for Particle Physics (CERN). A CD-rom that contains the final report of that study and also a computer animation of the Riesenrad gantry is available from the CERN library or the author.

---

# Table of Contents

<b>Deutsche Kurzfassung</b>	<b>4</b>
<b>English Summary</b>	<b>9</b>
<b>1 Introduction</b>	<b>18</b>
1.1 The Cancer Disease	18
1.2 The Principle Ideas of Radiation Therapy and the Promises of Ion Treatment	21
1.2.1 Basics of Radiation Therapy	21
1.2.2 The Benefit of (Carbon) Ions	28
1.3 Rationale and Structure of the Thesis	33
1.3.1 Rationale for the Thesis	33
1.3.2 Structure of the Thesis	38
<b>2 Investigation</b>	<b>44</b>
2.1 Conventional Gantries	44
2.2 Proton Gantries	48
2.2.1 Proposals to Avoid the Need for a Rotating Gantry	48
2.2.2 Loma Linda University Proton Treatment Center (LLUPTC)	52
2.2.3 National Cancer Center (NCC) Kashiwa & Northeast Proton Therapy Center (NPTC) Boston	58
2.2.4 The Eccentric Proton Gantry at the Paul Scherrer Institute (PSI)	71
2.3 Neutron Gantries	81
2.4 Ion Facilities	85
2.4.1 HIMAC	85
2.4.2 GSI Pilot Project	87
2.5 Summary	92
<b>3 Definition of the Carbon-Ion Gantry</b>	<b>94</b>
3.1 The Processes to Take Place	94
3.1.1 People Involved: Objectives, Tasks, Consequences	94
3.1.2 Patient Flow and Activities	97
3.1.3 Material Flow	102
3.1.4 Functional Relationship and Space Program	103
3.2 Strategic Objectives	104
3.2.1 Safety	104
3.2.2 Flexibility	107
3.3 Beam Optics	108
3.3.1 The Accelerator	108
3.3.2 Rotator	110
3.3.3 Beam Scanning	111
3.3.4 The Last Dipole	116
3.4 Treatment Precision	120
3.5 Specifications	121
3.6 Gantry Structure Considerations	124
3.6.1 Isocentric Ion Gantry Solutions	126
3.6.2 Ion Gantry Solutions with Patient and Beam Eccentric	131
3.6.3 Exocentric Riesenrad Gantries	135
3.7 Conclusion: to Go for the Riesenrad-Approach	142
<b>4 Generation of Variants for the Riesenrad Ion Gantry and Resolution</b>	<b>145</b>
4.1 Structural Principles, Methodology and Idealisations	148
4.2 Wheel Gantry	152
4.3 Cantilever Gantry	155
4.4 Centrally Supported Riesenrad Gantry	156
4.4.1 Principal Elements and Structural System	158
4.4.2 Deformations	163

4.5 Riesenrad Gantry with an Independent Telescopic Cabin	171
4.5.1 Principal Elements and Structural System	174
4.5.2 Deformations	179
4.6 Comparison and Resolution	185
4.6.1 Comparison	185
4.6.2 Evaluation and Resolution	194
<b>5 Design of the Riesenrad Ion Gantry</b>	<b>198</b>
5.1 Quadrupoles and the 90° Dipole	202
5.2 The Central Cage	210
5.2.1 Structural Design of the Central Cage	211
5.2.1.1 The Principal Elements	211
5.2.1.2 Support Considerations	219
5.2.1.3 Cage Assembly	222
5.2.2 Structural Analysis of the Central Cage	224
5.2.2.1 Elastic Deformation	230
5.2.2.2 Temperature Effects	237
5.2.2.3 Interpretation of Elastic Deformations and Temperature Effects	238
5.3 The Patient Cabin	239
5.3.1 Mechanical Structure of the Patient Cabin	239
5.3.2 Structural Analysis of the Patient Cabin	244
5.3.3 The Patient Couch	250
5.3.4 Lift	254
5.4 Operational Procedure, Flexibility & Safety	254
5.4.1 Standard Operational Procedure	254
5.4.2 Available Treatment Angles and Flexibility	257
5.4.3 Safety	263
5.5 Analysis of the Beam Position Accuracy	265
5.5.1 Beam Transport System of the Riesenrad Gantry	265
5.5.2 Error Analysis	268
5.5.2.1 General Considerations	268
5.5.2.2 Effects of Misalignments	270
5.5.3 Beam Transport Calculation	273
5.5.3.1 Systematic Misalignments	273
5.5.3.2 Random Misalignments	275
5.6 General Concept of Alignment and Beam Position Control, or: How to Assure That the Beam Meets the Tumour?	288
5.7 Gantry Hall	296
5.7.1 Geometry	296
5.7.2 Radio-Protection and Shielding	300
5.7.3 Civil Engineering	303
5.7.4 Dipole Cooling and HVAC	306
5.7.5 Integration of the Riesenrad Gantry into a Therapy Facility	314
5.8 Cost Estimate	316
5.9 Summary	319
<b>6 Conclusion</b>	<b>326</b>
6.1 The New Status Quo and Outlook	326
6.2 Other Scenarios	335
<b>Acknowledgements</b>	<b>337</b>
<b>References</b>	<b>339</b>
<b>Annex A: Design Drawings</b>	<b>348</b>
<b>Annex B: Design Calculations</b>	<b>358</b>
<b>Annex C: The Roller Supports (FEM-Study)</b>	<b>359</b>
<b>Glossary</b>	<b>388</b>
<b>The Author</b>	<b>419</b>



# 1 Introduction

## 1.1 The Cancer Disease

*Current situation*

*1 in 3 faces cancer*

The word "cancer" stands for more than 100 different kinds of malignant tumours and it is characterised by the uncontrolled multiplication of abnormal cells in the body. If this multiplication of cells occurs within a vital organ or tissue, normal function will be impaired or halted, with possible fatal results. In Europe, at present, one in three of us will have an encounter with cancer during his life and more than half of those will, sadly, die of the effects of that disease. As life expectancy is increasing, the disease is affecting more and more parts of the human population and the occurrence of cancer rises between 1% and 2% per year.

Cancers are generally said to be in one of three stages of growth:

- *local*, when a tumour is still confined to the tissue of origin or primary site,
- *regional*, where cancer cells from the tumour have invaded adjacent tissue or have spread only to regional lymph nodes,
- *metastasised*, when cancer cells have migrated to distant parts of the body from the primary site, via the blood or lymph systems, and have established secondary sites (metastases) of infection.

It is now known that cancer can be caused by a variety of factors acting either singly or in concert. These include a wide variety of chemical substances, various types of ionising radiation and various classes of viruses. There is even some evidence for genetic variations in radiation risks. This knowledge has accrued from a composite of epidemiological studies of cancer in humans and from experimental studies in the laboratory. Although much is known about how cancer is caused, the precise mechanism or group of mechanisms involved remains unknown and continues to elude researchers.

Current methods of cancer treatment rely on surgery, radiation therapy, chemotherapy or a combination of these.

*There are 3 principal kinds of cancer treatment: surgery, radiation therapy and chemotherapy.*

- Surgery must be performed before the cancer has spread into organs and tissues that cannot be safely removed. The malignant cells must be completely removed in order to reduce significantly the risk of developing metastases (secondary tumours) through the migration of cancer cells. When severe pain accompanies cancer, surgery may bring relief by severing the nerve pathways that carry the painful sensations. Surgery is also valuable as a preventive measure in controlling cancer.
- Radiation therapy makes use of *ionising* radiation to destroy cells by impairing their capacity to divide. The type of radiation can be photons (X-rays or gamma rays) and electrons or comparatively heavy *particles* like pi-mesons, protons, neutrons and ions). The radiation directed at the cancer may destroy normal tissue in adjacent areas, however, sophisticated techniques have been developed to minimise this occurrence. Some cancers do not respond to radiation therapy.
- Chemotherapy can cure certain forms of cancer as for instance acute leukaemia of childhood. Many other forms of cancer benefit temporarily or partially by chemotherapy. Some cancers are (or become) resistant to drugs, however. Another problem is that cancer drugs damage normal, as well as cancer cells and tissues.

Successful treatment of cancer requires the complete removal or destruction of all cancerous tissue otherwise the disease recurs. Surgery and radiation are the most effective forms of treatment. However, once a tumour has metastasised to diffuse areas of the body, it is much more difficult to remove the secondary tumours surgically; they may be numerous and inaccessible, and chemotherapy may be the only option. The "success" of the common forms of cancer treatment as well as their estimated cost is shown in Table 1-1.

The available data on costs depends considerably on national reimbursement procedures and technical standard. Radiation therapy for instance ranges from about 10000 Euro for a conventional radiation therapy up to 30000 Euro for a sophisticated conformal stereotactic treatment. Nevertheless, studies show that the economic benefit of a successful treatment by far exceeds the cost of an unsuccessful one, which necessitates subsequent treatments and costs (Brady et al., 1984, p. 1; Galle et al., 1998b, p. 190).

Various cancer treatment possibilities in comparison				
Type of Treatments	Primary tumour (local & regional)	Metastasised tumour	Total	Cost per treatment [Euro]
Surgery (alone)	22%			7000 - 28000
Radiation therapy (alone)	12%			3000 - 9000
Both combined	6%			
Chemotherapy alone, in combination with the above and other kind of treatments		5%		12000 - 51000
Successfully cured patients	40%	5%	45%	
Not or not successfully treated patients	18%	37%	55%	

Table 1-1 Comparison of different forms of cancer treatment, their cure rates and estimated costs. 100% represent all people suffering from cancer disease. Source: Vermoken et al., 1994; Galle et al., 1998a, p. 175; Amaldi, 1999, p. 381c.

## 1.2 The Principle Ideas of Radiation Therapy and the Promises of Ion Treatment

### 1.2.1 Basics of Radiation Therapy

#### Principal idea

*Accurate delivery of a prescribed dose to a target volume, while sparing surrounding healthy and critical tissue is the principal objective of radiation therapy.*

The principal idea of radiation therapy is to destroy the malignant tissue with some type of ionising radiation while at the same time restrict the delivered dose (i.e. the radiation energy *per unit mass*) of the healthy tissue - inevitable involved in the irradiation process - to a level that does not cause irreversible damage or complications. Hence, "attacking the tumour" is only one side of the medal, it is equally important that normal tissue - and here in particular tissue of critical organs - is spared from the irradiation. The risk of missing part of the cancer cell population must be balanced against the reduction of the risk of severe and serious treatment-related normal tissue complications. This decision-making is the (daily) responsibility of the radiation-oncologist.

It is evident that any improvements in equipment and radiation sources, which allow a concentration of the dose in the tumour tissue, are beneficial because one could

- either - for a given dose to the tumour - reduce the dose absorbed by the surrounding healthy tissue (and thus decrease the probability of complications),
- or increase the delivered dose to the tumour and thus the probability of tumour destruction or at least local control, while the dose to the healthy tissue remains unchanged.

*Improvements aim at the spatial conformation of the dose to the tumour.*

Spatial conformation of the dose to the tumour has been the major objective of all recent developments in radiation therapy, which goes hand in hand with an increased demand on accuracy of therapy procedures and technical equipment.

#### Risk of radiation therapy?

High doses such as those used in radiation therapy are used to kill cancerous cells but they can also damage normal tissue, hence a radiation therapy always has the potential to initiate a secondary cancer, but usually, this risk is low compared with that of leaving the disease untreated. Radiation risks can be estimated on the basis of epidemiological findings, such as those of the Japanese atomic bomb survivors. The level of risk depends on a number of factors. Among them, the size of the radiation dose is very important. Generally, the risk

varies in direct proportion to the dose<sup>1</sup>. Therefore, *the benefits to be obtained in the treatment of the disease (and also from medical diagnostic procedures) must be balanced against these potentially harmful effects.*

Estimations of the risk to develop a secondary cancer following a radiation therapy vary considerably, however, at most about 5% of all secondary cancers could be convincingly linked to the radiation treatment (Boice et al., 1988, p. 3). Table 1-2 shows typical effective doses and fatal cancer risks for some common X-ray examination. Equivalent periods of natural background radiation, which will result in the same effective dose as the medical examinations, are also shown for comparison. As it may take many years or even decades for a cancer to develop after exposure to radiation, children and young people undergoing a radiography or radiation therapy suffer from a higher risk than people who are elderly at the time of exposure.

*Fractionated treatment gives less damage to the healthy tissue*

Radiation risks are also affected by the degree to which the dose was protracted. For a given total dose, risks may be higher if received acutely rather than over a prolonged period. In addition, cancerous cells show inferior repair characteristics compared to normal tissue. This is the reason why in radiation therapy the prescribed dose is usually given in several fractions (sessions). In a typical treatment one delivers to the tumour about 2 Gray per fraction (absorbed dose). A treatment usually comprises about 30 fractions within 6 weeks, thus the target volume will have eventually received about 60 Gray.<sup>2</sup>

The risk of X-ray examinations			
Type of X-ray examinations	Typical effective dose (mSv)	Equivalent period of natural background radiation*	Risk of fatal cancer per examination**
Teeth (panoramic)	0.01	1.5 days	1 in 2 million
Chest (single PA film)	0.02	3 days	1 in a million
Skull	0.07	11 days	1 in 300,000
Cervical spine (neck)	0.08	2 weeks	1 in 200,000
Hip	0.3	7 weeks	1 in 67,000
Lumbar spine	1.3	7 months	1 in 15,000
CT head	2	1 year	1 in 10,000
CT chest	8	3.6 years	1 in 2500

\* UK average = 2.2 mSv per year; regional averages range from 1.5 to 7.5 mSv per year.  
 \*\* Approximate lifetime risk for patients from 16 to 69 years old, for paediatric patients multiply risks by about 2, for geriatric patients divide risks by about 5.

Table 1-2: Typical effective doses and fatal cancer risks for some common X-ray examinations. Equivalent periods of natural background radiation are shown for comparison. Source: extracted from National Radiological Protection Board (NRPB), UK, "Radiological Protection - Background Information" [online], available from: <http://www.nrpb.org.uk/Qmedical.htm#TABLE> [accessed 2000-05-04]

### Conventional photon treatment

Today, the principal technique used in radiation therapy is to produce a photon beam in some kind of apparatus and direct this beam at a point at the patient's skin where it is believed that the entering beam will eventually reach the inner tumour in an optimal way (external conventional radiotherapy). Usually, the apparatus is a linear accelerator (electron LINAC) capable of producing a continuous photon beam (bremsstrahlung), originating from an electron beam in the millions-of-electronvolt (MeV) region that is spontaneously decelerated in a heavy target.

When the photon beam enters the human tissue a series of interactions starts, leading to ionisation and hence to the generation of ions and secondary electrons which are eventually

<sup>1</sup> Epidemiological studies function as a basis for recommendations on radiological protection and maximum allowable doses (e.g. Publication 60, ICRP, 1991). By their nature, the conclusions drawn from epidemiological studies apply to groups rather than to specific persons. However, information on levels of risk associated with radiation exposure can be used in assessing the *probability* that a disease suffered by a given person was induced by such an exposure.

<sup>2</sup> For comparison, if the *whole body* is subjected to an effective dose, i.e. the absorbed dose weighted according to the type of radiation of 2 Sievert within a short period of time, the consequences are usually lethal. Note that the units Sievert (Sv) and Gray (Gy) are per unit mass!

responsible for the biological effect on the cells. Shortly beyond the skin the deposited energy and hence the absorbed dose decreases exponentially. The situation is illustrated in Figure 1-1 (dotted curve). Similar depth-dose curves are obtained for neutrons and electrons. It is evident that the exponential fall-off in deposited dose inherent to photon beams (which are frequently called "X-ray beams" by medical doctors) is a highly unsatisfying constraint to the treatment of deep-seated tumours.

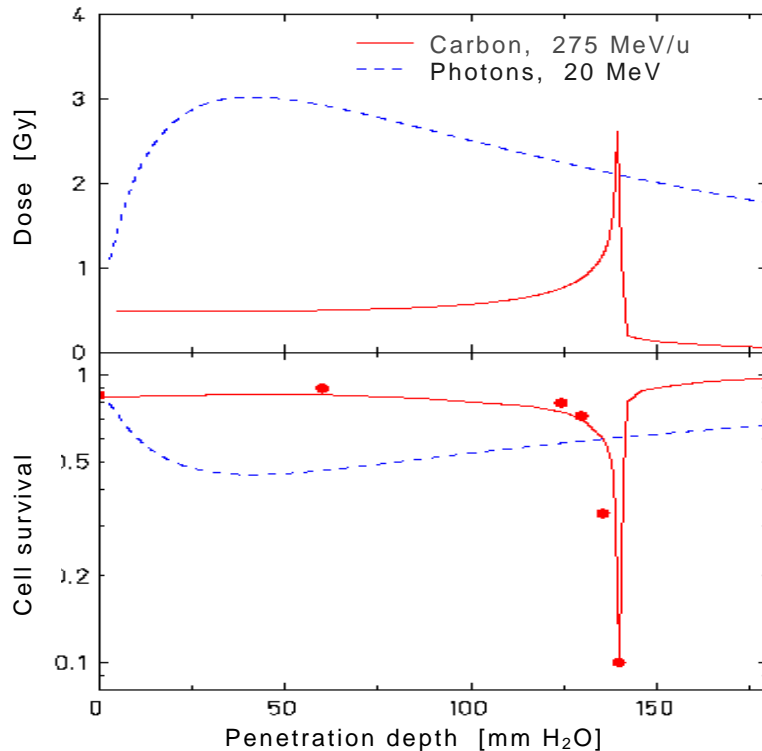


Figure 1-1 shows the physical dose distribution (upper half of the diagram) and the survival rate of cells (lower half) as a function of penetration depth in water for a photon beam (generated by a 20 MeV electron linear accelerator) and a 275 MeV/u carbon-ion beam.<sup>3</sup> The photon beam shows the characteristic exponential decrease of the dose with depth. Contrarily, the ion beam is characterised by an enhanced energy deposition *at the end* of the particle range and a corresponding dramatic decrease of cell survival, making it an excellent tool for the treatment of deep-seated tumours. Source: GSI, Heavy Ion Radiotherapy @ GSI [online], available from: <http://www-aix.gsi.de/~bio/therapy.html> [accessed 2000-05-03]

### Multiple beam entry ports achieved by a medical gantry

It is evident that by entering the patient's body with several photon beams from different ports (sides) the conformity of the dose to the tumour volume can be increased. The multiple beam entry ports focus on the centre of the tumour. Thus some kind of plateau in the intersecting region can be created while the normal tissue in the various entrance channels is subjected to the dose caused by one single beam only. Further improvements have been achieved by varying the intensity of the beam across the irradiation field with the help of individualised absorbers and shaping the (large) fields to the contours of the tumour by means of computer-controlled "multi leaf" collimators (*conformal intensity modulated radiotherapy*).

*A (medical) gantry is a machine capable of delivering a therapy beam to the patient from several different directions.*



In order to apply these techniques, it is necessary to rotate the electron linear accelerator around the supine patient (or vice versa). A mechanical machine capable of doing so - delivering a therapy beam for cancer treatment from any direction to the patient - is called a medical *gantry*. A standard version of such a gantry is shown in Figure 1-2.

Figure 1-2: Example for a (photon) gantry that allows the irradiation from multiple entry ports. The electron linear accelerator is mounted directly in the head of the rotating machine. Source: Varian Medical Systems [online], available from: <http://www.varian.com/prd/prd102.html>, [accessed 5.5.2000].

<sup>3</sup> "MeV/u": mega-electronvolt per nucleon

## 1.2.2 The Benefit of (Carbon) Ions

### The Bragg peak

As can be seen from Figure 1-1 carbon ions (and similarly also protons and other ions) show an *inverse* depth-dose profile with respect to photons. This is due to the fact that ions are slowed down successively in an absorbing matter (such as tissue) and the energy transfer increases with decreasing speed of the particle. The resulting effect is a relatively low "plateau" region of energy deposition in the entrance channel followed by a sharp peak at the end of their range (given by the initial energy of the particle). This phenomenon is called the "Bragg peak" and its potential for radiation therapy was realised already in the 1940s by Bob Wilson (at that time referring to protons only). He set up a modest therapy facility at Fermilab and later proposed the adaptation of the Harvard cyclotron for this purpose, which eventually became the facility with the longest continuous history of proton therapy.

*Protons and ions show a favourable, "inversed" depth-dose profile when passing through human tissue compared to the (classical) photons.*

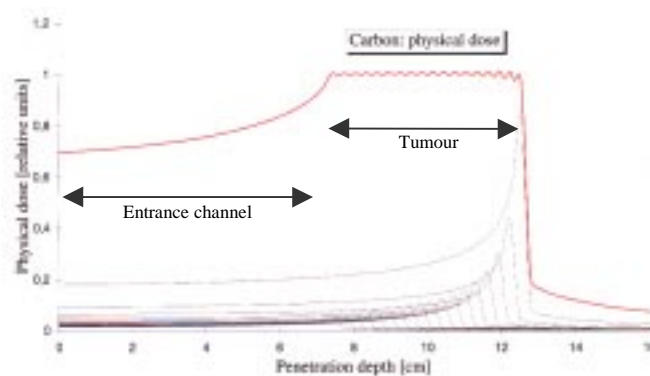
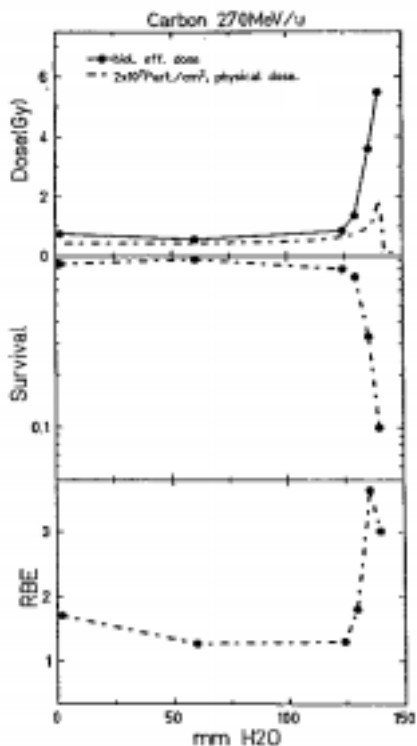


Figure 1-3: The spread-out Bragg peak (SOBP) permits the irradiation of a 3D-target volume by stacking several individual Bragg peaks of different energy and intensity. Source: Debus et al., 1998, p. 14

The Bragg peak effect offers the possibility to conform the dose very closely to the tumour by carefully controlling the energy (and hence the penetration depth) of the particles. Through the weighted superposition of proton or ion beams of different energies (i.e. creating Bragg peaks at different ranges) it is possible to deposit a homogenous dose in the entire target region using only a single beam direction. The resulting (range-modulated) depth-dose profile is called "spread-out Bragg peak" (SOBP). An example is given in Figure 1-3.



### Double strand breaks and RBE

In addition to the improved depth-dose profile of ions (including protons) compared to photons (physical selectivity), for ions heavier than helium nuclei a higher biological efficiency is observed. This *relative biological efficiency* (RBE) can be defined as the ratio of photon doses to particle doses necessary to produce the same biological effects, i.e. killing of cells. Figure 1-4 demonstrates the favourable RBE characteristic of carbon ions. In the plateau region the RBE value is similar to photon values (values between 1.3 and 1.5), whereas the RBE in the region of the Bragg peak increases to a value of about 3.

Figure 1-4: Physical dose, biological dose, cell survival rate and RBE value of cells exposed to  $2 \times 10^7$  carbon ions per  $\text{cm}^2$  having an initial energy of 270 MeV/u. Source: Selzer et al., 1998, p. 68.

The reason for this enhanced RBE is that - for a given *physical* dose - the carbon ions lead to a much higher intensity of secondary particles when interacting with tissue compared to protons; the probability of multiple ionisation events rises and therefore the chance of double strand breaks in the DNA yielding a greater probability of cell death (compare Figure 1-5).

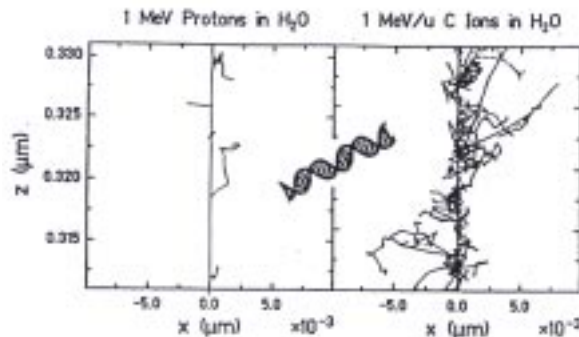


Figure 1-5: Monte-Carlo-simulation of tracks of proton and carbon ions in water. The tracks are compared with the dimensions of a schematic DNA molecule. Carbon produces much higher ionisation density causing more severe damage to the DNA in a cell. Source: Krämer et al., 1992

### Why carbon ions?

The choice of carbon ions for ion therapy is a trade-off between physical and biological characteristics. Carbon ions show - in general - the best ratio between biological effects in the tumour volume and the entrance channel (healthy tissue), which is crucial for the therapeutic effect.<sup>4</sup>

*Carbon ions show an optimal ratio between biological effects in the tumour volume and the entrance channel of the therapy beam.*

Carbon ions maintain sharp dose gradients when passing through tissue. This makes them ideally suited for high-precision irradiation where a small (pencil-) beam is "scanned" in three dimensions over the arbitrarily shaped tumour volume (active beam scanning). In addition, ions heavier than helium nuclei offer the possibility of a direct verification of the deposited dose via *Positron Emission Tomography* (PET) since the primary beam generates (to a small amount) radioactive isotopes in the region of interaction which decay by the emission of a positron.

On a macroscopic level, one has to consider that the heavier the particle chosen for therapy is, the larger will be the size of the facility and the equipment because the "stiffness" (magnetic rigidity) of the beam increases with the atomic mass of the particle. Simplistically spoken, it is more difficult to "bend" a (heavier) carbon-ion beam in a desired direction by means of a magnet than it is for a proton beam.<sup>5</sup> This is of particular consequence for the development of a medical gantry that is capable to direct the particle beam onto the patient from any desired position. Evidently, the particle of compromise must be the "lightest" one that still shows a desirable RBE characteristic. Carbon ions seem to meet best this criterion (Debus et al., 1998, p. 22).

## 1.3 Rationale and Structure of the Thesis

Table 1-1 indicates that 18% of all cancer treatments are not successful *although* the tumour was still locally confined (no metastases) at the time of first treatment. Radiation therapy applying carbon ions focuses at these 18% - or about a third of all cancer-related

<sup>4</sup> Ions heavier than carbon (oxygen, neon etc.) show even higher values for the RBE at the Bragg peak than carbon ions do, however, this is accompanied by an (unwanted) much higher RBE in the entrance channel. Additionally, ions heavier than carbon show an enhanced "tail" behind the Bragg peak in the depth-dose profile. This tail - which is to a certain, acceptable degree also present for carbon ions - is a consequence of fragmentation products causing secondary ionisation effects behind the target volume.

<sup>5</sup> For carbon ions with an initial energy of 400 MeV/u (corresponding to a penetration depth of about 27 cm in tissue) the magnetic rigidity is 6.3 Tm. With a non-superconducting dipole (usually) providing a magnetic field of 1.8 T, the required bending radius is 3.53 m - compared to 1.35 m for protons with a similar range (see Regler et al., 1998, p. 33).

deaths - since carbon ions allow a tight conformation of the dose to the tumour volume, hence increasing the dose to the tumour, reducing the dose on healthy tissue and sparing critical organs.

### 1.3.1 Rationale for the Thesis

Proton beams have been used successfully for cancer therapy in a number of countries and usually as a secondary application of a machine designed for physics research. The last decade saw a boom in proton therapy with the installation of dedicated hospital-based facilities (partly equipped with proton gantries). A major reason for this increased interest is due to the availability of better diagnostic imaging possibilities like computer tomography (CT), magnetic resonance imaging (MRI) and PET, which can identify the position and shape of tumours with a high precision.

*High-resolution diagnostic imaging is available*

Meanwhile, basic research in particular on the biological efficiency of ions heavier than protons has revealed carbon ions to possess optimal characteristics for the application in radiation therapy. The development of beam delivery systems capable of scanning the beam and of corresponding treatment planning systems are suited to considerably increase the conformity of the irradiation. Two test facilities were built to prove the feasibility of high-precision ion therapy and to gain clinical results (which are indeed very promising): at the HIMAC in Japan and at the GSI in Germany (see Section 2.4).

*Radiobiology of ions is known*

*Beam scanning is feasible*

In conventional therapy the photon beam is usually directed to the patient from several beam entry ports with the help of a gantry. Through the convergence of the beams on the target, it is possible to give more dose to the target volume than to the healthy tissue outside. The wish to apply the same strategy also with protons led to the development of first prototypes for proton gantries, which appeared in the middle of the 90s. These large proton gantries are commercially available these days.

*The next step: a carbon-ion gantry*

The recent promising results of carbon-ion therapy immediately call for the availability of a carbon-ion gantry in order to clearly demonstrate the advantages of ions compared to protons (and also stereotactic photon treatment). Actually, there are two concrete proposals for dedicated clinic ion-therapy facilities that intend to install a carbon-ion gantry, i.e. the German proposal for a facility in Heidelberg (Debus et al., 1998) and the Med-AUSTRON project in Austria (Pötter et al., 1998). Several others are pending like for instance in Italy (TERA-project; Amaldi et al., 1998), Stockholm and Lyon.

*So far, no ion gantry has ever been built, no detailed design has been made.*

*The objective: to find a viable solution for a carbon-ion gantry*

Traditionally, ion gantries were assumed to be too expensive and difficult to build. A few preliminary proposals for the design of an ion gantry exist, covering mostly the ion optical aspects only, however, there has never been an integrated approach leading to a viable design of an ion gantry. Such a design should link the beam optics with the structural design of the ion gantry and its building in order to evaluate the achievable beam stability in a following step. These issues are the objective of the present work. Not considering any of the above aspects might cause a major flaw in the proposed solution, which would therefore not be effective anymore. The need for an interdisciplinary approach is obvious.

*Why no industrial contract?*

One might ask the legitimate question why such a development was not simply handed over to an industrial contractor who would be in charge of the project for a "ready-to-use" turn-key ion gantry. First, one would have to see the history of proton gantries, where there has always been some major scientific research lab or university involved in the development and it was never a turn-key project supplied by a single contractor. Second, one has to realise the characteristics of such a project, which is a classic example of technology transfer. The development is still new and under way of making the step from basic research to an available technology. Such a state is characterised by the following aspects:

*Because the ion gantry is technology transfer...*

- There is an increasing involvement of various groups of actors (and their interests).
- Some major design parameters are not yet fixed. The process (activities and flows) due to take place inside the facility is *not* accurately defined yet, but will evolve during the

...which makes it impossible to formulate detailed and lasting specifications.

interdisciplinary planning phase. Therefore, *major* modifications during this phase have to be expected.

- The dimensions of technology, space, organisation and finance are *highly* interdependent - a change in one demands immediate changes in the others.
- Because of the novelty of the topic, the disciplines involved have - at the beginning - very different approaches to and (limited) personal views of the overall process. Naturally, they speak different "languages" and have different sets of values.

Such circumstances (as illustrated in Figure 1-6) make it impossible to formulate - at that stage - detailed and lasting (!) specifications necessary for contracting the project.

Currently, the technology of ion therapy is in the process of being transferred from basic research institutions to industry and it is the objective of the present thesis to provide a scientific document that paves the way for that transfer concerning the ion gantry. The generation of such a document needs the surrounding of a scientific institution since it is only there that one has "space and time" to optimise a system like the ion gantry - optimisation in a sense of combining different point of views from different disciplines involved in several different ways, judge them, remodel them and finally derive a not only efficient but - and this is the important aim - an effective solution. Such a dynamic and iterative process is very difficult under strong economic pressure.

Consequently, the present thesis was done at the European Laboratory for Particle Physics (CERN) in Geneva under the framework of the Proton-Ion Medical Machine Study (PIMMS) of which it forms part (Bryant et al., 2000). This constellation allowed - in close contact with accelerator physicists - the parallel development and mutual integration of the ion-optical and the structural design.

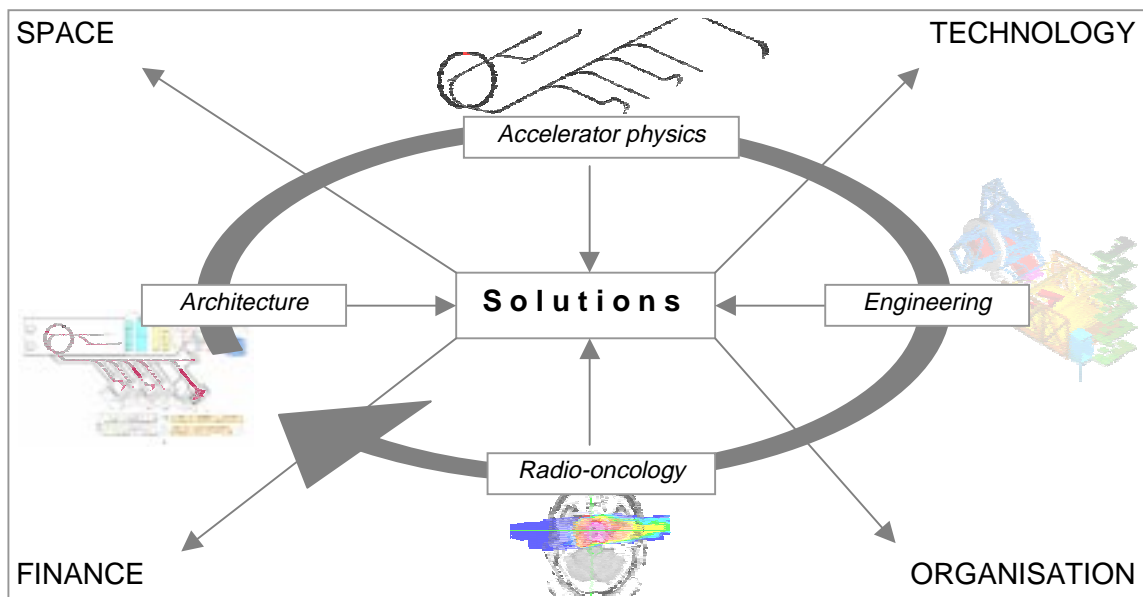


Figure 1-6: Characteristics and resulting requirements for the design process of a technology transfer project demonstrated on the example of the ion gantry development. Technological, spacial, organisational and financial arrangements are highly interdependent in such projects, more than they are in conventional industrial projects. The solution of one discipline involved has immediate impacts on the others. As a consequence, technology transfer projects require a dynamic and iterative design process, where real optimisation can take place. To find a viable solution means not to exclude a "player" from the process, since this would endanger the final solution to show a major flaw. It is the "design game" of finding the balance between fulfilling everyone's needs, providing flexibility and defining certain restrictions with the objective to reach an effective solution.



### 1.3.2 Structure of the Thesis

The present thesis is structured in four principal chapters focussing on the questions

- What exists? (Investigation)
- What is needed? (Definition)
- What solutions seem appropriate and which one is best suited? (Generation of variants and resolution)
- How can it be done? (Design)

The first three headings can be interpreted as a (architectural) program for the ion gantry, whereas the fourth one represents the first step in the design process.

This "core" is assisted by an Introduction explaining

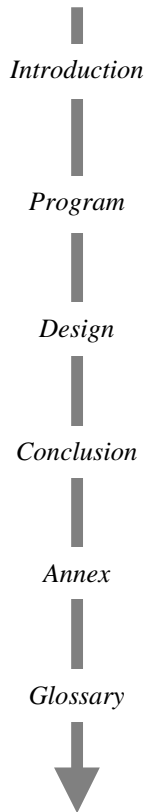
- Why is it done?

and a Conclusion to outline the new status quo. It contains an outlook on how to proceed and on what still needs to be done and touches some alternative scenarios. A summary - usually in the form of a table - finishes each chapter, thus giving brief information on the important facts.

The Annex contains a set of design drawings as well as the input and output data of the structural calculations. An additional section is devoted to a detailed analysis of some specific problems concerning the gantry structure.

The cross-functional topic requires the use of specific vocabulary of various disciplines. It was tried to explain such expressions in the text at first occurrence. Nevertheless, for convenience, a glossary was added at the end of the thesis where readers are invited to obtain definitions and further explanations of terms, which were used throughout the work, as well as of related expressions.

The structure of the thesis is illustrated and explained in Figure 1-7.



Chapter	1 Introduction	2 Investigation	3 Definition	4 Generation & Resolution	5 Design	6 Conclusion	7 Annex & Glossary
Focussing on the question	Why is it done?	What exists?	What is needed?	What solutions are possible and which one is best suited?	How can it be done?	What is the new status? How to proceed?	Details?
Objective	Background information on radiation - and in particular ion - therapy; rationale for and objective of the thesis	Profile of the present, in order to know the historic development, to identify assumptions, characteristics, and critical issues of <i>present</i> facilities	Definition of needs and constraints, the function, systematic dependencies (systems), future developments; derivation of specifications	Generation of alternative solutions, reflection, evaluation and resolution	Preliminary structural design of the gantry and its crucial sub-systems; evaluation of the performance of the system	Summary of the work; derivation of conclusions; outlook and alternative scenarios	Design drawings and technical details; glossary
Sub-structure	1.1 The Cancer Disease 1.2 The Principle Ideas of Radiation Therapy and the Promises of Ion Treatment 1.3 Rationale and Structure of the Thesis	2.1 Conventional Gantries 2.2 Proton Gantries 2.3 Neutron Gantries 2.4 Ion Facilities 2.5 Summary	3.1 The Processes to Take Place 3.2 Strategic Objectives 3.3 Beam Optics 3.4 Treatment Precision 3.5 Specifications 3.6 Gantry Structure Considerations 3.7 Conclusion: to Go for the Riesenrad-Approach	4.1 Structural Principles, Methodology and Idealisations 4.2 Wheel Gantry 4.3 Cantilever Gantry 4.4 Centrally Supported Riesenrad Gantry 4.5 Riesenrad Gantry with an Independent Telescopic Cabin 4.6 Comparison and Resolution	5.1 Quadrupoles and the 90° Dipole 5.2 The Central Cage 5.3 The Patient Cabin 5.4 Operational Procedure, Flexibility & Safety 5.5 Analysis of the Beam Position Accuracy 5.6 General Concept of Alignment and Beam Position Control, or: How to Assure That the Beam Meets the Tumour? 5.7 Gantry Hall 5.8 Cost Estimate 5.9 Summary	6.1 The New Status Quo and Outlook 6.2 Other Scenarios	Annex A: Design Drawings Annex B: Design Calculations Annex C: The Roller Supports (FEM-Study) Glossary The Author

Figure 1-7: Structure of the present thesis

## 2 Investigation

Before deriving a detailed specification and general design variants for a novel ion gantry, the present chapter is dedicated to a - partly historical - overview on existing types of medical gantries. The objective is to investigate these systems and, by that, obtain an idea in what direction the design of an ion gantry might lead. The description of the advantages and disadvantages of the various types of gantries acts as an important basis for the development of an ion gantry. In addition, Section 2.4 presents the two existing prototype facilities for ion treatment: the test facility at GSI in Germany equipped with a horizontal fixed beam line and an active beam scanning system for carbon ions, and HIMAC in Japan, where patients in supine positions can be treated with a horizontal *and* a vertical beam (energy range up to neon ions).

### 2.1 Conventional Gantries

A medical gantry offers the advantage of using multiple beam entry ports to increase the spatial conformation of the dose to the tumour and thus reducing the dose on the healthy tissue. Usually, treatment with a gantry involves the following procedures:

- The (supine) patient is immobilised on a patient couch by means of individualised whole-body moulds, masks or bite blocks.
- The gantry head is rotated to the desired treatment angle.
- The couch is moved (rotated and shifted) so that the centre of the tumour coincides with the isocentre, i.e. the centre of rotation of the gantry.

As it can be seen from Figure 1-2, the head of the gantry can be positioned on a circular path in a plane rectangular to the axis of rotation and the tumour is always found at the centre point (the isocentre) of that rotation. Such an isocentric arrangement is the *classical* concept of gantries, which are consequently called classic (rotating) gantries, isocentric gantries or conventional gantries. Theoretically, in the extreme case of full 360° rotation capacity of the gantry and a possible couch rotation of  $\pm 90^\circ$ , the central tumour can be irradiated from every point situated on a sphere around it, i.e. a  $4\pi$ -beam access to the patient ("full  $4\pi$ -irradiation") is realised. In practice, this is always limited by geometrical constraints to avoid collisions between patient and equipment.

*The classic approach in photon therapy is the conventional isocentric gantry where the central tumour can be irradiated from virtually every point situated on a sphere around the tumour.*

Figure 2-1 illustrates a typical arrangement of a treatment room equipped with a gantry for conventional radiation therapy. The gantry head houses the linear accelerator (LINAC) and the target to produce the photon beam, which can "escape" in direction of the patient only. Collimators and other equipment can be fixed to the head for shaping the beam more closely to the tumour. The whole apparatus is mounted eccentrically on a rotatable support structure (following the principle of a *cantilever*). The room is shielded in order to reduce the level of radiation for the personnel and the public to the allowable limit. The treatment is supervised remotely from a control room.

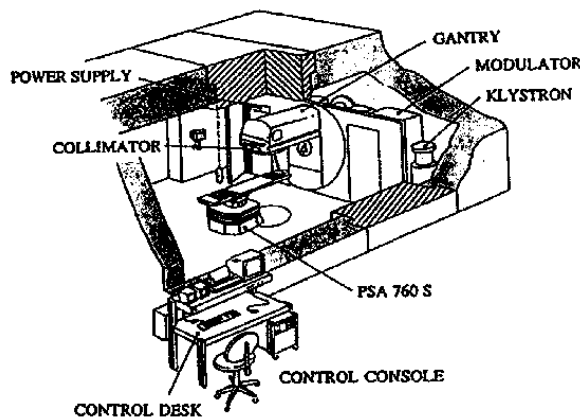


Figure 2-1: A treatment room for conventional radiation therapy. The gantry houses the linear accelerator producing an electron or - indirectly - a photon beam. By rotating the gantry the beam can be guided to the target from any desired direction. Source: Amaldi, 1999, p. 397c

Figure 2-2 illustrates the development of conventional gantries over the last decades. The size of the gantry was determined by the technology of the LINAC and the way it was mounted on the gantry head. Its continuous reduction in size has eventually lead to the state-of-the-art 360° rotating gantries of today.

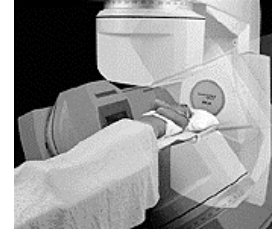
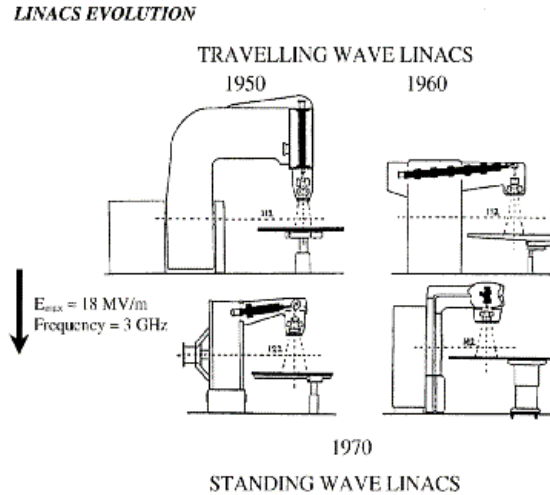


Figure 2-2: The development of conventional gantries. Improvements in the technology of the linear accelerator (LINAC) made the gantries more and more compact (left). Eventually, it was possible to rotate the head 360° around a supine patient (right). Source: IBA (Scanditronix); Rossi, 1998

## 2.2 Proton Gantries

### 2.2.1 Proposals to Avoid the Need for a Rotating Gantry

By definition, a gantry should be able to rotate 360°, in addition it should be compact, light, easy to maintain and cheap. This is more or less achievable for conventional (photon) gantries, however, when it comes to the task of building a gantry for protons, the constraints become more severe: the accelerator can no longer be mounted on the rotating arm of a gantry, since the (usually) required cyclotron weighs several hundred tons. Therefore, a beam line has to direct the beam to the rotating gantry structure. Dipole magnets mounted on the structure are used to first bend the beam out of axis and eventually direct it back onto the centrally positioned patient. The radius of such a gantry structure becomes large (up to five meters) and the weight is in the region of 100 tons.

*The first possibility:  
a set of several fixed  
beam lines*

Facing such difficulties, it is reasonable to search for alternatives to an expensive rotating proton gantry. One strategy could be to substitute the gantry by a *set of fixed beam lines* that provide a discrete choice of treatment angles. Figure 2-3 shows a proposal where the incoming beam is bent radially outwards by 90° and directed into various independent treatment rooms. Shielding should be sufficient so that the set-up of a patient in one room could be performed while treatment is carried out in another. The drawback of such a system is - besides the limited range of treatment angles - the need for a patient positioning system (PPS) in every single treatment room.

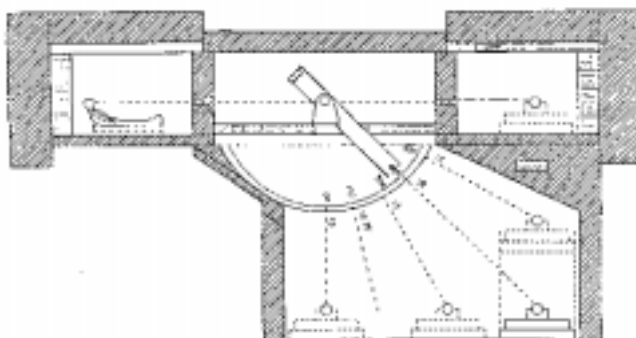


Figure 2-3: Proposal for a proton beam delivery system where the beam is directed to various (eccentrically placed) treatment rooms. A central 90° dipole can be rotated around the incoming horizontal beam axis. Thus, the beam can reach a treatment room below beam level or either of the two horizontal-beam treatment rooms at beam level. Each room is equipped with a patient positioning system (PPS). Source: Martin, 1990, p. 1803

A practical realisation of such a "gantry substitute" is currently under construction at the National Accelerator Centre (NAC) in South Africa where two fixed proton beam lines with a common isocentre will be installed: one horizontal line and one line inclined at an angle of  $60^\circ$  to the horizontal plane (see Figure 2-4). These two non-orthogonal beam lines together with a robotic patient positioning system (with 6 degrees of freedom, i.e. including pitch and roll of the couch) will provide a versatile treatment facility. It is expected that the new treatment facility will be commissioned during 2001.

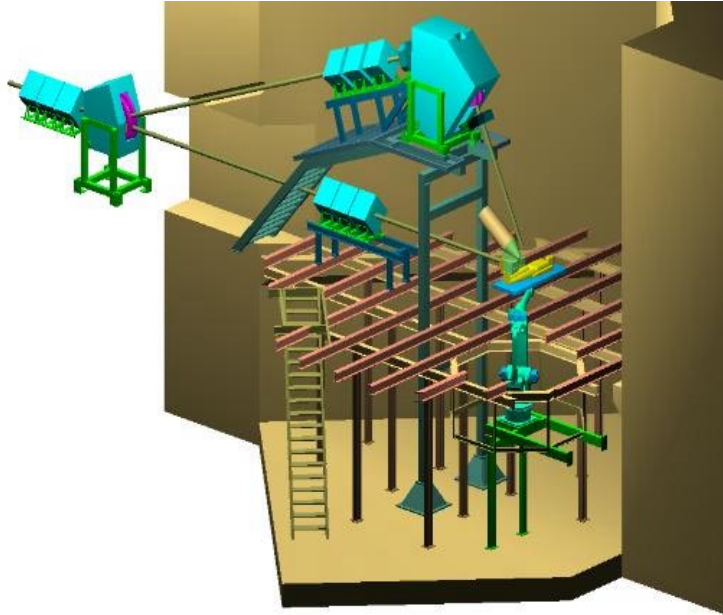


Figure 2-4: CAD image of the two fixed beam lines with a common isocentre (horizontal and  $60^\circ$ ) for proton therapy currently under construction at the National Accelerator Centre (NAC), South Africa. Source: The National Accelerator Centre (NAC), South Africa [on-line], available from: <http://medrad.nac.ac.za/npther.htm> [accessed 2000-05-16].

*The second possibility: to rotate the accelerator*

A completely different proposal to avoid the need for a large and expensive proton gantry was made by H. G. Blosser. The idea is to axially support a superconducting cyclotron by two wheels (disks). On either side of the wheels a proton beam is directed (through synchronously rotated shielding walls) into two separate treatment rooms, that can be used alternately (see Figure 2-5). The compactness of the solution is ingenious, however one accelerator can serve maximum two treatment rooms. In addition, therapy in these two rooms can not be scheduled independently.

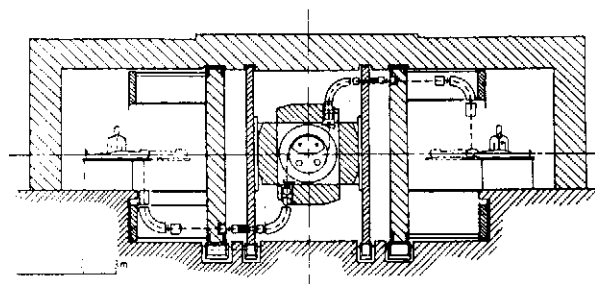


Figure 2-5: Proposal to mount a 250 MeV superconducting cyclotron on a gantry-like, rotating structure. The accelerator could serve two treatment rooms for proton therapy, one on either side. Source: Mandrillon, 1990, p. 264

## 2.2.2 Loma Linda University Proton Treatment Center (LLUPTC)

The proton therapy centre at the Loma Linda University Medical Centre (LLUMC) was the first dedicated clinic for proton therapy in the world. It is integrated into a large hospital complex. It opened 1990 and so far about 5000 patients were treated there. A synchrotron provides protons with a maximum energy of 250 MeV. The facility offers four treatment rooms, three of them are equipped with a rotating gantry (see Figure 2-6).

The proton gantries, which were also a novelty at that time, were built by SAIC (Science Applications International Corporation) from which the present company Optivus Technology Inc. emerged. However, the basic design considerations for these gantries can be found in Koehler et al., 1987 and Sisterson et al., 1987, featuring the idea of performing the majority of the necessary beam bending in a plane perpendicular to the axis of rotation and hence achieving a more compact gantry than with a classical design (see Figure 2-7). 360° of beam bending are necessary and, due to the 3D-beam transport, such a type of gantry was named "Corkscrew gantry". The version realised in Loma Linda is extremely narrow and hence does not allow any couch rotation (permitting  $2\pi$  irradiation only).

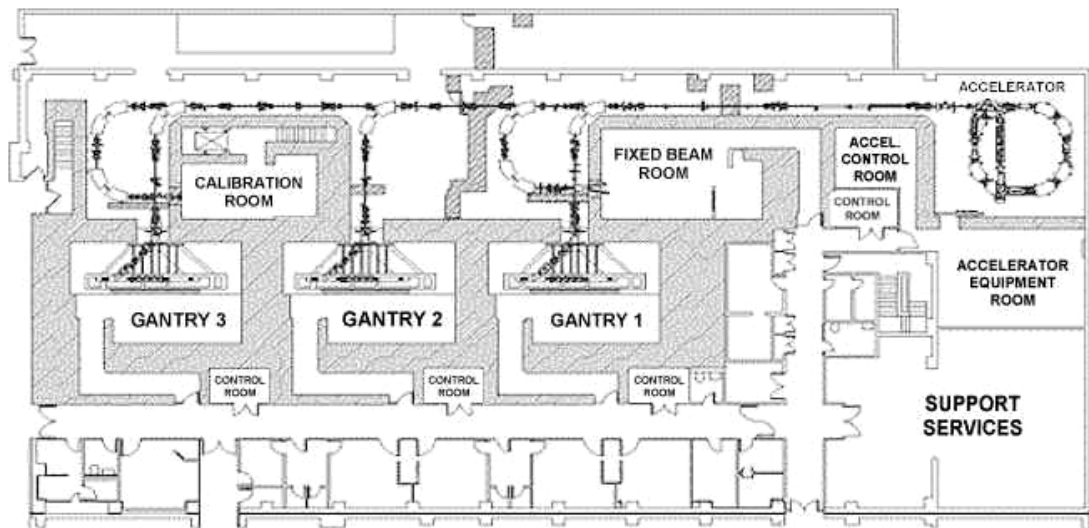


Figure 2-6: Plan of the LLUPTC (treatment level). Source: Optivus Technology.

### Gantry beam optics

The corkscrew gantries in Loma Linda bend the incoming beam by two times  $45^\circ$  (in-plane bending) followed by two  $135^\circ$  bends in a plane perpendicular to the incoming beam axis. In-between these two pairs of dipoles, 4 quadrupoles each focus the beam. A nozzle situated immediately after the last dipole houses the two scatterers (passive beam spreading) which allow field sizes up to 26 cm diameter. With a distance between the exit of the last dipole and the isocentre of 3 m, an effective source-to-axis distance (SAD)<sup>6</sup> of 2.75 m can be achieved (Flanz, 1995).

### Gantry structure

The gantry body consists of two steel rings about 3 m apart and stiffened with struts, which form a lying cylinder that can rotate around its central axis. The front ring ( $\varnothing$  4 m) rests on two pendular bearing units<sup>7</sup> with four rollers each, the rear ring, which is slightly smaller, on one unit. Column-like concrete foundations support these bearings. The gantry is driven via a roller on the front ring (friction drive). Several rollers are equipped with breaks to allow rapid gantry stops.

An octagonal, trussed disk ("gantry truss") of approximately 8 m height which supports the large dipoles ( $45^\circ$  plus  $2 \times 135^\circ$ ), the counterweight and the nozzle<sup>8</sup>, is mounted close to the front ring. Two inclined, ladder-like stiffening struts transfer parts of the load to the rear ring (see Figure 2-7). The trussed disk is assembled from 8 sections small enough to be transported into the gantry room.

<sup>6</sup> The "effective source-to-axis distance (SAD)" is defined as the distance between the (possibly virtual) point source of the beam - here: the first scatterer - and the point of interaction with the tumour (the Bragg peak) - here: the isocentre of the gantry.

<sup>7</sup> Such pendular bearing units provide a *statically determinate* support, which guarantees an *equal* load distribution on *all* rollers for all operating conditions.

<sup>8</sup> The nozzle is the apparatus between the last dipole and the patient containing all necessary equipment for beam shaping and beam monitoring. It is usually attached to the gantry structure.

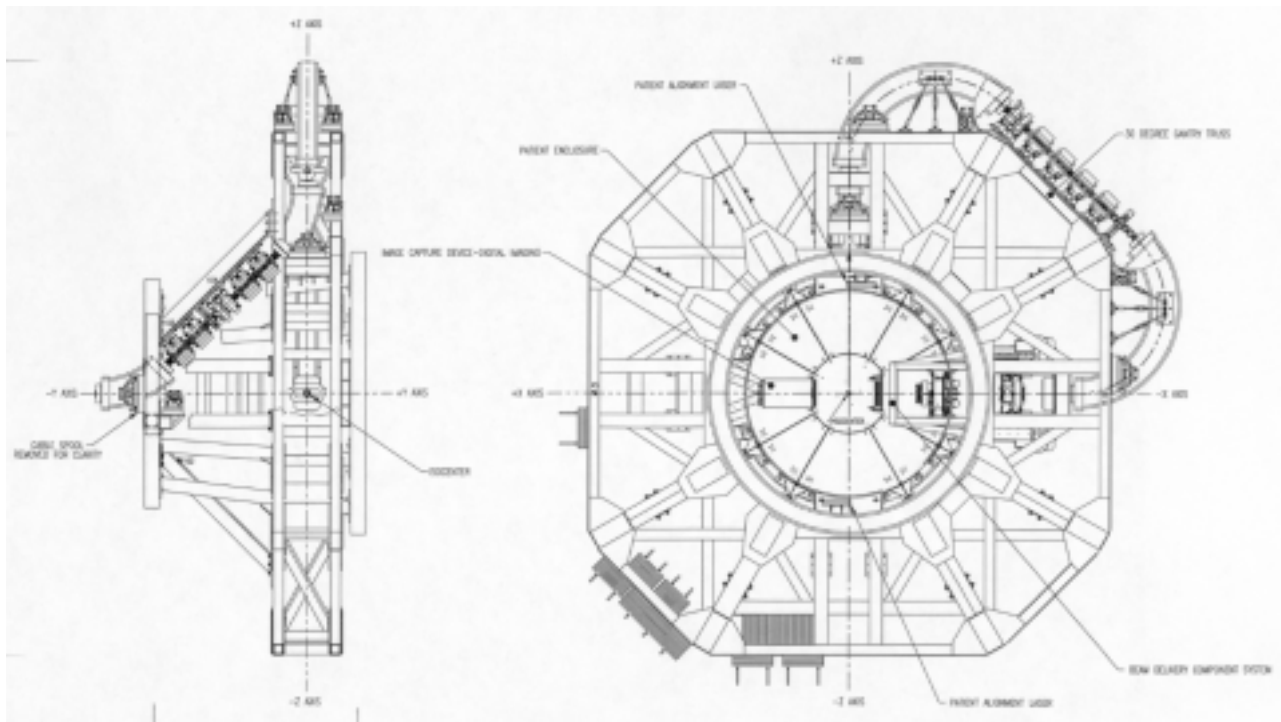


Figure 2-7: Front and side view of the corkscrew gantry operating at the LLUPTC. Source: Optivus Technology.

The overall gantry weight is approximately 96 t (Flanz, 1995) of which around 45 t are due to the structure and the counterweight. The fixation of the gantry in axial direction is via several small rollers ("seismic support assemblies"), which are mounted to the walls of the gantry hall pushing temporarily against the lateral surface of the two main rings. The clearance between these rollers and the rings (gantry structure) is checked regularly and the gantry position adjusted accordingly. Any twisting of the gantry is also corrected by this procedure.

#### Accuracy

The angular positioning accuracy of the gantry is around  $0.15^\circ$  (Optivus, 1998). Flanz (1995) quotes measurements indicating a maximum displacement of the (mechanical) isocentre due to elastic deformation of the gantry structure of  $\pm 0.8$  mm. The gantries are equipped with a portal X-ray system (for taking images in beam direction). It is current practice to use these devices before *each* irradiation to measure the tumour position and compare it to a reference image; observed differences are corrected by adjusting the couch position.

#### Gantry hall

The floor area of the gantry hall is approximately  $75 \text{ m}^2$ , of which about half of this area is occupied by the gantry structure, the other half functions as an area for patient handling and preparation. The height of the hall is about 13 m.

#### Cost

Slater et.al. (1997, p. 186) state fabrication costs for replicating one of the Loma Linda gantries to be approximately 6.5 M\$ (costs for development not included).

### 2.2.3 National Cancer Center (NCC) Kashiwa & Northeast Proton Therapy Center (NPTC) Boston

In the late 90s two similar proton therapy centres were built: the Proton Treatment Facility at the National Cancer Center (NCC), Kashiwa, Japan and the Northeast Proton Therapy Center (NPTC) at the MGH in Boston, USA. Both centres are equipped with a cyclotron

(235 MeV) and two isocentric gantries. The system was designed by the Belgian company Ion Beam Applications (IBA), partly in co-operation with Sumitomo Heavy Industries, Ltd. (NCC) and General Atomics (NPTC). The NPTC also provides a fixed beam room that can - in the long-term future - be adapted to house a third gantry (see Figure 2-8). The first patient treatment is envisaged for the beginning of 2001, whereas the Japanese facility has already started operation by the end of 1998. In addition, IBA is currently delivering three more proton therapy systems (including gantries) to TENET Healthcare Corporation, California.

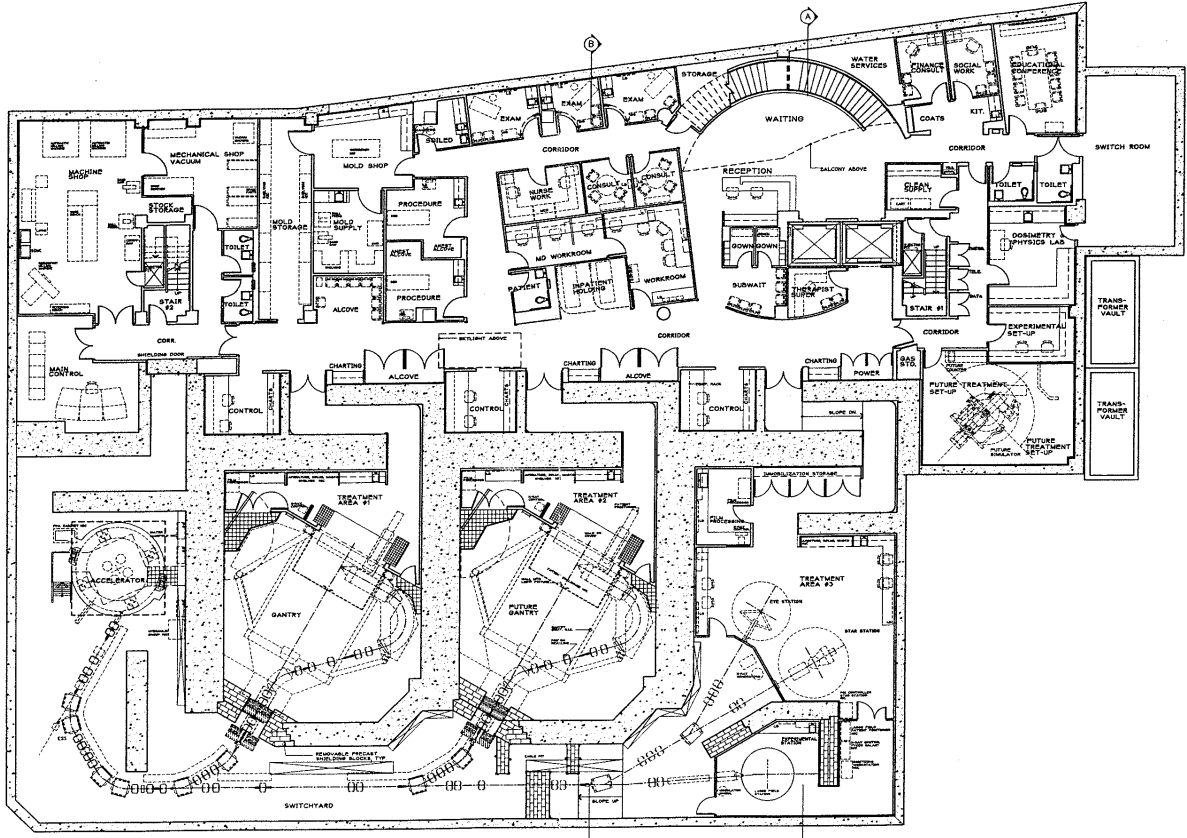


Figure 2-8: Plan of the underground level in the NPTC where all patient-related functions are concentrated. Each of the two gantry rooms is equipped with a conventional isocentric proton gantry. A third gantry can later be installed in the room currently housing the two fixed-beam treatment areas. Source: Bechtel Corporation.

The installed proton gantries are so-called conventional, "large throw" or conical isocentric gantries, which means that the incoming beam is first bent out of axis (by say a 45° dipole) and then - after some metres where the beam has gained sufficient eccentricity - directed back to the centre line radially (by a 135° dipole). All beam bending is done in a single plane. The dimensions within the gantry are such that the patient couch, which rests on a recess of the wall in front of the gantry and correctly positions the patient with respect to the gantry, can not only be moved in all three dimensions, but also be rotated around a vertical axis through the isocentre without colliding with the gantry enclosure. In combination with the gantry rotation of  $\pm 190^\circ$ , this gives 5 degrees of freedom and hence allows a full  $4\pi$ -irradiation of the patient.<sup>9</sup> In the NPTC, the couch is also equipped with pitch and roll degrees of freedom with small dynamic range to accomplish fine scale adjustments.

<sup>9</sup> Note that 5 degrees of freedom permit the description of every point on a sphere (representing the tumour) with a fixed radius. This is sufficient for treatment since the remaining 6<sup>th</sup> degree of freedom is provided by the variation of the beam energy (determining the penetration depth).



### Gantry beam optics

The beam transport inside the gantry (starting from the vacuum window) typically contains a set of four matching quadrupoles, a 45° dipole, 5 quadrupoles, the 135° dipole and finally the nozzle housing the two scatterers for "passive beam spreading". The nozzle is also foreseen to incorporate two scanning magnets ("sweepers") in order to upgrade the gantries to "beam wobbling" (enabling an enlarged field size) and "beam scanning" (in a second step). The distance between the exit of the last dipole to the isocentre is 3 m, the nozzle configuration allows an effective source-to-axis distance of 2.2 m (IBA, 1997).

### Gantry structure

The mechanical design of the gantry is governed by three principal objectives:

- Minimisation of interference with the beam delivery system
- Accessibility to the patient
- Confinement of the isocentre position of the proton beam to  $\pm 1$  mm during gantry rotation (IBA, 1997).

As it can be seen from Figure 2-9 the overall geometry of the gantry is determined by the 3 m distance between the isocentre and the end of the last dipole. The rotating part of the gantry is formed by two rings of about 5 m diameter with a space frame in-between thus providing the necessary bending and torsion stiffness for the gantry. Shear wall elements are used along both sides of the final 135° dipole and the counterweight. The space frame is made out of 4 major quarters bolted to each other and to the rings. The cable drum and the first set of quadrupoles are supported by a conical structure bolted to the rear ring.

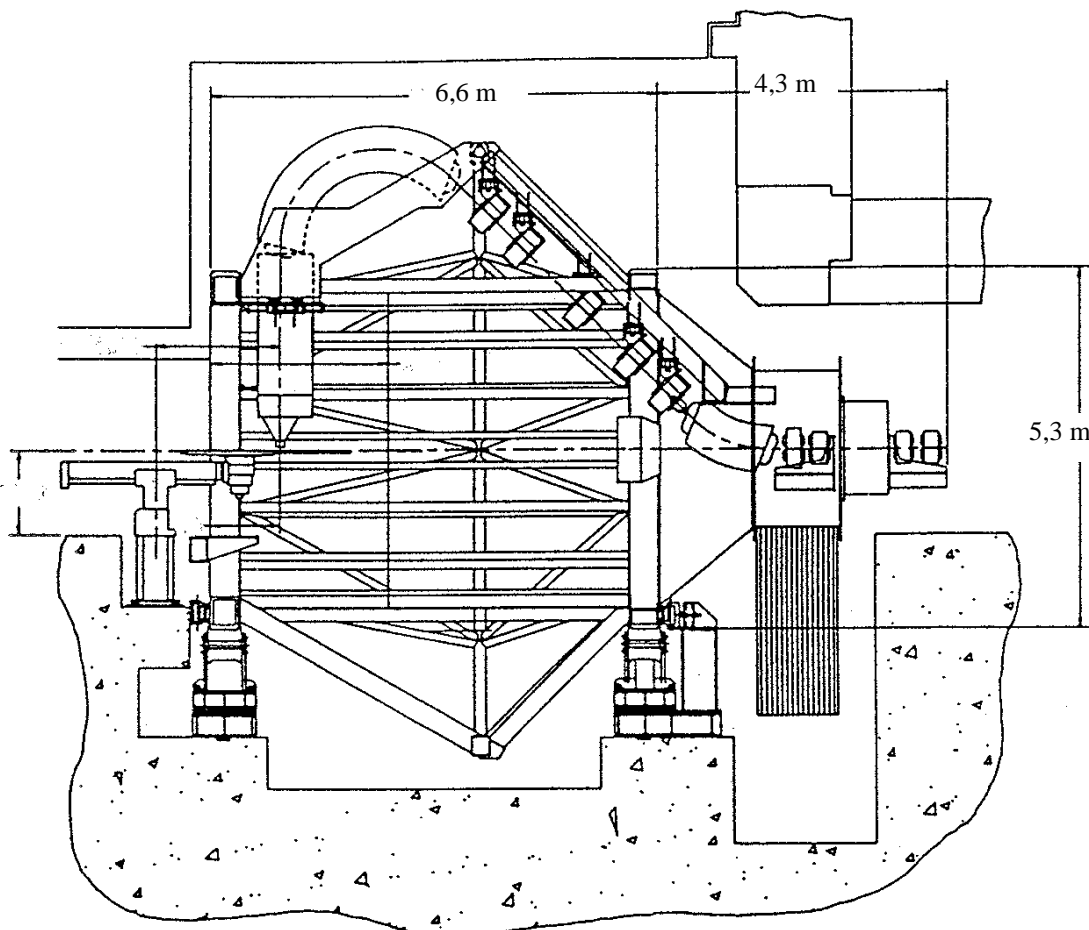


Figure 2-9:  
Section drawing  
of the IBA proton  
gantry. Source:  
IBA, 1997.

Each of the two rings is supported statically determinate by two sets of pendular bearing units à 4 rollers (see Figure 2-10 and Figure 2-11). These bearings are equipped with an additional rotating axis (parallel to a tangent of the ring) to secure a smooth stress distribution on the roller surfaces - even when the structure has sagged elastically. In addition, these units can float axially on linear bearings. The rotating structure - or more precisely the bottom point of the front ring - is pushed against a set of rollers which are

mounted on the building wall (below the support for the patient couch) by a spring-loaded roller bearing at the rear ring (see Figure 2-9). Therefore, the front wall acts as a reference point for gantry and couch alignment.

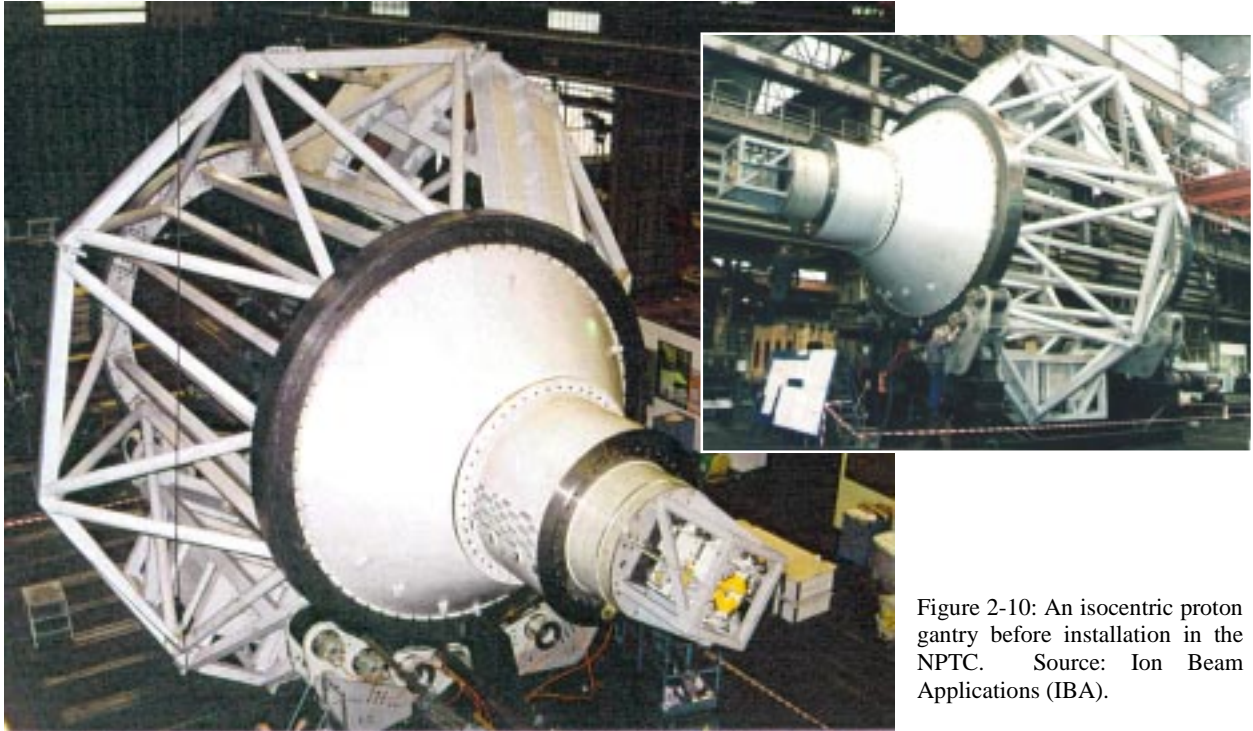


Figure 2-10: An isocentric proton gantry before installation in the NPTC. Source: Ion Beam Applications (IBA).



Figure 2-11: An isocentric proton gantry before installation in the NCC. Source: Ion Beam Applications (IBA).

The rotating structure is driven by two rollers (friction drive); fail-safe breaks are installed on four rollers of the rear ring. These breaks are capable of stopping the gantry (rotating at full speed of 1 rpm) within 30° under operating conditions and within 5° in case of an emergency. The gantry and its bearings rest on a base frame, which can be jacked up and re-adjusted if necessary.

The weight of the gantry without magnets and nozzle (but including the counterweight) is around 85 t, total weight is 120 t for the NPTC version (IBA, 1997) and about 155 t for the NCC version (Kataoka et al., 1999).



Figure 2-12: Images showing the assembly process of the isocentric proton gantry at the NCC. Source: Kataoka et al., 1999

### Accuracy

The dead load of the structure, the weight of the magnets and of the nozzle lead to an elastic deformation of the gantry, concerning in particular the two support rings and the nozzle itself. Naturally, these deformations vary during gantry rotation and they strongly influence the beam accuracy in the isocentre. For the NPTC, preliminary measurements of the *mechanical* isocentre indicated maximum (elastic) deformations of approximately  $\pm 0.6$  mm during gantry rotation (Flanz, 1998, p. 322). As illustrated in Figure 2-13, their effect on the beam turned out to be of similar magnitude in the plane of gantry rotation, whereas in direction of the gantry axis *beam displacements up to  $\pm 1$  mm* were encountered during gantry rotation (Barkhof et al., 1999, p. 2435). About 90% of these measured isocentre displacements appear to be *systematic* and could therefore be automatically compensated with the patient couch. The latter (2.5 t) is equipped with several load sensors to enable a patient specific correction of the couch deformation. The gantry drive is programmed to stop within  $0.25^\circ$  of a pre-selected gantry angle.

### Gantry hall

By fitting the gantry diagonally into the gantry hall - the angle between gantry axis and the longer side of the rectangular gantry hall is about  $30^\circ$  - a very compact room geometry is achieved: the floor area is approximately  $95 \text{ m}^2$ , the height of the hall is about 11 m (see Figure 2-8). The thickness of the concrete walls is between 2 m and 2.5 m (shielding). The

demanded precision of the gantry requires the temperature inside the hall to be maintained within  $\pm 1.5$  K. The heat release to the air is about 5 kW.

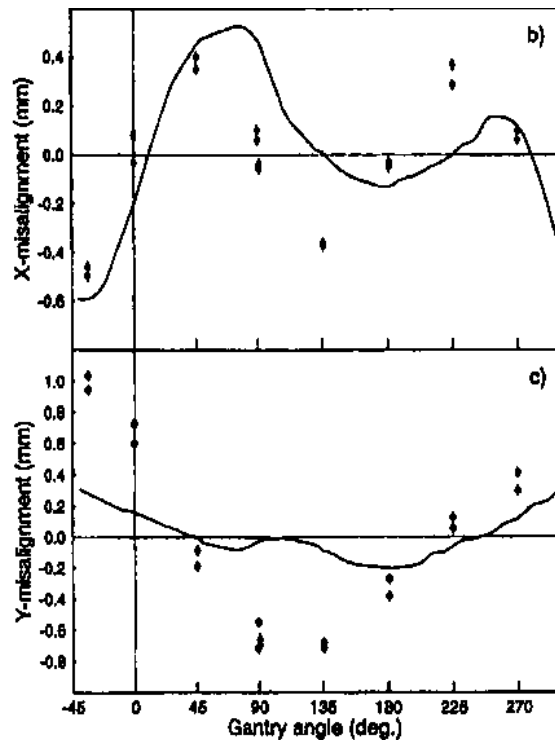


Figure 2-13: Effects of elastic isocentre deformations (solid curve, taken from the acceptance tests) of the NPTC proton gantry on the proton beam, indicated for various different gantry angles. The data points of the upper graph show the measured beam displacement (alignment error) in X-direction, i.e. the axis lying in the plane of gantry rotation being perpendicular to the beam. The lower graph represents the measured beam displacement in direction of the gantry rotation axis. The error bars at the data points indicate the standard deviation of the measurements:  $\sigma_x = 0.05$  mm and  $\sigma_y = 0.09$  mm. Since the accuracy of the measurement system is considerably higher ( $\sigma = 0.025$  mm), most of these random errors seem to be caused by the gantry. Source: Barkhof et al., 1999, p. 2435

### Cost

According to Goitein (1997, p. 149) the price paid by the NPTC for one proton gantry - including nozzle and patient couch but excluding the control system and the building - was about 4.5 M\$ (gantry 2.2 M\$, nozzle 1.5 M\$ and couch 0.8 M\$).

## 2.2.4 The Eccentric Proton Gantry at the Paul Scherrer Institute (PSI)

In 1996, the Paul Scherrer Institut (PSI), Villigen, Switzerland, started using their proton gantry for the irradiation of deep-seated tumours. The innovative design of placing not only the final dipole but - opposite to it - *also the patient eccentrically to the axis* of gantry rotation reduces the overall radius of the proton gantry to 2 m. Schär Engineering AG was the designer of the mechanical part.

Before each treatment, a specially adapted CT checks the correct position of the immobilised patient - notably the tumour - with respect to the patient couch in a separate room. For this task, the couch will be coupled to the CT table using the same clamping mechanism as later at the proton gantry. After the position check, the patient (plus couch) is transported to the gantry (with a special carriage system) and coupled to the gantry table. In addition, if necessary, the position of the patient (tumour) with respect to the gantry can be checked directly at the gantry with X-ray imaging or proton radiography.

### Beam optics

The proton therapy beam is delivered from a cyclotron with 590 MeV and is subsequently degraded to energies between 80 MeV and 270 MeV. This procedure increases the phase space of the beam, hence the aperture (and consequently the weight) of the gantry magnets ( $35^\circ - 35^\circ - 90^\circ$ , see Figure 2-14) has to be slightly larger than for an optimised machine dedicated to radiation therapy only (Pedroni, 1994, p. 450).

The PSI proton gantry is, so far, the only gantry working in an active beam-scanning mode. This system, called "spot scanning", uses a pencil beam to irradiate step by step small

volume elements ("spots") of the tumour, thus being in principle able to irradiate conformely any arbitrarily-shaped volume. No patient specific hardware (such as compensators or collimators) is needed for the spot scanning technique, except from the immobilisation device.

The motion of the pencil beam from one spot to the following is always performed with the beam switched off. For the fastest movements, a small bending magnet ("sweeper") *in front* of the final 90° dipole is used (see Figure 2-14). The motion along the second axis of scanning is realised with a range shifter system, which rapidly varies the dose spot in depth. The third - and slowest - direction is covered by the *motion of the patient couch* (circa 2 cm/s). The beam is a parallel beam with about 7 mm FWHM (full width at half maximum) and is scanned in an orthogonal matrix in steps of about 5 mm. For a one-litre target volume typically about 10000 spots are delivered in less than 5 minutes.

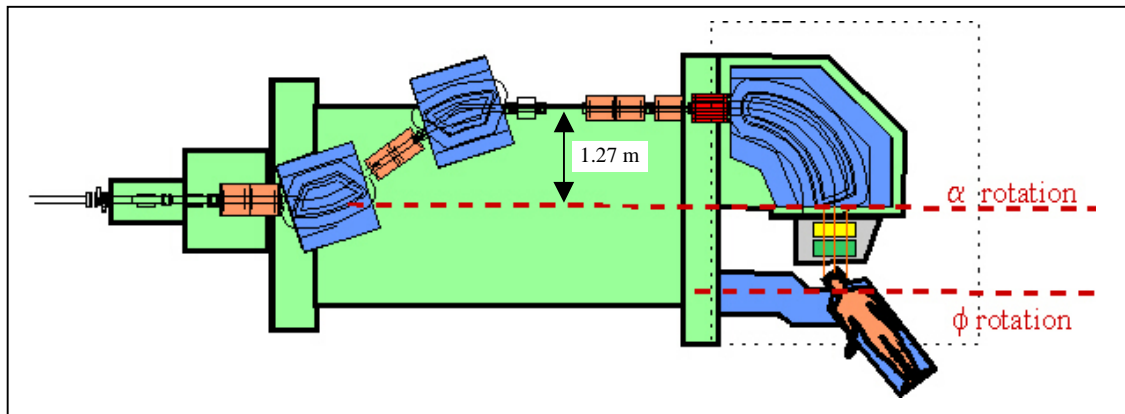


Figure 2-14: Arrangement of the beam transport system in the PSI proton gantry: bending magnets: blue, quadrupole: orange, sweeper (scanning dipole): red, structure: light green, beam monitoring system: yellow, range shifter: green. Source: PSI, 2000.

### Gantry structure

It can be seen from Figure 2-14 that the beam transport is similar to a conventional isocentric gantry, however, by placing the patient eccentrically to the axis of gantry rotation ( $\alpha$ ), the eccentricity of the large 90° dipole can be reduced accordingly. In addition, the active scanning system and a compact design of the nozzle allow a distance between the exit face of the dipole and the patient (axis) of only 1.1 m. Consequently, the overall *diameter* of the gantry can be limited to just 4 m.



Figure 2-15: The rear ring of the PSI proton gantry showing its chain drive and the roller supports. Source: Schär Engineering AG

The patient couch is mounted eccentrically and forms part of the gantry structure. In order to keep the couch horizontal during gantry rotation, a second axis of (couch) rotation ( $\phi$  in Figure 2-14), parallel to the gantry axis, has to be introduced. The chain drives (see Figure 2-15) for both axes are not coupled, which has the advantage that in case of a collision involving the patient, only the couch rotation has to be stopped immediately thus preventing any further relative movement between patient and gantry. A signal to stimulate such a situation could for example come from the collision-sensitive cover of the nozzle.

Irradiation angles where the proton beam has to come from below the patient imply that the latter is positioned somewhere close to the top of the gantry with a maximum of 2.4 m vertical distance to the solid floor, i.e. out of direct reach for a person standing on the this floor. In case of complete mechanical breakdown during such a gantry position, the patient couch can be slowly lowered with the help of a small crane. This issue has provoked some criticism in particular among medical doctors, since it could excessively delay intervention in case of an emergency.

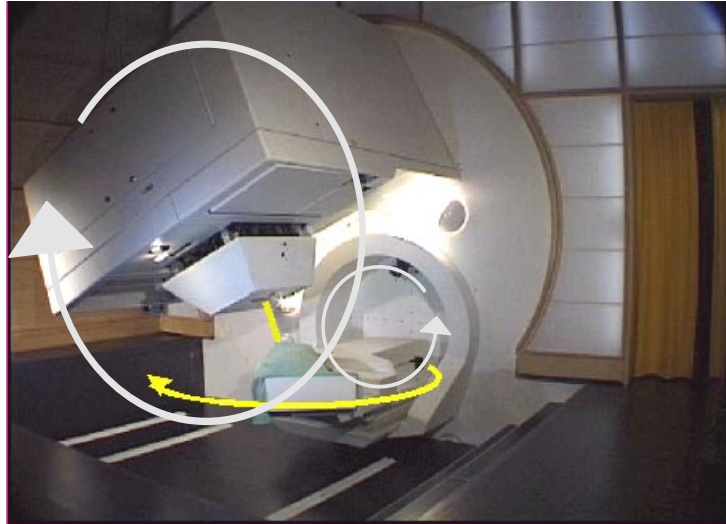


Figure 2-16: Kinematics of the eccentric PSI proton gantry. The gantry body can be rotated 360°, while a second axis of rotation keeps the patient couch horizontal. A couch top rotation (forming a maximum angle of 120° with the gantry axis) is also possible. Source: adapted from PSI, 2000.

The gantry can be rotated by 360°. With the help of a special support mounted on the gantry couch, the latter can be rotated up to 120° in a horizontal plane ("top rotation"), thus achieving (more or less)  $4\pi$ -beam access to the patient (see Figure 2-16).

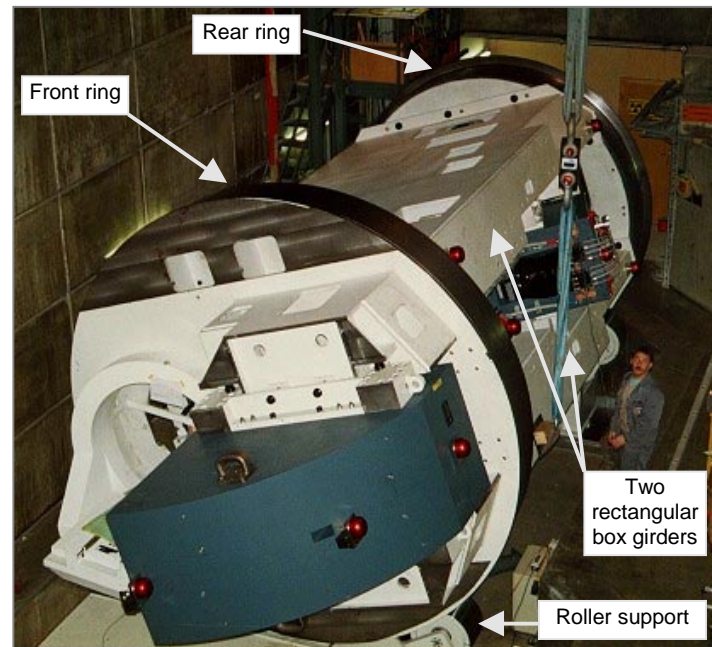


Figure 2-17: The PSI proton gantry during assembly. The main elements are indicated. Source: Schär Engineering AG

The principal elements of the gantry structure are the two main rings, supported by four rollers each (see Figure 2-15), and the two rectangular box-girders spanning in-between (see Figure 2-17 and Figure 2-18). These two girders act as shear walls and give support to the beam transport elements. They are rigidly connected to a third shear wall (orthogonal to the two others) opposite to the eccentric beam line. Most of the counterweight is actually integrated into this element. Eventually, the three girders together form a very rigid, "U"-shaped and torsion resistant structure.

The two box girders continue through the front ring and give support to the 90° dipole (25t, aperture: 20 × 5 cm<sup>2</sup>). Since the dipole and the patient couch can be seen as cantilevers built in the front ring (Ø 4 m), the latter does not need to be a "ring", but can rather be a - far more rigid - disk.

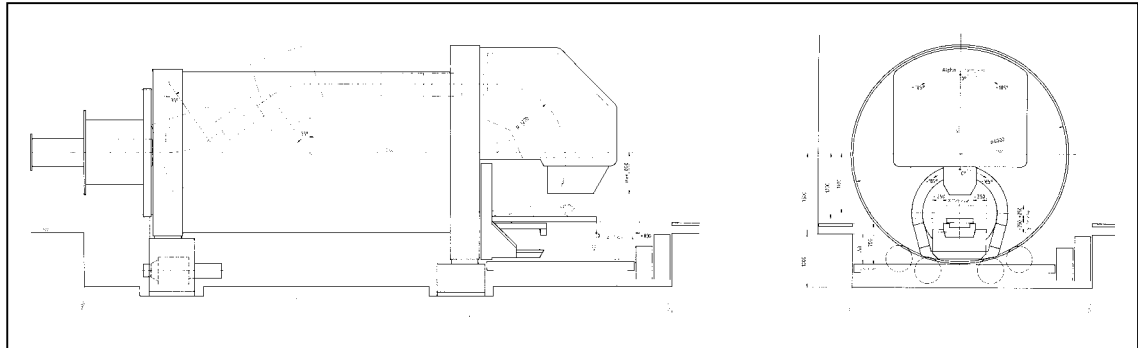


Figure 2-18: Construction drawings (side and front view) of the PSI proton gantry. Source: Schär Engineering AG.

The total weight of the gantry is 110 t, its overall length is about 11 m. The longitudinal fixation of the gantry is achieved by a set of roller bearings at the rear ring. However, this issue is not critical, because the patient couch is mounted directly on the gantry structure, hence guaranteeing mechanically the correct relative position.

Although a CT checks the correct alignment of the patient with respect to the couch before each treatment, the gantry is equipped with a X-ray unit that can telescope from the dipole face towards the patient, thus providing images orthogonal to the beam. On the same sliding supports, also two detectors for proton radiography are mounted, which can be inserted into the beam (in front and behind the patient, see Figure 2-19). The images obtained from proton radiography are similar to the X-ray ones, however, the main advantage is the possibility to check indirectly the calculation of the proton range in the patient (PSI, 2000).

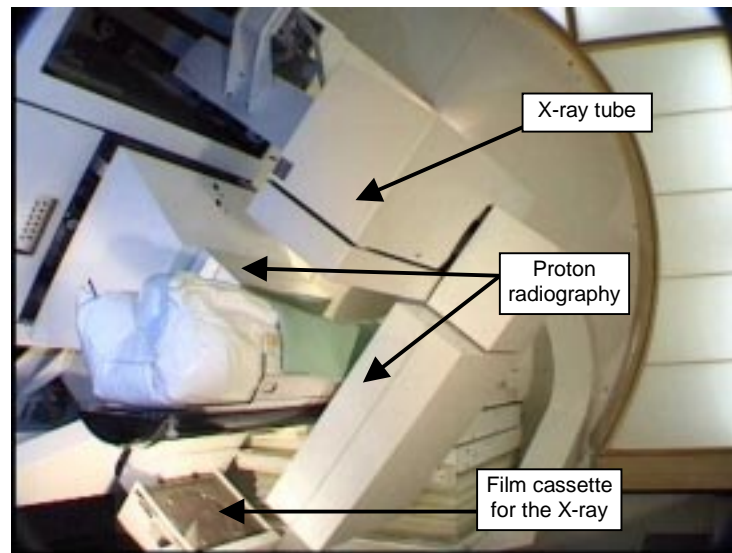


Figure 2-19: The X-ray and proton radiography at the PSI proton gantry. Source: PSI, 2000

### Accuracy

According to Schär Engineering, the maximum elastic sagging of the gantry is lower than 0.5 mm. Detailed beam measurements indicated that the maximum random error in the (local) iso-centre during beam scanning, i.e. the difference between expected and measured spot position, is below 0.5 mm (PSI, 2000).

### New developments

Due to the accelerator limitations mentioned above, the PSI intends to install a new cyclotron dedicated to proton therapy only. In addition, a novel "second generation" gantry (see Figure 2-20) is foreseen in order to exploit proton therapy on a commercial basis (Pedroni, 2000).



Figure 2-20: Proposed concept for a second, but this time isocentric, proton gantry at the PSI. The gantry turns only  $\pm 90^\circ$ , the patient couch performs a continuous  $180^\circ$  rotation in the horizontal plane. Source: Pedroni, 2000

## 2.3 Neutron Gantries

For certain specific kinds of tumours fast neutrons are the particle of choice for external radiation therapy. Neutrons show a better RBE compared to photons but a similar (unfavourable) depth-dose distribution. Nevertheless, a couple of neutron gantries were built, most of them following a similar *structural* design as conventional gantries (cantilever), but showing a considerable increase in dimensions to accommodate the beam line. This beam line directs the primary (proton) beam into the gantry and onto the target where the neutrons are finally produced (see Figure 2-21).

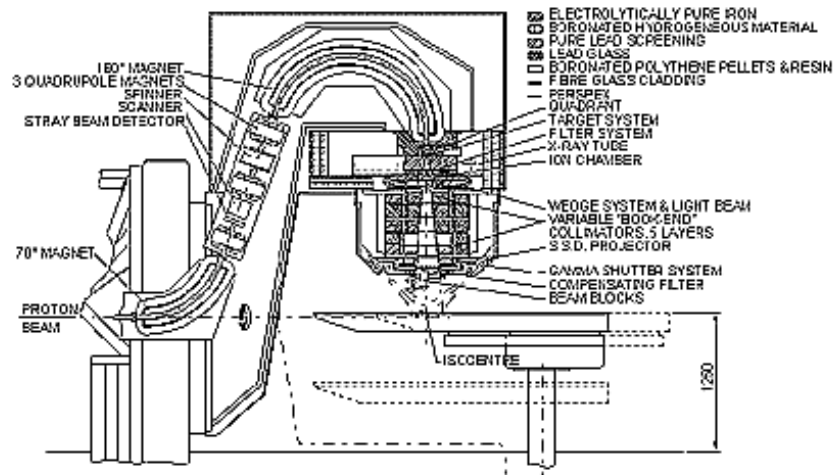


Figure 2-21: View (left) and section (right) of the isocentric neutron gantry installed at the NAC, South Africa. The neutrons are produced from a 66 MeV proton beam hitting a beryllium target. Source: The National Accelerator Centre (NAC), South Africa [on-line], available from: <http://medrad.nac.ac.za/neuts.htm> [accessed 2000-05-16]

A different and unique approach to a neutron gantry was realised at the Harper Hospital in Detroit; regular treatment started in 1992: A superconducting cyclotron is mounted directly on the rotatable gantry structure (see Figure 2-22). The mechanical concept is similar to that of conventional proton gantries. Two large rings form a cylinder that houses the treatment room. The 25 t magnet of the cyclotron is supported eccentrically. The patient couch is supported from outside of the gantry and cantilevers into the treatment room.



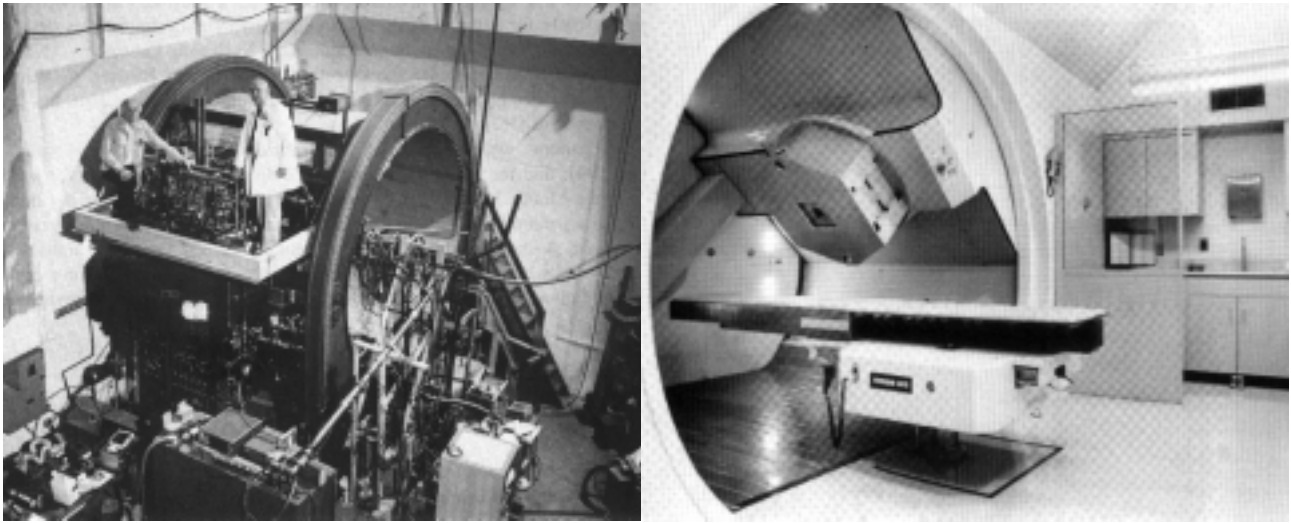


Figure 2-22: The neutron gantry at the Harper Hospital in Detroit. A superconducting cyclotron is supported by two large rings (left) that house the treatment room (right). Source: Maughan et al., 1994

## 2.4 Ion Facilities

### 2.4.1 HIMAC

In 1994, when the HIMAC (Heavy Ion Medical Accelerator in Chiba, Japan) treated the first patients with carbon ions, it was - and it still is - the first *ion* therapy facility dedicated to medical use only.

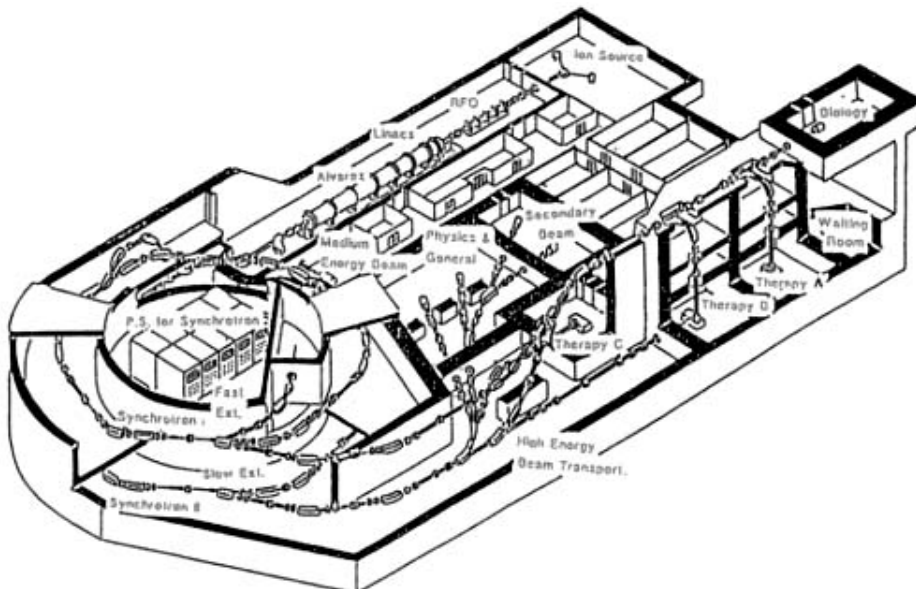


Figure 2-23: Facility layout of HIMAC, where regular ion treatment is carried out in a hospital-like environment. Source: HIMAC, 2000

Two 800 MeV/u synchrotrons vertically separated by approximately 10 m provide ions up to Xenon, however, the principal type of ion used for therapy is carbon ( $^{12}\text{C}$ ) at energies of 290, 350 and 400 MeV/u. HIMAC provides three treatment rooms: one with a horizontal, one with a vertical and one with both horizontal and vertical beams (see Figure 2-23 and Figure 2-24). The beam delivery applies the "wobbler" method: a beam scatterer *together* with scanning magnets forms a *large uniform* field, individually shaped with a multi-leaf

collimator. The beam range is adjusted by an individualised compensator ("bolus"). HIMAC also provides the possibility for "beam gating", i.e. the synchronisation of the particle extraction and the breathing cycle of the patient in order to mitigate the effect of organ movements *during* irradiation.

Currently, a forth treatment room is being commissioned, with a radioactive  $^{11}\text{C}$  beam produced by passing the  $^{12}\text{C}$  primary through a beryllium target and magnetically separating the  $^{11}\text{C}$  (Alonso, 2000). Such a beam provides excellent intensities for PET imaging in order to precisely measure the range distribution of the ions in the tumour (quality assurance).

So far, nearly 800 patients have been treated with carbon beams at HIMAC and the average rate of local tumour control after a one-year period is 82% for 510 available cases. These figures seem even more promising if one considers that only those patients have been selected for ion treatment, who are not curable with other types of therapy (Takada, 2000).



Figure 2-24: A treatment room with a horizontal and vertical beam line at HIMAC. The room is also equipped with a CT for checking the patient-to-couch position (on the left). Source: HIMAC, 2000

## 2.4.2 GSI Pilot Project

Since 1997, GSI<sup>10</sup> in Darmstadt is operating a horizontal beam line for carbon-ion therapy (Figure 2-26) using active energy variation and a beam scanning system ("rasterscan technique") to achieve a 3D tumour-conformal dose delivery (see Figure 2-25 and GSI, 2000).

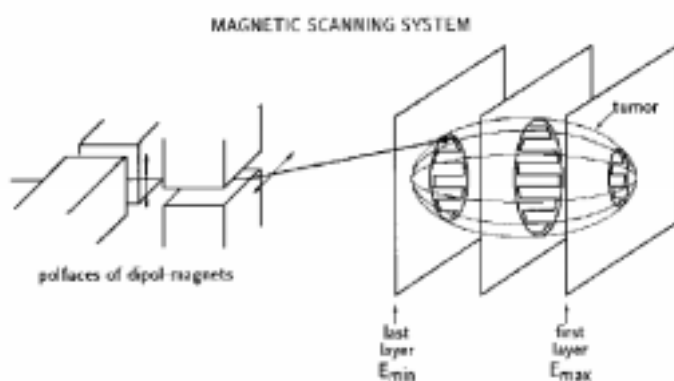


Figure 2-25: The rasterscan technique. The tumour is discretised in slices, each slice made out of small volume elements called "voxels". Irradiation starts with the most distant slice, corresponding to a maximum energy (and hence penetration depth) of the particle. Scanning magnets direct the beam to the next voxel as soon as the pre-calculated dose for the present voxel has been delivered. The size of a voxel is typically a 3 mm cube - which is only possible with ions - and it takes only about 1 ms to deliver the required dose to such a volume. The voxels are overlapping manifold to avoid hot and cold spots. When one slice has been "filled", the energy of the synchrotron is lowered actively and the procedure starts again for the next slice. Source: Eickhoff et al., 2000

Another remarkable innovation has been the full integration of PET imaging into the treatment process giving some feedback on the delivered dose after the treatment session has been finished (no on-line read-out possible yet). At the GSI, the PET image is taken

<sup>10</sup> The facility was set up in co-operation between the Radiologische Universitätsklinik Heidelberg, the Deutsche Krebsforschungszentrum Heidelberg (DKFZ), the Forschungszentrum Rossendorf (FZR) and the Gesellschaft für Schwerionenforschung (GSI).

during and immediately after irradiation when the patient is still immobilised. The amount of produced  $^{11}\text{C}$  is adequate for useful images, in particular for the head and neck region. In some cases beam deviations as high as 5 - 6 mm from the calculated *range* were detected by PET - errors arising from imprecise handling of inhomogeneities in the treatment planning programs (Alonso, 2000).

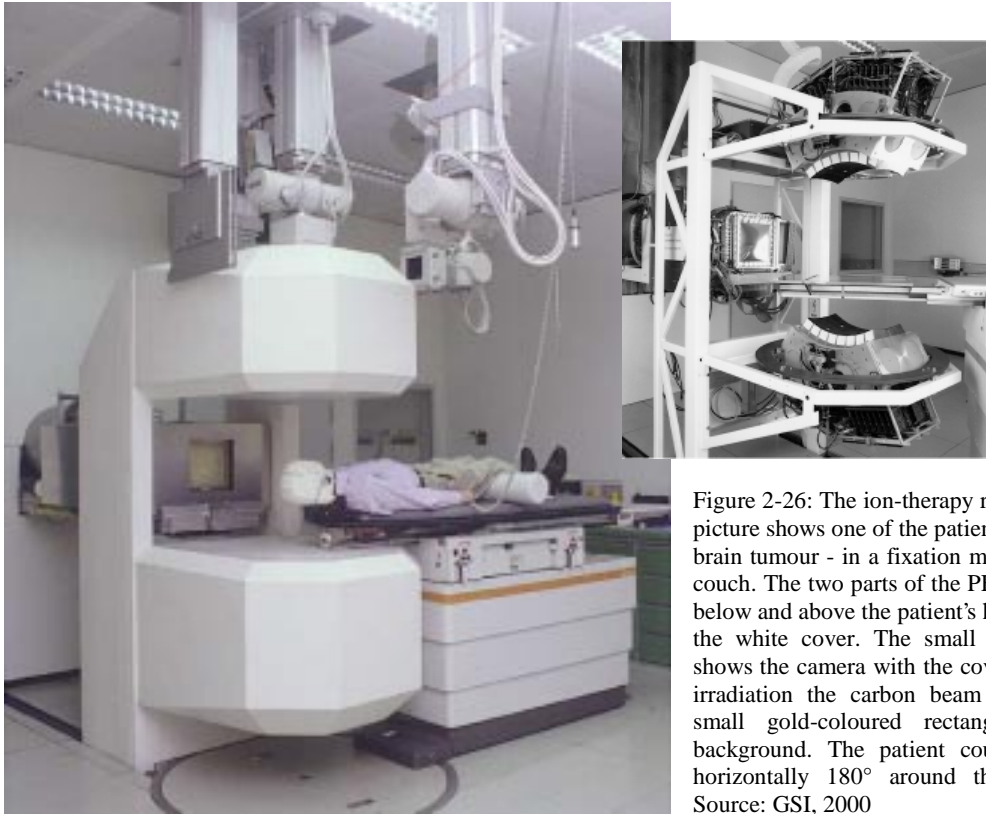


Figure 2-26: The ion-therapy room at the GSI. The picture shows one of the patients - suffering from a brain tumour - in a fixation mask on the treatment couch. The two parts of the PET camera are found below and above the patient's head - hidden behind the white cover. The small image on the right shows the camera with the cover removed. During irradiation the carbon beam enters through the small gold-coloured rectangular area in the background. The patient couch can be rotated horizontally 180° around the incoming beam. Source: GSI, 2000

Till today, about 60 patients have been treated at GSI, and the encouraging clinical results stimulate a rapid planning for a dedicated proton-ion cancer therapy facility at Heidelberg. The treatment level of the proposed centre is illustrated in Figure 2-27 featuring the three treatment rooms, of which two shall be equipped with an ion gantry. Final project approval is expected in 2001 and the first patient treatments are scheduled for 2006 (Eickhoff et al., 2000).

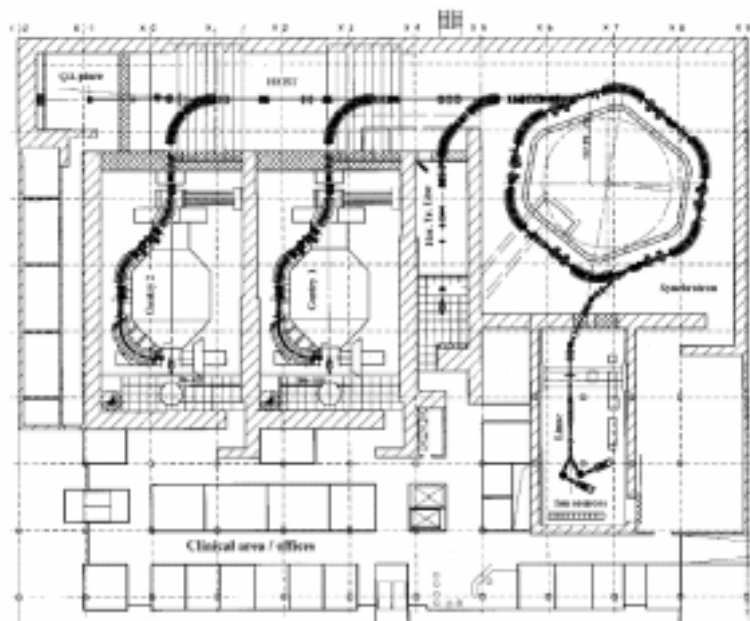


Figure 2-27: Plan of the treatment level of the proposed heavy-ion cancer therapy facility at Heidelberg. Source: Eickhoff et al., 2000

## 2.5 Summary

Comparison of existing proton gantries			
	NCC / NPTC	LLUPTC	PSI
Design and manufacturing	IBA & SHI / IBA & GA	SAIC (Optivus)	Schär Engineering
Type of proton gantry	Isocentric, conventional large-throw gantry	Isocentric, Corkscrew gantry	Eccentric gantry (patient and beam transport)
First operation	1998 / 2001	1991 (Gantry 2 + 3: 1994)	1996
Beam access to patient	4 $\pi$ -irradiation	2 $\pi$ -irradiation	4 $\pi$ -irradiation
Beam delivery	passive beam spreading (prepared for beam wobbling)	passive beam spreading	active spot scanning
Distance dipole exit to isocentre	3 m	3 m	1.1 m
Effective source to axis distance	2.25 m	2.75 m	$\infty$ (parallel scanning)
Maximum field size	$\varnothing$ 26 cm	$\varnothing$ 26 cm	20 cm $\times$ couch movement (max. 50 cm)
Total weight	150 t / 120 t	96 t	110 t
Overall dimensions	$\varnothing$ 9.5 m / 10.9 m long	$\varnothing$ 10.5 m / 4.5 m long	$\varnothing$ 4 m / 11 m long
Maximum gantry rotation	380°	370°	370°
Maximum turning speed	1 rpm	0.75 rpm	1 rpm
Energy consumption	~150 kW		~185 kW
Maximum beam displacement in the isocentre	$\pm$ 1 mm		$\pm$ 0.5 mm

Table 2-1: Comparison of existing proton gantries

## 3 Definition of the Carbon-Ion Gantry

The ion gantry is no standard piece of equipment for which specific medical and beam-optical objectives and constraints could be formulated easily. Instead, specifications are vague and the novelty and complexity of the task requires the careful definition of all "players" involved, parameters to consider, objectives, desired performance, foreseen activities and interdependencies of the various systems. Questions to ask in such a definition phase are: "*Which processes will happen in the future ion gantry facility?*", "*What interrelationships exist in the various technical systems relevant for the design?*" and "*What should be built in order to support best these intended processes?*" Since uncertainty about future operation scenarios is high, one should examine "*What could be needed in the future?*" Answering the above questions in a structured and documented decision-making process - which is the primary objective of this chapter - already involves the investigation of principal systems for the ion gantry. The process (automatically) leads to the definition of specifications as well as to first systematic decisions on the proposed ion gantry.

### 3.1 The Processes to Take Place

#### 3.1.1 People Involved: Objectives, Tasks, Consequences

It is beneficial for the understanding of the process to identify the people involved in the design and operation of the future ion gantry facility. Therefore, this section will very briefly describe their principal tasks as well as their individual expectations and objectives, which might be contradicting sometimes.

##### **Investor**

Even very cautious estimations about the type and the number of future indications suited for treatment with ions in Europe by far exceed the capacity of the few facilities currently planned, hence the market is there (see for example Debus et al., 1998, p. 31). An expanded catchment area would be required if one wants to study particularly seldom tumours.

The objective of a private investor would be to build a novel health-care facility equipped with an ion gantry for therapy that is competitive with other therapies (relative to its merits) and guarantees a certain return of investment. Therefore cost efficiency with respect to facility life-cycle costs and daily operation (cost of staff) is a major objective of the investor. However, the novelty of ion therapy in general and specifically the ion gantry (prototype) suggest to fund parts of the project publicly and establish a world leading research facility ("centre of excellence"), possibly related to a university clinic. This implies that the community of users does not only consist of patients and staff, but also scientists. The number of staff members will be higher compared to a conventional radiotherapy and the facility hosting the ion gantry must provide adequate resources for these people (laboratories, conference rooms, "think cells", etc.); but apart from that the built surrounding should enhance formal and informal communication and therefore stimulate information exchange, the joint development of new knowledge and creativity.

##### **Patient**

The patient is also the customer, who is in this case probably psychologically weak (facing a difficult situation in his life) but physically in a good shape (ambulant treatment). Nevertheless, it has to be expected that a small percentage of the patients will not be able to walk without help and hence be transported on stretchers. Relevant rooms, circulation and waiting areas have to be designed accordingly. During treatment, patients will judge the quality of the treatment by the staff they meet and by the building they see. A holistic view requires the facility not only to fulfil technical specifications but also to mitigate the

patients' fears, encourage their self-confidence, dignity and will to overcome the illness and give them guidance, in order to positively influence their physical health. To support these objectives the whole facility shall provide:

- Simple, understandable and logically arranged procedures (short distances, compact design, transparency, communicative surrounding, information systems etc.)
- A comfortable and reassuring impression (no bunker-like building, daylight, generous room geometry, colours, natural ventilation where possible, discreet access controls and safety measurements, respect of patients privacy etc.)
- A layout favouring personal contact between personnel and patients

#### **Radiation-oncologist**

The medical doctor is responsible for the diagnosis of the tumour and develops - in close co-operation with the medical physicist - the method of treatment, i.e. the *treatment plan* (What dose to be delivered to what region? From what ports?) It is his task to identify and delineate the tumour volume with the help of various diagnostic-imaging techniques (MRI, CT). Although this procedure is standardised (e.g. ICRU Report 62, 1999), it always involves a compromise that relies upon the experience and the judgment of the radiation-oncology team (How much dose can be applied without destroying critical healthy tissue? What safety margins should be considered?). Errors made at that stage persist throughout the whole treatment process. Before treatment, the medical doctor examines the patient, he usually also performs a final check of the patient set-up immediately before irradiation starts.

#### **Medical physicist**

The medical physicist - in close co-operation with the radiation-oncologist - is responsible for the more technical part of the treatment plan by developing an irradiation scheme that results in the desired dose distribution. It is obvious, that the facility layout must facilitate communication between the physicist and the oncologist.

#### **Assistants**

Radio-technical assistants are responsible for the correct set-up of the patient (patient immobilisation, transportation, alignment of patient couch, imaging, etc.)

#### **Accelerator physicist / Engineer**

The engineers are responsible for the operation of the accelerator, the beam lines, the beam delivery system (scanning), and - partly - for the correct alignment of the patient.

### **3.1.2 Patient Flow and Activities**

The patient flow and its related activities represent a *major* basis for planning, hence a detailed description of this process is absolutely necessary. A regular treatment session, i.e. a *fracture*, will see an ambulant patient having himself announced at the reception. The patient waits in the waiting and information area until he is called for treatment. He proceeds to one of the three dressing rooms (Figure 3-1). A sub-waiting area also functions as the waiting area for accompanying persons. Toilet facilities shall be adjacent. The lightly dressed patient will then see the physician in an examination room or directly proceed through a chicane (shielding) into the gantry room where he enters the patient cabin. The patient cabin is the apparent "room" where irradiation is happening. Its atmosphere and enclosure should make a smart impression to the patient.

*Patient immobilisation*

The set-up procedure requires the patient to get immobilised first. This can be achieved by an individualised whole-body mould, or - for the head only - thermoplastic mask or any other type of head holder. X-ray images or a CT scan will be taken for exact localisation of the target volume towards the actual isocentre of the ion beam. Necessary adjustments to the patient's position are applied and a physician performs a final check. The whole patient immobilisation and alignment procedure lasts for about 10 to 20 minutes, the actual irradiation for about 2 minutes. None except from the patient is allowed to be in the gantry room during irradiation, which is supervised by the therapists from the adjacent gantry control room.

*Patient alignment*

*Irradiation*

PET-imaging

Irradiation with carbon ions offers the possibility of monitoring the deposited dose by means of a PET camera, thus offering a unique tool to control the precision of irradiation as well as the treatment plan. The measurement can be done during and/or immediately after irradiation. Principally, such a PET camera could be mounted directly on the gantry or installed in a designated PET room. If the camera is fixed to the gantry and taking the image lasts longer than the irradiation, then the gantry is blocked while the PET image is taken, which results in a reduced patient throughput. Additionally, a clinic facility would certainly have another ion treatment room (probably with a fixed beam) for which the use of the PET would be desirable too. On the other hand, the longer the time between irradiation and PET imaging is, the poorer will be the quality of the image, since the positron emitters migrate in the body and decay rapidly. Additionally, a transfer of the immobilised patient out of the gantry, through the chicane into a PET room immediately after the irradiation seems not very practicable since it could alter the position of the patient with respect to the couch; for the patient this also prolongs the - not very comfortable - state of being immobilised.

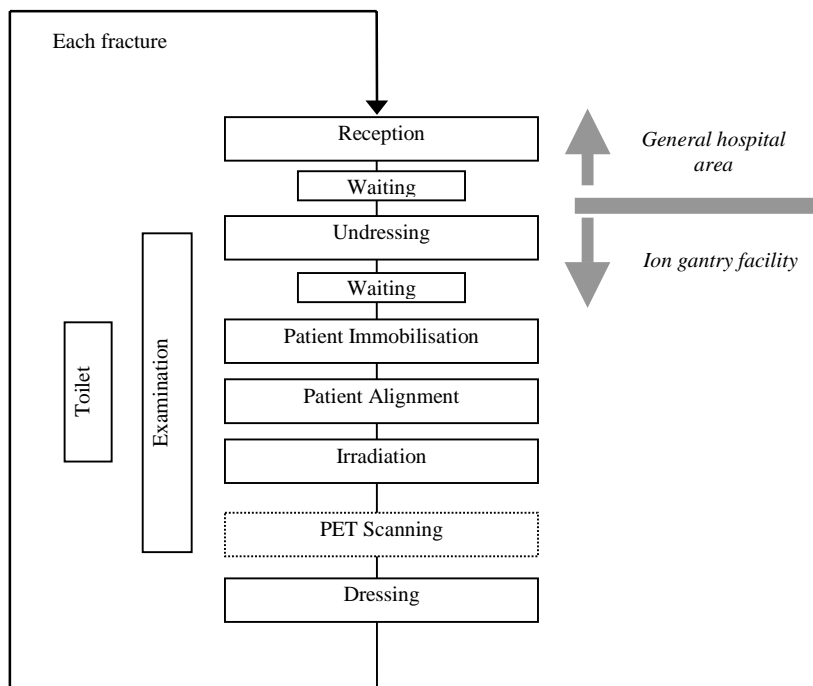


Figure 3-1: The process “fracture” from the patient point of view.

**Automation of the alignment procedure?**

In current proton-therapy practice, more than 50% of the time the patient occupies the gantry room is used for patient alignment (set-up, position check and correction). Automatic comparison between the X-ray images or CT-scans (made for position checking) and a reference image would significantly speed up the treatment and increase the utilisation of the gantry.<sup>11</sup> If somehow the localisation process could be shifted to a separate “preparation room”, the patient occupancy of the gantry room will be reduced even further.<sup>12</sup> In principle, the location of the tumour has to be defined relative to an accurate local reference system (e.g. a patient couch, on which the patient can be fixed in a reproducible way). This system and the actual isocentre of the beam (gantry) must then be related in a coordinative way (mechanical connection, optical recognition, etc).

<sup>11</sup>IBA for example calculated the gantry occupation time in proton therapy for the scenario outlined above to be 12.5 minutes (IBA, 1998).

<sup>12</sup>Compare for example the proposals by Baroni et al (1997) for an automated patient alignment with two preparation rooms per treatment room. However, when it comes to increasingly high throughput rates per treatment room, then limitations by the availability of the accelerator could arise. For instance, in a therapy centre with 5 treatment rooms and a throughput of 4 patients per hour and room, the “window of beam availability” per patient would already be limited to - unrealistic (!) - 3 minutes.

As a consequence, for the design of the ion gantry it has to be foreseen that

- patients walk in, lie down on the couch, and set-up starts,
- patients are carried in on a stretcher, are shifted manually on the couch, and set-up starts,
- the patient set-up takes place outside the gantry hall and the patients are carried in on a specially designed moveable device that can be docked to the gantry (compare the PSI gantry).

### 3.1.3 Material Flow

The only flow of material relevant from a logistical point of view concerns the supply and storage of the immobilisation devices (Figure 3-2) and here in particular the bulky whole-body moulds. For every treatment the right device has to be supplied for the immobilisation of the patient and removed to the storage, after the treatment. Therefore, the immobilisation-device storage room must be as close as possible to the gantry room.

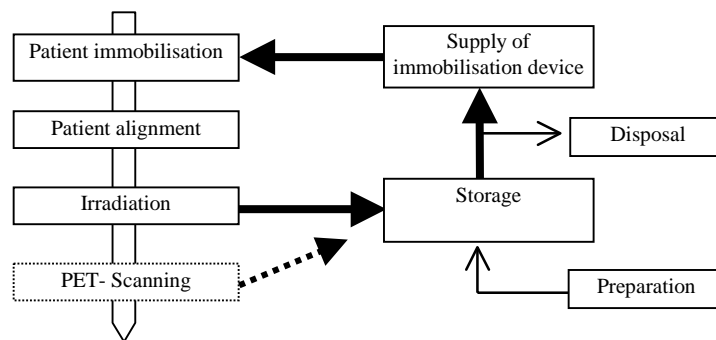


Figure 3-2: The major material flow in the ion gantry facility: supply and storage of the immobilisation devices.

### 3.1.4 Functional Relationship and Space Program

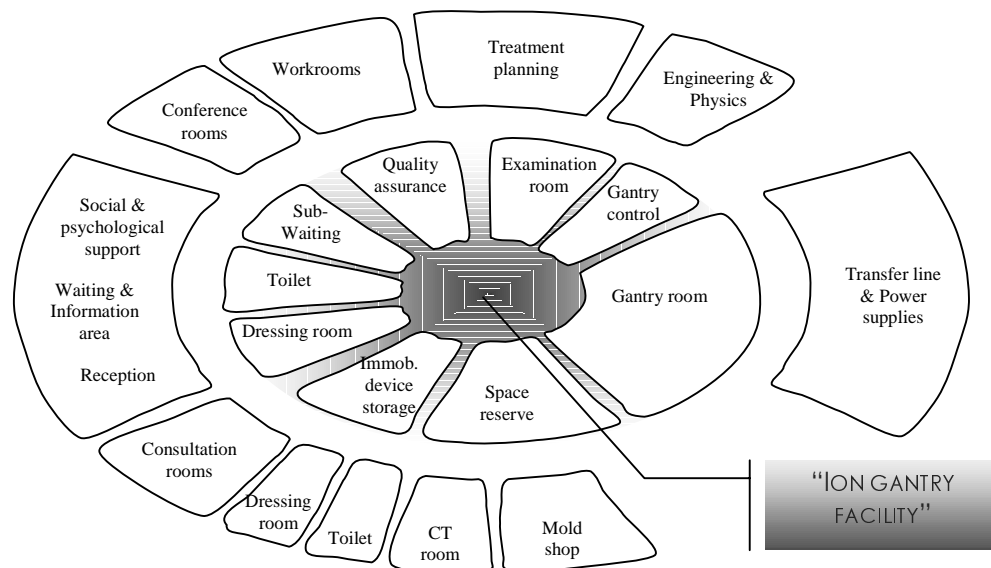


Figure 3-3: The ion gantry facility embedded in an ion-therapy centre. Operation scenarios and various flows (patient, staff, information and material) can be superposed, checked and improved.

Figure 3-3 shows the functional integration of the ion gantry unit into a clinic for ion therapy and represents a sound basis for preliminary architectural planning. Quantity (area) and quality requirements (standards, adjacencies) for every room will be assigned and specified during the design phase of the facility. Special attention has to be paid to the possibility of installing, removing and exchanging the heavy equipment inside the gantry



room. Considerable space for the power supplies of the gantry must be provided in the building housing the transfer line or in a separate room. A space reserve shall be foreseen adjacent to the gantry room in case a PET room, preparation room or re-mobilisation zone is needed in the future. The number of dressing rooms, toilet facilities and the capacity of the storage must be easily adaptable to an increased patient throughput.

## 3.2 Strategic Objectives

In order to focus the efforts, the development of the ion gantry is guided by two strategic objectives: safety and flexibility.

### 3.2.1 Safety

*Accidents related to ionising radiation*

Generally, in radiation therapy safety is one of the crucial issues concerning in particular the human patient since he is

- placed directly in a very intense radiation beam,
- he is intentionally receiving very high doses, and
- not only an overdosage but also an underdosage may have severe consequences for his health.

As a consequence of this, the whole treatment process (involving many professionals participating in a large number of steps) has to be exactly defined, technical systems need to be redundant and regular quality checks have to be foreseen with several levels of intensity.

The technical system of an *ion gantry has to assure that the delivered beam is directed accurately to the cancerous tumour*. This means that the positions of the

- structure(s) towards the building,
- beam transport elements towards the mechanical structure(s),
- patient couch (or patient table) towards the beam transport elements,
- patient towards the patient couch, and
- the position of the tumour inside the patient

is known, controlled (partly redundantly) and adjusted on a regular basis. Obviously, a systems approach for the design of the ion gantry is necessary.

In order to protect the personnel from radiation, the ion gantry design - and here in particular the design of the building - has to respect the various codes of radiation protection. The principal consequence is that the (concrete) walls of the building have to be sufficiently thick to reduce the radiation level originating from the treatment inside to a level that is safe for the personnel and the public outside.

*Accidents related to the mechanics and the building*

A more common aspect of safety is related to the mechanical (probably kinematic) structure of the gantry and the fact that this gantry is installed in a shielded and therefore not easily accessible room. Possible accidents might be due to collisions between humans and moving technical equipment and due to fire, however, such types of accident are not specific to radiation therapy and the common standards for hazard prevention can be applied. Again the person most likely to be victim of such a kind of accident is the patient - in particular when he has been prepared for irradiation and hence is immobilised. The following guidelines have to be considered in the gantry design:

- In case of a (technical) emergency, the patient must have the possibility to re-mobilise himself.
- In case of a medical emergency access to the patient must always be possible within a time not considerably longer than in conventional therapy.
- Patient and personnel present in the gantry must be able to leave the room without having to rely on sophisticated mechanical equipment.

*The way to achieve safety: simplicity, operability and maintainability.*

Usually, conventional radiotherapy involves several sessions, in each of which several parameters have to be set correctly in order to avoid any accidents. This is equally true for ion therapy. In addition, its technology is certainly on the upper limit of what is feasible. As a consequence of this and of the above said, the design of the ion gantry should hence (as far as possible) be *simple in order to keep the complexity of the whole system as low as possible* (or pessimistically spoken: under control). One has to remember that the ion gantry will be operated in a hospital environment and run by physicians and not engineers or scientists. This calls for reliable and not over-engineered solutions, which are understandable and easy to handle for the staff in order to avoid operational errors. A cautious and conservative approach to new technical developments is mandatory due to safety reasons.

### 3.2.2 Flexibility

Continuously, clinical experience and research results as well as new technical developments will have to be incorporated into the design of the ion gantry as well as in the operation once the ion gantry is built. Usually, this uncertainty makes it difficult to set reasonable specifications for the development, since the less is known the more people tend to specify that they need everything and the design becomes not feasible or not competitive. It is therefore necessary to design an open system and *prefer solutions that offer a maximum of flexibility*. Certainly, unavoidable constraints have to be identified and communicated to all persons participating in the design process.

## 3.3 Beam Optics

### General Remarks

The development of the beam-optical concept for a proton-ion therapy facility including an ion gantry was done - parallel to the first engineering studies of the ion gantry - under the framework of the Proton-Ion Medical Machine Study (PIMMS) hosted by CERN (Bryant et al., 2000). Although this section will present the final status - being in ideal harmony with the final design of the ion gantry - beam-optical constraints were not always so clear during the present work but evolved continuously. In addition, when investigating variants for an ion gantry, some fundamental questions are strongly related to ion-optical solutions, in particular the systematic interdependencies between

- type of scanning system chosen,
- type, weight and size of the bending magnet to deflect the beam onto the patient, and
- movements that have to be performed by the gantry and the patient positioning system (PPS).

A short, but not at all exhaustive, introduction to these relationships will be given in this section. Since the final layout of the beam transport system corresponds to a specific type of ion gantry, this will be presented in the design chapter (Section 5.5.1).

### 3.3.1 The Accelerator

The primary objective of PIMMS was to present a design of a facility that would allow the direct clinical comparison of protons and carbon ions for cancer therapy using high-precision active scanning. As a secondary aim, the facility should also be capable of delivering proton beams by passive beam spreading. For these tasks a synchrotron using a slow extraction was chosen, which offers the flexibility needed for dual-species operation and the variable energy needed for active scanning. The principal design requirement was that of a smooth particle spill, but as much emphasis as possible was given to reliability and simplicity of operation. The principal parameters of the proposed machine are listed in Table 3-1.

### PIMMS performance parameters for active scanning (pencil beam) with carbon ions

Extraction energies for carbon ions	120-400 MeV/u
Beam distributions	Gaussian in direction perpendicular to scan, near-rectangular in scan direction
Nominal treatment times with carbon ions	60 spills in 2.4 min
Nominal dose delivered	2 Gray in 2 litres
Number of carbon ions in one spill at patient	$4 \times 10^8$
Start of spill can be triggered for synchronisation of breathing	Yes
Spot size variation at all energies (FWHM)	4-10 mm
Energy levels	The number of energy steps is limited only by the control system

Table 3-1: Performance parameters relevant for carbon-ion treatment of the accelerator proposed by the Proton-Ion Medical Machine Study (PIMMS). Source: Bryant et al., 2000, p. 2

### 3.3.2 Rotator

Before the ion beam arrives at the gantry it passes a so-called rotator. This is a 10 m long string of quadrupoles that is turned around the beam axis by half of the angle of the gantry. It has the effect of making the beam optics of the gantry-based delivery system (scanning system) completely independent of the gantry rotation (by rotating the phase spaces to match the gantry angle). The theory is covered in Volume I Sections 8.5 and 8.6 of the study (Bryant et al., 2000).

### 3.3.3 Beam Scanning

The principle of scanning is to divide the arbitrarily shaped tumour into small volume elements (mm-region) and irradiate each of those elements separately using a pencil-shaped beam.<sup>13</sup> No patient-specific hardware is necessary (except from the immobilisation device) allowing multiple-field treatment in one single session without intervention of the personnel. The ion beam has to be directed actively and very rapidly over the tumour volume, requiring *three degrees of freedom*:

- The entrance depth is varied by *energy variation done by the synchrotron* every cycle (~2.4 s). This represents the slowest dimension of motion. The tumour will be irradiated slice by slice starting with the most distant one (iso-energy slices).
- A *scanning magnet*, i.e. a small dipole, performs the fastest movement.
- The remaining third dimension should direct the beam over the whole diameter of an (iso-energy) slice within a cycle of the synchrotron. Performing this movement continuously would require a minimum speed of ~20 cm/s at the tumour (Figure 3-4, left). This rules out the use of the patient couch for this dimension of freedom, but possibly small rotations of the dipole around the gantry axis could perform this task. However, one would also have to rotate the rotator and the gantry quadrupoles synchronously, which seems unpractical. For safety reasons it is also desirable *not* to perform any mechanical motions in the system *during* irradiation. In addition, with the very inhomogeneous irradiation patterns expected for a tumour slice, such a procedure would suffer from considerable dead times, since it is not possible to quickly skip some lines in the irradiation pattern of an iso-energy slice. Therefore, stepwise movement for the third dimension is preferred. In case the beam is not switched off during movement the required velocity for both scanning directions should be the same (Figure 3-4, right).

<sup>13</sup> Passive spreading is not proposed for carbon ions because (a) to get sufficiently large scattering angles the losses would be high and the particle intensity from the accelerator is too low, (b) the scattering causes fragmentation and neutron background, (c) this would ignore one of the principal advantages of carbon ions, that is the small, high-precision beam spots preserved by the low scattering.

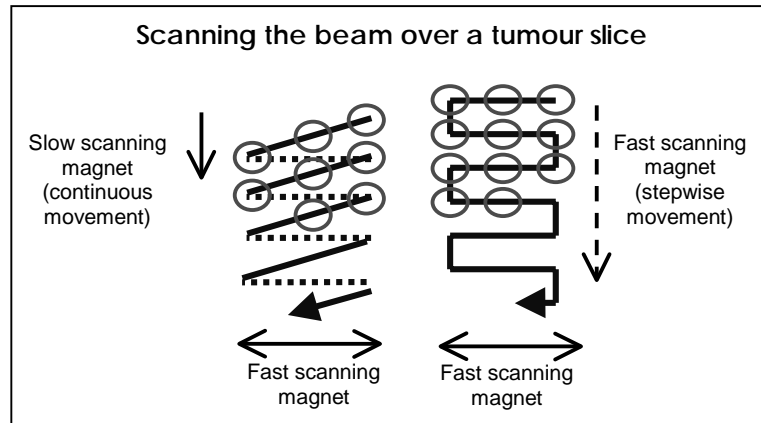


Figure 3-4: Impact of the scanning method on the necessary performance of the scanning magnets.

Summarising the considerations above, the active energy variation by the synchrotron suggests to use (fast) scanning magnets for steering the beam in the two transversal dimensions. Substituting one scanning dimension by movements of the whole gantry structure, the dipole or the PPS seems not reasonable.<sup>14</sup> Flexibility in treatment planning and shorter irradiation times favour similar scanning velocities for both dimensions.

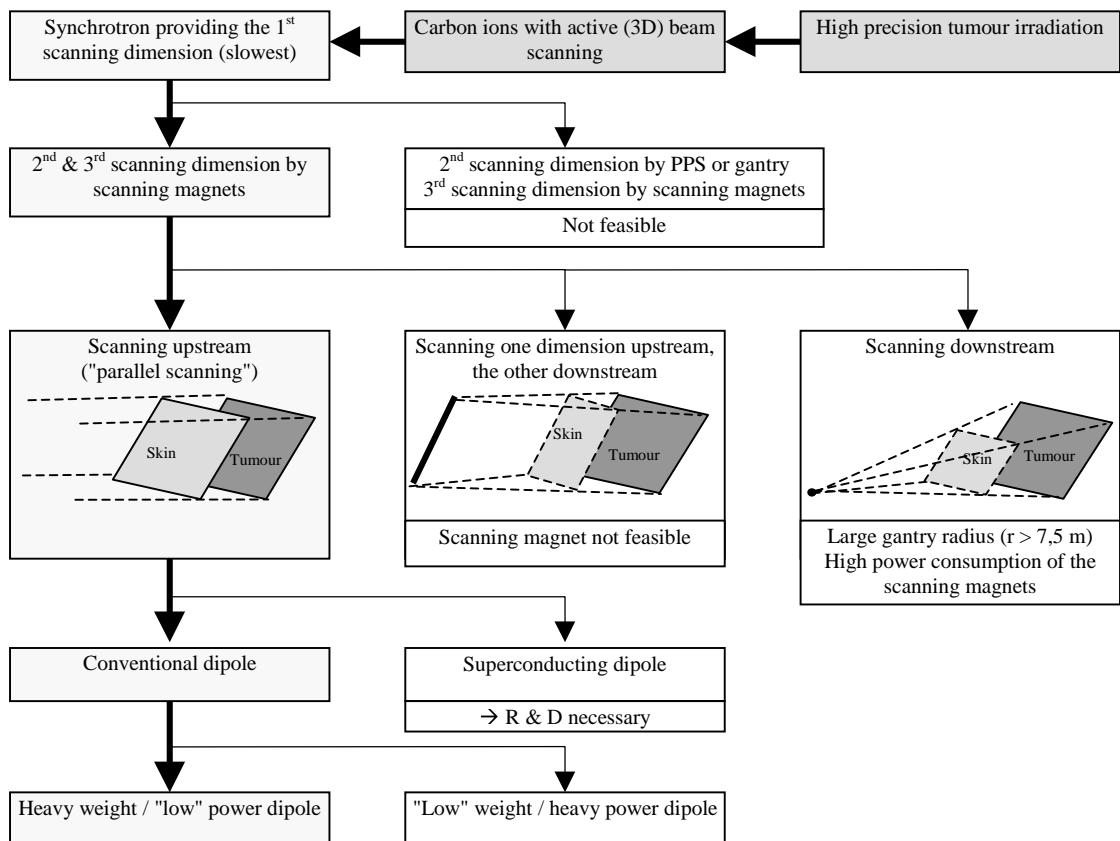


Figure 3-5: Decision making process concerning beam optics relevant for the ion gantry.

Generally, an ion gantry - no matter what type will finally be chosen - needs to bend the particle beam by approximately 90° towards the patient with the help of one or several bending magnets (dipoles). The size and weight of such a magnet depend largely on the

<sup>14</sup> The proton gantry at the Paul Scherrer Institut (PSI) uses a fast range shifter for energy variation, which is mounted in the nozzle. Velocity is high enough to cater for the second scanning dimension, consequently the slowest motion can be performed by the PPS.

beam optics but represent a crucial input parameter for the gantry design. Figure 3-5 summarises very briefly the theoretically possible decision paths - each of them leading to a special characteristic of that final bending magnet.

As it is indicated, the scanning magnets could in principal be placed before (upstream) or after this last bending dipole (downstream). With the scanning magnets upstream of the main dipole the gantry radius is minimised but therefore it is necessary to construct the dipole with an aperture approximately equal to the area to be scanned. This large aperture is required more or less over the complete length of the magnet, hence driving its weight to something between 40 t and 80 t having a power consumption of approximately 700 kW and 300 kW respectively. Downstream scanning would be a nice alternative since the gap of the dipole could be reduced to a few centimetres only (in both directions), weight and power consumption would be low. Unfortunately, this would result in a - probably prohibitive - increase in the gantry radius in order to

- limit the necessary beam divergence and thus the power of the scanning magnets to a reasonable value,
- maintain an acceptable source-to-axis distance (SAD).

The tempting "compromise" of placing only one scanning dimension downstream is even more unsuited, since the downstream scanner would need to provide its tough performance over an already largely spread (scanned) beam.

### 3.3.4 The Last Dipole

With carbon ions, it is not possible to put the scanning magnets after the main dipole and maintain a reasonable radius for the gantry. Therefore, the scanning magnets are positioned just before the main dipole and the main dipole itself has a large aperture.

Regarding a conventional, i.e. non-superconducting dipole, its developed magnetic flux density (magnetic induction  $B$ ) for an applied magnetic intensity can be seen as being composed of two components:

- The original part due to the powered coils
- An additional part due to the facilitating ("field supporting") effect of a ferrous core.

The power consumption of a dipole is proportional to its magnetic reluctance. This reluctance can be reduced by decreasing the gap of the magnet, which is impossible in our case, or by improving the magnetic permeability of the iron core. The latter is done on one hand by keeping the required magnetic flux well below saturation of the iron core<sup>15</sup> – say 1.8 T – and on the other hand by providing a large cross-sectional area of the iron core. Certainly, both these measures have adverse effects on the gantry structure, as the radius and the weight of the magnets are increased respectively. In the case of our large aperture dipole, the principal variables are power consumption and weight, which show a relationship that is indirect proportional. This means that the power to drive the magnet can be reduced - to a certain degree - by placing more iron on the magnet.

The final design for the 90° dipole as foreseen by PIMMS represents a "low" power / heavy weight approach (62 t, 364 kW), its principal parameters are listed in Table 3-2, the geometry can be seen in Figure 3-6. Although these exact values were only available towards the end of the present study, similar data was used from the beginning and actualised regularly.

In contrast to the PIMMS design one has to see for example the first proposal for the German ion-therapy facility made by Kalimov und Wollnik suggesting a 2.0 T, 40 t, 720 kW dipole providing a similar good-field region of 20 cm × 20 cm (Kalimov et al., 1998, p. 512). Such a high power magnet would certainly increase the demand on the cooling system of the dipole and the ventilation of the gantry hall in order to avoid any excessive temperature-related deformations affecting the dipole, the gantry structure and hence the

<sup>15</sup> As long as the iron core is unsaturated, its permeability is manifold the one of free space, when saturation commences the permeability decreases continuously to meet the value of free space asymptotically.

precision of the treatment adversely. A more recent version of the dipole shows characteristic values of 68 t and 660 kW (Spiller et al., 1999).

**Principal parameters of the main dipole**

Yoke length along central orbit [m]	5.5400
Bending radius on central orbit [m]	3.5269
Overall width of cross-section [m]	1.5300
Overall height of yoke [m]	1.0700
Overall height with coil at end [m]	1.4460
Gap height on central orbit [m]	0.2080
Weight [t]	62
Nominal maximum field [T]	1.8
Current for maximum field [A]	4370
"Good-field" region (all field levels) [mm]	±100 horizontal; ±90 vertical
Field quality, $\Delta B/B$ (all field levels)	At least $\pm 2 \times 10^{-4}$
Resistance (magnet) [ $\Omega$ ]	0.019
Maximum power dissipation [kW]	364

Table 3-2: Principal parameters for the 90° main dipole of the ion gantry designed by PIMMS. Note the modifications proposed in Section 5.7.4. Source: Bryant et al., 2000, p. 299

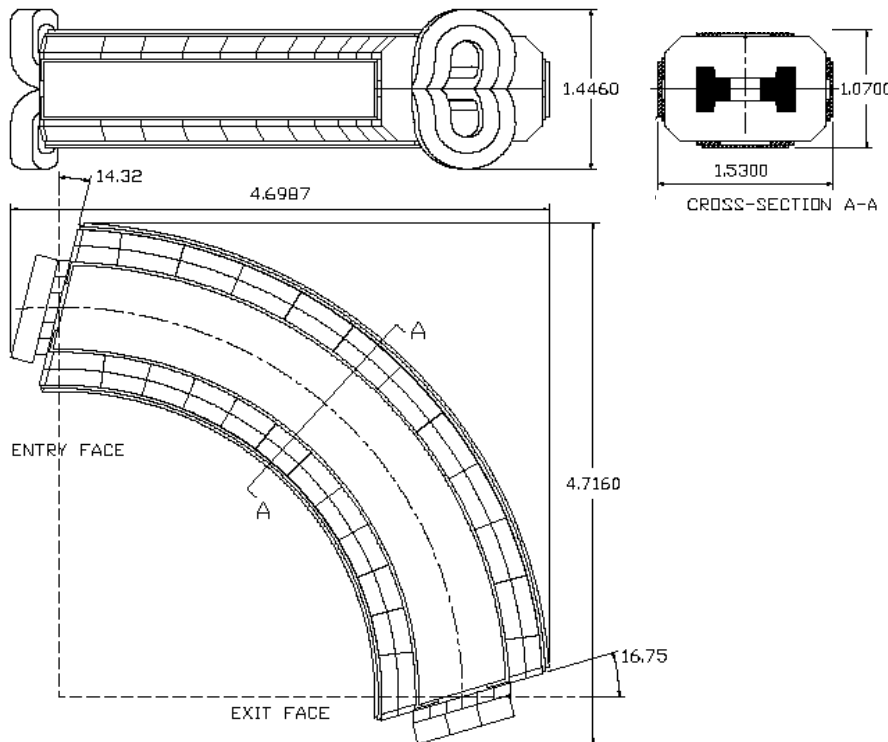


Figure 3-6: The 90° dipole of the ion gantry as designed by PIMMS. Dimensions are in metres. The yoke is split into two halves, each of them split into segments. Source: Bryant et al. 2000, p. 300

**Superconducting dipole?**

Superconductivity (SC) offers the possibility of reducing the radius and in particular the weight of the large bending magnet; a more compact and light gantry design would be feasible. Proposals in that direction were - among others - done by Vorobiev et al. (1997) suggesting an isocentric gantry (gantry radius about 3 m) equipped with a SC-beam delivery system. However, even if the technology of rotating a SC-magnet were available, a lot of development for the intended use of SC-magnets in the gantry would be necessary, addressing in particular the following crucial questions:

- Which amount of iron is needed to avoid harmful magnetic stray fields acting on the beam monitoring equipment, the scanning magnets and the patient? Does this jeopardise the original saving in weight?

*An ion gantry with SC magnets would need additional research and development.*

- Quenching of a SC-magnet, i.e. the sudden transition from superconductivity to normal conductivity, may happen accompanied by a rapid, explosion-like expansion of the liquid helium. What effects does such an event have on the close patient and the accuracy of the system?

A compromise could be the use of a dipole with a "warm" iron core (in order to avoid any long-distance stray fields) plus superconducting coils (Vorobiev et al., 1998).

Regarding the strategic objective of safety (including reliability and operability), it has to be said that the use of SC-magnets and their complicated cooling system would add a critical technology to the already complex system of an ion gantry and should therefore be avoided in the design. Nevertheless, the question of using SC-dipoles could become interesting again in a few years time.

### 3.4 Treatment Precision

The precision of the treatment is affected by various systematic and random errors due to

- the imaging systems, diagnostics and the ongoing treatment planning (see Leunens et al., 1993),
- the patient himself (e.g. organ movements due to respiration),
- the beam generation and the beam optics as well as the lateral scattering and fragmentation of the ion beam,
- the patient positioning system (PPS) including the patient couch and the immobilisation of the patient (see Sweeney et al., 1998), and
- the mechanical gantry structure.

This study deals mainly with the last two items, however, it is essential to always keep in mind the whole system and the relative contribution of each part in order to identify the most suited areas of improvement.

The mechanical gantry structure, the PPS and the beam optics are highly coupled sub-systems. Jointly they are responsible for delivering the beam to the patient with a desired accuracy, which is frequently stated to be - rather imprecisely - "sub-millimetric" for ion therapy.

There is, of course, the principal possibility that one of the sub-systems involved corrects errors made by the others. For example, the PPS or additional correction magnets can be used to compensate deformations of the structure. Errors like that are called *systematic*, since they are reproducible, which distinguishes them from so-called *random* errors. These errors are statistically distributed errors (e.g. backlash) and any envisaged correction mechanism for random errors would require some on-line feedback system during irradiation. However, excessive use of correction algorithms and devices will considerably *increase the complexity* of the system, make it more difficult to operate and in particular prolong the installation and testing procedures, which can easily take some years (compare the history of the NPTC). Such an increased "time-to-market" would act as a deterrent for private investors. *Therefore, having the objective of simplicity, operability and reliability in mind, an as high as possible initial accuracy and rigidity of the mechanical gantry structure shall be achieved.* Even if this does not completely avoid any correction action, it simplifies them considerably. As a first target value one should try to restrict elastic deformations of the gantry structure along the beam line to a value well below 0.5 mm.

*The precision is determined by several sub-systems, each of them affecting the remaining error budget for the others*

*A high mechanical rigidity of the gantry reduces complexity*

### 3.5 Specifications

The technical specifications presented in Table 3-3 are the result of the previous chapters and the strategic objectives. They represent a basis for the development of the ion gantry

and not necessarily a "must". The rationale for some items involves complex interdependent systems and it is logical that these issues are a frequent matter of discussion among experts.

### Specifications for the ion gantry

<i>Patient position</i>	Supine to restrict organ movements to a minimum.	<i>Supine</i>
<i>Irradiation sites</i>	It has to be assumed that treated indications will comprise all regions of the human body.	<i>All regions</i>
<i>Treatment time</i>	The time to deliver a usual fraction of about 2 Gray is 2 - 3 minutes. Up to 30 fractions comprise a treatment.	<i>Max. 30 fractions à 2-3 min.</i>
<i>Treatment angles</i>	The author found no large-scale statistics about treatment angles actually used in routine clinical operation. Full $4\pi$ -irradiation to a patient in a supine position is the optimum to achieve (gaining a maximum of flexibility). Limiting the available gantry angles to small discrete steps (say a few degrees) seems acceptable. Limiting or even blocking the rotation of the patient positioning system (PPS) around the vertical axis (corresponding to a transformation from $4\pi$ to $2\pi$ -irradiation) would result in a slight reduction of the overall gantry-dimensions and the complexity of the PPS only.	<i><math>4\pi</math>-irradiation</i>
<i>Field size</i>	No medical studies about the statistical distribution of field sizes in radiotherapy were found. Quadratic field sizes are preferred to rectangular ones for flexibility reasons, since the former do not de-favour particular gantry positions. The maximum extension of a tumour can be as large as 40 cm. From the medical point of view minimal field sizes of $25 \times 25 \text{ cm}^2$ are desirable. However, it is expected that this parameter will have a <i>decisive</i> impact on the design, the overall dimensions and the cost of an ion gantry. When demanding large field sizes one clearly has to realise that this specification could <i>endanger</i> the financial and technical feasibility of the ion gantry. Therefore, economically reasonable values will be in the region of $15 \times 15 \text{ cm}^2$ to $20 \times 20 \text{ cm}^2$ . For those tumours where the field size is not sufficient, techniques of combining several fields could be developed.	<i><math>&gt; 15 \times 15 \text{ cm}^2</math></i>
<i>SAD (source to axis distance)</i>	Considering a point source of the beam, a decrease in the effective SAD leads to an over-proportional increase of the relative dose on the patient surface (skin); the skin dose to target dose ratio decreases with an SAD-increase, making a large SAD desirable. Usually, an effective SAD larger than 2 m is considered as acceptable, but 3 m are highly preferred. <sup>16</sup> (see for example Tosi et al., 1994)	<i>Effective SAD <math>\geq 3 \text{ m}</math></i>
<i>Beam delivery system</i>	Precise conformal tumour treatment offering maximum flexibility in treatment planning requires the ion beam to be actively directed ("scanned") over the arbitrarily shaped target area.	<i>(Active) Scanning</i>
<i>Beam rigidity</i>	Reaching deep-seated tumours requires the carbon beam to have a beam rigidity of about 6,3 Tm (corresponding to a penetration depth of 27 cm in water). A normal conducting bending magnet having a magnetic field of 1,8 T would need to have a radius of 3.5 m.	<i><math>\sim 6,3 \text{ Tm}</math></i>
<i>Positioning accuracy</i>	It is assumed that the ion gantry is used primarily for high precision irradiation requiring sub-millimetre accuracy (e.g. brain tumours).	<i>Tolerance: <math>\pm 0,5 \text{ mm}</math></i>
<i>PET</i>	The ion gantry should be capable of supporting intensive use of PET imaging.	<i>PET compatible</i>

Table 3-3: Medical and beam optical specifications for the ion gantry.

## 3.6 Gantry Structure Considerations

The choice of the type of gantry is not a straightforward one but governed by an optimisation process involving mechanics, beam optics and beam delivery, medical aspects, safety considerations and cost. Principal possibilities how to translate the idea of an ion gantry into a mechanical structure are shown in Figure 3-7 and will be explained in the following sub-sections.

Certainly, one can find many other - more or less different - gantry solutions in the literature, however they usually refer to protons only. A nice compilation can be found in Eros Pedroni's Como paper (1994, p. 445).

<sup>16</sup> In the extreme case of having 30 cm between the irradiated slice of the tumour and the skin, a 2 m and 3 m effective SAD is responsible for a relative (!) dose increase on the skin of 39 % and 23 % respectively.



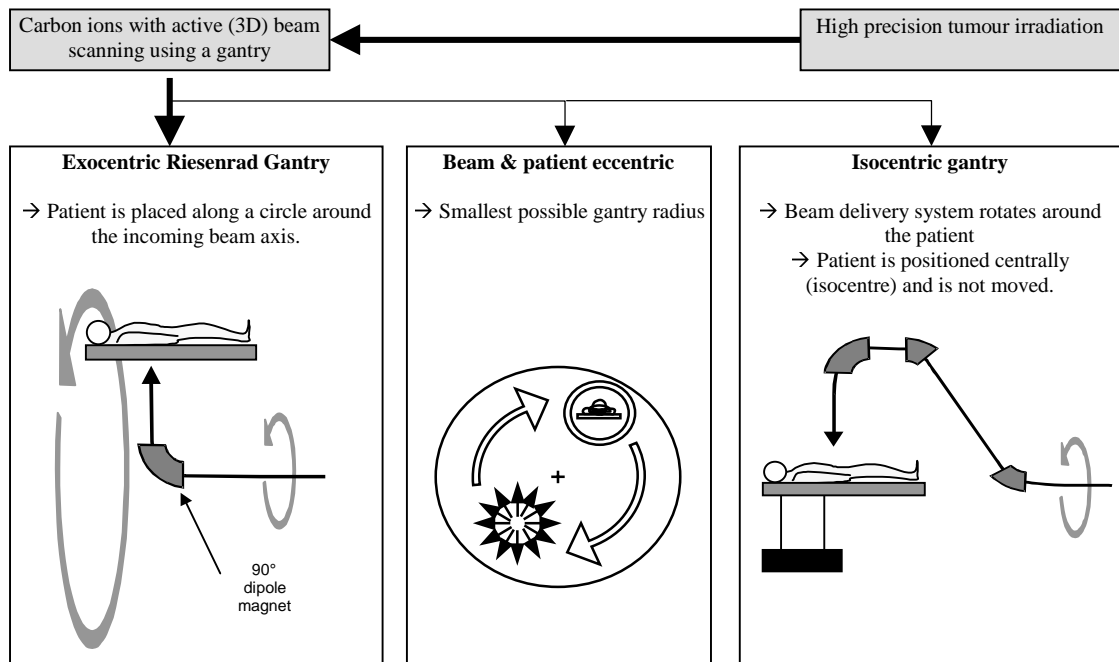


Figure 3-7 highlights the principal possibilities for an ion gantry (seen from a structural point of view).

### 3.6.1 Isocentric Ion Gantry Solutions

Gantry systems where the patient is placed in the centre of the machine are called isocentric gantries. All the proton gantries except from the one at the Paul Scherrer Institut (PSI) have so far been based on this approach. The PPS is mounted for instance on the floor of the building and cantilevers into the gantry. The incoming beam is guided away from the axis and eventually bent down towards the patient. The whole delivery system rotates around the (iso-) centre. A special version of this is the corkscrew gantry (as applied in the Loma-Linda proton gantries), where the beam is bent not only in one, but also in two planes, giving a shorter construction length. However, about 315° of the total necessary 360° of the heavy bending magnets have to be mounted eccentrically, therefore not favouring an efficient structural solution in the case of carbon ions.

The construction of a conventional gantry for ions would imply to have an - at least - 15 m long (depth) mechanical structure to accommodate the necessary beam transport elements. A desirable structurally determinate support on two bearings generates large bending moments. To avoid excessive flexure the structure would reasonably be some kind of heavy cylindrical ("barrel type") or conical shell structure or space frame, also capable of transferring large torsion forces. A critical part would be the design of the front ring, which has to carry most of the load coming from the final dipole and the counterweight; its diameter has to allow access for the patient and the PPS, thus restricting propping of the ring to perimeter regions. Forces will have to be carried by bending, resulting in large deformations or very heavy dimensions of the ring (to gain the necessary stiffness). A solution to this problem could be to cantilever out the final heavy dipole from the bearing ring, as it is shown at the PSI-gantry, thus the bearing ring could be made more solid.

Detailed ion-optical studies for an isocentric ion gantry were performed in the framework of the proposed German ion-therapy facility in Heidelberg (see Vorobiev et al., 1998). The ion optical concept was called "short-barrel" version and said to be the "most space-saving concept for isocentric single-plane gantries" (p. 4). It is shown in Figure 3-8. The gantry radius was estimated to be 5 m (including a 1.4 m free drift between last dipole and the patient), the length of the off-axis part of the gantry was supposed to be 14.5 m.

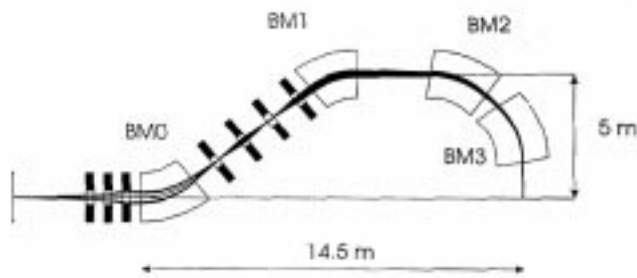


Figure 3-8: Beam optics layout of the isocentric ion gantry (called "short-barrel") foreseen for the German ion-therapy facility. The beam scanning is done upstream of the final 90° bend. Source: Vorobiev et al., 1998, p. 13

*An isocentric carbon-ion gantry: 675 t; required volume of the gantry hall  $\approx 6400 \text{ m}^3$*

Towards the end of the present study (August 2000), first solutions for the mechanical realisation of the above ion-optical concept appeared (Spiller et al., 2000) proposing a box girder solution somehow similar to the proton gantry at the PSI (see Figure 3-9). However, tribute has to be paid to the large dimensions and heavy loads: the total weight of the gantry is estimated to be 675 t, of which 460 t alone rest on the front ring, which is supported by 12 rollers. The required dimensions for the gantry hall are about 25 m × 15 m × 17 m (height). Maximum elastic deformation along the beam axis is around 0.3 mm. The design is already close to the point where - due to the domination of the dead load - any additional material thickness does not lead to any reduction in elastic deformation. An innovative idea is the use of the counterweight for shielding purposes, hence reducing the necessary thickness of the building walls accordingly.

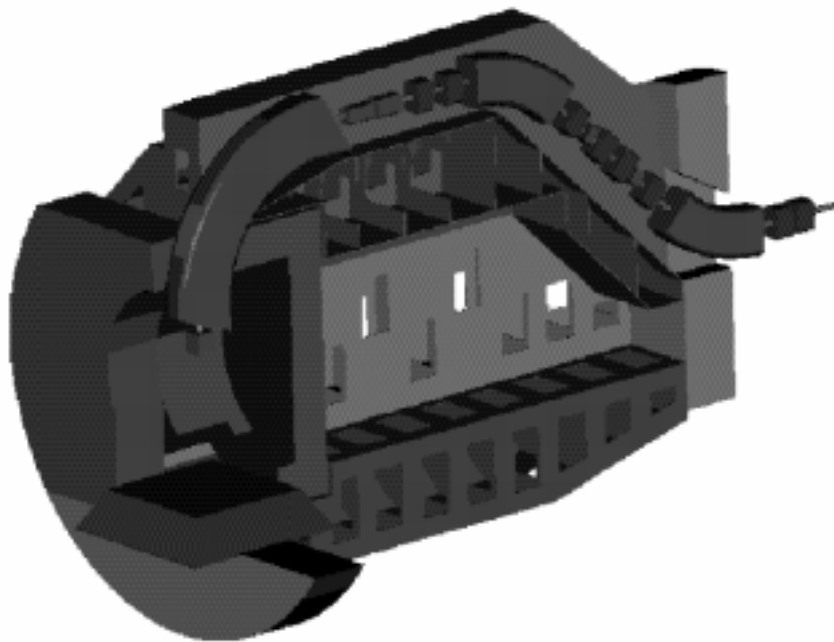


Figure 3-9: Proposed structural design of the carbon-ion gantry for the planned German ion-therapy facility in Heidelberg. Source: Spiller et al., 2000

A proposal on how to reduce the overall diameter of an ion gantry while still keeping the attractive isocentric patient position was made by Pavlovic (1999). He suggested to reduce the final bending of the beam from 90° to 60°, since it is the remaining 30° that contribute massively (about 1.75 m) to the gantry radius. Such an "oblique gantry" would allow a gantry radius of about 3 m. The price one has to pay for this is the impossibility to cover all treatment angles, in particular no top or bottom irradiation is feasible. Relief could be afforded by a complementary treatment chair to cover the rest of the angles (Figure 3-10). Another possibility to ameliorate the situation would be to introduce some pitch and roll in the patient couch. Nevertheless, flexibility with such a type of gantry would be limited. In addition, the relationship between treatment angle and corresponding gantry and PPS position is not straightforward anymore but fairly complicated, which could make it more difficult for the personnel to perform visual position checks.

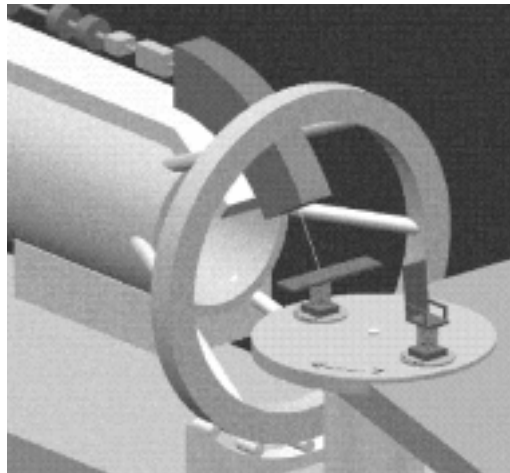


Figure 3-10: 3D-view of the bend-down shoulder of the 60° "oblique gantry" with a special patient positioning system allowing to irradiate the patient either in supine or sitting position.

### 3.6.2 Ion Gantry Solutions with Patient and Beam Eccentric

A possibility to achieve a moderate radius of an ion gantry is to have the beam delivery system *and (!)* the patient eccentric with respect to the axis of gantry rotation, as it was done at the proton gantry at the PSI. Compared to a conventional gantry the structural complexity would rise, since a second axis of rotation (patient axis) has to be introduced, while the required amount of beam bending remains more or less unchanged. Therefore, this solution would show its power when space is very restricted.

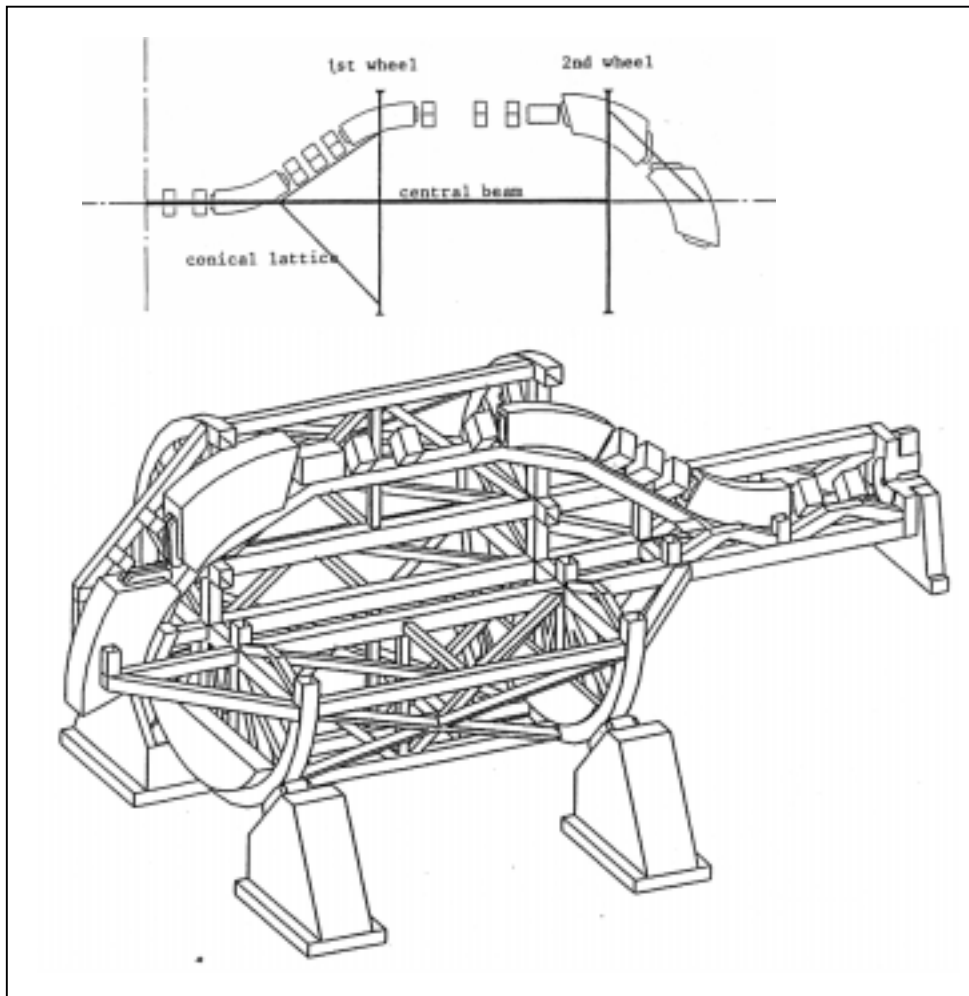


Figure 3-11: Scheme of the gantry optics and 3D-view (with one quarter of the structure cut-off) of the proposed eccentric ion gantry for EULIMA. Total weight is about 145 t, mechanical deformations of the isocentre are calculated to be within a sphere of 0.7 mm. Source: Rocher et al., 1991

Nevertheless, a preliminary structural design for such a type of ion gantry was done in the framework of the EULIMA (European Light Ion Medical Accelerator) study in the early 90s (see Rocher et al., 1991). Bending magnets were assumed to be of conventional type (Figure 3-11, top), the final 90° bend (separated in two dipoles) accounted for about 46 t, the counterweight for 18 t. The proposed cylindrical gantry structure (Figure 3-11, bottom) consists of two large wheels of 7.5 m in diameter, 7.75 m apart and trussed by a set of beams in order to form a stiff and rigid lying cylinder.

Along the centre line spans a trussed girder (1.4 m × 1.4 m) that continues 7.75 m beyond the rear wheel, thus supporting the first quadrupoles and the first small dipole of the gantry. A conical lattice is used to increase the rigidity of the connection between cylinder and central beam, giving the whole gantry the shape of a lying bottle. The last dipole is supported by a set of triangles cantilevering from the front ring. The whole structure is modelled out of rectangular hollow sections (RHS beams) having cross-sections up to 400 mm × 400 mm. The dead load was calculated to be 55 t, total weight 145 t. Reaction forces on the front ring turned out to be approximately 900 kN (vertically). The structural analysis showed that stresses in the members would not exceed 50 N/mm<sup>2</sup>. The maximum deformation always occurred at the isocentre; during rotation this point performed movements that were within a sphere of radius 0.7 mm from its starting point. Maximum absolute deformations were about 1 mm from the ideal (unloaded) position.

The authors of that study also investigated a more conical type of gantry, consisting of two rings with different diameter and more close to each other, leading to similar results. Contrarily, the attempt to substitute these two rings by a single one, resulted in excessive deformations and the version was abandoned.

Finally, it has to be said that the design does not give any suggestion on where and how to fix the patient couch to the structure and on how to guarantee satisfyingly a continuous access to the patient.

### 3.6.3 Exocentric Riesenrad Gantries

The principle of the Riesenrad<sup>17</sup> gantry allows a remarkable simplification<sup>17</sup> of the beam delivery system compared to the conventional gantries. In the Riesenrad, the 90° bending magnet terminating the transfer line is placed on the axis of gantry rotation that coincides with the axis of the incoming beam. The magnet is rotated around the incoming beam axis and can be set to any angle. The beam deflection will correspond to the magnet angle. The patient must be in this case placed *eccentrically* in a special cabin that follows the magnet rotation.

*The Riesenrad approach minimises the moment of inertia, hence the total weight and the maximum deformation of a gantry.*

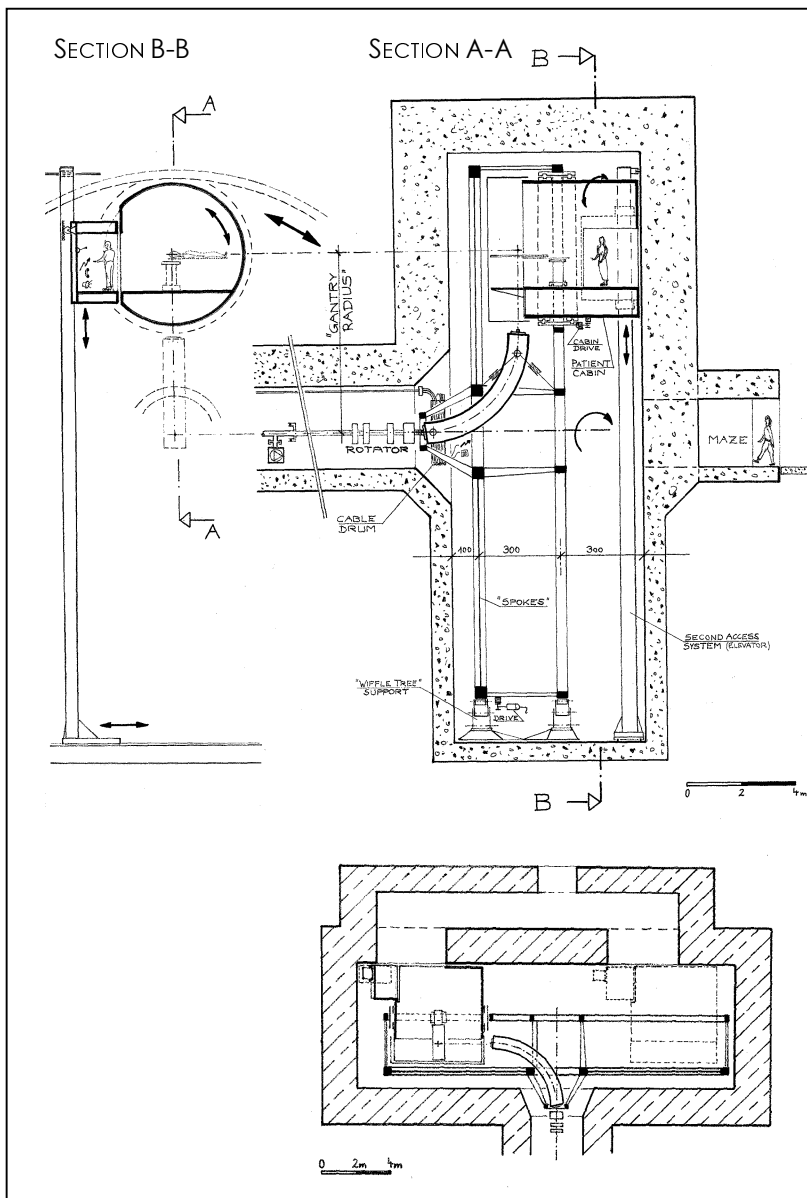
It is obvious that the concept of a Riesenrad gantry reduces the amount of beam bending and simplifies the mechanical design of the gantry compared to any isocentric variant. Placing the heavy dipole on-axis minimises the moment of inertia of a rotating gantry structure<sup>18</sup>, since far less counterweight is required to balance the structure. Consequently, the total weight as well as the deformation can be kept comparatively low.

A challenge is to find satisfying solutions for "secondary" issues such as the positioning of the patient on a circular path around the gantry axis, emergency access to the patient etc. in order to be as close as possible to the common standards of conventional radiotherapy facilities.

A principal possibility of such a Riesenrad gantry - which also perfectly justifies this name - would be to mount the central magnet close to the hub of a wheel, which is supported on its perimeter by roller bearings, as indicated in Figure 3-12. The version

<sup>17</sup> The name "Riesenrad" is derived from the large Ferris wheel in Vienna.

<sup>18</sup> The moment of inertia is given by  $I_{Gantry} = \sum_i m_i \times r_i^2$  where  $r_i$  is the radius from the turning axis of a point mass  $m_i$ .



should be referred to as a "wheel gantry". The overall radius of the machine would be around 8 m. The access level is placed at medium height and *two* entrances to the chicane are provided. Therefore the maximum rotation of the gantry necessary in an emergency is limited to 90°, corresponding to 15 s when a speed of 1 rpm is assumed. By cantilevering the cabin from the second bearing wheel, space is available for a second access system which could be a rack and pinion lift with two axes similar to systems used to serve high-rise stores. Such a system has to dock to the cabin from the side, whereas the exit to the chicane would be via the front. The supporting rails are either mounted on the floor or on the wall. To increase security it is possible to add another lift opposite the first one. The overall depth of the wheel gantry is below 7 m. Basically, the load of the heavy 90° magnet will be carried by normal forces only, resulting in a high rigidity of the structure.

Figure 3-12: Basic system of a Riesenrad gantry, type wheel gantry. The gantry radius  $R$  was taken as 6.6 m. Assumed radius of the bending magnet: 3.5 m.

A completely different structural approach to a Riesenrad gantry would be to support the 90°-bending magnet and the eccentric patient cabin by a *central* axis ("cabin gantry"). A group from the Harvard Cyclotron developed such an idea for a *proton* gantry already during the 80s. P. Negri recently presented a preliminary design for a "mobile cabin gantry" for ions following a similar structural principle (1998).

In a cabin gantry, the patient cabin and the opposite counterweight are mounted on two girders fixed to a central axis (see Figure 3-13). The majority of the weight of the 90°-bending magnet will be carried directly by a central space frame. The principle of supporting the patient cabin on its end panels requires the cabin to be a comparatively rigid structure, spanning between its two supports (i.e. the girders). Due to the necessary beam-entrance channel, no full 360° rotation of the cabin is possible. Nevertheless, a 180° rotation of the gantry starting from top position will be sufficient, if the PPS can turn *at least* 180° around the (local) isocentre as indicated in Figure 3-13. Eventually, the "restriction" turns into an advantage, because the building volume could be reduced by approximately one third. Unfortunately, the counterweight will become fairly heavy due to the small lever arm.

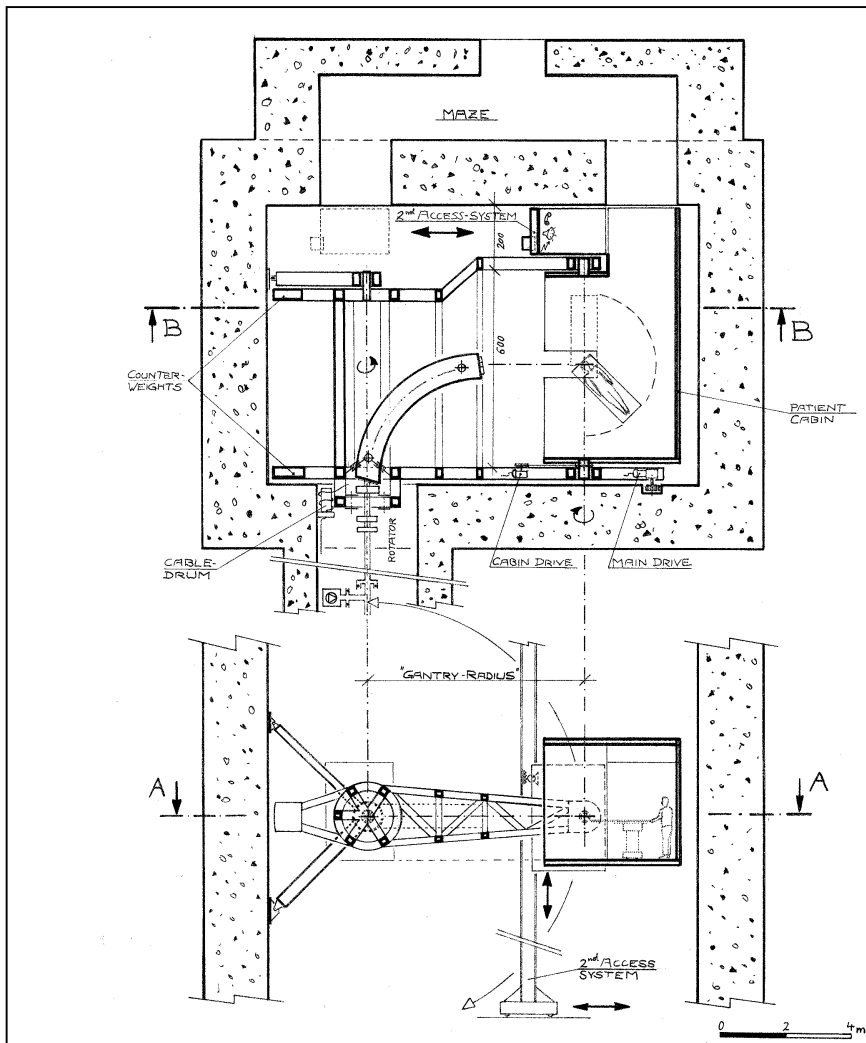


Figure 3-13: Principal system of a Riesenrad gantry, type cabin gantry. The gantry radius  $R$  was taken as 6.6 m. Assumed radius of the bending magnet: 3.5 m.

An alternative would be to support the cabin only by one girder; the cabin would cantilever into the beam line in a similar way as it is shown for the wheel gantry thus gaining about 0.5 m in depth, which is about 9 m in the current design. Transition to a 360° rotation would reduce the required space for the PPS, gaining another 1 m in depth. On the other hand, the 360° rotation eradicates a main advantage of the cabin gantry, which is the (approximately 30%) reduction in building size (breadth) due to the limited rotation.

The axis of the gantry is simply supported: upstream on some rollers (fixes support) and opposite to it on an "A"-shaped support, which is fixed to the sidewall of the gantry hall. Therefore, the total length of the central axis is kept low and space is made available for the installation of a second access-

system, which in principle could be similar to the one explained for the wheel gantry. Its central location with a separate entrance from the chicane avoids any interference with the gantry in an emergency situation.

A discussion regularly coming up in gantry design is whether it would be more efficient to have several fixed beam lines instead of a gantry and how this could be achieved. Suggestions in that direction came for example from Vorobiev et al. (1997, p. 13, "static gantry"), a practical example can be found at the HIMAC (see Section 2.4.1), where the patient is positioned in the common isocentre of a horizontal and vertical beam line. The advantage of such a solution is that common technology of fixed beam lines can be applied, even the step to SC-magnets seems attractive, since no rotation is required. However, for each desired treatment angle, a separate beam delivery system has to be provided, which immediately eradicates any cost savings if more than two treatment angles are demanded (compare the cost estimation done by Böhne, 1998).

*The "multi room" concept: a central structure supporting the heavy dipole and directing the beam to various treatment rooms situated at the perimeter.*

The corresponding principle following an exocentric approach would be to have a so-called "multi room" concept, where the actual gantry is reduced to accommodate the rotation of the centrally placed 90°-bending magnet - similar to the proposal of Martin (1990) for a proton gantry, which is shown in Figure 2-3. The patient "cabins" are provided by the building itself, giving direct access to the patient at all times. The challenge is shifted to the design of a cheap PPS, which has to be installed in every treatment room. By providing a certain pitch and roll capability for the PPS, one could ameliorate the main disadvantage of all such systems, i.e. the limited spectrum of treatment angles. However, this would make the PPS system more costly - and one needs several of them...

### 3.7 Conclusion: to Go for the Riesenrad-Approach

Based on the studies of potential procedures, specifications for the ion gantry (and partly the surrounding facility) were derived. They are summarised in Table 3-3. During the ongoing decision making process attention should be paid to the two strategic objectives, which are flexibility and – crucial to a machine running in a hospital environment – safety. At first sight, the latter is in favour of isocentric gantry solutions, where direct access to the patient is intrinsic. In addition, this principle represents the current practice in radiation therapy and it has to be assumed that any other gantry configuration will only be accepted, if the safety standards are the same as in conventional radiotherapy with isocentric gantries.

"Static" gantries or multi-room concepts only show - if any - small cost advantages but the major disadvantage of supporting only a view discrete treatment angles, thus reducing the flexibility of the system. Another aspect of flexibility concerns the size of the treatment area inside the gantry. Uncertainty on future procedures clearly favours large patient areas, as it is possible for example in the "cabin gantry". For this version one can also expect the smallest gantry hall volume of all possible variants, however, the effect on the overall cost of the gantry is not decisive. From the mechanical point of view an exocentric Riesenrad gantry promises a unique competitiveness. Its structural efficiency would be considerably higher than any isocentric variant, since the Riesenrad gantry keeps the heavy loads close to the axis. This results in a corresponding increase in rigidity and hence treatment precision. The Riesenrad approach is also superior concerning the beam optics, since only the minimum 90° of beam bending is required, saving pro rata costs of dipoles, power supplies, vacuum chambers and cooling devices.

Summing up the arguments, a Riesenrad gantry shows clear advantages concerning mechanical feasibility, achievable treatment precision, cost and flexibility. *Provided* that a satisfying solution for the patient access is found, the concept will certainly have the power to make a gantry-based ion therapy with active beam scanning competitive with other forms of radiation therapy. Therefore, and in accordance with the beam-optical development done in PIMMS, *the Riesenrad approach is selected for further investigation*. The next step will see the simultaneous development of various principle structural concepts for the Riesenrad gantry (Chapter 4) based on the specifications that are summarised in Table 3-4.

#### Basic guidelines for the development of a Riesenrad ion gantry

Patient position	Supine
Irradiation sites	All regions
Treatment angles	4 $\pi$ -irradiation
Patient access	Permanent access guaranteed by two independent access systems
PET compatibility	Yes
Beam optics	Based on a particle beam that is derived from a slow-extraction scheme in a synchrotron (PIMMS design)
Beam delivery system	(Active) spot scanning, performed upstream of the final 90° dipole
Treatment time	2 - 3 min. (to deliver 2 Gray)
Beam rigidity	6.35 Tm
Dipole bending radius	3.6 m
Dipole cross-section	150 cm x 100 cm
Good field region	20 x 18 cm <sup>2</sup>
Dipole weight	60 tons
Drift dipole – isocentre (Bragg peak)	2 m
Drift centre scanning magnets – start dipole	1.5 m
Max. elastic deformation	< 0.5 mm
Shielding requirements for the gantry hall	Equivalent to 2 m - 4 m ordinary concrete

Table 3-4: Specification for the design of a Riesenrad ion gantry. The listing is the result of an investigation of the basic processes taking place inside the gantry area and the mutual interrelationships between the crucial *systems* of an ion gantry as highlighted in the present chapter.

## 4 Generation of Variants for the Riesenrad Ion Gantry and Resolution

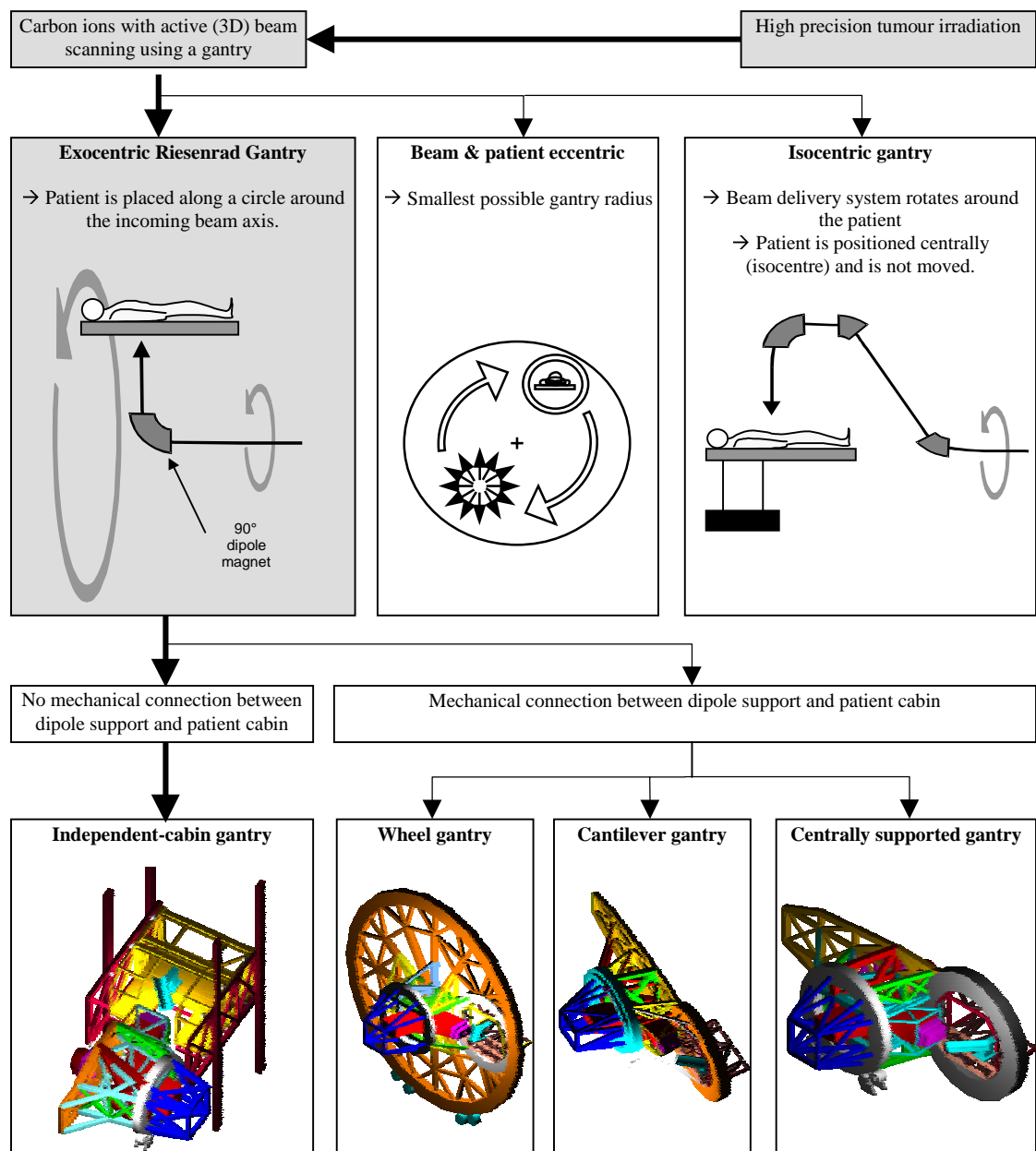


Figure 4-1: Decision making process for the development of an ion gantry focussing on the mechanical structure.

Based on the specifications for an ion gantry derived above, this chapter is dedicated to the more detailed investigation of a so-called *Riesenrad gantry*. The basic idea of this concept is to deflect the ion beam with a single 90° dipole, which rotates around the incoming beam axis, and directs it towards the eccentrically positioned patient cabin. The objective of this



chapter is to present and – to a certain degree – evaluate different versions of a Riesenrad gantry with clear focus on the mechanical performance. The driving questions were: "What structural concepts seem promising for a Riesenrad gantry?" and "How small can elastic deformations of the gantry reasonably be kept?"

The process of finding a suitable design for a novel gantry is an iterative one: defining requirements, developing variants and deciding for a solution will see many feedback loops. Nevertheless, some crucial questions determining this process always crystallise (Figure 4-1). In the previous chapter the principal decision to take was to go for an exocentric gantry solution or not. Now, one has to address the question whether it is possible to reach the specified precision of  $\pm 0.5$  mm while relying on mechanical rigidity only (i.e. no active position correction). From the point of simplicity and reliability such a system would be preferable. Three such gantry variants are generated, of which only one is proposed for further investigation. Nevertheless, the other two versions are shortly presented as well because they represent extreme solutions demonstrating the structural limits. Eventually, the proposed variant following the above principle is a *centrally supported Riesenrad Gantry* with a cabin that is "plugged-in" at the far end of a girder. Maximum absolute deformations are slightly above the specified value. However, on one hand they can be partly corrected by modifying the gantry rotation angle, on the other hand *absolute* maximum deformations are less significant when the patient is mounted directly on the gantry structure - it is the relative movement between dipole and patient that counts.

To achieve a further reduction of absolute elastic deformations one has to consider an active (feed back) alignment system for the PPS with respect to the magnet. The structural consequence is the - now reasonable - mechanical separation of the patient cabin from the central part carrying the dipole, because precision requirements for the two parts are different. The Riesenrad gantry with an *independent telescopic cabin* allows having a large patient cabin continuously accessible via an emergency staircase. However, this separation of the structure will considerably increase the complexity of the control system.

The last section of this chapter provides an evaluation of the two variants mentioned above, summarising their strengths and weaknesses and leading to a final proposal for the ongoing design phase.

## 4.1 Structural Principles, Methodology and Idealisations

When addressing the actual structural design of a Riesenrad gantry some general principles evolve:

- As the  $90^\circ$  dipole is the main load of the system, one would always like to support it as close to its centre of gravity as possible, which suggests to fix it on a ring supported on rollers. The geometrical position of the ring is a trade-off between its necessary radius and the actual percentage of magnet weight taken.
- The main difficulty of the design is – when the gantry is in horizontal position – to provide a second, sufficiently stiff magnet support close to the magnet's downstream aperture.

In all following drawings and graphs, the plane of gantry rotation is represented by the  $Z$  (vertically upwards) and  $X$  co-ordinate.  $Y$  points in the direction of the incoming beam axis.

The structural analysis of the various gantry proposals was performed with the software CUBUS, using the modules Statik-3 (analysis of space frames) and Fagus-3 (analysis of cross-sections). Standard square profiles between RHS 100/100/5 and RHS 400/400/20 (steel grade S235) were used. Because of the slow turning speed of a gantry, its structure was analysed as being static.

Due to the high precision requirements the structural design of the ion gantry is governed by permissible deflections and no problems concerning stability and maximum stress were observed: generally, maximum equivalent stresses occurring in the members are in the region of 0 to 2 kN/cm<sup>2</sup>. Consequently, the analysis was carried out applying safety factors of 1.0 for resistances and loads. The latter were: gravity, main dipole (600 kN), the patient positioning system (PPS) in the patient cabin (25 kN), scanning magnets (20 kN) and necessary counterweights to *balance* the structure. For the PPS a conservative approach was taken: the (upper limit) weight of 25 kN was split into two point loads acting on the structure at the most adverse positions depending on the gantry rotation angle.

The nodes of the analysed static model were assumed to be rigid, shear deformations were taken into account (increasing the deflections by approx. 10%). The magnet was modelled not to be rigid but to deflect elastically. Generally, a three-point magnet support was assumed in the analysis: two supports in a kind of "front ring" and another further downstream. Increasing the number of the supports for the magnet would have a beneficial impact on the structural performance of the gantry. A mass-less beam cantilevering perpendicular from the (deforming) magnet aperture represented the movements of the local isocentre.

Apart from the idealisations mentioned above, which led to the models eventually analysed, several uncertainties remain and certainly they will have an impact on the real system. The following list of possible effects is non-comprehensive and confined to structural matters. It should act as a warning to interpret the results of the elastic analysis as an *approximation*:

- Supports are never perfectly aligned as assumed in the analysis.
- Manufacturing tolerances will alter the intended geometry. Reasonable tolerances for the machining of bearing rings with several metres diameter are in the region of 0.1 mm.
- Local deformations due to high contact pressures were neglected in the analysis. This concerns mainly the rollers of the supports.
- Settlement of the extremely heavy gantry room (concrete shielding) will be considerable over the time (perhaps even in the cm-region). Certainly the gantry supports will be made re-adjustable, but this error – as other systematic errors – has to be detected and corrected during operation.
- Measurement tolerances, backlash of driving motors and clearance of bearings will add random errors.
- A uniform temperature rise in the gantry room by 1° C would enlarge the structure roughly by 0.15 mm. The effect of temperature gradients may be even more severe and has to be analysed in detail at a later stage.

## 4.2 Wheel Gantry

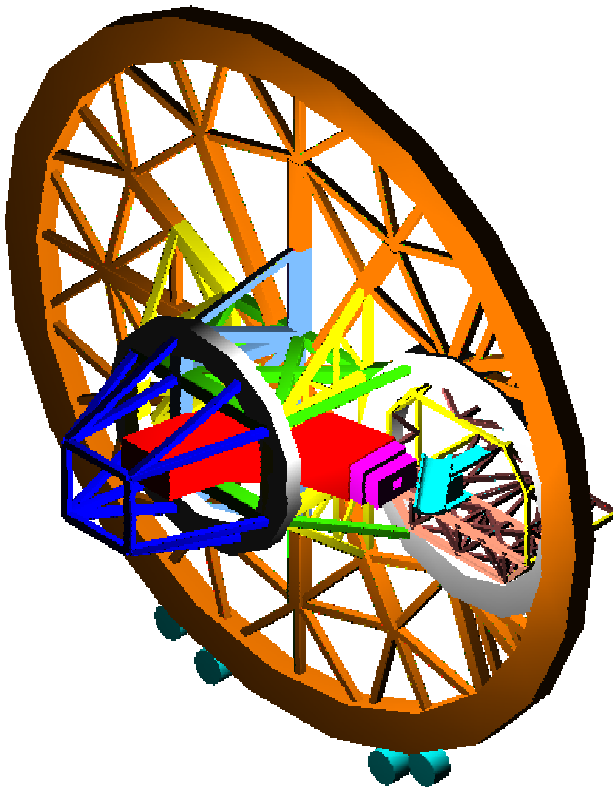


Figure 4-2: Perspective of the Wheel gantry

In the wheel gantry - being literally a kind of Riesenrad - the weight of the central 90° dipole is shared by the smaller front ring (taking approximately two thirds, outer diameter 5.6 m) and a large, trussed "wheel" of 18 m outer diameter (Figure 4-2). Wheel and ring are 3 m apart and both are supported by cylindrical rollers. The patient cabin is inserted into an eccentrically-placed "hole" of the large wheel. From this hole it cantilevers towards the chicane. The cylindrical cabin can rotate around the centre of the hole in order to stay horizontal during gantry rotation. The PPS is mounted on rails running in the plane of the wheel to transfer its load directly onto the wheel and avoid large bending moments acting on the cabin structure. The cabin was modelled separately; its reactions were applied as forces to the main model.

The counterweight (35 t) is distributed on the two rings as not to introduce any torsion to the system. A lift travels vertically and horizontally in front of the wheel and serves the cabin laterally providing a second access system. The rails for horizontal travel can be mounted on the floor, the ceiling or – in a recess – the front wall.

The difference in diameter between the ring and the wheel results in their different (absolute) elastic deformation. The level of the bearings of the (smaller) ring is adjusted in a way, that the centres of both, wheel and ring, show similar vertical displacements of about 0.3 mm. However, the changing stiffness of the large wheel leads to corresponding ups and downs during gantry rotation. Because the smaller front ring runs more stable there will be considerable differential movements resulting in tilting and thus unwanted horizontal deformation of the wheel. This tilting also affects the dipole and yields out-of-plane isocentre deformations of around  $\pm 0.5$  mm.

The gantry system is based on the provision of a mechanically fixed distance between the incoming beam and the isocentre. The rigidity is maximised by transferring the loads directly to the supports via normal forces resulting in deformations, which are within the specification of  $\pm 0.5$  mm. However, a consequence of this rigidity are the large overall dimension of the gantry and the heavy cross-sections, which have to be used throughout the entire structure. Its weight exceeds 75 t, giving a total weight of the gantry of around 185 t. The two roller bearings on the front ring have to withstand forces of about 550 kN each.

The design of the big wheel is dominated by its dead load and not by giving support to the patient cabin. The effort to achieve smooth rolling (avoiding ups when a spoke crosses the bearing) is considerable (one third of the structural weight - 25 t - is due to the large rim of the wheel); and still the hole remains a weak spot in the rim, resulting in high deformations when – during a rotation – bearing forces eventually act on this part. Additionally, accurate machining of such a large ring would be extremely difficult to achieve. All these arguments suggest that competitiveness will not be reached with such a gantry variant.

### 4.3 Cantilever Gantry

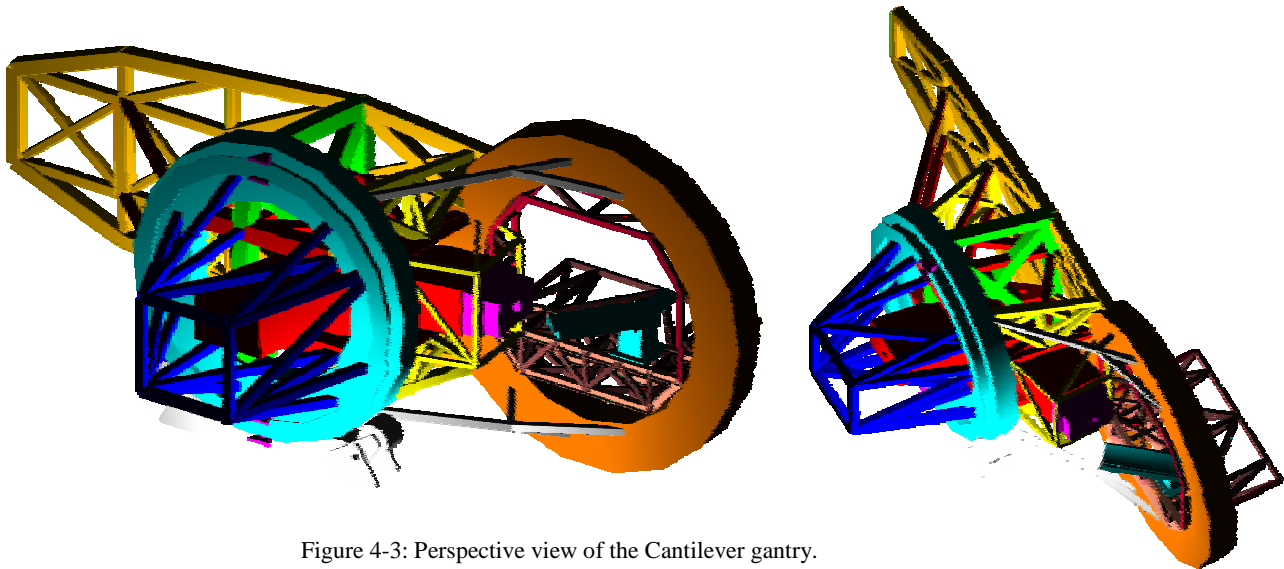


Figure 4-3: Perspective view of the Cantilever gantry.

The basic idea of this gantry proposal is to reduce the structural elements to the absolute necessary, i.e. a balanced girder carrying the eccentrically-placed patient cabin and the counterweight, one main ring taking all the loads and one vertical and two horizontal shear walls (modelled as trusses) connecting the two parts. The *whole* structure cantilevers out from the ring, which transfers the vertical loads *and* the resulting moment (via a pair of horizontal forces) into a wall of the gantry hall (Figure 4-3).

The balanced girder is a high truss to maximise bending resistance. It has to provide a ring-like opening to support the cylindrical patient cabin. This ring is a very sensitive part - even though the loads of the patient cabin are comparatively small. Nevertheless, the ring has to provide large cross-section resistances in both planes and against torsion. Despite the effort the elastic deformations in plane and out of plane *exceed* considerably the value of  $\pm 0.5$  mm.

The benefit of studying such a "puritanical" gantry solution is to get some information on the feasibility and the structural limits of such a system when reducing its weight (40 t) to the absolute minimum. The deficiencies turned out to be:

- The specification for the permissible deflections cannot be reached (hence an on-line position correction system for the patient couch would be needed). Additionally, the excessive deformation of the cabin ring spoils the mechanics and position accuracy of the patient cabin.
- With conventional roller supports it would be difficult to provide the required load capacity ( $2 \times 800$  kN) in an efficient way, therefore demanding more sophisticated bearing techniques.
- Space for the magnet itself and its maintenance is very limited.

However, the solution could become interesting again if the dipole could be made considerably lighter and smaller.

### 4.4 Centrally Supported Riesenrad Gantry

This gantry version is based on the extreme approach of a cantilevering gantry, however, several crucial design changes were made in order to restrict the elastic deformation to the specified maximum while still relying on a mechanically rigid connection between dipole supporting part and patient cabin. The most obvious difference is the additional support (rear support) of the gantry, which - from a mechanical point of view - changes the (static)

system from a cantilever towards a simply supported beam (with the beam axis being the axis of gantry rotation inside the gantry). The *Centrally Supported Gantry* - centrally supported compared to the wheel gantry, which is supported at the perimeter - is originally derived from the cabin gantry approach mentioned in Section 3.6.3. There, the patient cabin was not cantilevering out of a ring-like hole of a large girder, as it is the case here, but was supported on its side panels by two girders. However, in a brief analysis, this solution was found to be not satisfying and the present version was developed instead.

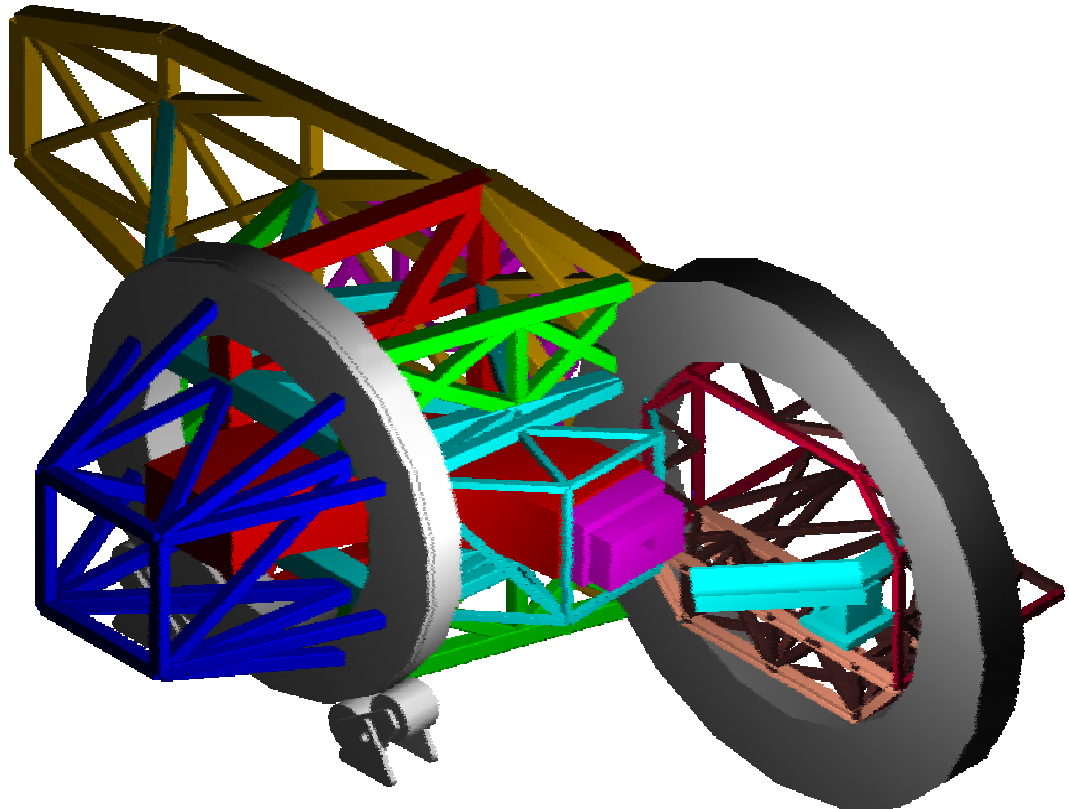


Figure 4-4: Perspective view of the centrally supported Riesenrad gantry

#### 4.4.1 Principal Elements and Structural System

The gantry, which can rotate 360°, is supported on a *front ring* (two self-aligning roller supports) and an additional support at the opposite end of the structure (*rear support*). The main bearing elements spanning between the supports are:

- in horizontal position a *main shear wall* slightly tilted out of axis and assisted by *two lateral assistant shear walls* of similar stiffness,
- in vertical position the *two transverse shear walls* (see Figure 4-4, Figure 4-5 and Figure 4-6).

Perpendicular to the shear walls runs the *trussed girder*, which gives support to the eccentrically positioned *patient cabin* and the opposite counterweight. The *cabin ring* provides the support for the cylindrical patient cabin, which cantilevers towards the chicane (exit) and rotates around its longitudinal axis. The patient couch is inserted into the beam, a light casing around the isocentre (not shown in the above figure) that is fixed to the magnet frame gives the patient the impression of being in an isocentric treatment room.

A *front structure* cantilevers from the *front ring* towards the transfer line and supports the scanning magnets. Compared to the previous cantilever gantry, the third support reduces

the global bending moments in the structure (and therefore the normal forces acting in every truss member). Cross-sections can be made smaller or – with the same dimensions used above – deformations reduced. The necessary counterweight is also smaller because a higher proportion can be put on the far edge of the trussed girder. Loads to the front bearings are reduced to around 600 kN. The rear support is lifted by 0.1 mm to counter-balance part of the vertical deformation. A higher value would – while generally being beneficial to the gantry deformations – lead to an increased sagging of the scanning magnets (approx. by half the value applied to the support).

In comparison to the cantilever gantry, the trussed girder is placed further away from the isocentre, thus the patient cabin is better balanced (reducing the out of plane moment acting on the ring) and thus considerably lighter (3.5 t). Improvements seem possible with the cabin ring, where conservative dimensions were assumed. A higher slenderness ratio of the cross-section could be used to increase its height or decrease the weight of the ring.

The analysed gantry model is supported in a statically determinate way and balanced. Remaining turning forces are (conservatively) taken by a support acting in X-direction at the central bottom of the front ring. The cabin was modelled separately, its reactions were applied as forces to the main model. The maximum deformation of the rotating cabin platform itself is less than 0.1 mm and was neglected. The second access system is provided by two elevators (e.g. rack and pinion system) which can also travel horizontally to serve the patient cabin laterally (see Figure 4-6).

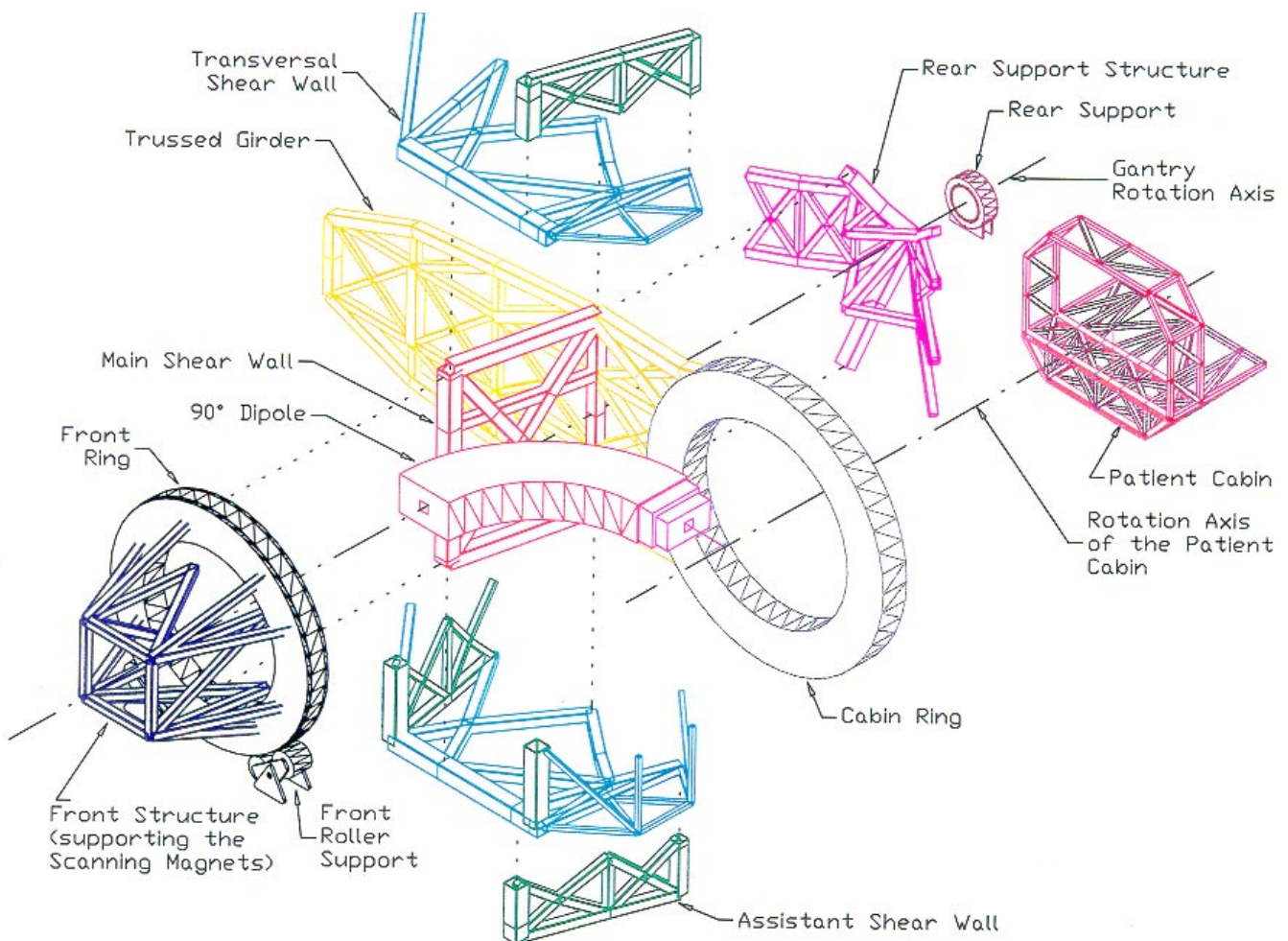


Figure 4-5: Principal elements of the centrally supported Riesenrad gantry.

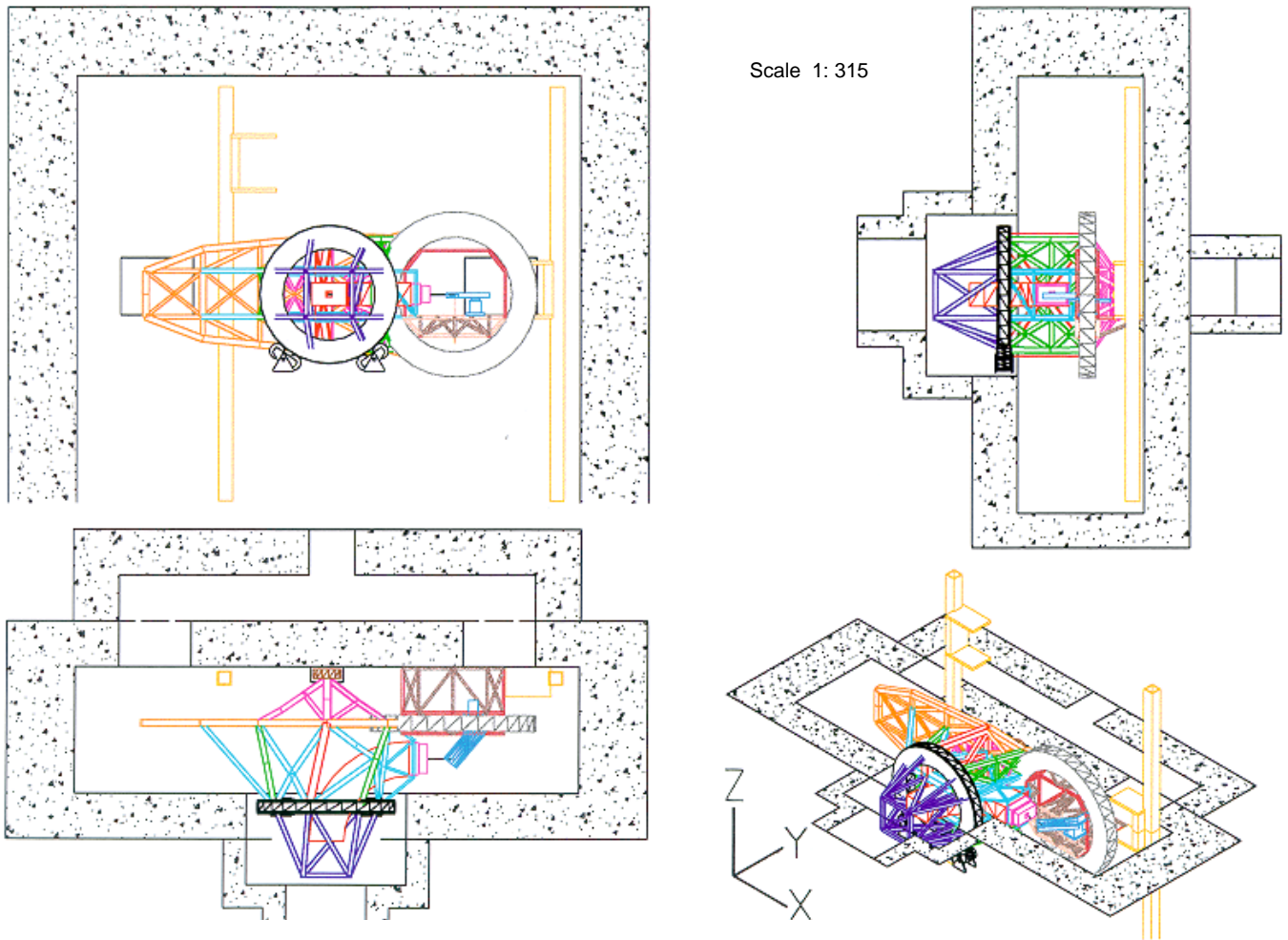


Figure 4-6: Plan, front-view, side-view and perspective of the centrally supported Riesenrad gantry

#### 4.4.2 Deformations

A qualitative impression of the elastic deformation of the gantry can be obtained from Figure 4-7, which shows a deformation plot of the analysed model. The primary concern of the design was to limit the vertical deformation of the local isocentre when the gantry is in horizontal position ( $0^\circ$ ). Eventually, in this respect the current design does not quite reach the desired specification of  $\pm 0.5$  mm (Figure 4-8). However, adjusting the angle of gantry rotation can to a great extent compensate this excessive flexure. For example, to eliminate the calculated maximum of  $-0.7$  mm, an angular correction of  $0.007^\circ$  would be necessary.

When the gantry is in horizontal position approx. 40% of the vertical deformation of the cabin ring centre is due to the dead load of the structure, another 40% is caused by the cabin and the PPS, and only 20% by the dipole. Contrarily, when regarding the isocentre deformation modelled as a straight line from the aperture of the magnet, around 80% of the vertical deformation is caused directly by the weight of the magnet. Consequently, the following steps would seem most promising when trying to meet the specification directly:

- A more rigid fixation of the magnet onto the structure to couple the deformations more intensively
- A reduction in the weight of the PPS
- A stiffness increase of the main girder and the cabin ring.

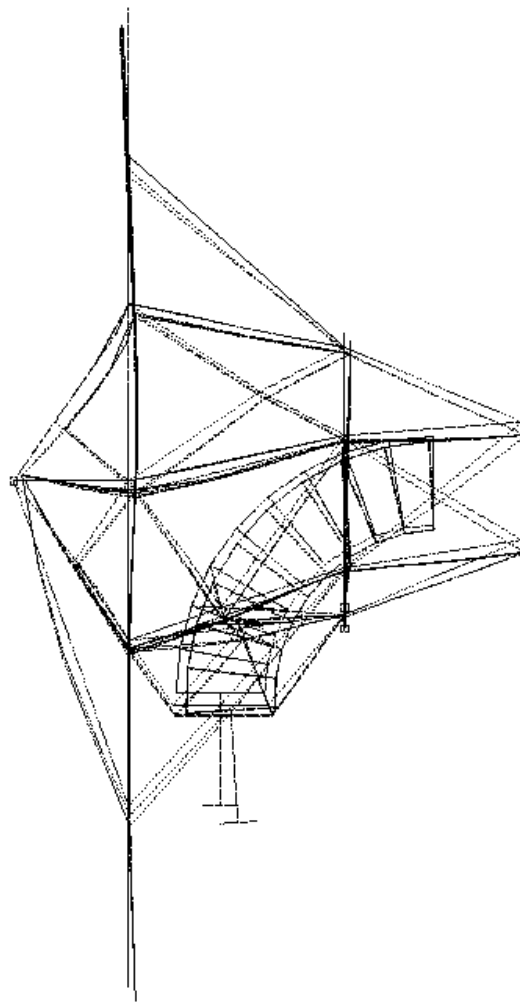


Figure 4-7: Deformation plot of the Centrally Supported Riesenrad Gantry pointing downwards (top irradiation).

Figure 4-8 gives an impression of the mechanical isocentre stability during gantry rotation. Graphs are drawn for the actual isocentre (modelled as a straight prolongation of the beam from the magnet aperture) and the centre of the cabin ring. As mentioned above, for a single gantry position, relative contributions of the various load-cases are quite different for each of the two points. The absolute differences are strongly governed by the modelling of the dipole and the dipole fixations in the structural analysis. In a refined model – with more precise stiffness data of the magnet available – it will be possible to further reduce these differences (in all three dimensions).

The difference of the two curves also indicates how the patient cabin deforms relative to the magnet (or vice versa). A gantry concept where the patient cabin is *not* mounted on the same structure as the magnet would have to compare its patient cabin alignment capability to these values.

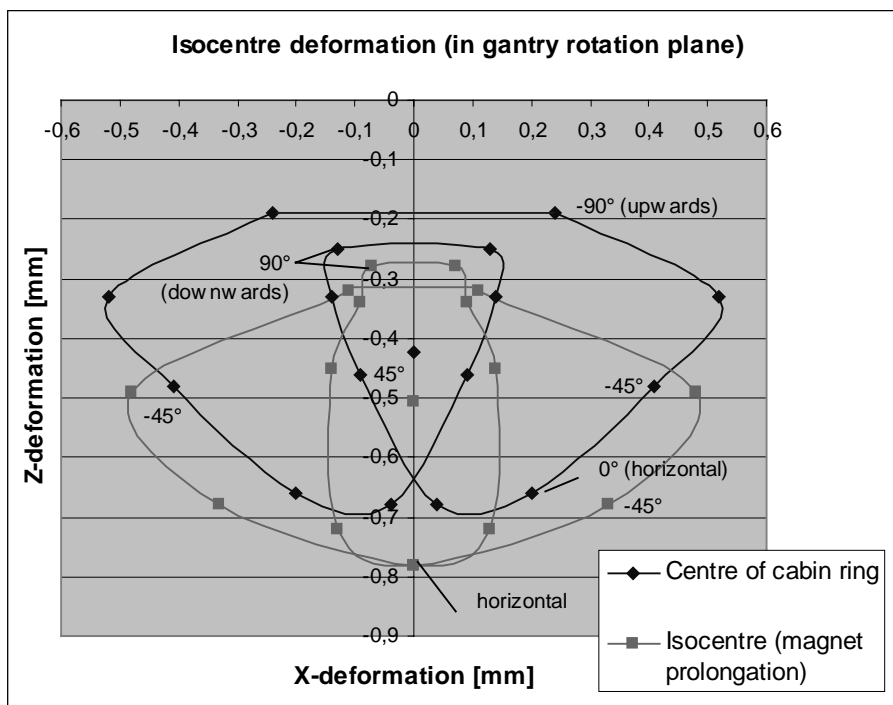


Figure 4-8: Isocentre deformation of a Centrally Supported Riesenrad Gantry during a 360° turn. Deformations in Z (vertical) and X (horizontal) direction are shown, i.e. deformations in the plane of the gantry rotation. The PPS was considered to be in its most adverse position. In the top and bottom gantry position the PPS was shifted from one side to the other, which is indicated by two separate points for the single position.



When the gantry is pointing virtually upwards, the system reacts very sensitively and shows considerable horizontal (*X*-) deformations depending on the position of the PPS. The symmetric (to the *Z*-axis) counterparts for the points indicating the upward- and downward-pointing gantry positions in Figure 4-8 represent the horizontal shift of the gantry when moving the PPS from the far right to the far left position and vice versa.

The maximum calculated *X*-deformation is 0.5 mm (when the gantry is around 18° from the upward-pointing position). About 0.2 mm of this horizontal deformation is already present at the top points of the *front* (!) ring suggesting that increased bracing is needed there, which can be achieved economically by structurally incorporating the counterweight inside this ring. Additionally, with a refined modelling of the PPS the horizontal deformation can be expected to decrease considerably.

Out-of-plane deformations (in *Y*-direction) are – due to the dipole and the cantilevering cabin – most critical when the gantry points downwards. Values of ±0.3 mm are encountered. In particular the dipole shows the tendency to "rotate" out of plane (see Figure 4-7). This movement strongly depends on the magnet stiffness and the magnet fixations; again improvements seem possible here. The lifting of the rear support by 0.1 mm is responsible for beneficial effects in the order of 0.05 mm both with the in-plane as well as out-of-plane deformations.

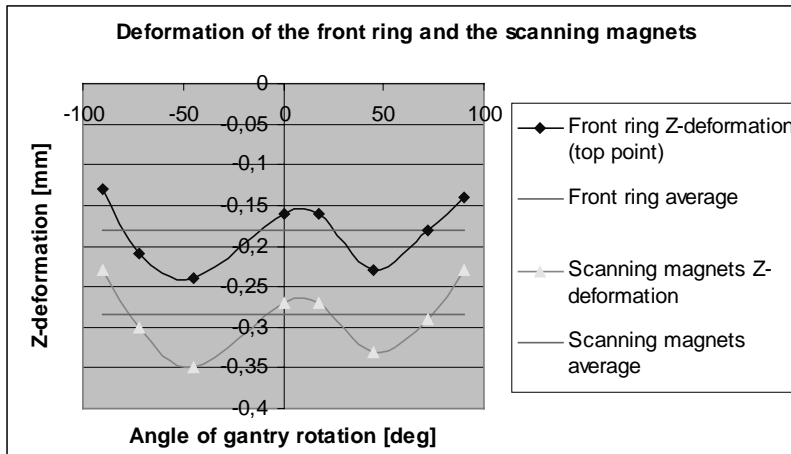


Figure 4-9: Deformation of the front ring and the scanning magnets at the Centrally Supported Riesenrad Gantry. For each rotation angle of the gantry the vertical (*Z*-) deflection of two points is indicated: the *top* point of the main ring and the (virtual) intersection point where the beam enters the front structure carrying the scanning magnets.

As it can be seen from Figure 4-9 the top point of the front ring is sagging between -0.15 mm and -0.25 mm during gantry rotation. For the virtual point in the centre of the ring half the average value, i.e. -0.1 mm average vertical deformation, can be expected. The scanning magnets follow the movements of the front ring on a "lower" level, average *Z*-displacement is around -0.3 mm. From the structural analysis one obtains an idea of the vertical deformation of the beam path inside the gantry (Figure 4-10).

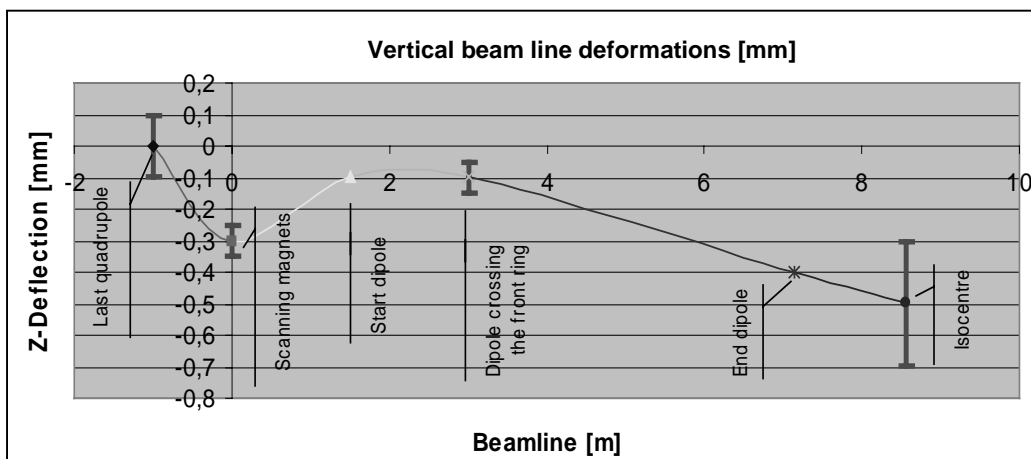


Figure 4-10: Vertical (*Z*-) deformation of the beam path in the Centrally Supported Riesenrad Gantry. The error bars - only those values were calculated - indicate the variation during gantry rotation. The line in-between is smoothed and does not represent the true situation.

## 4.5 Riesenrad Gantry with an Independent Telescopic Cabin

The basic idea of this gantry is to *separate the patient cabin from the magnet-supporting structure* in order to reduce the masses of the movable sub-structures, increase their rigidity and hence minimise elastic deformations. A central rotating "cage" is carrying the 90° dipole whereas a telescopic platform functions as a lateral patient cabin and supports the PPS. Only 180° of gantry rotation are necessary (Figure 4-11, Figure 4-12 and Figure 4-13).

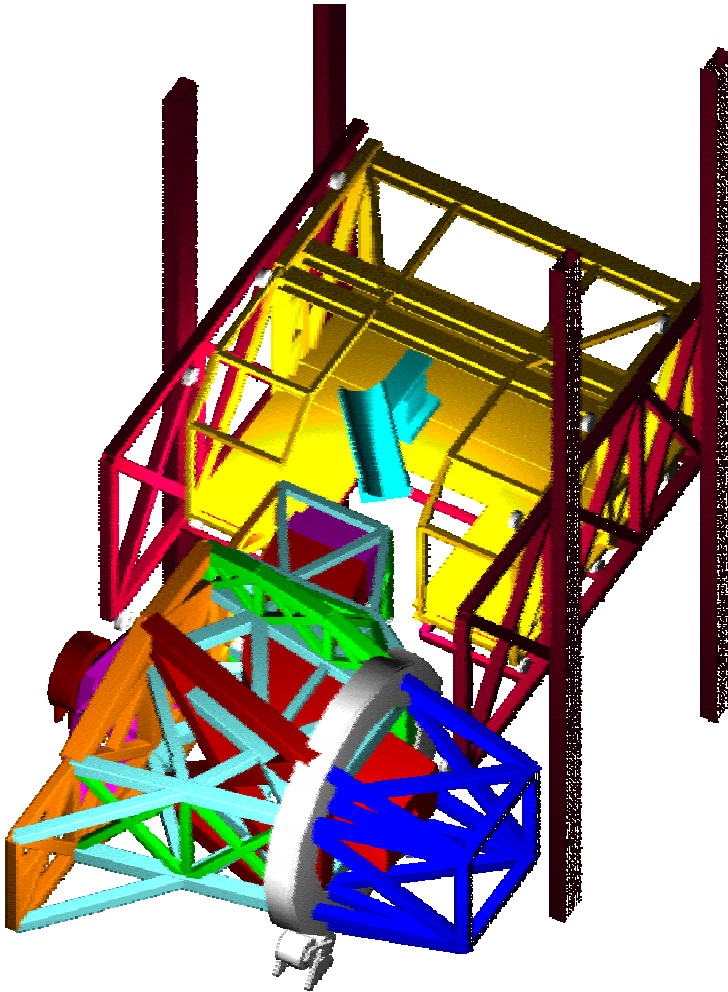


Figure 4-11: Perspective view of the Riesenrad Gantry with an Independent Telescopic Patient Cabin. The patient cabin follows the rotational motion of the magnet (and hence the isocentre) by travelling vertically on guiding rails and telescoping back and forth.

For the structural independence of the two sub-systems the mechanically secured correctness of the "gantry radius" is sacrificed, the correct position of the platform has to be maintained "artificially" and collision protection requires a considerable effort.

Since magnet support (cage) and patient cabin are separated structures, there is no point in demanding a high initial rigidity for the whole system. It is in this case sufficient and reasonable to align *only* the actual patient couch with respect to the high-rigidity, magnet-supporting structure. Positioning of the platform and the rigidity of the platform itself is less critical - perhaps some commonly available industrial system can be adapted for this purpose. Consequently, competitiveness of this gantry variant depends a lot on the development of a cheap and reliable alignment system for the patient couch.

### 4.5.1 Principal Elements and Structural System

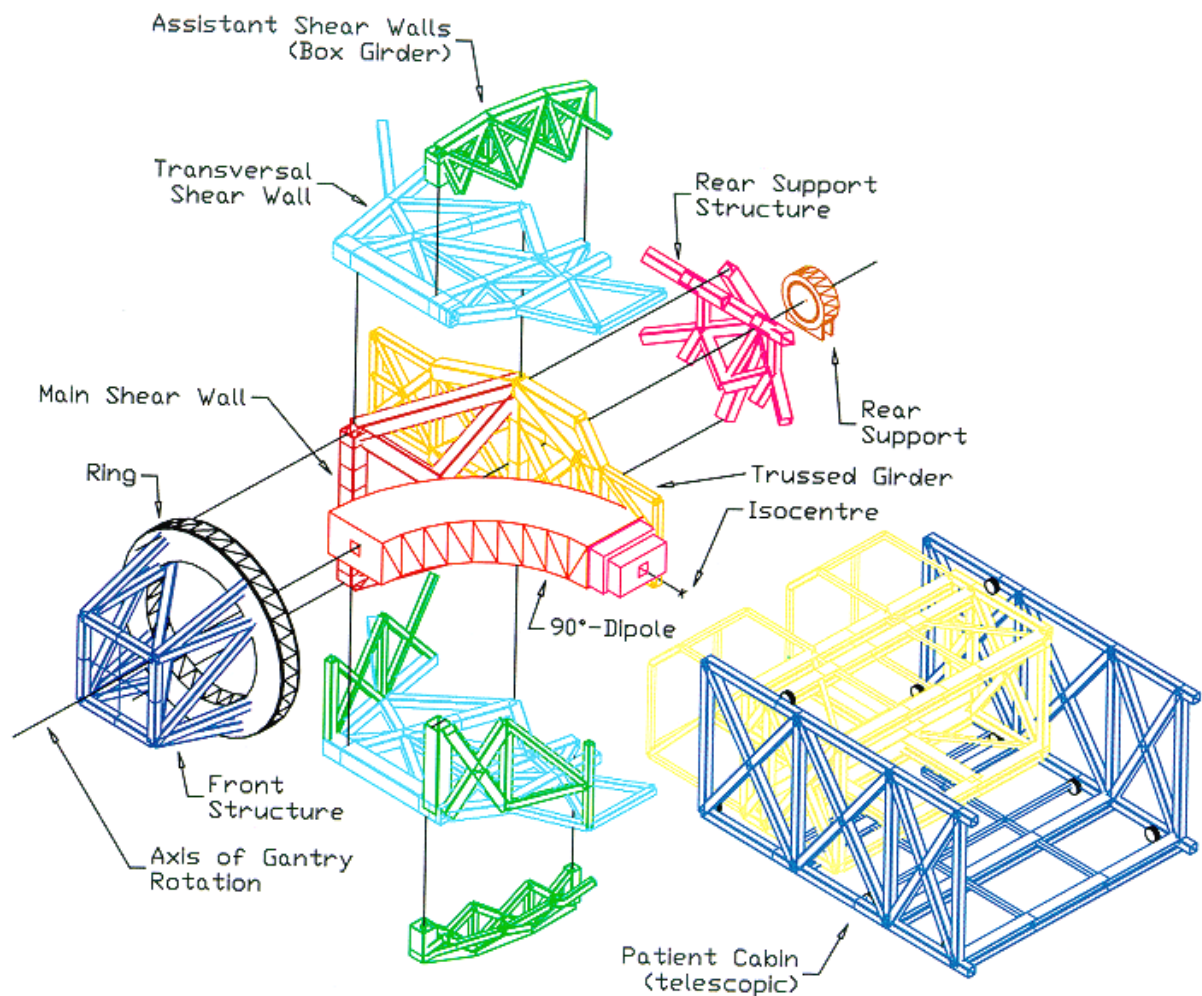


Figure 4-12: Principal elements of the Riesenrad gantry with an independent telescopic patient cabin.

The cage is basically an arrangement of shear walls – most of them modelled as trusses – similar to the previous gantry version. The gantry is supported structurally determinate on two pairs of rollers, acting on a large *front ring* (outer diameter 4.5 m), and a single *rear support*. To span the distance in-between two *transversal shear walls* and a single *main shear wall* take the load when the gantry is in a vertical and horizontal position respectively. The main shear wall is slightly tilted to make way for the dipole. It is relieved by two smaller lateral *assistant shear walls*, one of them itself is made out of two *triangular shaped box girders* to let the dipole pass.

The ring supports the dipole close to its centre of gravity, taking about two thirds of its weight. When the gantry is in vertical position the other third is taken by the transversal shear walls, guiding the forces directly to the supports. However, in horizontal position the two triangular-shaped box girders running to the 3.6 m high *trussed girder*, perform this task. A *front structure* cantilevering from the front ring towards the rotator supports the scanning magnets. Counterweights of 130 kN and 148 kN are acting on the front ring and the trussed girder respectively. The independence of the telescopic platform allows generous dimensions of this "*patient cabin*" therefore improving flexibility. A PPS being able to rotate horizontally around the (local) isocentre reduces the need for gantry rotation to  $\pm 90^\circ$ .

The necessary (relative) alignment of the PPS towards the magnet can be done by means of *photogrammetry* (optical non-contact co-ordinate measuring system). Standard systems provided by industry easily achieve an accuracy better than 0.15 mm ( $\sigma$ ). A feasible solution would be to mark the PPS with reflective targets (also at the bottom) and attach some cameras on the end face of the dipole or the frame carrying the beam position monitors.

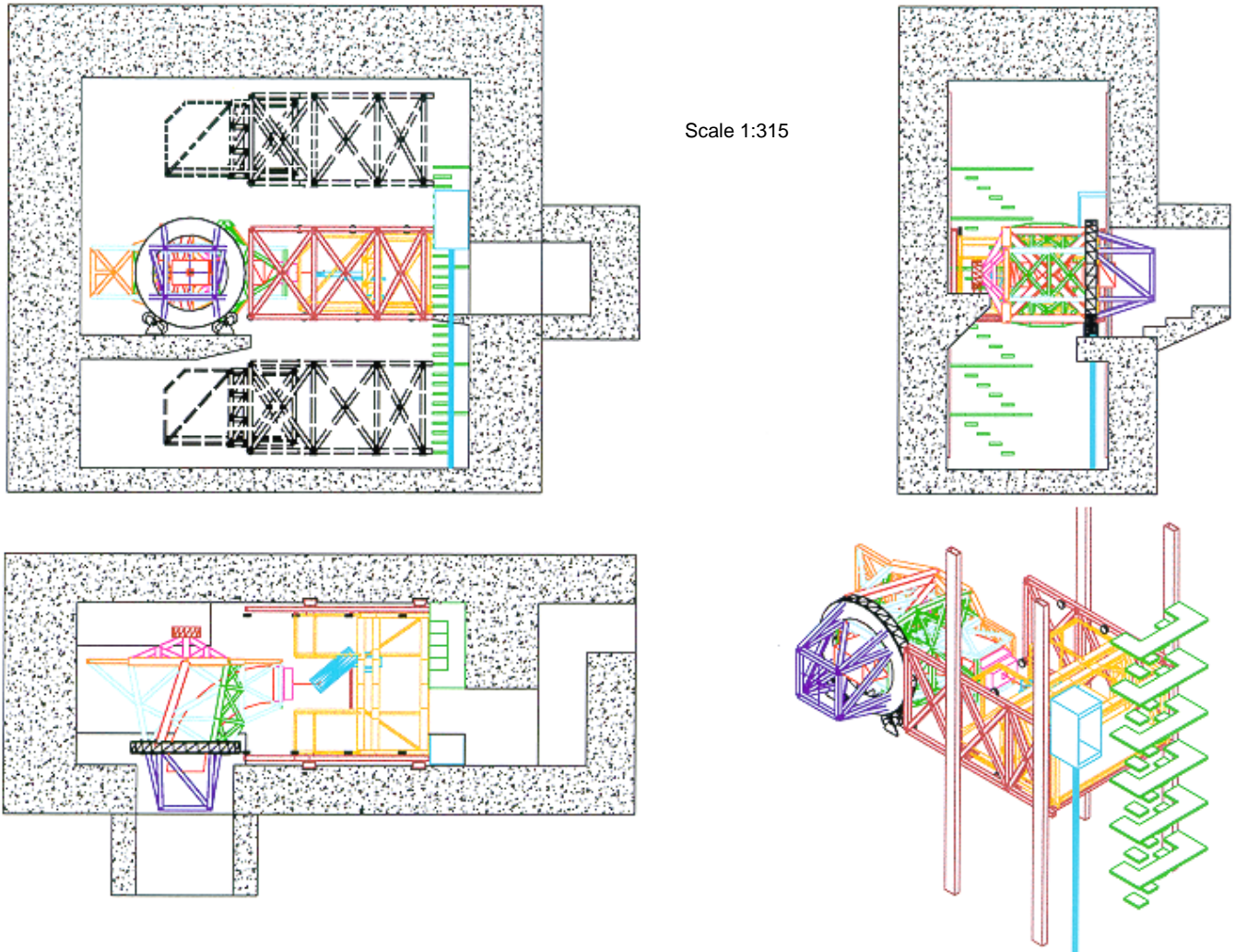


Figure 4-13: Plan, elevation, side view and perspective view of the Riesenrad Gantry with an Independent Telescopic Cabin.

The patient cabin is designed to travel 11 m vertically and to telescope 5.5 m horizontally, which allows a *constant* contact to the lateral wall of the gantry hall. This gives the advantage that a continuous access to the cabin via a staircase is feasible (intrinsic safety system). A lift provides quick access to the cabin during regular operation. A possible solution for the vertical motion of the cabin would be to use two guiding rails on each side of the gantry room, which take the moment and the vertical load of the platform by a pair of normal forces. For the cabin a rack and pinion drive seems suited.

The patient cabin dictates the depth of the gantry hall. By enlarging the room size in the longer dimension the counterweight at the trussed girder could be reduced.

## 4.5.2 Deformations

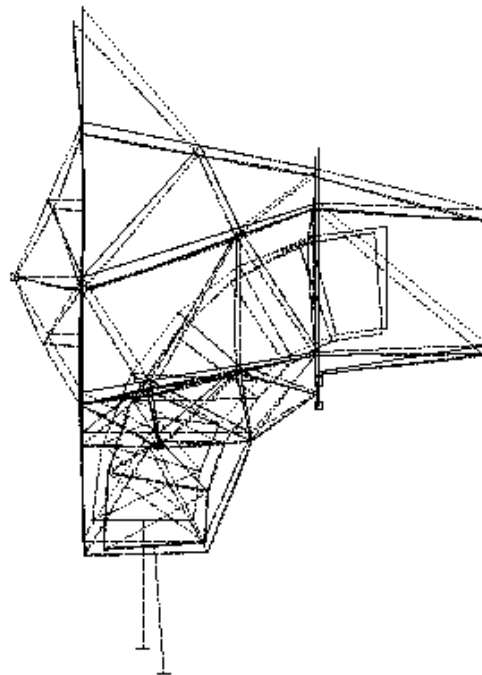


Figure 4-14: Plot of the elastic deformation of the Riesenrad Gantry with an independent telescopic cabin (gantry pointing downwards).

Figure 4-14 gives a qualitative impression of the elastic deformation of the gantry for the downwards-pointing gantry position. Due to the comparatively low weight of the dipole-supporting cage, elastic deformations are very small and the corresponding specifications can be easily met. However, because the gantry is not one solid structure but comprises two independent sub-systems, the problem of precision is shifted to the accurate relative alignment of the two. This is performed by the photogrammetric system, which adjusts the position of the couch.

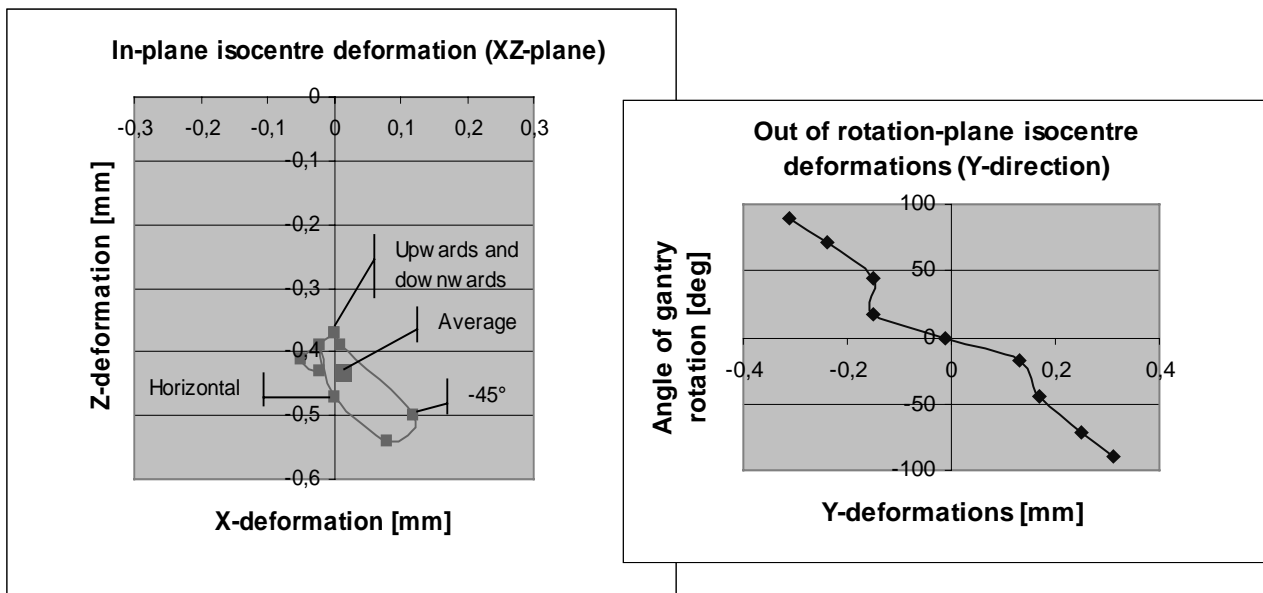


Figure 4-15: Deformations of the isocentre of the Riesenrad Gantry with an Independent Telescopic Cabin for various different gantry angles. Deformation in Z (vertical) and X (horizontal) direction are shown on the left, i.e. deformations in the plane of the gantry rotation. The deformation in the (Y-) direction (out of the gantry rotation plane) is presented on the right. The isocentre position was modelled by a 2 m long, straight line originating perpendicular from the centre of the deformed magnet aperture.

When regarding the (local) isocentre deformations (Figure 4-15) during 180° of gantry rotation one can observe that:

- The downwards (Z-) deformation is more or less stable at around 0.4 mm.
- The horizontal deformation in the rotation plane (X) is negligible.
- An out of plane (Y-) deformation of ±0.3 mm is building up when the gantry is rotated from a horizontal into a vertical position.

The small increase in vertical deformation when moving from horizontal position upwards can be explained by a then less beneficial position of the rollers supporting the ring (larger sagging of the ring). With a more detailed modelling of the magnet and the magnet fixations to the structure even lower values for the elastic deformation can be expected; a further reduction could be achieved by slightly lifting the rear support.

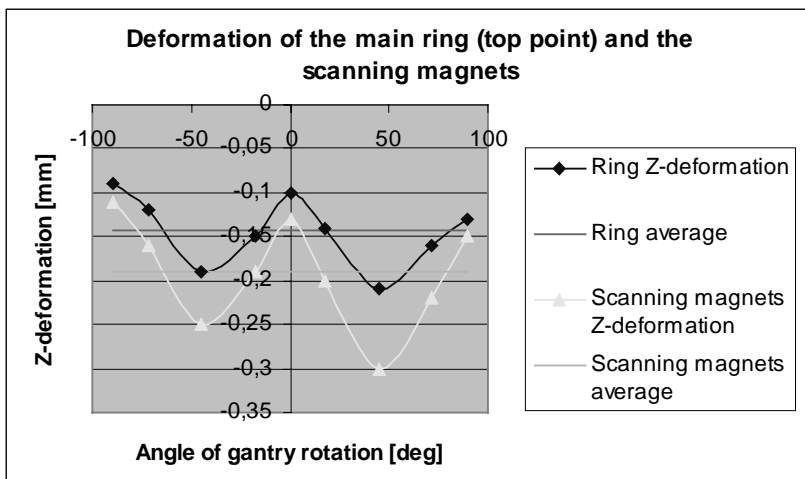


Figure 4-16: Vertical movements of the top point of the ring and of the scanning magnets during rotation of the Riesenrad Gantry with an Independent Telescopic Cabin. The virtual point where the beam line enters the front structure models the deformation of the scanning magnets.

Figure 4-16 shows the up and down of the top point of the ring during gantry rotation. The range is about 0.1 mm. Correspondingly, the ring shows – at some gantry positions – a considerable deformation at the supports in the order of ±0.1 mm. Both displacements can be expected to be considerably lower in reality since a calculated reaction force will be taken by two rollers. Scanning magnets oscillate around a vertical (Z-) deformation of -0.2 mm. Larger cross-sections in the front structure could improve this value, a stiffer ring would help to reduce the amplitude.

Figure 4-17 gives an idea of the vertical deformation of the beam line in the gantry due to elastic sagging of the structure and the dipole. The latter rests comparatively stable in a slightly inclined position (i.e. a more or less rigid body rotation around the X-axis) during gantry rotation. The faces of the magnet show maximum rotations of about 0.004°.

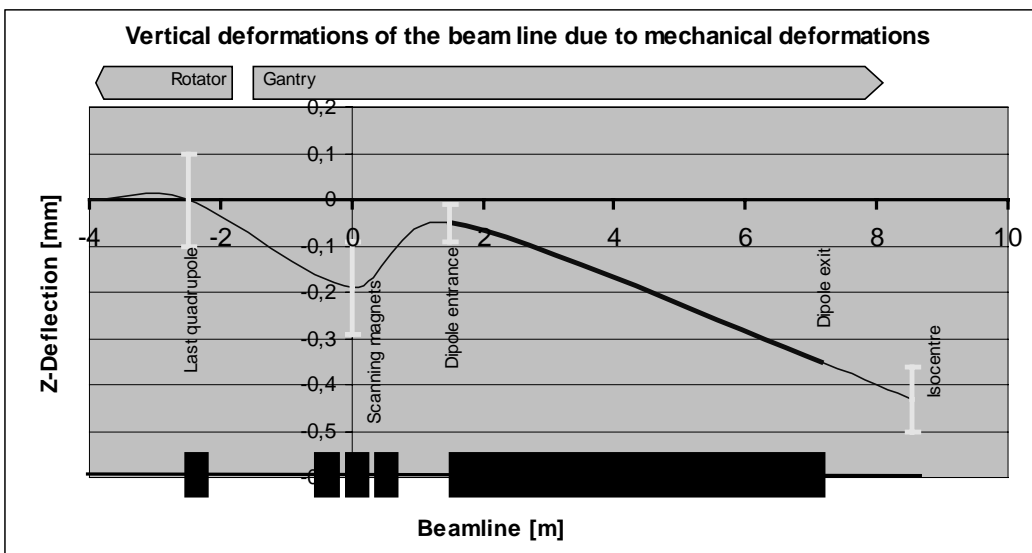
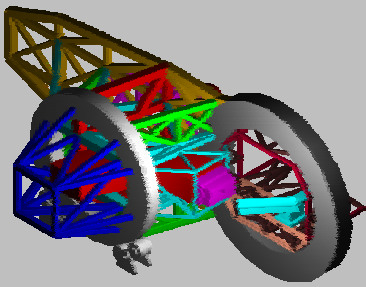
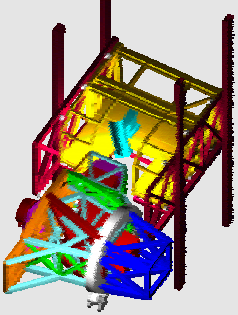


Figure 4-17: Vertical deformations of the beam path due to the elastic sagging of the structure and the magnet in the Riesenrad Gantry with an Independent Telescopic Cabin. The line represents the average values. Error bars (only these values were calculated) indicate the variation during gantry rotation.

## 4.6 Comparison and Resolution

### 4.6.1 Comparison

The following Table 4-1 summarises and compares the two most suited variants for the Riesenrad ion gantry, the centrally supported solution consisting of a single structural unit vs. the solution where the patient cabin is independent from the central cage that holds the dipole.

Comparison of the two principal variants for the Riesenrad ion gantry		
	<b>Variant 1</b> <b>Riesenrad gantry – Centrally supported</b>	<b>Variant 2</b> <b>Riesenrad gantry – Independent telescopic cabin</b>
		
<b>Function</b>	<p>The central dipole and the eccentric patient cabin are mounted on <i>one single mechanical structure</i>, which can rotate <math>360^\circ</math> and is supported on one large ring and a small bearing unit.</p> <p>The cylindrically shaped cabin is plugged into a hole in the central girder. To keep the patient horizontal during gantry rotation the cylindrical cabin can rotate around its axis.</p> <p>The PPS cantilevers into the beam, it can move laterally and forward as well as rotate <math>\pm 90^\circ</math> around the vertical axis.</p> <p>Direct access to the cabin is possible only when the gantry is in a horizontal position. Two vertically and laterally moving lifts secure access and exit (for the personnel) during all other gantry positions and in case of gantry breakdown (active redundancy).</p>	<p>A central rotating part (the cage) is carrying the <math>90^\circ</math> dipole whereas an <i>independent telescopic platform</i> functions as a <i>lateral patient cabin</i> supporting the PPS. Only <math>180^\circ</math> of <i>gantry rotation</i> are necessary because the PPS can rotate <math>360^\circ</math> around the (local) isocentre.</p> <p>During gantry rotation the platform (patient cabin) follows the rotational movement of the beam by travelling up to <math>\pm 5.5</math> m vertically and by telescoping 5.5 m horizontally.</p> <p>When the gantry is not in horizontal position access and exit to the cabin is via a (standard) lift. In case of an emergency the cabin can always be accessed via a staircase because the cabin <i>constantly</i> keeps contact to the lateral wall.</p>
<b>Structural principle</b>	<p>The precise deposition of the dose is achieved by mechanical rigidity of the whole gantry. Scanning magnets, dipole and the patient cabin are mounted on the same support structure. The correct gantry radius is guaranteed <i>mechanically</i>. The high precision structure secures intrinsically - to a certain extent - the correct position of the patient relative to the beam.</p> <p>The gantry transfers the loads towards one large front ring (outer diameter 6 m) and a small bearing unit at the rear. The support is statically determinate. Concrete consoles guide the forces to the (diaphragm) walls of the building.</p> <p>A large balanced girder gives support to the patient cabin through a large ring, in which the cylindrically-shaped, plugged-in cabin is free to rotate around its axis.</p>	<p>Magnet support and patient cabin are two independent structures. Moveable masses and lever arms are minimised, however, the correct "gantry radius" is not intrinsic but has to be secured by an alignment procedure: Minimum 4 cameras guarantee the correct <i>relative</i> position of the patient (-couch) with respect to the dipole by means of photogrammetry.</p> <p>Scanning magnets and dipole are positioned accurately by means of a high precision support structure ("cage") that transfers the loads towards one large front ring (outer diameter 4.5 m) and a small bearing unit at the rear. The support is statically determinate. Concrete consoles guide the forces to the (diaphragm-) walls of the building.</p> <p>A separate platform acts as a patient cabin carrying the PPS. For travelling vertically it uses two guiding rails on each side of the cabin that are fixed to the walls. Horizontal motion is achieved by telescoping forward. Because the PPS is aligned automatically towards the dipole, a moderate positioning accuracy of the cabin is sufficient.</p>

<b>Design characteristics</b>		
Structural weight	55 t including the patient cabin	30 t
Counterweight	28 t (13 t front ring, 15 t main girder)	the independent telescopic cabin around 20 t
Total load	146 t	28 t
Normal forces on bearings	2 × 600 kN, 1 × 400 kN	120 t + 20 t separate cabin
Systematic misalignment due to elastic deformations of the loaded structure	Because dipole and cabin are one single unit, the cabin (automatically) has to follow the movements (and deformations) of the dipole, hence restricting relative movements between the two to a negligible level. Additionally, the effects of some absolute misalignments are eased (e.g. shift along and rotation around the axial direction).	2 × 500 kN, 1 × 390 kN The separation of the patient cabin from the magnet support structure minimises absolute deformations of the latter. Deformations of the cabin are irrelevant because they will be automatically corrected by the PPS and its photogrammetric alignment system, which makes the couch follow all the deformations of the dipole (simulating a rigid connection).
Calculated maximum isocentre-deformation	±0.3 mm	±0.3 mm
-out of rotation plane	±0.7 mm (vertical and horizontal)	vertical 0.5 mm / horizontal negligible
-in plane	Large dimensions increase the susceptibility to temperature effects. Backlashes and free plays have to be expected in the gantry drive, the gantry support, the cabin drive, the PPS and in particular in the connection cabin ring – cabin.	Due to the minimum of mechanical connections, random errors are governed by the precision of the photogrammetric alignment system and the PPS.
Susceptibility to random errors	2300 m <sup>3</sup> ; long and narrow floor geometry; minimum height 19 m.	1700 m <sup>3</sup> ; minimum height 19 m; large consoles for gantry support necessary.
Gantry hall	The 360°-rotation requires having the maximum shielding wall thickness along both lateral walls and the entire ceiling. Two chicanes are required, which can be situated along the rear wall.	Because gantry rotation is only 180° the maximum shielding has to be applied to half of the building only. The chicane is situated in direction of the beam, requiring a very heavy design.
Shielding walls		
<b>Safety</b>		
Emergency access and evacuation	Apart from the gantry itself, two vertically <i>and</i> horizontally movable lifts provide a second, independent and redundant access system to the patient cabin. Gantry and lifts act as a rescue system for each other, the <i>evacuation procedures rely on the availability of one of the two systems in an emergency</i> . Additionally, the elevators can be lowered manually providing an emergency exit via a (maintenance) staircase leading to the bottom of the room.	The access to the cabin is possible at all times (via an emergency staircase). Emergency procedures do not have to rely on the availability of <i>any</i> mechanically driven system. In addition, a conventional lift provides (redundant) access to the cabin.
Collision protection	In case of a collision it is sufficient to break only the lightweight cabin immediately (and not the whole and heavy gantry) to avoid any additional relative movement. Unfortunately, this benefit can not be exhausted because there has to be a quick responding anti-collision system between the gantry and the two elevators requiring the possibility of rapid breaking also for the gantry (150 t).	Collision between the cabin (plus PPS) and the gantry has to be avoided requiring the possibility of rapid gantry stops (120 t). The situation can be ameliorated by the following guidelines: -The cage is only moved when the cabin is in retracted position -The cabin and / or the cage are only moved when the PPS is in reference (backward) position (highest priority). Additionally, as the gantry rotation is restricted to ±90° the gantry speed (and therefore the breaking capacity) can be relatively low.
<b>Manufacturing / Installation / Maintenance<sup>19</sup></b>	The large front ring (perimeter 19 m) and the inner surface of the cabin ring have to be machined very accurately and in the correct position towards each other.	Only 270° of the front ring (perimeter 11 m) have to be machined. Smaller dimensions facilitate manufacturing, transport and installation. Cabin can be easily installed in the lowest position. The cabin can partly be used as a service platform for maintenance work at the cage and the downstream part of the dipole.
<b>Alignment control</b>		
Components (differences only!)	Correct gantry radius is intrinsic, thus the relative position of the cabin towards the magnet is	The necessary relative positioning of the PPS towards the magnet is done with a

<sup>19</sup> In both gantry variants space is foreseen inside the gantry to access and maintain the dipole. Changing the dipole is possible without dismantling the gantry. For this purpose the dipole is moved (rotated) out of the structure into a small hall between the last quads and the gantry hall, where there is a removable lateral wall to enter during these rare occasions. Initial installation will also be via this "door".



Compensation of elastic deformations	secured mechanically and only the levelling of the cabin has to be controlled. Position and anti-collision control for the two lifts (travelling vertically <i>and</i> horizontally) with respect to the (rotating) cage necessary. A correction map has to be done for every gantry angle applying several PPS positions each.	photogrammetric system that has to be integrated. Rotational movements of the gantry have to be transformed into orthogonal movements of the cabin.  The correction map has to be done for every gantry angle.
<b>Ergonomics</b> Impression for the patient	Patient will hardly realise the gantry motion.	Patient will hardly realise the gantry motion. The rectangular and quite generous patient cabin will help not to intimidate the patient.
Treatment procedure	Staff enters the cabin with the patient, gantry rotates to treatment position, set-up, staff leaves via special lifts, irradiation, staff enters via special lift or: PPS is retracted, gantry is rotated back and staff enters, patient leaves.	Cage rotates to treatment position, meanwhile staff enters the cabin with the patient, cabin travels to treatment position, set-up, staff leaves via lift, irradiation, staff enters via lift or: PPS is retracted, platform is retracted and lifted or lowered back to access position, staff enters, patient leaves.
To irradiate two coplanar fields perpendicular to the body axis: Handling	PPS stays in place and the gantry is rotated to the other side (max. 180°)  Space in the patient cabin and the special lift is very restricted.	PPS is rotated (max. 180°), gantry (cage and cabin) does not move.  The large working space in the cabin facilitates handling and the set-up of the patient. The standard lift is not restricted in size and provides fast access to the cabin (maximum 5.5 m vertical movement)
<b>Flexibility</b> Expandability	No	The design offers – in a later stage – the principal possibility of having a second patient cabin opposite to the first one. They would be served by the gantry alternately.
Patient cabin	The small floor area in the patient cabin restricts the possibility of adding or changing medical equipment. In particular, the limited space and bearing capacity complicate a possible use of a PET inside the cabin. Changes in the cabin always affect the whole gantry (deformation, alignment, etc.).	The large patient cabin gives high flexibility in the arrangement and positioning of medical equipment and provides a generous working space. Cabin loads can be increased without affecting the alignment procedure and precision.
Design, construction and operation	A larger gantry radius would affect the structure adversely. The gantry precision is sensitive to a heavier dipole.	Gantry and cabin are independent structural systems and can – to a certain degree – be optimised, installed and tested separately. A larger gantry radius would effect the cabin only and could be realised without major modifications.
<b>Control system</b>		Photogrammetric system has to be included.

Table 4-1: Descriptive comparison of two possible variants for the Riesenrad ion gantry: the Centrally Supported Gantry (left) consisting of a single structural unit vs. the solution where the patient cabin is independent from the central cage that holds the dipole (Independent Telescopic Cabin Gantry; right).

### 4.6.2 Evaluation and Resolution

Having compared the two variants in question gives a sound basis for decision-making on what variant to proceed. Judging is based on the following criterions: the two strategic objectives, i.e. safety and flexibility, as well as technical performance and estimated cost effectiveness.

#### Safety and simplicity of design and operation

Generally, as variant 1 relies much more on the mechanics than variant 2, its complexity is comparatively low; interfaces are minimised, steering the gantry and controlling the position of the patient is facilitated. Unfortunately, the effort for the integration of the second access system - a lift with two axes of motion - counterbalances this advantage (collision protection!). The extreme stiffness of the magnet supporting part of variant 2 guarantees a very stable position of the magnet. The mechanical structure of variant 2 is simpler and more reliable, the photogrammetric system linking the two sub-structures is commercially available. The access problem in variant 1 is not solved satisfyingly (evacuation procedures rely on the availability of one of the two systems in any emergency)

whereas in variant 2 there is a convincing, efficient and simple solution, capable of overcoming potential acceptance problems.

**Flexibility**

The fact that it is still uncertain what kind of medical equipment will be present in the patient cabin clearly favours variant 2, its cabin can be easily adapted to changing requirements during operation and also late in the design phase.

**Technical performance**

Generally, the same quality of treatment can be achieved with both variants. The ergonomic situation is better with variant 2.

**Cost effectiveness**

Cost of the mechanical structure will be in the region of 4 MEuro, variant 2 can be expected to cost slightly less than variant 1. Concerning the building, variant 2 yields moderate cost savings of about 0.2 MEuro. It is extremely difficult to estimate the cost for the control system, but at least half the values claimed for the structure should be taken into consideration. Slightly higher software costs for variant 2 can be expected.

	Variant 1: Riesenrad gantry – Centrally supported	Variant 2 Riesenrad gantry – Independent cabin
Safety		
Simplicity of design and operation	+	0
Safety in case of an emergency	–	+
Flexibility	0	+
Technical performance	0	0
Cost	0	0

Table 4-2: Evaluation of the two gantry variants. Criteria are the strategic objectives.

Based on the statements above and Table 4-2, which summarises the arguments, *it is decided to investigate the concept of a Riesenrad gantry with an independent telescopic patient cabin in more detail* (leading to a preliminary design). This task is the objective of the following chapter.

*The Riesenrad Gantry with an Independent Telescopic Cabin for the patient is considered to give the best value for money and hence proposed for a preliminary design.*

## 5 Design of the Riesenrad Ion Gantry

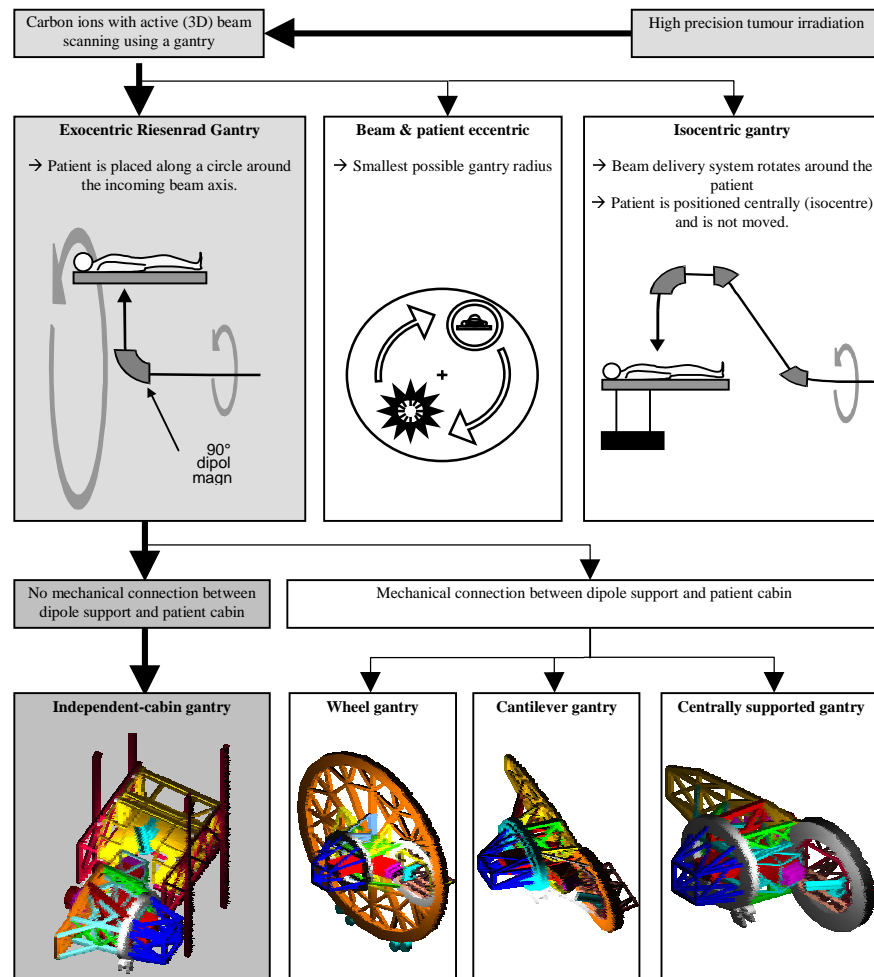


Figure 5-1: Principal steps in the decision-making process favouring the Riesenrad gantry with an independent telescopic patient cabin.

Several technical realisations of a Riesenrad gantry were investigated and compared in the previous chapter. The preferred solution with respect to the mechanical engineering, beam-optics and safety aspects is based on the so-called independent-cabin approach. Figure 5-1 briefly recalls the underlying decision-making process. The proposed design, which is schematically shown in Figure 5-2, has the following advantages:

- The central cage ("gantry") and the patient cabin are two independent structures. That is why, the central cage, which supports only the heavy bending magnet sitting on axis and its counter-balance weight, is relatively small and compact, hence reducing its moment of inertia and increasing its rigidity.
- The patient cabin is spacious and essentially unlimited in size, hence facilitating an easy patient handling and set-up, as well as the installation of auxiliary medical equipment.
- The patient cabin is a low-precision lift structure with a telescopic floor. Only the patient couch requires precise alignment, which can be done photogrammetrically with respect to the exit face of the bending magnet.
- The patient cabin has continuous contact with the lateral wall of the gantry hall and, by virtue of this, has permanent emergency access by a staircase.
- The inner volume of the gantry hall is small compared to other variants.

The objective of the current chapter is to prepare a preliminary design of the Riesenrad gantry, its auxiliary equipment and the building. The sections deal with the following crucial questions:

- How does the dipole itself deform under gravity? How are the rotator and the gantry quadrupoles supported and what deformation has to be expected there? (Section 5.1)
- How far can the elastic deformation of the central cage be reduced in a revised design? And what impact will temperature effects have on the structure? (Section 5.2)
- What does the interface cage - patient cabin look like? (Section 5.3)
- What treatment angles can be achieved? What flexibility does the design offer? What is the exact sequence of treatment procedure and gantry motions? (Section 5.4)
- How do the deformations of the structures affect the actual ion beam passing through? And what misalignment has to be expected for the beam in the isocentre, where its energy is eventually deposited? (Section 5.5)
- Which patient positioning, set-up and alignment control methods seem suited? (Section 5.6)
- What are the requirements for the gantry hall and how is the Riesenrad gantry integrated into the planned therapy facility? (Section 5.7)
- How much will it cost? (Section 5.8)

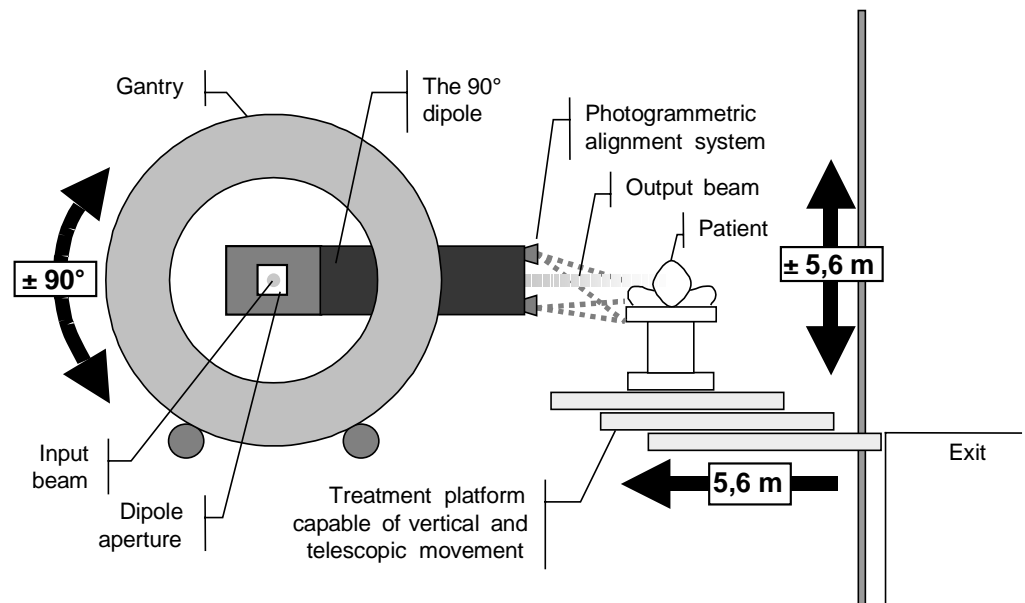


Figure 5-2: The Riesenrad Gantry with an Independent Telescopic Cabin. The patient cabin is positioned corresponding to a particular angle of gantry rotation by vertical translation and horizontal telescopic movement. The gantry supporting the dipole can rotate  $\pm 90^\circ$  and the patient couch can rotate  $360^\circ$  (horizontal plane) so as to achieve effectively any treatment angle.

## 5.1 Quadrupoles and the $90^\circ$ Dipole

The structural design of the gantry is largely influenced by the arrangement of the beam transport system, which is explained in detail in the Proton-Ion Medical Machine Study (PIMMS; see Section 3.3). Relevant for the mechanical design is the fact that upstream of the main dipole, the beam passes through a rotatable set of seven quadrupoles (a so-called "rotator"), which turns with half the angle of the gantry, followed by a set of four quadrupoles ("gantry quadrupoles") turning with the same angle as the gantry.

*Gantry and rotator quadrupoles are supported by two separate, very stiff structures.*

From the mechanical point of view, the rotator and the gantry-quads structure are similar items. In a preliminary design, both are foreseen to be girders about 10 m long with a

square cross-section (1.2 m diagonal, see Figure 5-3). The "flanges" are rectangular beams (RHS 250/150/8), the webs will be braced by RHS 100/100/10 (or equally stiff members) in order to facilitate access to the quads and the vacuum chamber. The fixations of the quadrupoles need to be adjustable with 6 degrees of freedom. Each structure has two bearings (simply supported beam) at optimal distances to minimise elastic deformation. At the bearings, a ring is welded around the girder. Support to the ring is given - statically determinate - by a set of two rollers. The weight of each structure is about 2 tons, not taking into account the quadrupoles, which are around 170 kg each. The maximum elastic sagging is lower than 0.05 mm. Temperature fluctuations of 1 K uniform and 2 K along the axis are responsible for a vertical deformations of 0.04 mm and an X-rotation of about 0.007 mrad.

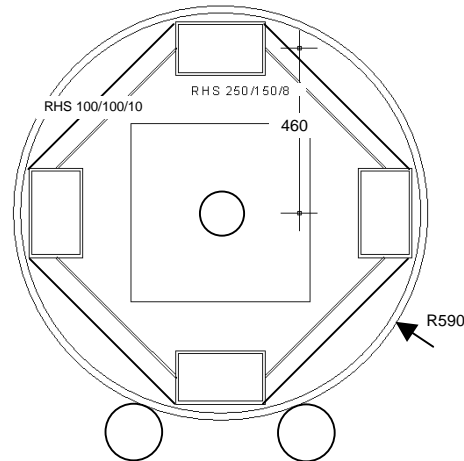


Figure 5-3: Cross-section of a rotating support structure for the quadrupoles. The trussed girder is about 10 m long, supported statically determinate on two rings with two rollers each. Dimensions are in mm.

Crucial input information for the structural design of the gantry are the relevant parameters of the 90° dipole supported by the central cage, which were listed in Table 3-2. An important aspect, however, is the mechanical behaviour of the magnet itself.

*What are the stiffness properties of the 90° dipole?*

The 90° dipole is made out of two half-yokes. Each half-yoke comprises several laminated segments (2 mm thick laminations). A segment is constructed by gluing the laminations and then machining the block to the correct "wedge" angle. When assembling a half-yoke, the segments are first glued and then welded between thick end plates by tie bars. The mechanical stiffness properties of the glue are low compared to iron<sup>20</sup>. Their effect on the rigidity of the entire half-yoke depends on the number of laminations (joints), hence the thickness of the laminations should be as high as reasonably achievable in the punching process without deteriorating the punching precision. For the current design of the Riesenrad dipole a lamination thickness of 2 mm was assumed, however, a (beneficial) increase of that value seems possible. As a result the iron half-yoke shows a (comparatively low) shear and Young's modulus of  $G = 27000 \text{ N/mm}^2$  and  $E = 114000 \text{ N/mm}^2$  respectively<sup>21</sup> (compared to  $81000 \text{ N/mm}^2$  and  $210000 \text{ N/mm}^2$  for a solid iron yoke).

In order to hold the two half-yokes together and to increase the stiffness of the magnet, the latter is reinforced by a "corset" of tie bars and cover plates (see Figure 5-4). Note the importance of the lateral cover plates: the more shear force they take, the more bending-stiffness can be expected from the cross-section (then acting as a composite system). Therefore, these lateral plates should not be substituted by an X- or frame bracing. Depending on the final fixation of the dipole inside the gantry, the top and bottom cover plates could alternatively be welded directly onto the laminations. Another possible modification would be to bolt the two magnet halves together to facilitate the changing of the vacuum chamber or the coils in case of failure. However, space limitations at the interface between dipole and front ring of the gantry favour the welded design.

<sup>20</sup> For example Araldit 2014 (two-component glue based on epoxy resin): Shear modulus  $G \approx 1000 \text{ N/mm}^2$ , Young's modulus  $E \approx 6000 \text{ N/mm}^2$  at room temperature.

<sup>21</sup> The average stiffness moduli depend on the ratio between the thickness of the lamination towards the thickness of the glued joint. The latter was assumed to be 0.05 mm.

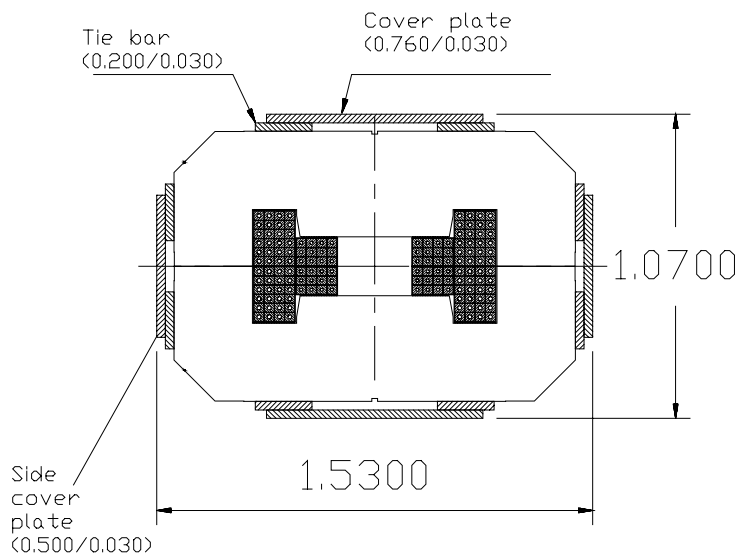


Figure 5-4: Cross-section of the 90° dipole. Dimensions are in metres. Note the additional side and top cover plates that have been added to increase its mechanical rigidity.

It is now possible to model the cross-section - which is not at all straightforward since it consists of three parts having different stiffness properties - and eventually the entire dipole in a structural analysis in order to investigate its primary elastic deformation and the load-sharing between the different parts. The "corset" adds ~5 t to the weight of the dipole, while taking approximately one third of its bending and shear force. Varying the two supports of the dipole inside the gantry structure showed that the optimum support positions were around 1 m from the two faces of the dipole. Supported at these positions, *the reinforced dipole could be regarded as being virtually rigid* (maximum deformations smaller than 0.03 mm) and thus performing rigid body movements only.

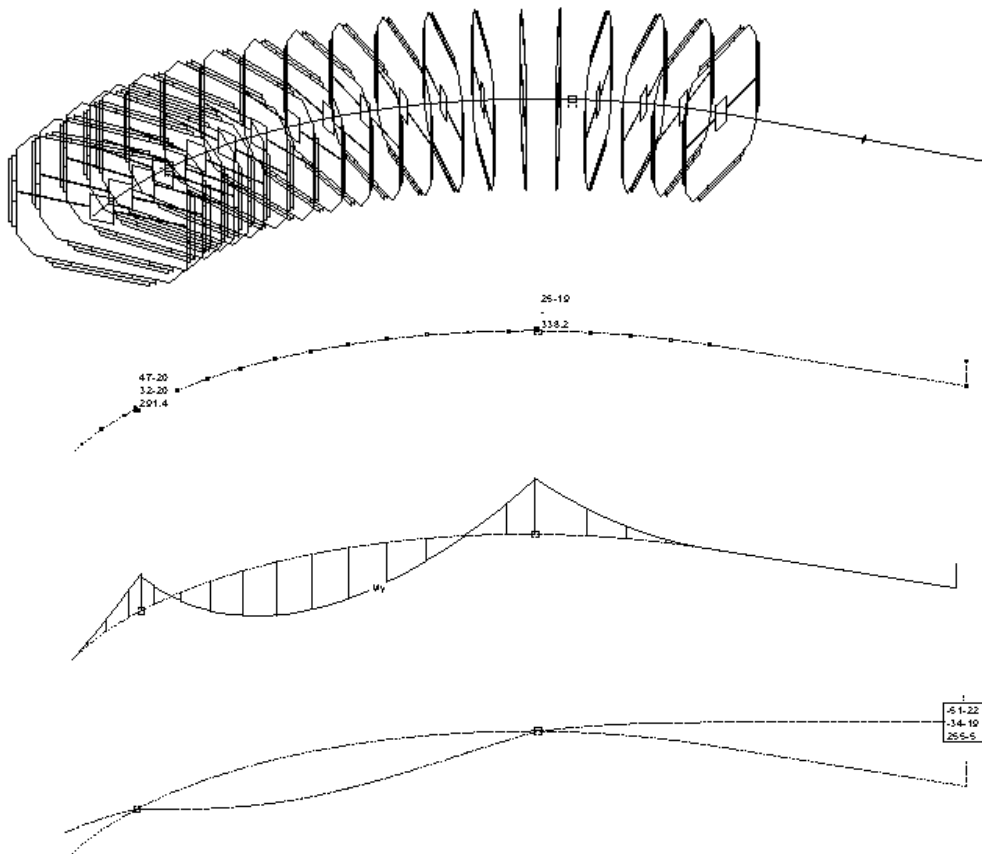


Figure 5-5: Structural analysis of the dipole showing the static model, reaction forces (X,Y,Z in kN), bending moment distribution and deformation plot (values in cm).

## 5.2 The Central Cage

The central cage of the Riesenrad gantry supports the three scanning magnets (1.5 t) and the large 90° dipole (62 t). The total weight is ~127 t, 23 t of which are due to the counterweight. The design of the central cage is driven by the desire to minimise sagging of the dipole no matter what gantry position is considered. The principal elements of the cage are shown in Figure 5-6 (left part of the gantry). Compared to the preliminary design presented in the previous chapter, several improvements have been introduced. The most important modification - although hardly visible - concerns the downstream support of the dipole by two "balancing tongs". This idea allows a partial compensation of vertical deformations.

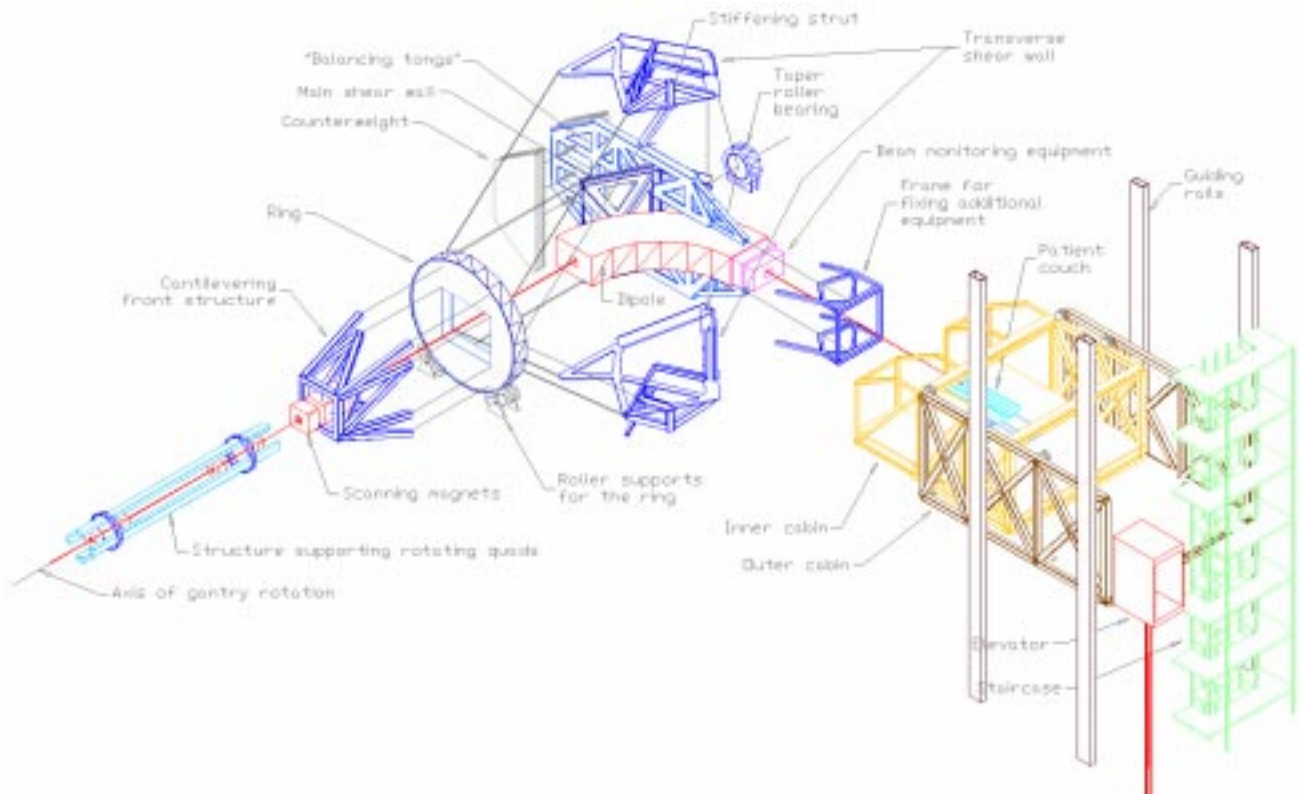


Figure 5-6: Principal elements of the Riesenrad gantry structure. The cage supporting the heavy dipole is shown on the left, the independent patient cabin on the right.

### 5.2.1 Structural Design of the Central Cage

#### 5.2.1.1 The Principal Elements

As mentioned above the principal task (and difficulty) of the central cage is to provide two equally stiff support points for the 90° dipole, the first one - quite obvious - is a stiffened ring supported by two pairs of rollers. The heavy weight of the dipole will be transferred to the ring by adjustable fixations along the top and the bottom of the dipole - depending on the angle of gantry rotation either by normal forces (horizontal position) or shear forces (vertical).

*The transverse shear walls*

This is not the case for the second dipole support, which is situated about one meter upstream from the exit face of the magnet. Let us consider the vertical gantry position first, since this is easier to cope with. When the dipole points vertically upwards or downwards, it can be flanked by two vertical "walls" - acting as slabs or shear walls - that span from the front ring to a rear support that rests on a console of the building wall. The free distance

between the two walls is 1.5 m so that the dipole and in particular its bent-up coils at the ends fit through. The large "height" of the shear walls gives a high bending resistance of the cage. In Figure 5-6 the so called *transverse shear walls* are represented by plane trusses, the final version will see these walls more closed (each of them consisting of two 20 mm sheets, 30 cm apart and stiffened) - thus resembling a more classical shear wall design as indicated in Figure 5-7 (plan) and Figure 5-9 (section).

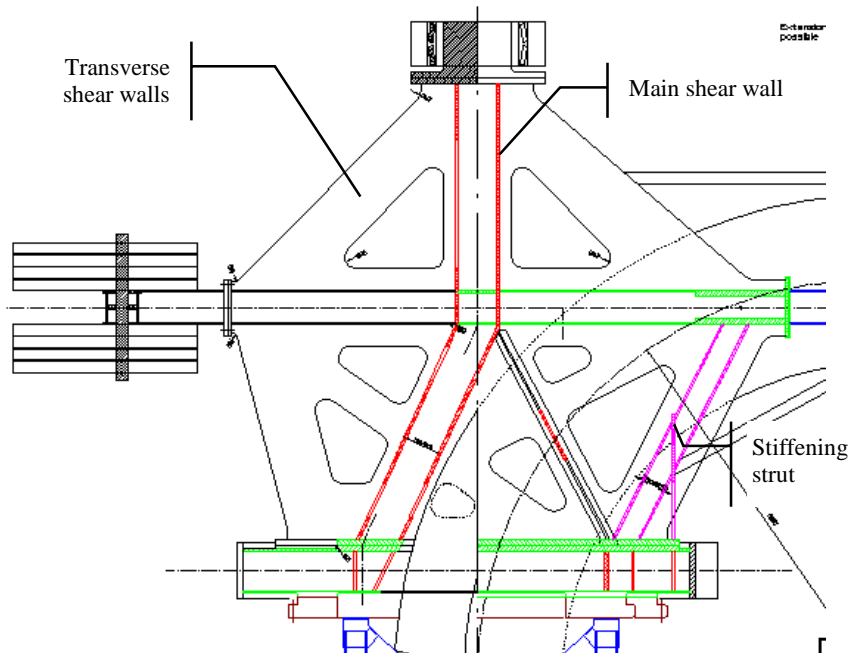


Figure 5-7: Horizontal gantry section parallel to the transverse shear walls (horizontal gantry position). Holes are cut into the sheets where structurally feasible in order to reduce the dead load and facilitate the assembly process (welding).

For the other extreme gantry position when the dipole is in horizontal position, a more sophisticated approach for the downstream dipole support had to be found, since the dipole's presence prohibits large shear walls spanning between two supports. Therefore, in the preliminary design, two triangular-shaped girders span in direction of the gantry axis above and below the dipole. Certainly, the rigidity of those girders was limited due to their restricted height. To further reduce deformations, a new approach using a pair of "balancing tongs" is introduced: the principle behind is that a very small (stabilising) force can alter the equilibrium position of a centrally supported and balanced girder (see Figure 5-8).

*The balancing tongs*

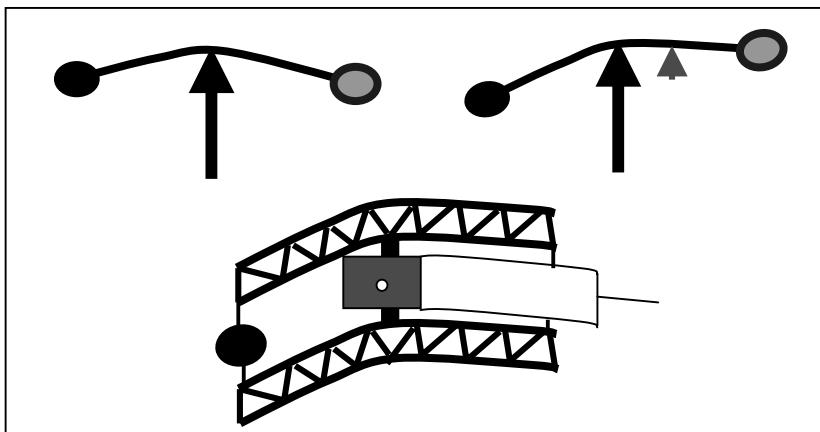


Figure 5-8: The principle of a centrally supported, balanced girder (left). A small force can easily alter its equilibrium position (right). This principle can be applied to compensate deformations on the dipole side of the cage (bottom).

*The stiffening struts guide the dipole side of the balanced tongs in the desired position.*

In the cage, the girder is loaded by a certain portion of the weight of the dipole (on the right side) and the equivalent counterweight (on the left) The central support of the girder is provided by the *main shear wall* spanning between the ring and the rear support of the cage. The stabilising force comes from the so-called *stiffening struts*, which cantilever from the front ring (see Figure 5-7). This system is doubled: one girder below and one above the dipole. Both together hold the magnet like a pair of structural tongs. These truss-like tongs transfer their balanced load via the central diagonals and the inner girder onto the main shear wall. The outer girder is free to glide over the main shear wall (i.e. no mechanical



connection) in order to provide the required rotation capability of the tongs at their central support (see Figure 5-9). With such an arrangement, vertical elastic deformations on the dipole-side of the structure, and hence at the local isocentre, can be partly compensated (by a corresponding increase on the counterweight side). The achievable degree depends on the stiffness of the struts, the stiffness of the transverse shear walls (perpendicular to their principal plane) and on the stiffness of the joints between main shear wall and tongs.

Cross-sections of the members of the tongs are in general RHS 300/300/16. The counterweight (23 t) is made of several steel plates that can be lifted by a small crane and attached on both sides of the tongs. If necessary, a frame for holding additional equipment (e.g. for beam monitoring or medical imaging) in front of the exit face of the dipole can be added to the structure. However, it seems more likely that such a frame - if not too heavy - will be directly bolted to the magnet face. Of the two-metre drift between dipole aperture and the isocentre, 80 cm are currently foreseen for the installation of monitoring equipment, the remaining distance has to be kept clear. Unfortunately, part of this space is occupied by the coils that extend out of the yoke, hence this point should be addressed carefully in a detailed design.

*The fixation of the dipole to the cage*

Both, ring and the pair of balancing tongs, support the dipole on the bottom and at the top. These 4 fixations must permit the adjustment of the dipole's position in all 6 degrees of freedom while being fully loaded. It is foreseen to use a combination of U-shaped profiles (the long dimension pointing towards the isocentre) that are pre-stressed by pairs of spindles, one pair for each dimension. The system is roughly indicated in Figure 5-9.

*The main shear wall*

Similar to the transverse shear walls, the *main shear wall* is kind of a box - made out of two steel sheets (25 mm thick) approximately 40 cm apart. Large holes were cut into the sheets where structurally reasonable in order to save weight and provide access for the welding of stiffening ribs in-between the sheets.

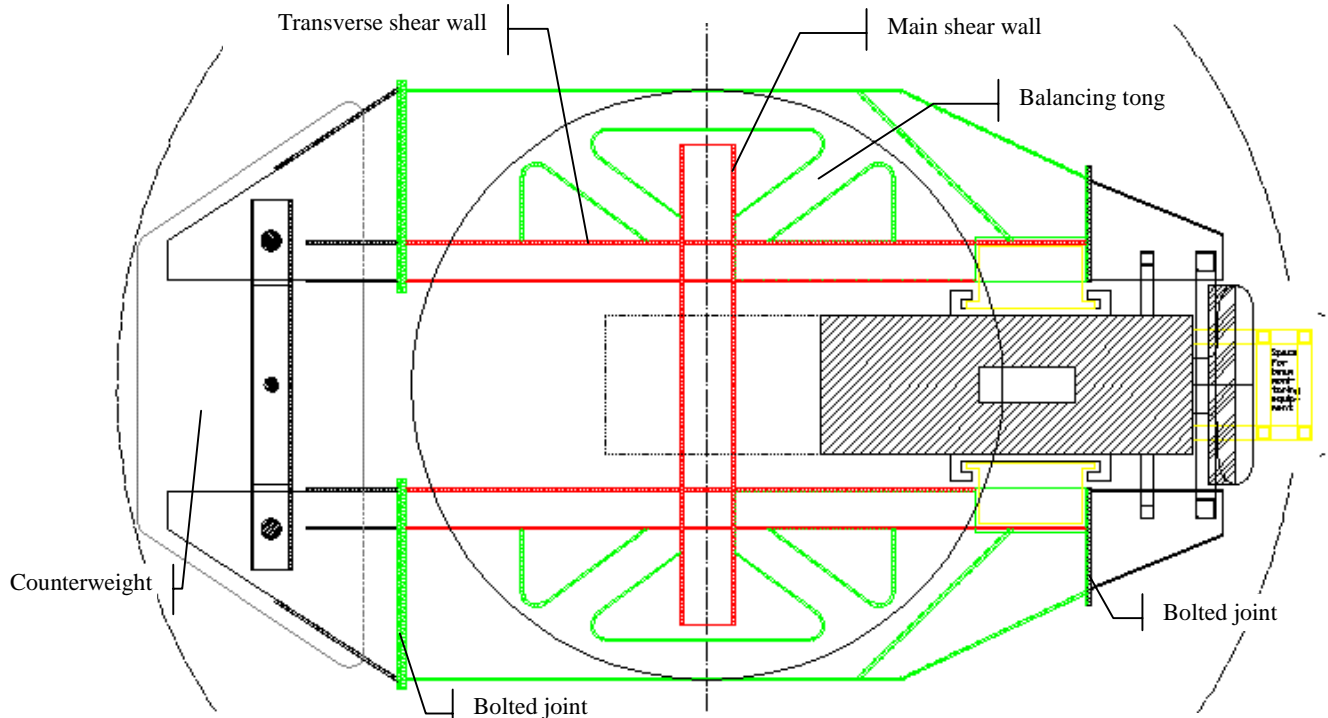


Figure 5-9: Vertical section through the balancing tongs of the cage (horizontal gantry position). For better orientation the shape of the front ring is indicated. The vertical box in the centre is the main shear wall, to which only the inner girder of each tong is welded. The inner girders also form part of the transverse shear walls. The type of fixation of the dipole to the tongs is schematically indicated. The outer prolongation of the tongs on the right hand side is optional. The structure farthest right is bolted to the dipole face and cantilevers into the patient cabin, giving support to the beam monitoring equipment and the photogrammetric cameras.

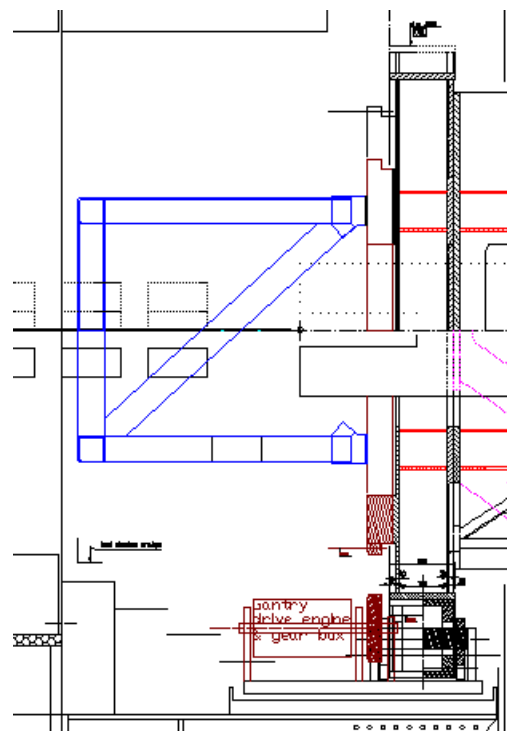
*The ring*

The front ring ( $\varnothing$  4.3 m, thickness 0.5 m) is in fact an extremely rigid cylindrical box with a relatively small "window" of 1.85 m  $\times$  1.5 m in the middle to allow the dipole to pass through. The thickness of the rolling surface is 50 mm in order to minimise local deformation in the region of contact to the 4 supporting rollers. The rolling surface has to be machined very precisely (tolerance for circular run-out  $<$  0.1 mm) since any deviation there will be seen directly by the dipole and hence the beam. As the gantry only turns  $\pm 90^\circ$ , only  $280^\circ$  of the ring have to be machined. The inner "flange" of the "beam" forming the ring is made out of sheets (500 mm  $\times$  50 mm) surrounding the window for the dipole. The ring, which is in fact a cylindrical box (or disk), is stiffened by several cross members (400 mm  $\times$  50 mm), which assist to transfer the forces from the various connected shear walls and trusses into the front and rear "web" of the ring and guide them to the roller supports. Generally, the webs are 20 mm thick, however, where connections appear, the thickness is increased to 50 mm (Figure 5-10).

*The drive*

The gantry will be rotated by a *chain drive*, that applies its force to a toothed wheel ( $\varnothing$  3.6 m, weight  $\approx$  4 t) that is bolted to the ring (Figure 5-10). The engine will be placed on the same base plate as the roller supports of the front ring. Since geometry is constrained, the chain is a triplex chain (DIN 32 B-3) having an ultimate load of 670 kN. This capacity is sufficient to break the gantry in case of an emergency within 0.25 seconds, which equals a movement of approximately 10 cm at the interface between cage and cabin. The applied safety factor is about 5. In addition, the chain can prevent the gantry from turning when only half of the counterweight is put on with a safety factor of about 3. Nevertheless, a cross girder spanning between the two walls of the gantry hall will hold the gantry during assembling. The fixation height of the engine and the gear box can be adjusted to allow chain tightening.

*The front structure to hold the scanning magnets*



A stiff *front structure* made out of RHS 200/200/10 cross-sections cantilevers 3 m from the centre of the ring towards the rotator. Its opening of about 2 m  $\times$  1.6 m provides space to support the three scanning magnets and the cable drum to roll on and off all the cabling (power, cooling water and data) during gantry rotation. When a detailed design of the scanning magnets and the necessary fixation beams is available in the future, one will probably fit the front structure more tightly to the actual needs.

Figure 5-10: Lateral section through the front structure, the large toothed wheel for the drive, the ring and a roller to support the ring. Rollers and drive rest on a thick steel plate that can be adjusted in all three dimensions.

**5.2.1.2 Support Considerations**

The high precision requirements for the gantry call for a *statically determinate* support in order to

- guarantee a distinct and known distribution of reaction forces, independent of the overall stiffness parameters of the cage, and hence

- avoid any constraints leading to (unknown) induced stresses or even plastic deformation.

When regarding the bearing designs of existing proton gantries, one could be surprised by the various approaches found (see Chapter 2) which show considerably difference in effort and design – namely the permitted degrees of freedom of the bearings. For the Riesenrad gantry, the choice of bearings was lead by the desire to

- use – as far as possible – industrial available components.
- avoid large support structures and restrict – if possible – the amount of self-aligning rollers for the ring to four (thus saving space and cost).

*The rear support is a fixed bearing.*

The rear support of the cage is a fixed support consisting of paired single-row taper roller bearings in X-arrangement, capable of taking radial and axial forces. By machining the intermediate ring one can reduce the axial play to virtually zero or even apply some pre-stress.

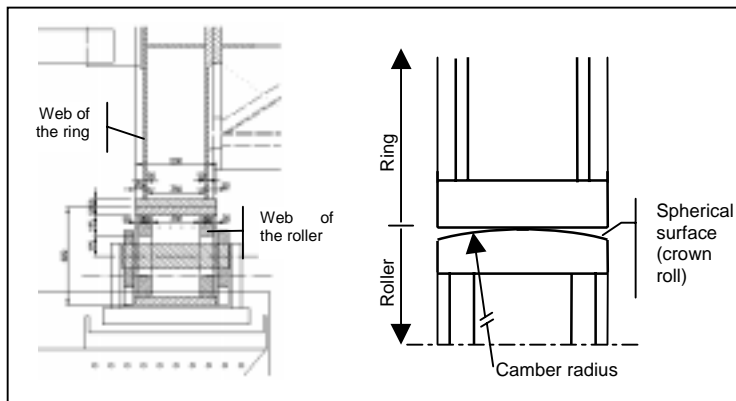


Figure 5-11: Ring-roller interface (left) and a schematic sketch of the spherical surface of the roller (right) thus having a convex contour or "barrel" shape. The "intensity" of this crown roll is defined by a camber radius.

The front ring is supported radially only by two pairs of self-aligning rollers of 0.6 m diameter that have to withstand a radial force of 240 kN each. This relatively high load raises two questions:

- Can the stress distribution on the contact surface be made smooth enough so that no plastic deformation will occur?
- What are the effects of a (very small) sagging of the cage (around the X-axis, i.e. between its two supports)?

*Four barrel shaped rollers support the front ring*

The approach chosen to deal with these problems was to give the roller surface a crown roll, i.e. a slight curvature in the axial planes to achieve some kind of barrel shape (see Figure 5-11). The establishment of the most suited radius as well as the check on the occurring stresses was performed with a finite element (FE) analysis, which is reported in Annex C. It was found that a camber radius of around 60 m - perhaps slightly higher – seems to give a maximised contact area while still keeping contact stresses comparatively uniform. The curvature also allows for a small rotation (caused by sagging of the cage) without generating large stress concentrations on the edges of the rollers.

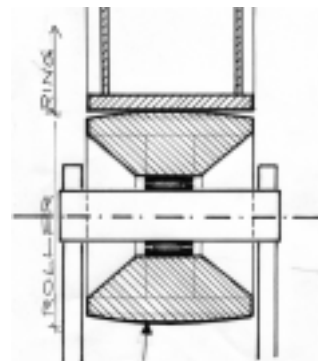


Figure 5-12: Variant for the support roller of the front ring using a toroidal roller bearing that would allow axial and rotational movements.

No axial play for the rollers is foreseen; it is assumed that any axial elongation of the cage will be compensated by a small relative displacement between ring and roller during gantry

rotation. An interesting alternative to the "classical" design of a roller (supported by two roller bearings along its axis) which provides also axial freedom would be to use only one so-called toroidal roller bearing per roller. Such a bearing combines very high load capacity with a small section height and a (limited) capability to cope with axial *and* rotational displacements of the axis. Therefore, a roller-arrangement as shown in Figure 5-12 would always guarantee a stable and constant stress distribution on the ring-roller interface.

Both, front and rear support of the cage rest on consoles that transfer the forces to the diaphragm walls of the gantry hall.

### 5.2.1.3 Cage Assembly

The structure of the entire cage consists of 8 major pieces, which are welded structures that can be brought to the site separately and which are bolted together on-site:

- rear bearing unit (pair of single-row taper roller bearings)
- body of the cage
- counterweight
- frame to hold the beam monitoring equipment and the cameras
- ring
- base plate with the roller supports and the drive
- toothed wheel
- front structure

*The cage is made out of 8 principal welded elements that are bolted together on-site*

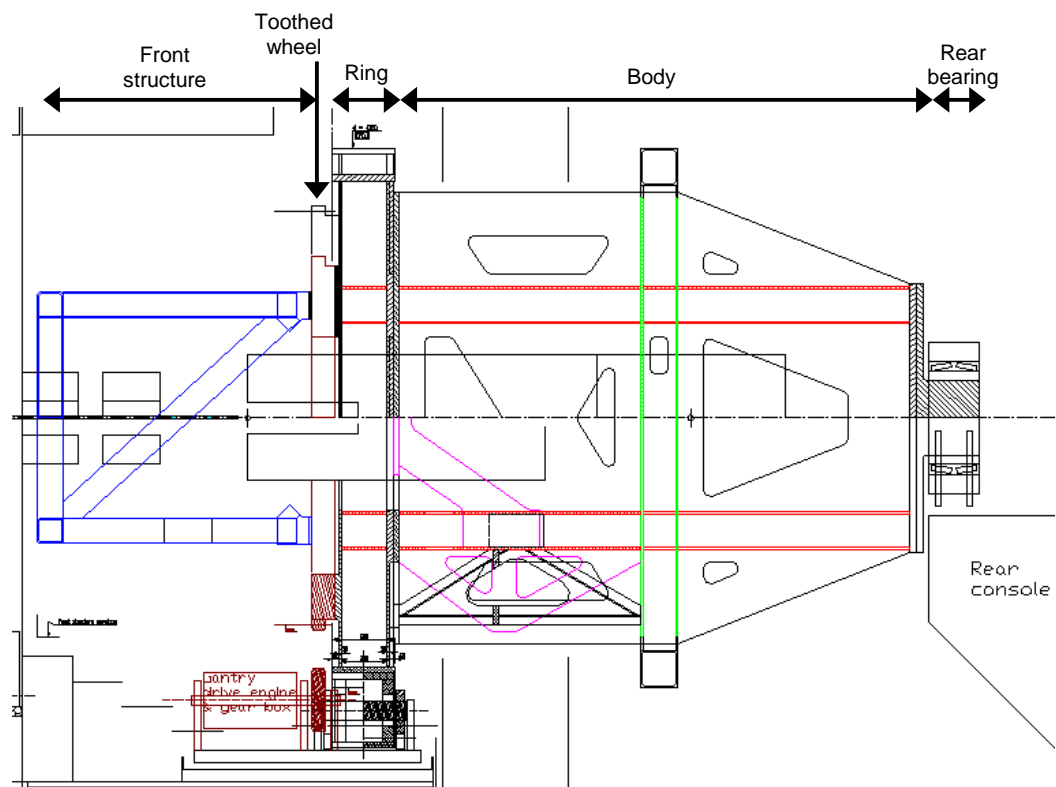


Figure 5-13: Side view of the cage showing its principal pieces that have to be bolted together (machined contact surfaces).

The contact surfaces between two pieces have to be machined very accurately; this is of particular importance for the interface ring-body and body-rear bearing (tolerance for perpendicularity 0.1 mm). The cage gains stability as soon as the body is connected to the ring and to the rear support. Depending on the access possibilities to the gantry hall, this "core" of the cage is either lowered from top (removable ceiling) onto the pre-installed base plate, or - preferably - it is shifted in laterally (together with the base plate) along the front

and rear console towards its final position. The next step will see the fixation of the counterweight structure, i.e. the outer part of the tongs on the left-hand side in Figure 5-9, followed by the insertion of the dipole and the subsequent mounting of the counterweight. After the dipole has been accurately fixed to the cage, the toothed wheel of the chain drive and the front structure will be bolted to the ring. Finally, the scanning magnets and the other remaining parts will be added.

Removing the dipole is only possible after the scanning magnets and the front structure have been dismantled.

### 5.2.2 Structural Analysis of the Central Cage

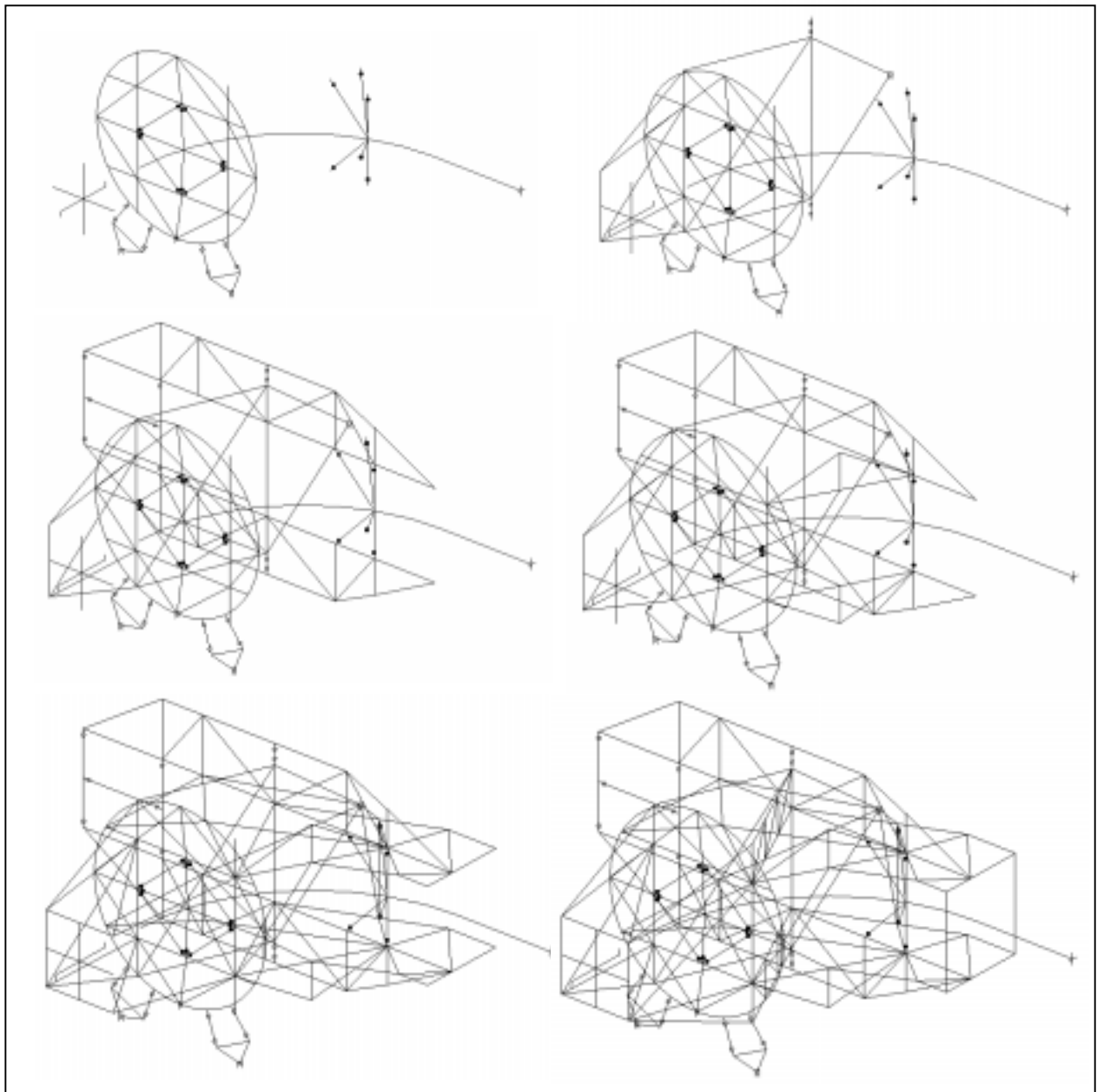


Figure 5-14: The development of the static system of the central cage. The upper left image shows the ring, its support modelling, and the central beam line with the final (mass-less) beam to the local isocentre. Successively, the main shear wall, the two tongs, the stiffening struts, the transverse shear walls and the rest of the front structure is added to form the entire model, which is shown at the bottom, right.

The structural analysis was performed with the software CUBUS (1998) using the modules Statik-3 (analysis of space frames) and Fagus-3 (analysis of cross-sections). The steel grade is S 355<sup>22</sup>. In the static model, as it is shown in Figure 5-14 and Figure 5-15, all shear walls were modelled as trusses of equal or slightly lower stiffness. The exact geometry, member cross-sections and properties as well as the calculated member forces and absolute deformations due to the various load cases can be found in Annex B (floppy disk).

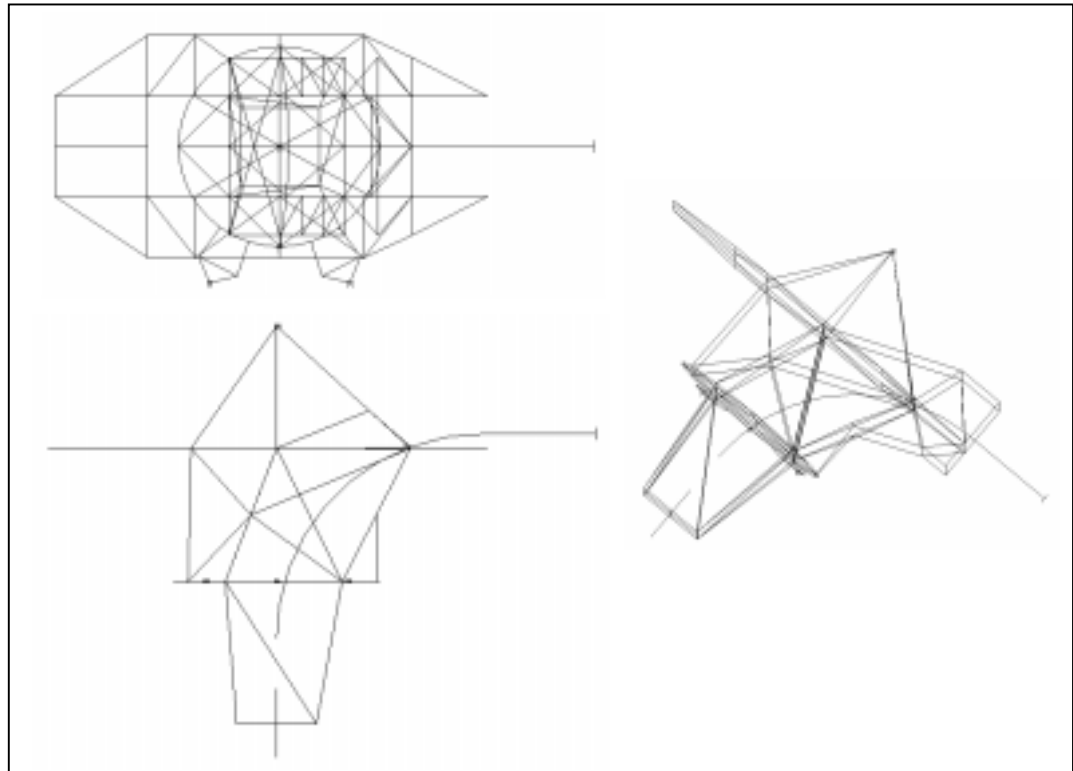


Figure 5-15: Top, front and axonometric view of the static model of the cage (horizontal position). Support points are marked as little squares.

All welded and bolted joints were modelled as being rigid. Shear deformations were generally taken into account (thus increasing the deformations by approx. 10%). Because of the slow rotation of the gantry, the structure was analysed as being static. A mass-less beam cantilevering from the 90° dipole aperture indicated the displacement of the local isocentre. The four roller supports of the ring were modelled accurately by pendulum-beams that transmit their normal force to a very stiff triangle that has a fixed support at the bottom (see Figure 5-14 top left). As a consequence, the total load is shared uniformly by the four rollers.

In order not to have a kinematic model of the structure (which is actually *meant* to rotate) an additional support at the bottom of the ring was added taking circumferential forces only and hence modelling – in a way – the chain drive. During the analysis, the counterweight was successively increased till a more or less balanced condition was reached and the additional support was free of load.

Due to the high-precision requirements, the mechanical design has been governed by the permissible deformations and, generally, no problems concerning maximum stress and stability were encountered (i.e. a deformation-driven design). Actual stress levels in the members rarely exceed 10 N/mm<sup>2</sup>, only a few highly-loaded struts of the tongs show

<sup>22</sup> S 355 (DIN EN 10025) – equal to Fe 510 (EC 3) – is a construction steel with a characteristic value for the yield strength of 355 N/mm<sup>2</sup> and 335 N/mm<sup>2</sup>, regarding member thicknesses up to 40 mm and above respectively. Young's modulus is 210000 N/mm<sup>2</sup>.

maximum (axial) stresses of about  $20 \text{ N/mm}^2$ . Consequently, the analysis was carried out applying safety factors of 1.0 for resistances and loads.

The applied loads were the following:

- Gravity on all members except from the beam line and the rollers (334 kN).
- A (very small) counterweight of 4 kN on the outer left-hand side of the ring.
- The principal counterweight of 222 kN at the outer edge of the tongs (i.e. with a distance of 4 m from the axis).
- Two times 7.5 kN on the front edge of the front structure (i.e. 2.5 m from the centre of the ring) representing the scanning magnets, cables etc.
- Gravity on the dipole, which was modelled in a slightly simpler way than in the detailed analysis reported on the previous section (nevertheless its - limited - elasticity was taken into account). Total weight was assumed to be 665 kN, i.e. about 45 kN heavier than the real one.
- In addition, various different types of temperature loads on the structure and the dipole.

The heavy 4-ton toothed wheel for the drive was not considered at that stage; it will increase the load on the rollers correspondingly. One also has to consider that the final design of the cage will show some increase in weight due to a stiffer design (mainly in the front ring) and due to auxiliary equipment in the gantry, which is estimated to sum up to around 7 t. Figure 5-16 indicates the reaction forces encountered for the fully loaded cage. One can summarise that approximately half of the dipole's weight (340 kN) is taken directly by the front ring. The other half (325 kN) is supported by the tongs, transferred to the main shear wall where the majority of the load is directed to the rear support (300 kN), the rest is taken by the front ring. The values remain constant during gantry rotation.

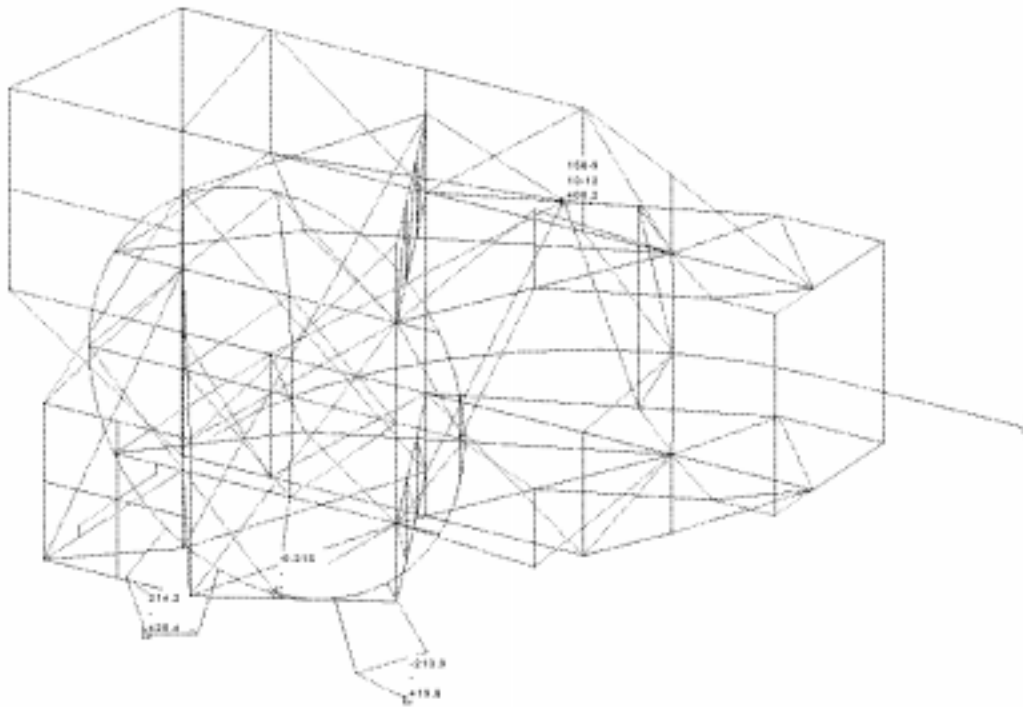


Figure 5-16 indicates the reaction forces in kN at the supports in X, Y and Z direction (room co-ordinates). The values remain constant during gantry rotation. The circumferential reaction force at the ring is nearly zero, hence the structure is well balanced. Each member modelling one of the four rollers withstands a compression force of 239 kN.

### 5.2.2.1 Elastic Deformation

Based on the results of the structural analysis, the effect of elastic deformations due to gravity has been estimated. Note the definition of the global (room) co-ordinate system  $[X, Y, Z]$  where  $X$  and  $Y$  are the horizontal axes ( $Y$  being aligned with the axis of the incoming beam) and  $Z$  is the vertical axis pointing upwards. Deformations are expressed in the room co-ordinate system as deflections of the mechanical axis of the beam transport system with respect to its ideal straight-line shape.

Figure 5-17 gives a qualitative idea of the deformation of the cage for three different gantry angles. In total 13 angular positions were analysed. Figure 5-18 demonstrates the effect of the intrinsic deformation compensation for horizontal gantry positions: the beam line towards the local isocentre rests more or less horizontal.

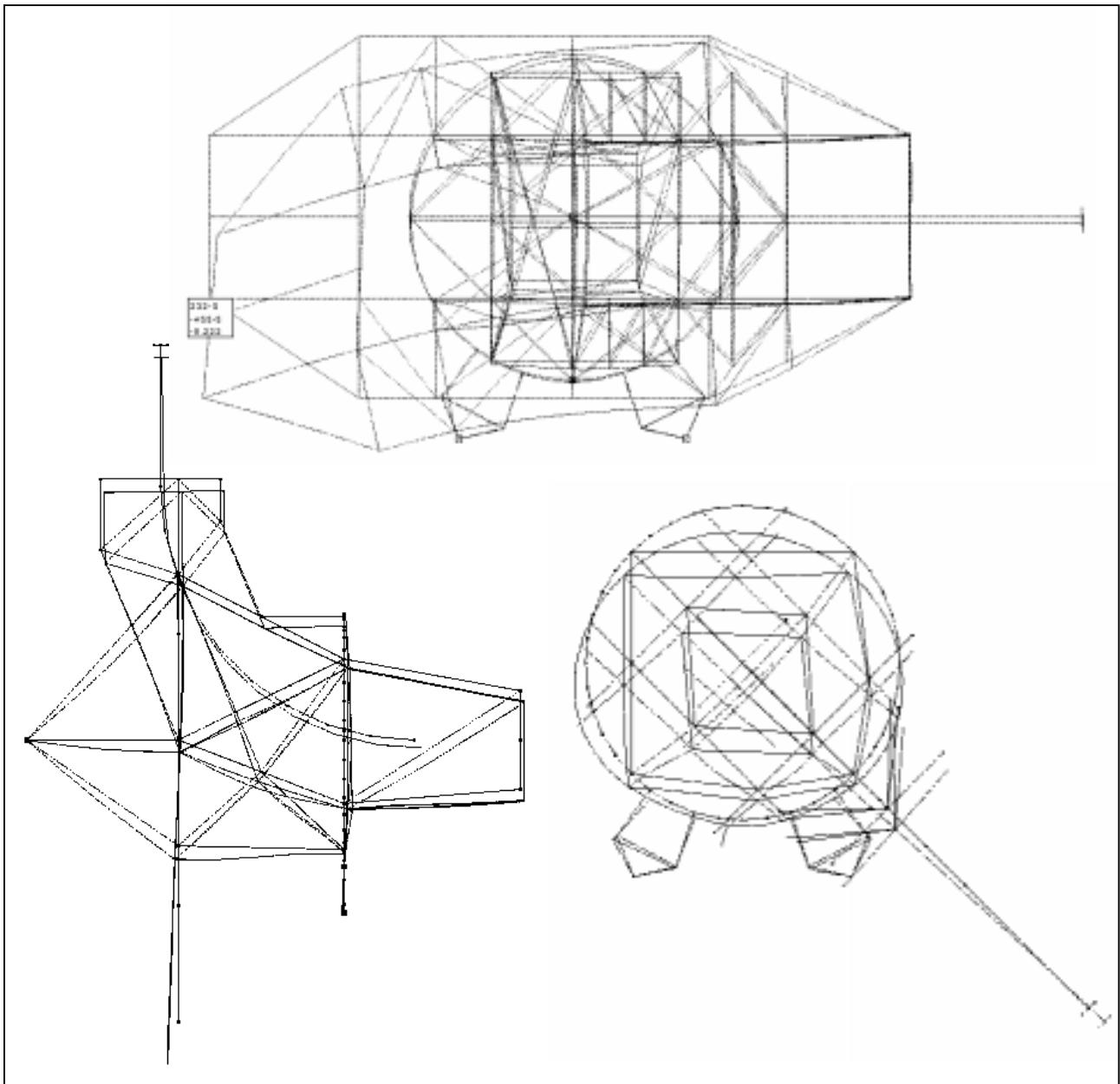


Figure 5-17: Deformation plot of the fully loaded cage in horizontal gantry position (front view, 500-fold enlargement, values in cm), vertical position pointing upwards (side view, 1000-fold), and 45° position (front view, ring and beam line only, 2000-fold).

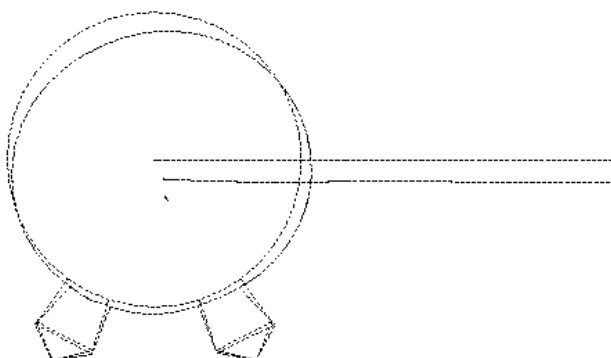


Figure 5-18: Plot of the elastic deformation (and the original geometry) of the cage (horizontal position). Only the ring and the beam line are shown. One can see the uniform sagging of the two, showing that the (commonly expected) additional deformation of the local isocentre is successfully compensated.



Figure 5-19 and Figure 5-20 illustrate the elastic deformation for the gantry isocentre and the beam transport system along the gantry, respectively. Note that the mechanically deformed path in Figure 5-20 represents *merely* the sagging of the beam transport elements but does not take into account any ion-optical consequences of these deformations. The ion-optical effect is studied separately and the results are reported in Section 5.5.

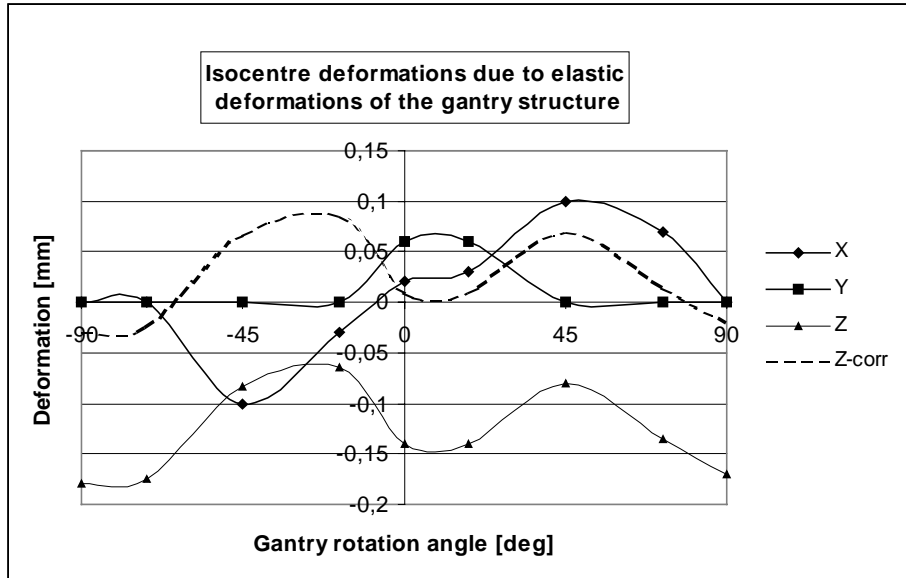


Figure 5-19: Calculated displacements of the (mechanical) isocentre due to the elastic deformation of the gantry structure in global room coordinates as a function of the angle of gantry rotation with respect to the ideal geometry. Resulting ion-optical effects were ignored.

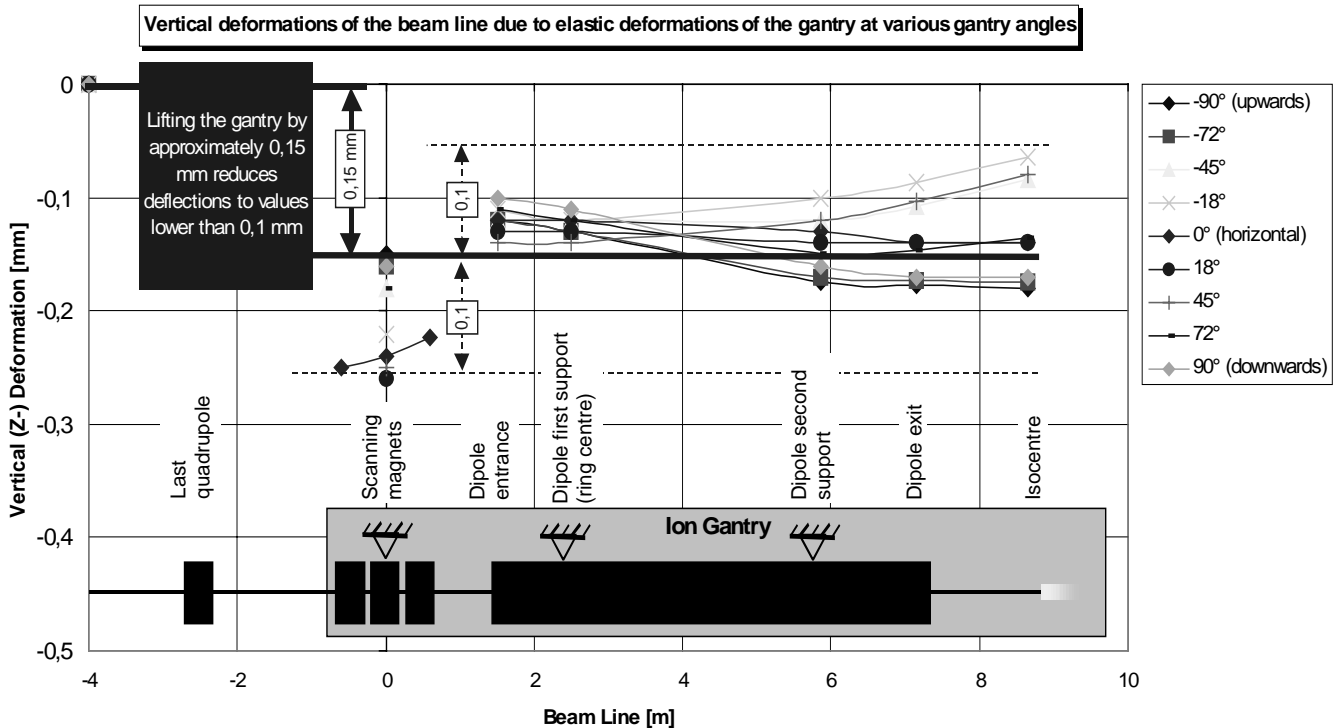


Figure 5-20: Calculated vertical (Z) deformation along the mechanical axis of the beam transport system due to the elastic deformation of the gantry structure. The deformed shape of the dipole and the sagging of the central scanning magnet are indicated for nine different gantry angles, the position of the other two scanning magnets is only shown for the horizontal gantry position. Resulting ion-optical effects were ignored.

The uniform vertical displacement of the dipole and its relative independence of angular position (see Figure 5-20) yield the opportunity to lift the whole structure by approximately

*Elastic deformations in any direction and at any point along the beam transport system of the gantry will hardly exceed  $\pm 0.1$  mm.*

0.15 mm at the bearings in order to better match the gantry to the preceding beam line. Under these circumstances, only the differential deformations of about  $\pm 0.1$  mm will have an influence on the beam transport (compare *Z-corr* in Figure 5-19). The comparatively large deformations (up to -0.25 mm vertical and 0.03 mrad rotational around the horizontal axis) occurring at the scanning magnets are not critical. Their influence on the beam transport can be eliminated if adequate margins for mechanical misalignments of the magnets are considered in the design so that the beam still stays in a good-field region.

Deformations in the two other directions (*X* and *Y*) also show values below  $\pm 0.1$  mm. These results suggest that the *elastic deformations* in any direction and at any point along the beam transport system of the gantry will hardly exceed  $\pm 0.1$  mm. The deformation of the patient cabin is irrelevant because the patient couch and its photogrammetric alignment system will ensure their correction before treatment starts.

### 5.2.2.2 Temperature Effects

It is foreseen to maintain the temperature in the gantry hall and the transfer line within  $\pm 1$  K. On this basis, the following temperature-related effects were investigated:

- A uniform temperature rise by 1 K in the gantry hall. This lifts the centre of the front ring by approximately 0.05 mm, the isocentre rises about one third of this value (Figure 5-21, left). Axial (*Y*) deformation of the front ring is -0.07 mm.
- A temperature gradient of 2 K from the lower (-1 K) towards the upper part (+1 K) of the gantry hall (Figure 5-21, right). The effects vary depending on the gantry angle, however, they are of the same order of magnitude as for the uniform temperature rise (maximum deformation 0.03 mm, maximum rotation 0.01 mrad).
- A heating of 1 K of the dipole relative to the cage. The resulting effect is quite sensitive to the design of the dipole fixations, namely to their rigidity. Maximum expected deformations are 0.04 mm / 0.005 mrad.

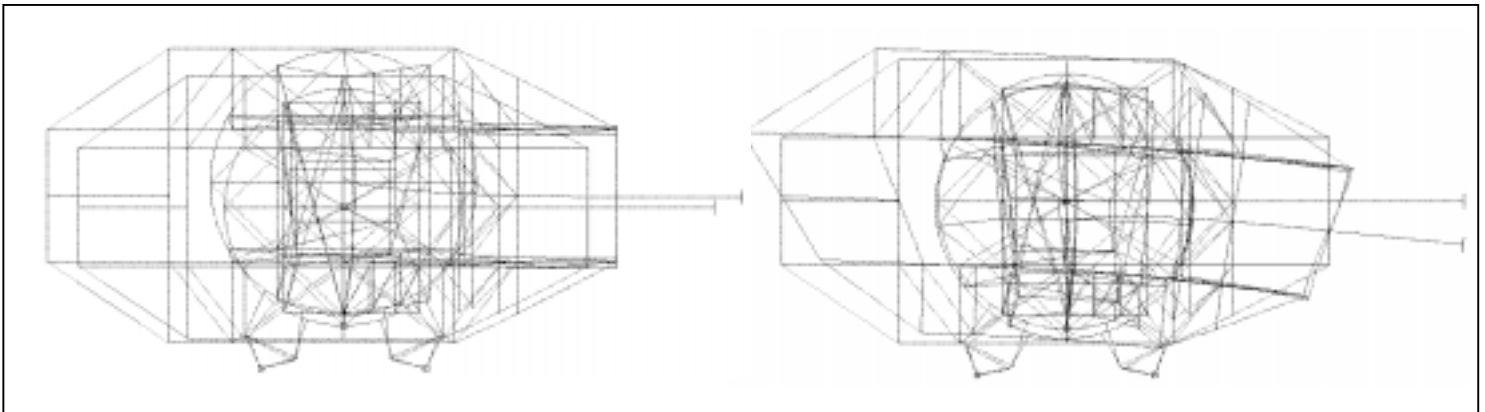


Figure 5-21: Plot of the cage (horizontal position) deformed due to a uniform temperature rise of 1 K (left) and a temperature gradient of 2 K (right); magnification 1000-fold.

### 5.2.2.3 Interpretation of Elastic Deformations and Temperature Effects

*Elastic deformations are systematic errors*

The elastic deformations are interpreted as *systematic* errors, which means they are expected to be a reproducible function of the gantry angle. Thus, a correction map can be generated to compensate for an incorrect beam position at the gantry isocentre due to the elastic deformations. The correcting action can be performed by the patient positioning system (PPS), by the scanning magnets or by dedicated corrector magnets inserted preferably upstream of the scanning system. This principle, called "mapping", also applies for the correction of other systematic errors such as manufacturing errors, initial alignment errors etc. Long-term systematic effects like differential settlement of the building or wear of the mechanics will call for a regular "re-mapping".

In contrast to this, the mapping, which is a feed-forward correction, is not feasible for compensating *random* errors. Random errors have to be either kept below a certain limit or

*Temperature effects  
are random errors*

their effects have to be measured and compensated on-line. Temperature effects are expected to be the main and typical random error contributor, other sources might be backlash of drive mechanics, free-play in bearings or non-reproducible alignment changes of individual beam transport elements during the gantry operation.

## 5.3 The Patient Cabin

### 5.3.1 Mechanical Structure of the Patient Cabin

The patient cabin (see Figure 5-6) is an independent structure with no mechanical connection to the central cage. The central cage therefore avoids an equivalent increase of its counterweight and is relieved of the task of holding a patient cabin rigidly at a large radius. This yields a considerable reduction in the total weight and moment of inertia of the central cage, which is consequently more rigid and easier to build.

The principal task of the patient cabin is to move a supine patient to a desired treatment position that is specified with respect to the main dipole. In order to reach all possible gantry angles, the patient cabin travels vertically up to  $\pm 5.6$  m with respect to the entrance level by using two guide rails on each side of the cabin. The rails are fixed to the building walls. The lateral movement is performed by a horizontal telescopic motion of the platform by a maximum of 5.6 m.

Theoretically, a robot arm with a patient couch at its end would also be able to act as a low-budget alternative for the cabin. However, apart from the expected precision problems, the following arguments lead to the current design:

- Prevention for someone or something falling down as the cabin can be positioned maximum 12 m above floor level of the gantry hall. (As a consequence, the "slot" for the incoming beam should be as small as possible.)
- Providence of space around the patient facilitates all processes before and after treatment and guarantees flexibility to adapt the system to future needs.
- The telescopic nature of the patient cabin secures contact to the lateral wall of the room where additional means of access – namely a lift and an (emergency-) staircase – are foreseen. The telescopic movement is achieved by moving an inner cabin relative to an outer one.
- Although a moderate precision and rigidity of the patient cabin is sufficient, a somehow over-dimensioned design is preferred in order to provide structural reserves for unforeseen loads and avoid vibration problems.

The *breadth* of the patient cabin is governed by the need to irradiate a tumour in the head of a patient laterally from both sides ( $2 \times 2.1$  m). 0.5 m was added to give the personnel the opportunity to pass the couch being in such an extreme position, additional 0.4 m facilitate the installation of a CT/PET inside the cabin, hence the total interior breadth is 5.6 m. Increasing this value, which is certainly possible, directly affects

- the necessary cantilever length of the two consoles for the gantry supports,
- the breadth of the gantry room.

The minimum length (in beam direction) of the outer cabin equals the required telescopic movement (i.e. 5.6 m). In the current design this value was enlarged by approximately 1 m to facilitate the installation of a CT/PET inside the cabin. The free height in the inner cabin is 2.4 m. This value is reduced towards the cage in order to avoid collision with the front console (supporting the front ring). The vertical difference between the floors of the inner and the outer cabin is governed by the height of the main girder of the inner cabin that is supporting the PPS. The current design foresees a step of 0.55 m. When the cabin is in reference position, the inner cabin "docks" at chicane-level, which allows to "roll on and off" with a patient bed without the need to overcome any vertical distance with the help of ramps. As soon as the cabin starts telescoping, the developing gap is bridged by a 1 m long

step that appears correspondingly. Two other steps – designed to finally overcome the entire 55 cm – follow when the total horizontal movement exceeds approximately 1 m and 2 m respectively. The exact value can be set in accordance to the agreed increments of the gantry angle in the final design in order to minimise inconveniences on the elevator-cabin-interface when the personnel enters the room through the lift.

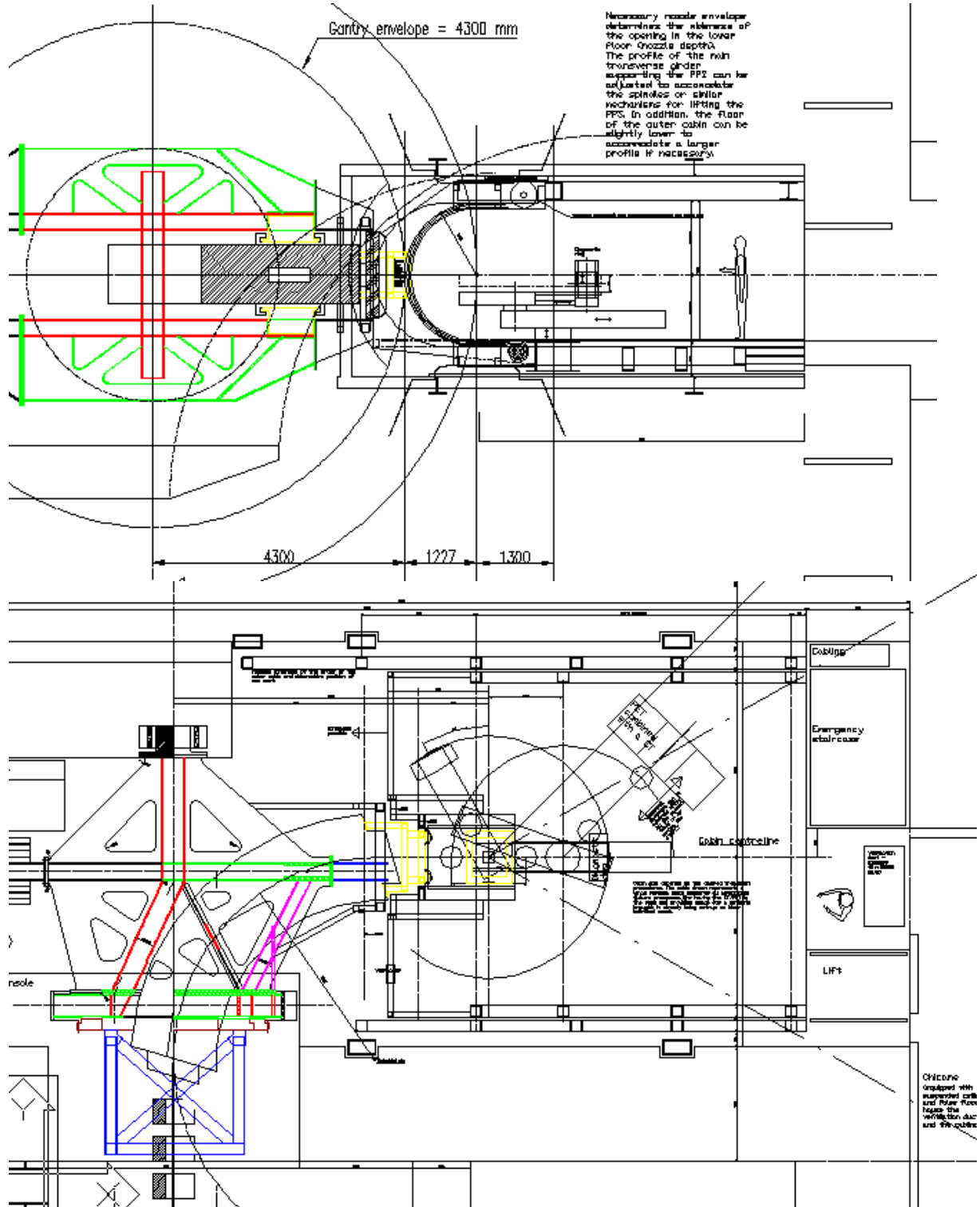


Figure 5-22: Vertical and horizontal section through the patient cabin. Gantry position is horizontal, hence the cabin is completely retracted.

The cabin is essentially closed except from a 1 m wide "slot" for the incoming beam. In elevation (Figure 5-22) this slot has the shape of a half circle (inner radius 113 cm). The slot allows the camera-carrying frame to watch the inside of the cabin, namely the couch. A rolling floor covers the slot between floor level and camera frame. Space is foreseen to have a similar solution for the top-part of the slot if felt to be necessary.

As mentioned above, the cabin structure does not have to meet particularly hard precision requirements, since accurate alignment will be done via the PPS. This could offer the opportunity to adapt some industrial available systems for this purpose. Similar applications can be found in elevators using rack and pinion techniques<sup>23</sup> or in the design of movable theatre stages, however, the need to telescope the inner cabin (generating a varying cantilever moment) will demand substantial adaptations of any of those systems.

The current design foresees to use the building walls on both sides of the patient cabin to give support to two masts each. These masts take the vertical loads of the cabin and – by forming two pairs of vertical forces – they can also take the cantilever moment of the fully telescoped cabin. Each mast can be combined to host a vertical drive for the cabin. Such a drive mechanism for vertical *and* telescopic movement should meet the following requirements:

- Drive velocity so that most extreme treatment position (5.6 m upward and 5.6 m forward) is reached within 1 minute maximum.
- Smooth acceleration.
- Positioning accuracy 2 cm.

Access to the cabin will be controlled by 3 *vertically-sliding* doors, which are all fixed to the outer cabin.

- Between cabin and emergency staircase. To be opened manually from inside and outside. Bottom edge at floor level of the outer cabin. Height of the opening 2.5 m.
- Between cabin and chicane. Opens automatically when cabin reaches 0-level (reference position). Bottom edge at floor level of the inner cabin. Height of the opening 2.0 m.
- Between cabin and lift. Opens automatically when lift has reached cabin level. Bottom edge at floor level of the inner cabin, the outer cabin or the steps bridging the gap (depending on gantry position). Height of the opening 2.5 m.

Finally, the cabin design should make a friendly, light and non-intimidating impression and be sound absorbing.

### 5.3.2 Structural Analysis of the Patient Cabin

A structural analysis of the cabin was performed for the most critical position, i.e. when the cabin is fully telescoped. The assumed static system is shown in Figure 5-23. The analysis of the space truss model was performed using the software CUBUS (1998). Shear deformations were taken into account. For the major lateral trusses of the inner and outer cabins quadratic steel cross-sections were chosen: RHS 200/200/6.3 for the girders and RHS 150/150/5 for the diagonals. The crossbeams show rectangular or I-shaped cross-sections with a height between 300 mm and 400 mm. A speciality is the heavy beam supporting the patient couch, which is 500 mm high and has a cross-section area of 330 cm<sup>2</sup>. The exact geometry of the static system, the member properties, and the results are listed in Annex C (floppy disk). The following load assumptions were made:

- Patient couch: 10 kN
- CT/PET: 18 kN
- Secondary support for the floor plus the floor weight: 0.5 kN/m<sup>2</sup>

<sup>23</sup> Compare for example the four-masted rack and pinion driven lift installed at the Royal Opera House in Covent Garden, which is capable of lifting trucks up to 24 t by 14 m (manufacturer: Alimak, Sweden).

The above loads act during *regular* gantry operation, which is called *service limit state*. For an *ultimate limit state* an additional payload of  $3.5 \text{ kN/m}^2$  according to DIN 1055 part 3 – loads on balconies, treatment rooms, etc. – was assumed.

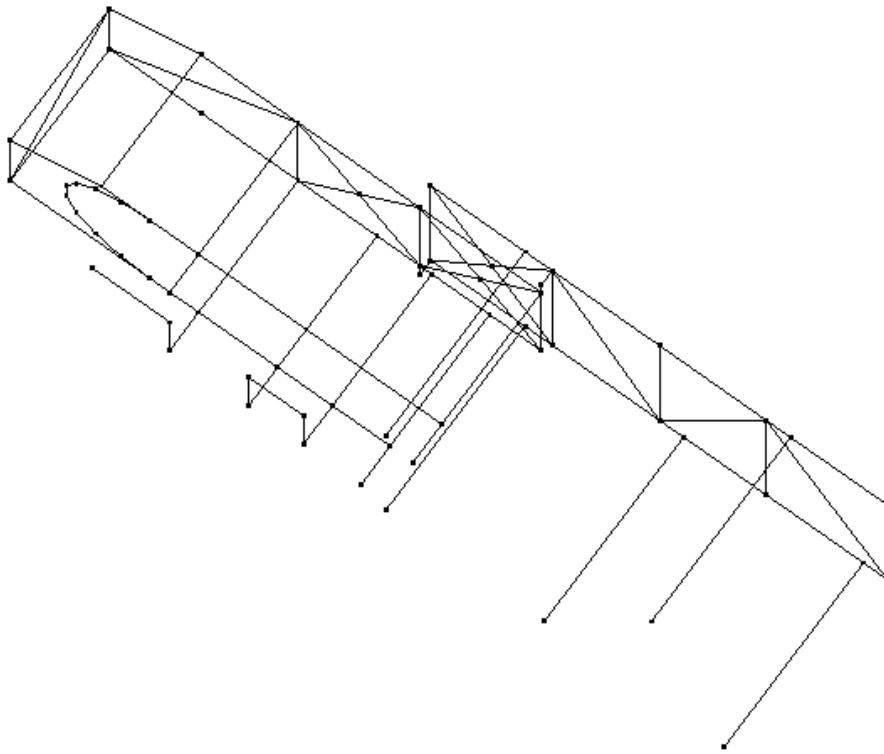


Figure 5-23: The static system of the patient cabin. The heavy single loads of the PPS and the CT/PET are applied at the centre line, hence modelling can benefit from symmetry.

Based on the results obtained from the analysis one can state that *for the service limit state*:

- The dead load of the inner cabin (including patient couch and CT/PET) is about 12 t, total weight of the cabin is 19.5 t.
- When fully telescoped, the two front masts have to withstand not only the full weight but – acting as a pair of opposite vertical forces with their rear counterparts - take the cantilever moment of the outer cabin, which is about 66 kNm *per side* (around the support point at the front masts).
- The two rolling disks / heavy-load carriages / pinions (or whatever) which take the cantilevering moment have to withstand a radial force of 93 kN (lower girder) and 33 kN (upper girder).
- Corresponding service load maximums for the front masts are 8.3 t each (1.4 t each for the rear units).
- Since vertical movement occurs only when the inner cabin is retracted, the service loads for each of the 4 vertical *drives* do not exceed 5.1 t.

*For the ultimate limit state* (applying a safety factor of 1.3 for the dead load, patient couch, CT/PET and a safety factor of 1.5 for the payload):

- The ultimate weight of the cabin would be 65 t.
- The front masts have to withstand a maximum normal force of 256 kN vertically downwards.
- Theoretically, in the extreme case of applying the payload only to the (fully telescoped) inner cabin, the rear masts can get tension of about 6 kN each.
- The highly loaded front rolling disks or pinions have to withstand an ultimate radial force of 286 kN.

*The maximum number of people accessing the cabin platform has to be restricted.*

The payload of  $3.5 \text{ kN/m}^2$  acting in the ultimate limit state increases dramatically the maximum forces in the system compared to the service limit state. In order not to endanger the competitiveness of the design one should investigate measures that allow payload

assumptions to be reduced, for example by restricting the maximum number of people accessing the cabin platform (in the event of guided tours through the facility). Additionally, to reduce the dead load of the cabin structure, secondary beams (e.g. for the floor structure) could be made of aluminium.

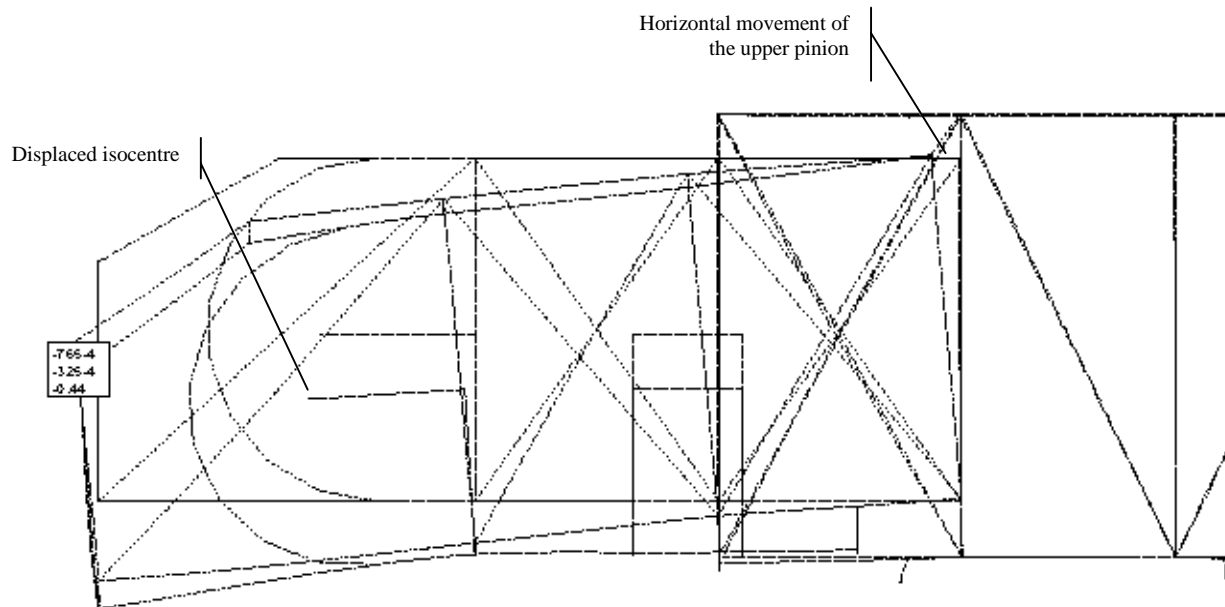


Figure 5-24: Deformed shape of the inner patient cabin. The numbers indicate the occurrence and magnitude of the maximum deformation in cm.

When the cabin is fully telescoped (in the service limit state), the downwards deformation of the local isocentre is approximately 2.6 mm, of which only 1 mm is due to the cantilevering inner cabin itself. The main contribution comes from horizontal movement of the interface between inner and outer cabin (disc or pinion; see Figure 5-24). The patient couch is subjected to an angular deformation around the Y-axis of 0.3 mrad. In a further step one would have to add to this value the angular deformation of the loaded patient couch itself and eventually evaluate whether this angular misalignment of the patient can be tolerated. If this were denied, one would have to implement a pitching mechanism into the couch. The differential deformation between the couch and the CT/PET is about 0.4 mm and 0.3 mrad.

The deformation state of the cabin is considerably ameliorated when relative horizontal (X-) translation between the inner and outer cabin is blocked, e.g. by achieving the telescopic movement via a rack on the bottom *and* on the top girder of the inner cabin. The cantilever moment is then mainly taken by a pair of horizontal forces (~20 kN each) that are transferred from the inner to the outer cabin via the (horizontal) drive mechanism. Due to the larger lever arm, overall forces onto the pinion would be reduced.

### 5.3.3 The Patient Couch

The patient couch has two principal tasks:

- To *accurately* move the patient to the desired treatment position, requiring four degrees of freedom for the couch (no horizontal pitch and roll is foreseen) in a mechanical design that should be as rigid as possible.
- To secure the exact alignment of the patient towards the beam, since the patient cabin provides only moderate positioning accuracy. This is performed by a photogrammetric alignment system.

The current couch design (see Figure 5-22) features two vertical axes of rotation, a horizontal telescopic arm in-between and a vertical drive mechanism in the base (i.e. two rotational and two linear axes).<sup>24</sup> The patient table, i.e. the final "arm" on which the patient is actually lying, is partly made of carbon in order not to interact with a beam from below. The kinematics allow the positioning of more than half the length of that table in the isocentre for couch angles  $\pm 120^\circ$  from the reference position, while still being able to perform position adjustments of  $50\text{ cm} \times 50\text{ cm} \times 30\text{ cm}$  (height). The other half of the body can be irradiated by inverting the direction of the patient on the couch. Table angles larger than  $\pm 120^\circ$  (up to  $180^\circ$ ) are possible for top-irradiation of head and neck regions. By turning the couch horizontally around its base, the table can be inserted into the combined PET/CT unit. The precision of the drives should be around  $0.1\text{ mm}$  ( $\sigma$ ). Sagging of the (cantilevered) patient couch *could* be roughly corrected by a correction map taking into account the couch position, patient position on the couch and the patient's weight. Nevertheless, the precise alignment will be guaranteed by the photogrammetric system.

*The mechanics of the couch: two rotational and two linear axes.*

*The photogrammetric alignment system*

This system, which is a standard optical, non-contact co-ordinate measuring system<sup>25</sup>, automatically controls and corrects the position of the couch. Reflectors on the patient couch are monitored by at least four cameras attached to a frame that is bolted to the exit face of the dipole (see Figure 5-25). The arrangement has to be done in such a way that for all possible irradiation positions at least three reflectors are visible for at least one camera. During patient set-up, the *relative couch-to-magnet position* (and this is the one which is interesting) is measured with an accuracy better than  $0.1\text{ mm}$  ( $\sigma$ ). During irradiation, the iris of the cameras is protected in order not to suffer from radiation damage.

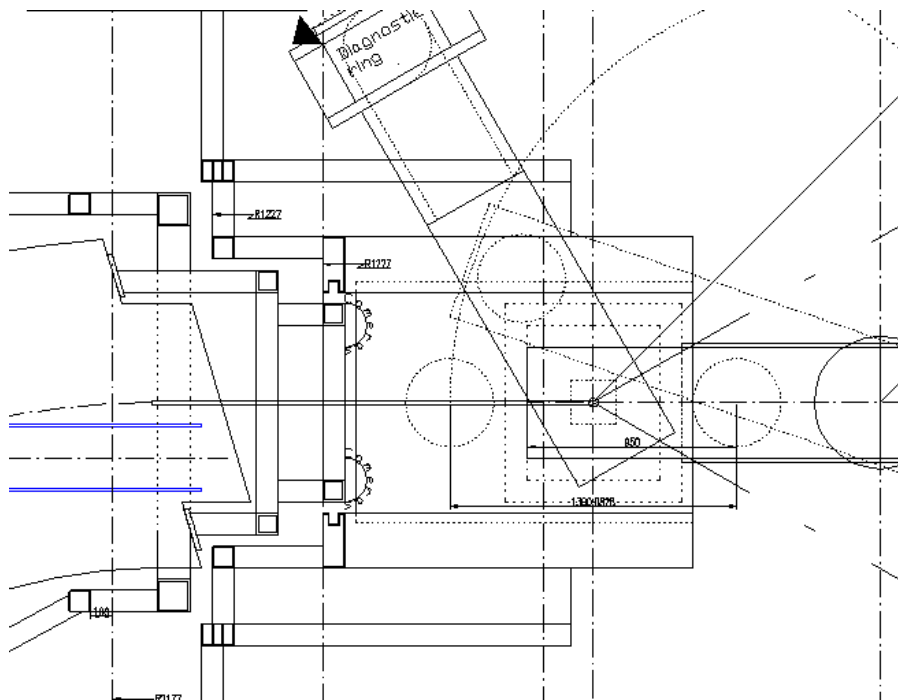


Figure 5-25: The interface cabin - cage (horizontal section) showing the frame bolted to the dipole face carrying the cameras.

*The diagnostic ring*

A so-called diagnostic ring allows the insertion of a beam position monitor close to the patient during irradiation – no matter what the couch position is. The mechanics of this ring are situated below the carbon plate of the patient table. The ring can be moved along the axis and around the head of the table. The monitoring unit can slide between two curved guide rails.

<sup>24</sup> The current design of the patient couch is based on a proposal by the Swiss company Schär Engineering AG.

<sup>25</sup> A suitable and commercially available system is, for example, provided by Oy Mapvision Ltd., Finland.



### 5.3.4 Lift

The lift provides the standard vertical connection between the 0-level of the maze and the cabin platform, whenever the latter is *not* in reference (0-) position. In particular, the personnel use the lift to leave the patient cabin immediately before treatment starts.

The interior of the lift should have a floor area of at least  $1.1 \times 1.4 \text{ m}^2$  to comfortably accommodate four people. Maximum travelling height is  $\pm 5.6 \text{ m}$  (from the central 0-level). The mechanics can support the lift from below (hydraulic lift) or from the side (rack and pinion drive). The lift has two opposite sliding doors:

- At the exit towards the chicane (to be opened at reference position only),
- A horizontally sliding door freeing the passage onto the patient cabin. This door must be fail-safe to avoid any unwanted opening.

Assuming a discrete distribution of possible treatment angles - say every 5 degrees - the foreseen stops of the lift sum up to 35.

## 5.4 Operational Procedure, Flexibility & Safety

### 5.4.1 Standard Operational Procedure

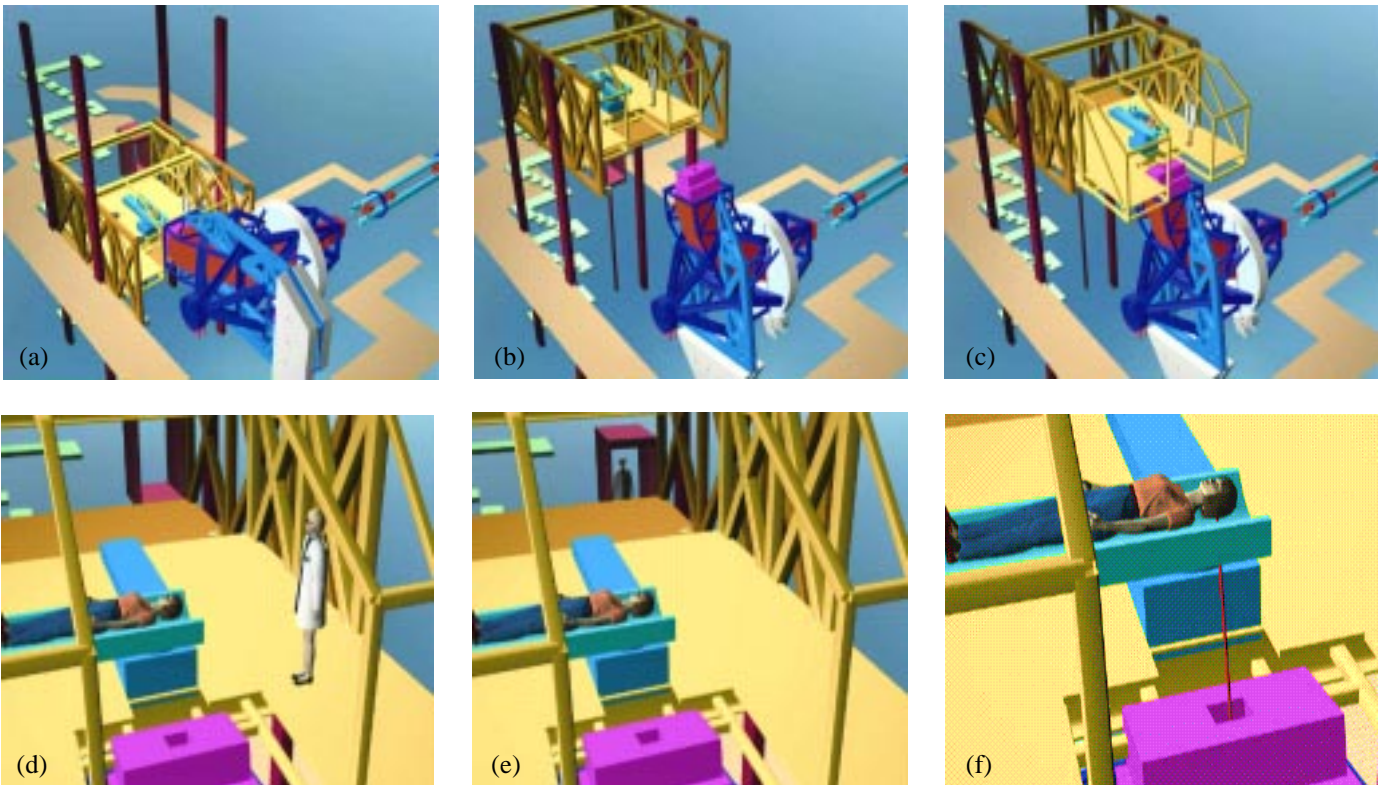


Figure 5-26: Example of a treatment with a lateral field. Patient and accompanying personnel enter the patient cabin directly from the chicane, the patient lies down on the patient couch and immobilisation and patient set-up procedures start. Meanwhile, the gantry is rotated from reference position to a particular angle that is going to be used for the treatment (a). Correspondingly, the cabin is lifted (b) and telescoped forward (c). Then, the patient positioning system brings the patient couch into its final position (d). After performing final checks the personnel leaves the cabin with the rear lift (e) and the beam is switched on (f).

The operational procedure is a sequence of the following main steps, which - except from the final one - take place with the beam switched off:

- The cage supporting the main dipole is set to the specified treatment angle. The rotator is concurrently turned to half this angle. The patient cabin rests in its initial reference position, vertically at entrance level, horizontally retracted.
- Meanwhile, the patient and the accompanying personnel can enter the patient cabin directly via the chicane. Possibly, the patient is already pre-positioned on a special transport device.
- The cabin is set to the actual treatment position using vertical and horizontal translations.
- The patient lies down on (or is transferred from the transport device onto) a patient couch and positioned with respect to the couch.
- The patient couch is brought into the treatment position and aligned precisely using the photogrammetric system with respect to the exit face of the dipole magnet.
- The final patient position is verified.
- The personnel leaves the cabin with the lift.
- The beam is switched on and the treatment session starts.

Figure 5-26 shows the gantry in several characteristic positions during a treatment with a lateral field. A flow chart of the gantry operation is listed in Chapter 6. Compared to conventional gantries (including classical LINACS) the geometry for applying dedicated fields is altered in the Riesenrad gantry, which affects the general positioning procedures. Since the beam points into the cabin in a similar way as in a fixed beam room, orthogonal fields are achieved by turning the patient table by a maximum of  $180^\circ$ , whereas irradiation along the patient axis (vertex field) does not require any table movement. Consequently, which is an advantage of the Riesenrad Gantry, positioning for opposed fields (being symmetrical to the vertical axis) does not require any gantry movement, only the patient table will be rotated.

#### 5.4.2 Available Treatment Angles and Flexibility

Figure 5-27 illustrates the available treatment angles. The couch can be shifted in all three directions and rotated around the vertical axis. The beam can be directed into the cabin at any angle between  $-90^\circ$  and  $+90^\circ$  (a beam pointing vertically downwards corresponds to the angle of gantry rotation  $+90^\circ$ , a horizontal beam is defined as  $0^\circ$  and a beam pointing vertically upwards is obtained by  $-90^\circ$  of gantry rotation). As it can be seen, the gantry covering the  $-90^\circ$  to  $+90^\circ$  angular sector together with a patient couch that can be rotated around its vertical axis.

*The gantry virtually supports  $4\pi$ -beam access to the patient*

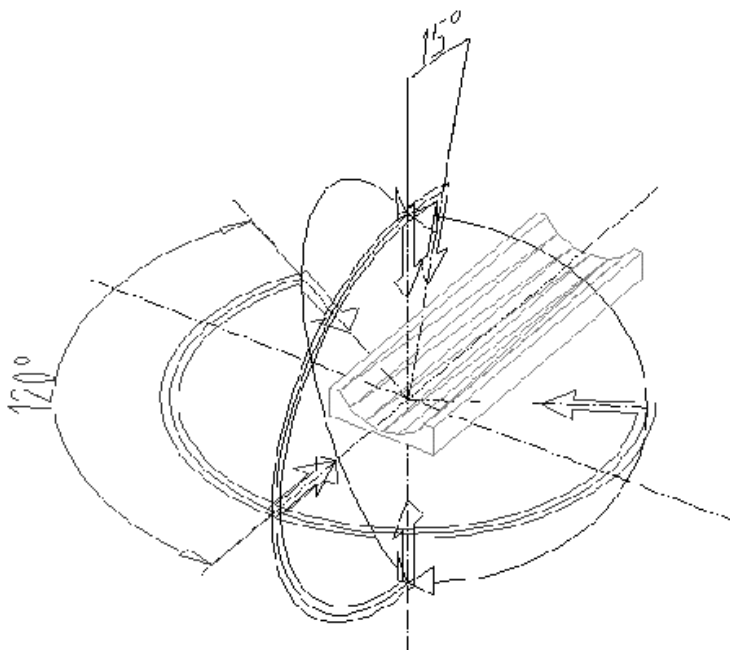


Figure 5-27: Range of possible treatment angles. The cabin and patient positioning system permit a  $360^\circ$  couch rotation. In combination with a gantry rotation of  $\pm 90^\circ$ , the theoretical  $4\pi$ -beam access to the patient is limited only by the need to avoid collisions between the nozzle and the patient couch. Inside the cabin, similar conditions as in a treatment room for a fixed beam line prevail, i.e. vertex fields are achieved when the patient couch is in reference position, opposed fields require the patient couch to be rotated by maximum  $180^\circ$ .

There is no practical experience with this type of treatment system and the operational procedure described above may be modified in the future. That is why, the gantry was designed as an open and flexible system that facilitates its adaptation to possible changes and new needs. Since the rotator, gantry quadrupole structure, central cage and patient cabin are independent systems, they can, to a certain degree, be optimised, installed, tested or even modified separately.

*The spacious patient cabin permits future modifications of equipment and procedures*

The large floor area in the patient cabin guarantees maximum flexibility for the installation of auxiliary equipment, facilitates the setting-up and positioning of the patient and provides a generous working space for handling devices (in particular, the bulky patient moulds). A CT scanner, possibly combined with a PET scanner, can be placed inside the cabin and can be directly accessible by the patient couch. Cabin loads can be increased without affecting the alignment procedure and precision. The 2 m drift between the dipole exit and the patient helps collision prevention. 0.8 m of this drift is reserved for beam diagnostics and dose verification instruments.

Changing the dipole is possible without dismantling the gantry. For this purpose, the central cage is moved to the horizontal position, the front structure and the scanning magnets are dismantled and the dipole is horizontally moved and rotated out of the structure into a small hall between the transfer line building and the gantry, where there is a removable lateral wall. Initial installation will also be done in this way.

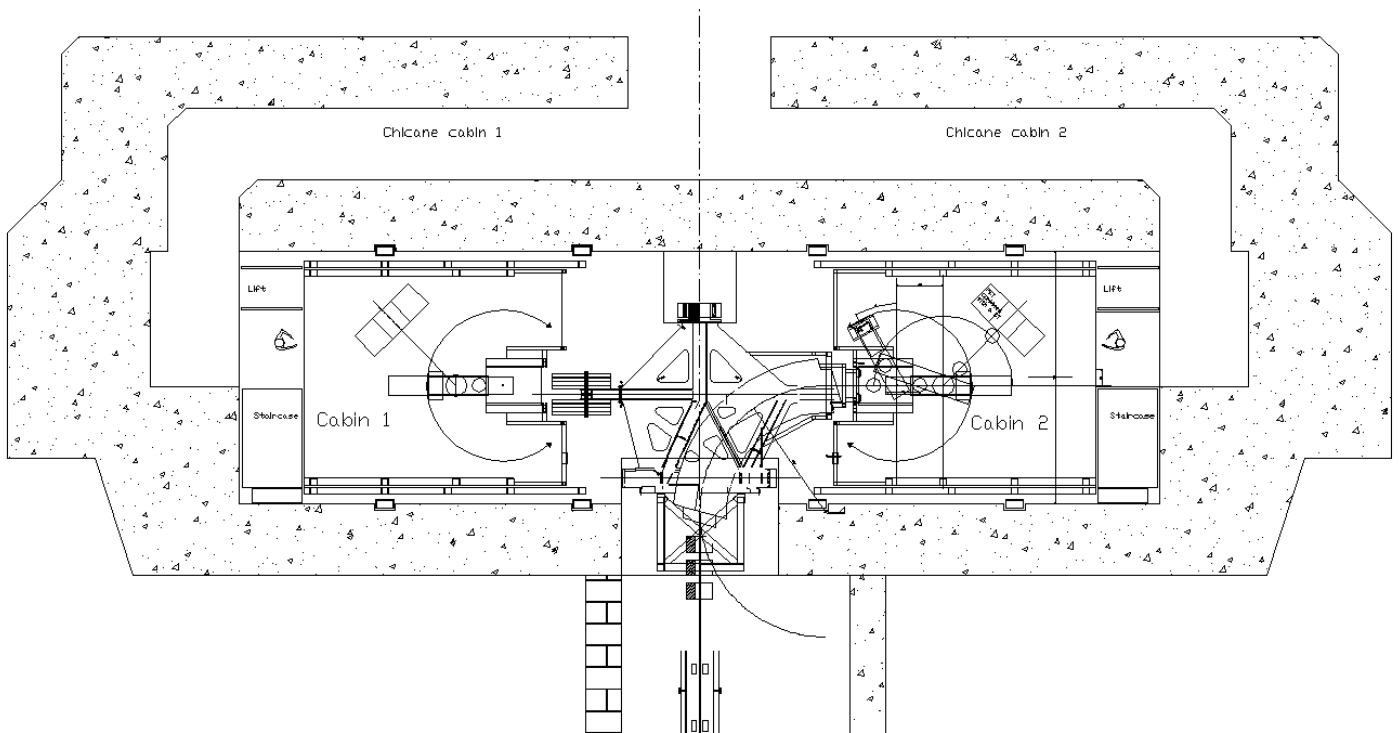


Figure 5-28: Principal layout of a Riesenrad gantry serving two patient cabins alternately.

*The design can be modified to house two cabins served by one cage, hence improving efficiency by more than 45%.*

The design offers a possibility of being extended by adding a second patient cabin, similar to the one described in Section 5.3, which is placed on the other side of the axis of gantry rotation, exactly opposite the first one. The gantry would then serve two patient cabins alternately (see Figure 5-28). Additional costs arise for the second cabin and a 45% enlargement of the gantry hall. During irradiation in one cabin, the other is empty. The economic advantage depends on the time it takes to free a cabin (PET-scanning, re-mobilisation, back to reference position), since it is this period which can already be used for the patient set-up in the other cabin. A first estimation suggests an increase in patient throughput by approximately 45% for a scenario assuming 20 min, 5 min and 10 min for patient set-up, irradiation and PET-scanning / re-mobilisation respectively (Figure 5-29). However, if process times before and after the irradiation can be harmonised, efficiency gains up to 75% are feasible.

The option of a second cabin could be realised at a later stage, since the enlargement of the gantry hall could - to a certain extent - take place during operation of the gantry. For the original sidewall, its possible removal at a later stage should be considered in the civil engineering design.

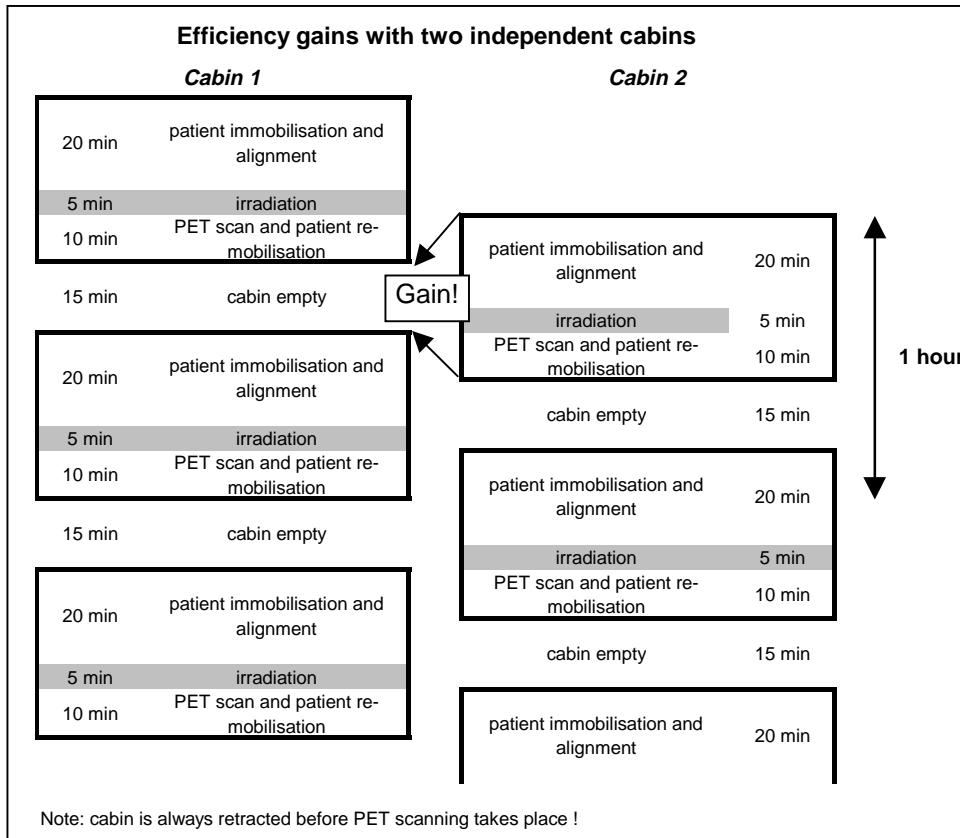


Figure 5-29: Possible treatment process for a Riesenrad gantry serving two cabins. Assumed scenario: 20 minutes for patient set-up, 5 minutes for test beam and irradiation (during which the second cabin can not be used), 10 minutes for re-mobilisation. The average patient throughput is 2.5 patients / h (compared to 1.7 patients / h for the single cabin variant).

### 5.4.3 Safety

For any gantry system, two safety aspects are of crucial importance:

- Quick access to the patient during all modes of operation.
- Avoidance of collisions between moving equipment and the patient.

These safety issues become even more decisive for exocentric gantries, where the patient is moved in space to the final treatment position *before* being irradiated. The Riesenrad gantry guarantees the access to the patient by providing two independent active systems connecting the entrance level (chicane) with the treatment position. First, the patient cabin itself with a maximum travelling time of ~60 s and, second, the lift with a maximum of 5.6 m to travel in ~15 s. Additionally, in the unlikely event of a complete system breakdown, access is always possible via the staircase, hence, emergency procedures do not have to rely on the availability of any mechanically-driven system.

Collisions between the cabin (including the patient couch) and the gantry have to be avoided calling for the possibility of rapid stops of all moving equipment. The situation is ameliorated by the following guidelines:

- *The patient cabin and/or cage can only be moved when the patient couch is in its reference (backward) position (highest priority).*
- *The cage is only rotated when the patient cabin is in the fully retracted position, however, the central cage and the fully retracted patient cabin can be moved independently. This is achieved by a minimum drift space without any monitoring equipment of 1.2 m in front of the isocentre.*

Since the gantry rotation is restricted to only  $\pm 90^\circ$ , the speed of gantry rotation can be relatively low (0.75 rpm). Therefore, the angular momentum to be absorbed is also comparatively low and a maximum over-travel of the cage at the isocentre in case of an emergency stop can be restricted to 10 cm only.

Since the cage and the cabin are steel structures (quickly losing stability above  $500^\circ\text{C}$ ), the possibility of a (longer lasting) fire has to be ruled out. This requires, as far as possible, the elimination of combustible materials and the installation of an automatic fire extinction system in the gantry hall.

## 5.5 Analysis of the Beam Position Accuracy

### 5.5.1 Beam Transport System of the Riesenrad Gantry

The part of the beam transport system that concerns the present analysis starts at the entry to the rotator and continues to the gantry isocentre (see Figure 5-30). Since the magnets in this part are supported by three different rotatable structures, they are expected to suffer larger misalignment errors than the elements of the upstream fixed beam line where the magnets are all static and mounted on individual stands directly on the floor. It is assumed that the monitors and steering units in the upstream line will guide the beam into the rotator perfectly on axis. The above assumptions justify that the analysis has been restricted merely to the rotating parts of the beam transport system.

Neither the gantry nor the rotator is involved in the control of the beam size at the isocentre. This task is accomplished by a dedicated phase-shifter-stepper in the upstream transfer line (Benedikt et al., 1999). This means that changing the beam size will not affect the position of the beam spot because the optical settings of the gantry and rotator are constant. However, the overall transfer matrix from the rotator entrance to the isocentre is a function of the gantry angle  $\alpha$ , because an angle  $\alpha/2$  appears between the exit of the rotator and the entrance of the gantry. That is why, ion-optical effects related to the misalignment of the beam transport elements of the rotator depend, in general, on the gantry angle.

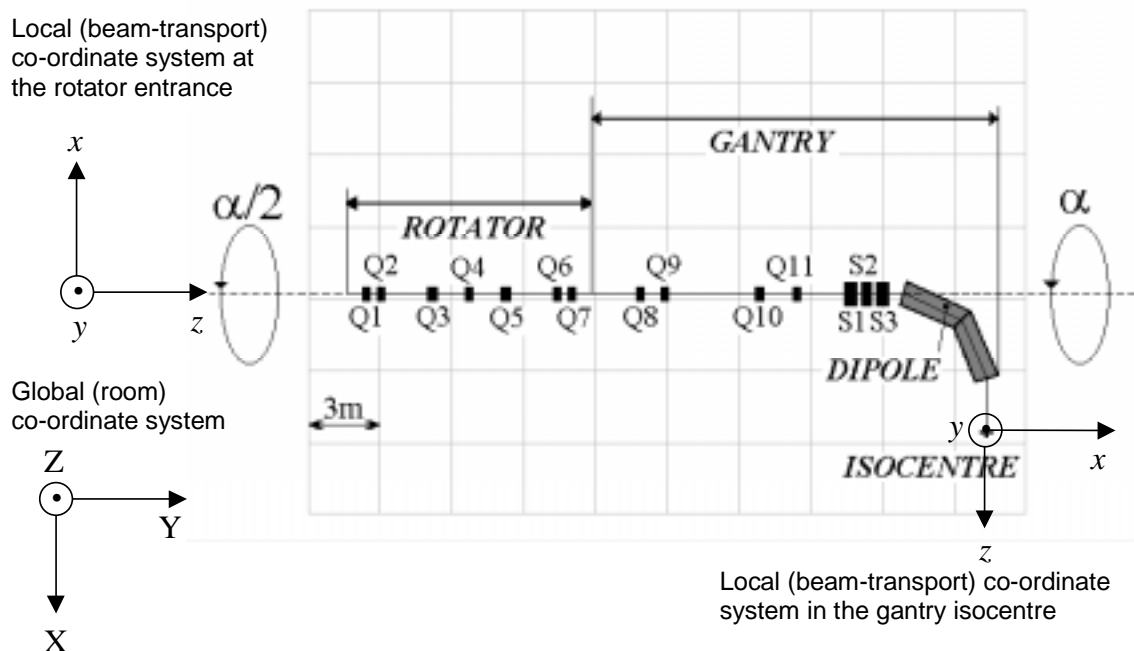


Figure 5-30: Beam transport system of the Riesenrad ion gantry including the rotator. The rotator consists of 7 quadrupoles (Q1-Q7) in one rotating structure. The gantry has 4 quadrupoles (Q8-Q12) in one rotating structure while scanning magnets (S1, S2, S3) and main dipole are supported by the central cage. Global (room) and local (beam-transport) co-ordinate systems are indicated as well.

## 5.5.2 Error Analysis

### 5.5.2.1 General Considerations

The present analysis has been restricted to errors leading to an incorrect beam position at the gantry isocentre, which is the most critical aspect of the gantry beam transport system. The effects causing focusing errors such as deviations from an exact beam size or deformations of an ideal round beam spot have been neglected. Therefore, only the misalignment of beam transport elements, which causes a deviation of the beam from the optical axis, has been considered. The beam transport elements are assumed to be perfectly manufactured, correctly powered, to have an ideal field quality, but to be slightly displaced along and/or rotated around each of the local co-ordinate system axes  $x$ ,  $y$  and  $z$  (see Figure 5-30). The action of the scanning magnets is not taken into account. In other words, it is investigated how precisely the centre of the non-scanned beam can hit the ideal gantry isocentre.

*It is investigated how precisely the centre of the non-scanned beam can hit the ideal gantry isocentre.*

Following the structural analysis, the misalignments have been classified into two categories: systematic and random. The main feature of systematic misalignments, caused for example by elastic deformations of the gantry and rotator support structures, is their short-term reproducibility as a function of the gantry angle. This category covers also errors of the initial magnet alignment during the assembling of the gantry. These systematic errors are assumed to be constant and independent of the gantry angle. However, their ion-optical effects *can* be a function of the gantry angle due to the angular dependence of the overall transfer matrix. Random misalignments represent all possible effects with no reproducibility as a function of the gantry angle (like temperature fluctuations). These misalignments are expected to have a gaussian distribution which is superimposed on the systematic misalignments. The position of each beam transport element is therefore characterised by a particular value of the systematic misalignment (element-specific) and a standard deviation of the random misalignment probability distribution. The situation is illustrated in Figure 5-31. The practical effect of random misalignments is that *for different fractions* the position of the non-scanned beam will vary around the ideal position (isocentre) according to a gaussian distribution (supposing that during a single fraction all conditions are stable).

*The practical effect of random misalignments is that for different fractions the position of the beam will vary around the ideal position according to a gaussian distribution.*

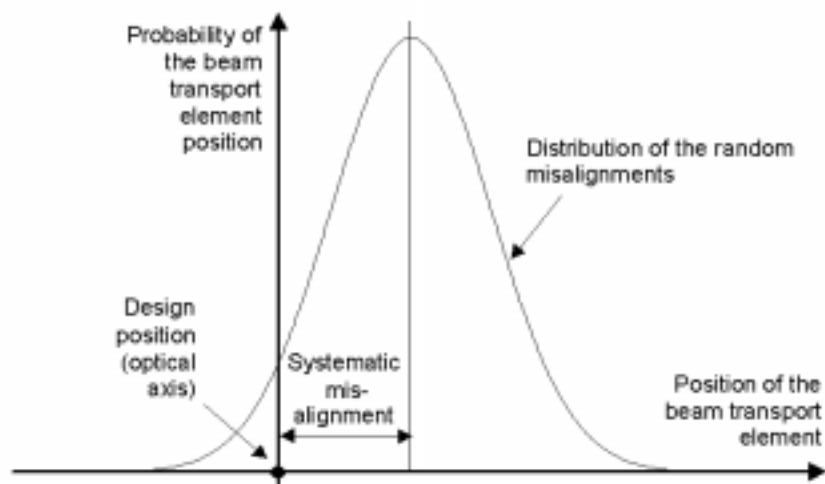


Figure 5-31: Position probability distribution of a beam transport element showing the systematic and random misalignment components.

### 5.5.2.2 Effects of Misalignments

The beam transport system of the Riesenrad ion gantry consists of quadrupole magnets and the main 90° dipole magnet. First, the misalignment effects of these two types of magnets have been evaluated separately.

A misaligned quadrupole causes a transverse "kick" to the beam, which can be calculated from the transfer matrix:

$$\begin{pmatrix} x_1 \\ x_1' \\ y_1 \\ y_1' \end{pmatrix} = \begin{pmatrix} \cos \sqrt{k}L & \frac{1}{\sqrt{k}} \sin \sqrt{k}L & 0 & 0 \\ -\sqrt{k} \sin \sqrt{k}L & \cos \sqrt{k}L & 0 & 0 \\ 0 & 0 & \cosh \sqrt{k}L & \frac{1}{\sqrt{k}} \sinh \sqrt{k}L \\ 0 & 0 & \sqrt{k} \sinh \sqrt{k}L & \cosh \sqrt{k}L \end{pmatrix} \begin{pmatrix} x_0 \\ x_0' \\ y_0 \\ y_0' \end{pmatrix} \quad (5.1)$$

for a quadrupole which focuses in the  $(x, z)$  plane, where  $x_0, x_0', y_0, y_0'$  are the particle co-ordinates at the entrance,  $x_1, x_1', y_1, y_1'$  are the co-ordinates at the exit,  $L$  is the quadrupole effective length [m] and  $k > 0$  is the strength [ $\text{m}^{-2}$ ] defined as  $k = g/(B\rho)$  where  $g$  is the gradient [T/m] and  $B\rho$  is the magnetic beam rigidity [Tm]. For a transverse misalignment  $\Delta x, \Delta y$  one gets for the kick, by putting  $x_0 = -\Delta x, x_0' = 0, y_0 = -\Delta y$  and  $y_0' = 0$ , (see Figure 5-32(a)):

$$x_1' - x_0' = (\sqrt{k} \sin \sqrt{k}L) \cdot \Delta x \quad (5.2a)$$

for the focusing plane and

$$y_1' - y_0' = (-\sqrt{k} \sinh \sqrt{k}L) \cdot \Delta y \quad (5.2b)$$

for the defocusing plane of the quadrupole. Note that the misalignment of a magnet which is positive in the local beam co-ordinate system causes the reference particle to be negatively displaced with respect to the optical axis of the misaligned magnet, hence  $x_0 = -\Delta x$  and  $y_0 = -\Delta y$ .

When tilting the magnet by angles  $R_x$  (about  $x$ -axis) and  $R_y$  (about  $y$ -axis), then  $x_0 = 0, x_0' = -R_y, y_0 = 0$  and  $y_0' = +R_x$  (see Figure 5-32(b)). The kicks are given by:

$$x_1' - x_0' = (-\cos \sqrt{k}L) \cdot R_y - (-R_y) = (1 - \cos \sqrt{k}L) \cdot R_y \quad (5.3a)$$

for the focusing plane and

$$y_1' - y_0' = (\cosh \sqrt{k}L) \cdot R_x - R_x = (\cosh \sqrt{k}L - 1) \cdot R_x \quad (5.3b)$$

for the defocusing plane.

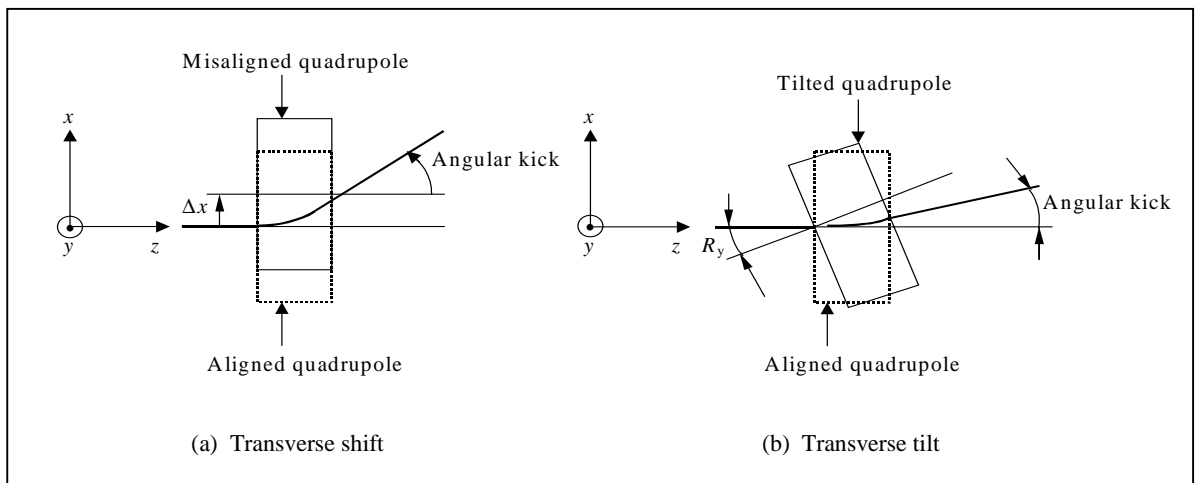


Figure 5-32: Effects of a misaligned quadrupole lens. Note that the outputs given by the transfer matrix of the quadrupole are in fact related to the optical axis of the misaligned element and have to be properly converted to the co-ordinate system following a design trajectory.

Similarly, the effects of dipole misalignments that are basically geometrical focusing and/or some trigonometric transformations in the local co-ordinate system can be calculated.

Systematic and random misalignments must be treated differently. The systematic misalignments represent the situation where all elements are misaligned by a known amount. For each gantry angle, the elements have definite positions different from the ideal design positions and the whole beam line represents a certain particular combination of element misalignments. The position of the beam in the gantry isocentre is obtained by tracing the beam through this misaligned beam line by a computer code. The random misalignments are interpreted as an uncertainty of the actual element position. In other words, the element position is given a certain probability distribution, which is assumed to be gaussian. All misalignments of all elements are assumed to be independent and their individual contributions to the beam displacement are added quadratically. If the parameters of the element misalignment are interpreted as one standard deviation of its position probability distribution, then the calculated beam position represents one standard deviation of the *beam position probability distribution*.

### 5.5.3 Beam Transport Calculation

The beam transport calculations were performed by two computer codes using different strategies for simulating the misalignment effects. TRANSPORT (Carey, et al., 1995) calculates first all individual contributions for all elements and then sums them. WinAGILE (Bryant, 2000) creates many lattices each representing a certain particular but randomly generated combination of misalignments and traces the beam through each lattice. The beam positions at a specified point of interest are collected and statistically evaluated. An excellent agreement between both computer codes has been observed.

#### 5.5.3.1 Systematic Misalignments

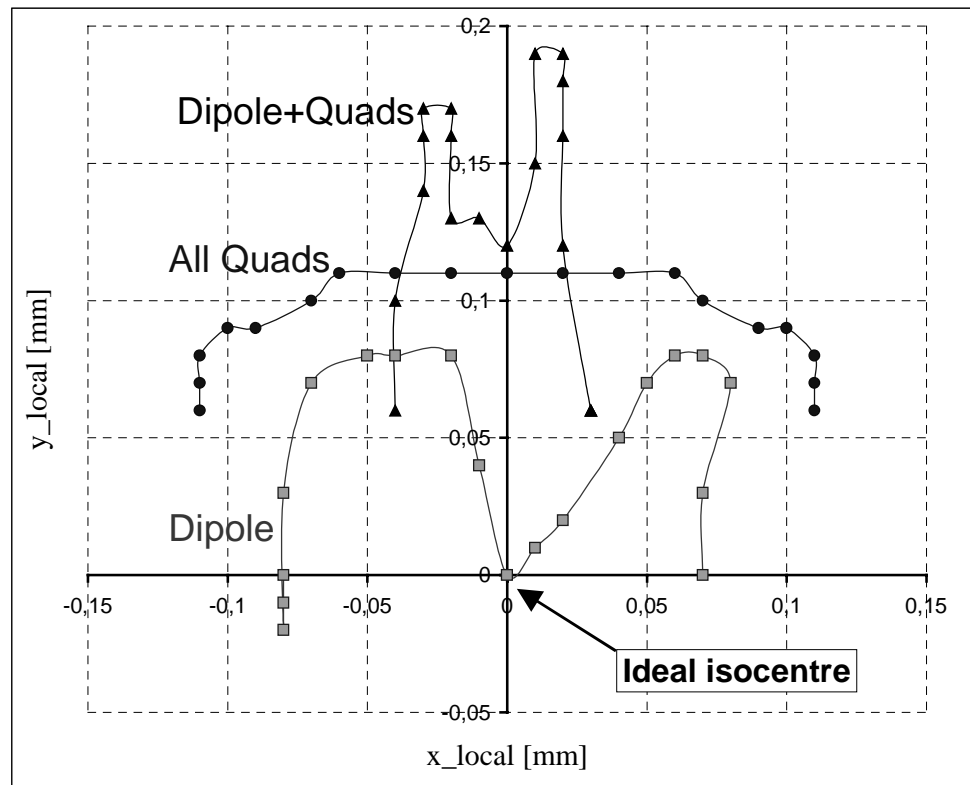


Figure 5-33: Beam position in the gantry isocentre for different angles of gantry rotation taking into account ion-optical effects. The deviations from the ideal isocentre are caused by elastic deformations of the support structures of the main dipole alone (squares), the quadrupoles alone (circles) and the dipole and the quadrupoles together.

Typical, and presumably the dominating component, of the systematic misalignments are the elastic deformations of the gantry support structures, i.e. the cage and the quadrupole



*Elastic deformations of the gantry support structures are a typical component of the systematic misalignment of the beam in the isocentre.*

support structures, as investigated in Section 5.2.2.1 and Section 5.1 respectively. The calculated values were converted from the global (room) co-ordinate system to the local (beam-transport) co-ordinate system that follows the bends and rotations of the beam line. In the local co-ordinate system, the  $z$ -axis always points in the beam direction and the  $[x-z]$  and  $[y-z]$  planes correspond to "horizontal" and "vertical" plane of the beam transport elements according to the usual convention in beam-optics. Because the local co-ordinate system follows the beam line rotations, the "horizontal" and "vertical" plane is identical with the bending and non-bending plane of the main dipole, respectively, independent from the angle of gantry rotation (see Figure 5-30).

The results of the beam transport calculations showing the response of the system to the misalignments caused by elastic deformations are shown in Figure 5-33. The position of the beam-centre in the gantry isocentre is given in the local co-ordinate system for different angles of gantry rotation from  $-90^\circ$  to  $+90^\circ$  in  $10^\circ$  steps. Three sets of data are presented corresponding to the misalignment of the quadrupoles alone, the gantry dipole alone and all elements together.

### 5.5.3.2 Random Misalignments

It is difficult to assess the random misalignments in the same way as the systematic ones and a different strategy has been chosen. The *sensitivity* of the beam transport system to random misalignments was investigated, thus giving the possibility to specify "backwards" the permissible tolerances for random misalignments of the beam transport elements. For this purpose, some approximations have been introduced into the model. The first approximation is to express the effect of a misaligned quadrupole as an angular kick with zero displacement at the exit of the quadrupole (thin-lens approximation). The angular kicks are given by (5.2) and (5.3). The kicks then cause a beam displacement at the gantry isocentre according to the transformation:

$$\begin{pmatrix} x \\ x' \\ y \\ y' \end{pmatrix} = \begin{pmatrix} t_{11} & t_{12} & t_{13} & t_{14} \\ t_{21} & t_{22} & t_{23} & t_{24} \\ t_{31} & t_{32} & t_{33} & t_{34} \\ t_{41} & t_{42} & t_{43} & t_{44} \end{pmatrix} \cdot \begin{pmatrix} x_0 \\ x'_0 \\ y_0 \\ y'_0 \end{pmatrix} \quad (5.4)$$

where  $x$ ,  $x'$ ,  $y$ ,  $y'$  are parameters of the reference trajectory (beam centre) in the gantry isocentre,  $x_0$ ,  $x'_0$ ,  $y_0$ ,  $y'_0$  are parameters of the reference trajectory at the exit of the misaligned element and  $t_{ij}$  are elements of the transfer matrix from the exit of the misaligned element to the gantry isocentre. The thin-lens approximation gives  $x_0 = y_0 = 0$  and  $x'_0$  and  $y'_0$  will be called  $H_{\text{kick}}$  and  $V_{\text{kick}}$  for the horizontal and vertical plane, respectively. Note that there is a coupling between the horizontal and the vertical planes due to the fact that the gantry is rotated by an angle  $\alpha/2$  with respect to the rotator,  $\alpha$  being the angle of gantry rotation. The terms in the off-diagonal sub-matrices are therefore not zero. For the same reason,  $t_{ij} = f(\alpha)$ . The final beam displacement due to the quadrupole shift is:

$$x = t_{12} \cdot H_{\text{kick}} + t_{14} \cdot V_{\text{kick}} \quad (\text{horizontal plane}) \quad (5.5)$$

$$y = t_{32} \cdot H_{\text{kick}} + t_{34} \cdot V_{\text{kick}} \quad (\text{vertical plane})$$

After evaluating the kicks using (5.2), one obtains:

$$x = t_{12} \cdot \sqrt{k} \sin \sqrt{k}L \cdot \Delta x - t_{14} \cdot \sqrt{k} \sinh \sqrt{k}L \cdot \Delta y = C_1 \Delta x + C_2 \Delta y \quad (5.6)$$

$$y = t_{32} \cdot \sqrt{k} \sin \sqrt{k}L \cdot \Delta x - t_{34} \cdot \sqrt{k} \sinh \sqrt{k}L \cdot \Delta y = C_3 \Delta x + C_4 \Delta y$$

where  $C_1$ ,  $C_2$ ,  $C_3$  and  $C_4$  are constants depending on the angle of gantry rotation and characterising the response of the beam position in the gantry isocentre to a misalignment of a given quadrupole. For the analysis of random errors, the misalignments  $\Delta x$  and  $\Delta y$

represent a standard deviation of the position probability distribution of a misaligned element and their effects – supposing independent random misalignments in any direction – are added quadratically:

$$\sigma(i)_H = \sqrt{(x(\Delta x, \Delta y = 0))^2 + (x(\Delta x = 0, \Delta y))^2} = \sqrt{C_1(i)^2(\Delta x)^2 + C_2(i)^2(\Delta y)^2} \quad (5.7)$$

$$\sigma(i)_V = \sqrt{(y(\Delta x, \Delta y = 0))^2 + (y(\Delta x = 0, \Delta y))^2} = \sqrt{C_3(i)^2(\Delta x)^2 + C_4(i)^2(\Delta y)^2}$$

where  $\sigma(i)_H$  and  $\sigma(i)_V$  now represent a standard deviation of the beam position probability distribution caused by the misalignment of the  $i$ -th quadrupole. The indexes H and V assign the horizontal and vertical plane, respectively. The second approximation in the model is a physically reasonable assumption that the position uncertainty for all quadrupoles in all directions is the same, that is  $\Delta x = \Delta y = \Delta z \equiv \Delta_{\text{shift}}$  where  $\Delta_{\text{shift}}$  is now introduced as representing the random misalignment of a quadrupole in any direction. Equation (5.7) then looks like:

$$\sigma(i)_H = \sqrt{C_1(i)^2 + C_2(i)^2} \cdot \Delta_{\text{shift}} = C(i)_H \Delta_{\text{shift}} \quad (5.8)$$

$$\sigma(i)_V = \sqrt{C_3(i)^2 + C_4(i)^2} \cdot \Delta_{\text{shift}} = C(i)_V \Delta_{\text{shift}}$$

Keeping in mind that the misalignment  $\Delta_{\text{shift}}$  is taken as a standard deviation of the position probability distribution of a misaligned element, equation (5.8) demonstrates that the standard deviation of the beam position probability distribution in the gantry isocentre is proportional to the standard deviation of the probability distribution of the element position. The proportionality constants are different in the horizontal and vertical plane  $C(i)_H \neq C(i)_V$ . If all quadrupoles are independently misaligned, the standard deviation of the beam position probability distribution in each plane will be given by:

$$\sigma_{\text{shift}} = \sqrt{\sum_i (\sigma(i))^2} = \sqrt{\sum_i (C(i)^2 \Delta_{\text{shift}}^2)} = \sqrt{\sum_i (C(i)^2)} \cdot \Delta_{\text{shift}} \propto \Delta_{\text{shift}} \quad (5.9)$$

where indexes for horizontal and vertical planes are no longer indicated since equation (5.9) differs for the different planes by only the proportionality constant.

The same strategy can be applied for effects of quadrupole-tilt, dipole-shift and dipole-tilt yielding the final expression for the standard deviation of the beam position probability distribution in a given plane,  $\sigma_{\text{total}}$ :

$$\sigma_{\text{total}} = \sqrt{(\sigma(\text{quads})_{\text{shift}})^2 + (\sigma(\text{quads})_{\text{tilt}})^2 + (\sigma(\text{dipole})_{\text{shift}})^2 + (\sigma(\text{dipole})_{\text{tilt}})^2} \quad (5.10)$$

where each contributing effect is simply proportional with a different proportionality constant to the corresponding type of misalignment. This enables a proportional scaling of results and specifying "backwards" the tolerable "budget" for random misalignments from the requirements on the beam position accuracy. In principle, calculations should be done for all gantry angles, because the proportionality constants depend on the angle of gantry rotation.

Since the exact values for random misalignments are difficult to specify, the sensitivity of the beam position in the isocentre to "reference" random errors was studied first. The reference input data applied were  $3\sigma_{\text{shift}} = 0.1 \text{ mm}$  and  $3\sigma_{\text{tilt}} = 0.1 \text{ mrad}$  for all quadrupoles and for the dipole. Specifying the  $3\sigma$  values means practically that the elements are always expected to be found within a  $-3\sigma$  to  $+3\sigma$  tolerance region (exceptional cases, so-called "accidental" errors, will be discussed later). The calculations were done for gantry angles from  $-90^\circ$  to  $+90^\circ$  with  $10^\circ$  steps. Figure 5-34 shows the results for two significant angles of gantry rotation  $+90^\circ$  and  $0^\circ$ . The values for other gantry angles were in-between these

two extreme cases. Maximum overall values for the beam position probability distribution in the isocentre were  $3\sigma_{\text{total}} = 0.96 \text{ mm} / 1.4 \text{ mm}$  (horizontal / vertical plane), obtained for  $\alpha = 90^\circ$ . Figure 5-35 presents the individual contributions corresponding to the quadrupole-shift, quadrupole-tilt, dipole-shift and dipole-tilt for  $\alpha = 90^\circ$ .

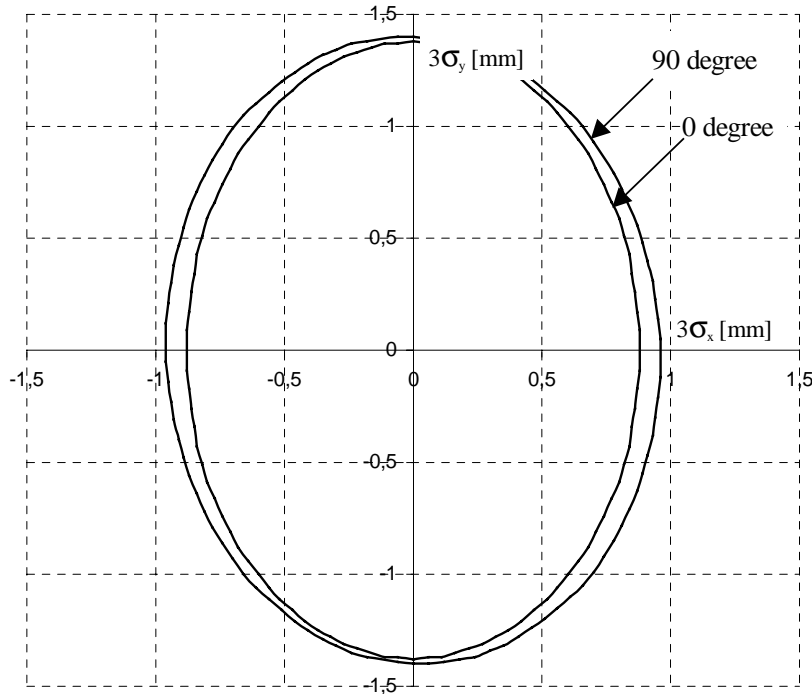


Figure 5-34: Uncertainty of the beam position in the gantry isocentre expressed as  $3\sigma$  of the beam position probability distribution for two angles of gantry rotation ( $0^\circ$  and  $90^\circ$ ) and reference random misalignments of all elements  $3\sigma_{\text{shift}} = 0.1 \text{ mm}$  and  $3\sigma_{\text{tilt}} = 0.1 \text{ mrad}$ .

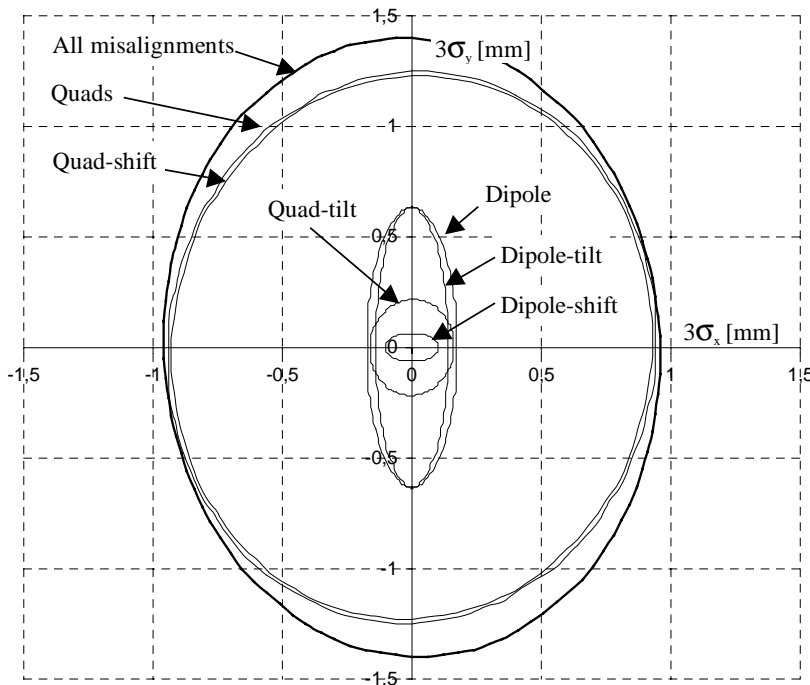


Figure 5-35: Individual components of the beam position uncertainty due to reference random misalignments of  $3\sigma_{\text{shift}} = 0.1 \text{ mm}$  for quadrupole-shift and dipole-shift and  $3\sigma_{\text{tilt}} = 0.1 \text{ mrad}$  for quadrupole-tilt and dipole-tilt. The angle of gantry rotation  $\alpha = 90^\circ$ .

In Figure 5-36(a), the results obtained for the reference misalignments are scaled to the expected random misalignments due to the temperature fluctuations reported in Section 5.2.2.2, which are considered as the main contributor to random errors. In order to be on the conservative side with the assessment as well as to be consistent with the model assumptions (equal random misalignments in all directions), the applied input values were obtained by taking the "worst" value of all directions for each temperature-related effect

and adding them quadratically. Therefore, the  $3\sigma$  input values were 0.09 mm for dipole-shift, 0.017 mrad for dipole-tilt, 0.04 mm for quadrupole-shift and 0.007 mrad for quadrupole-tilt. Finally, a contribution from the photogrammetric alignment system (PAS) of the patient couch ( $3\sigma = 0.3$  mm) was added to the position uncertainty due to the beam transport. The overall beam position uncertainty in the isocentre expressed as the  $3\sigma$ -region of the beam position probability distribution is indicated in Figure 5-36(b).

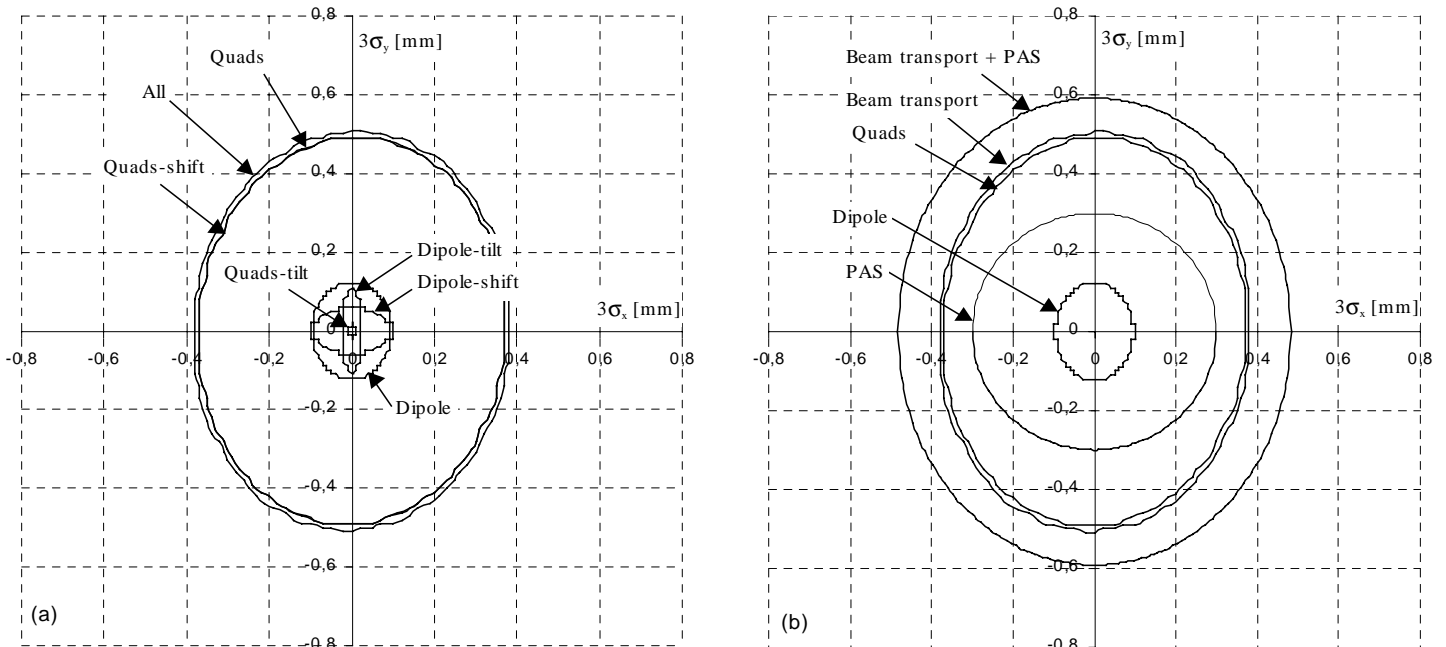


Figure 5-36: Beam position uncertainty due to expected random misalignments of the beam transport system. The outer curves represent the calculated  $3\sigma$ -region of the beam position probability distribution due to expected temperature fluctuations in the gantry hall (a), and due to temperature fluctuations *and* the resolution error of the photogrammetric alignment system, PAS, (b). Inner curves indicate individual components to the overall beam position uncertainty.

*The sensitivity of the beam position to random misalignments of the beam transport elements is rather high.*

The results show that the sensitivity of the beam position to random misalignments of the beam transport elements is rather high. In order to achieve the sub-millimetre precision defined as  $3\sigma_{\text{total}} < 1$  mm at the isocentre, the random misalignments have to be lower than the chosen reference values of  $3\sigma_{\text{shift}} = 0.1$  mm and  $3\sigma_{\text{tilt}} = 0.1$  mrad. However, not all misalignments are that critical. The dominating contribution comes from the quadrupole shift. A misalignment tolerance of  $3\sigma < 0.07$  mm is required for the transverse position of the quadrupoles. The effect of quadrupole tilt is about a factor of 6 lower. For the dipole, the angular misalignments are more critical compared to the shift, especially in the vertical plane. The reference misalignment tolerances are acceptable for the dipole, a reduction of tilt to  $3\sigma_{\text{tilt}} = 0.05$  mrad would, however, provide a higher - and urgently needed - tolerance budget for the quadrupole shift. The results of the random misalignment study are collected in Table 5-1. It has to be pointed out that the tough tolerances listed in the table do *not* represent the absolute misalignment tolerances, rather than the *stability* of the element position (see again Figure 5-31). The average misalignment may be larger, but, as this represents the systematic error, it can be corrected by the mapping. Only the non-reproducible, *random* components of the element misalignments are concerned by the above-derived tolerances.

It would also be possible to reduce the quadrupole contribution by steering magnets located downstream of the gantry quadrupoles and upstream of the scanning magnets. These correctors could be used to direct the beam into the centre of the scanning system and hence remove the position and angular errors of the incoming beam caused by the upstream misalignments. The corrector magnets would have to be controlled on-line by a permanent beam position monitoring system at the entrance to the scanning system.

Type of alignment error	Reference conditions		Temperature effects		Recommended tolerances for $3\sigma < 1$ mm	
	Misalignment ( $3\sigma$ )	Beam response ( $3\sigma$ )	Misalignment ( $3\sigma$ )	Beam response ( $3\sigma$ )	Misalignment ( $3\sigma$ )	Beam response ( $3\sigma$ )
Dipole: shift	0.1 mm	0.1 mm / 0.06 mm	0.09 mm 0.017 mrad	0.09 mm / 0.05 mm	0.1 mm 0.05 mrad	0.1 mm / 0.06 mm
Dipole: tilt	0.1 mrad	0.14 mm / 0.63 mm		0.02 mm / 0.11 mm		0.07 mm / 0.32 mm
Dipole: shift + tilt		0.17 mm / 0.64 mm		0.09 mm / 0.12 mm		0.12 mm / 0.33 mm
Quadrupoles: shift	0.1 mm	0.93 mm / 1.23 mm	0.04 mm 0.007 mrad	0.37 mm / 0.49 mm	0.07 mm 0.05 mrad	0.65 mm / 0.86 mm
Quadrupoles: tilt	0.1 mrad	0.16 mm / 0.22 mm		0.01 mm / 0.02 mm		0.08 mm / 0.11 mm
Quadrupoles: shift + tilt		0.94 mm / 1.25 mm		0.37 mm / 0.49 mm		0.65 mm / 0.87 mm
Beam transport: Dipole + quadrupoles		0.96 mm / 1.40 mm		0.38 mm / 0.50 mm		0.66 mm / 0.93 mm
PAS	0.3 mm	0.3 mm	0.3 mm	0.3 mm	0.3 mm	0.3 mm
Beam transport + PAS		1.01 mm / 1.43 mm		0.48 mm / 0.58 mm		0.72 mm / 0.98 mm

Table 5-1: Main results of the random misalignment study for the beam transport of the Riesenrad ion gantry. The beam position uncertainty in the isocentre (titled "beam response" in the Table) is given separately in horizontal / vertical plane and expressed as  $3\sigma$  of the beam position probability distribution. Individual contributions are added quadratically. Finally, the misalignment tolerance (resolution error) for the photogrammetric alignment system (PAS) is added.

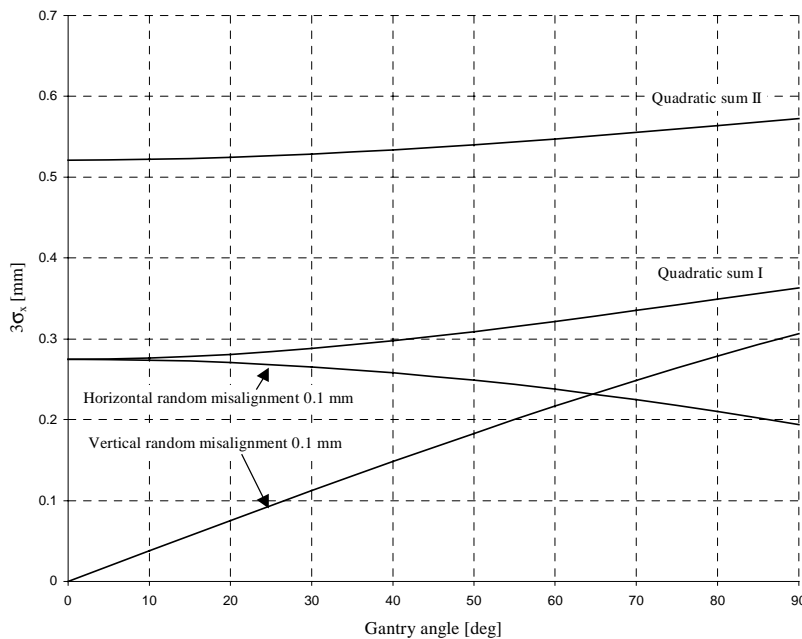


Figure 5-37: Demonstration of the summation of different random misalignment contributions leading to "vanishing" of the angular dependence of the beam position accuracy.

A further finding of the analysis is the fact that the angular dependence of the beam position uncertainty is practically negligible, which reduces drastically the calculations that have to be done in the future to refine the gantry design. There are two reasons for this very weak angular dependence. The first reason is that the standard deviation of the overall beam position probability distribution is given as a quadratic sum of many contributions, namely three independent shifts and tilts of each element, all elements being independently misaligned with respect to each other. Each individual contribution has its own angular dependence which may be increasing or decreasing with the gantry angle, so that in the quadratic sum the decrease of one contribution is well balanced by an increase in another.

The second reason is that there are also contributions from elements located downstream of the rotator-to-gantry coupling point. These contributions are independent of the angle of gantry rotation. The situation is illustrated in Figure 5-37 that shows the response of the beam (isocentre) position as a function of the gantry angle separately for horizontal and

vertical misalignments of  $3\sigma_{\text{shift}} = 0.1 \text{ mm}$  of the first quadrupole. The quadratic sum of these two effects is indicated as "Sum I" while "Sum II" is a quadratic sum of these effects *and* contributions from the elements downstream of the rotator-to-gantry coupling point. The overall angular dependence becomes practically negligible.

## 5.6 General Concept of Alignment and Beam Position Control, or: How to Assure That the Beam Meets the Tumour?

In the above analysis, the position of each beam transport element is characterised by a particular systematic misalignment and a standard deviation of the random misalignment distribution. All *systematic* misalignments can be *compensated* by the mapping strategy mentioned in Section 5.2.2.3, the random misalignments should be kept within the tolerances derived above.

During the treatment, the actual beam position must be measured permanently by an on-line beam position monitor placed as close as possible to the patient. In the case of intolerable beam excursions from the planned position, an interlock signal is sent to a special beam-stopping device and the treatment is interrupted.

The current practice in radiotherapy is to mount the monitoring equipment in the nozzle on the supporting frame of the beam line or the gantry. The obtained information is the relative position of the beam with respect to the nozzle and *not* with respect to the patient. This method is suitable for passive beam spreading techniques where the irradiated area is in fact defined by the collimators in the nozzle and not directly by the beam position. It may also be accepted for fixed beam lines where the relative position between the nozzle and the patient couch is fixed. For a gantry equipped with an active pencil-beam scanning, a different strategy is recommended. An optimum would be to attach the beam monitoring system to the patient couch, so that it measures the absolute position of the beam *with respect to the patient*. A possible technical solution of such a beam monitoring system is the "diagnostic ring", as described in Section 5.3.3 and schematically shown in Figure 5-38.

*The diagnostic ring permanently measures the actual beam position relative to the patient couch during patient irradiation.*

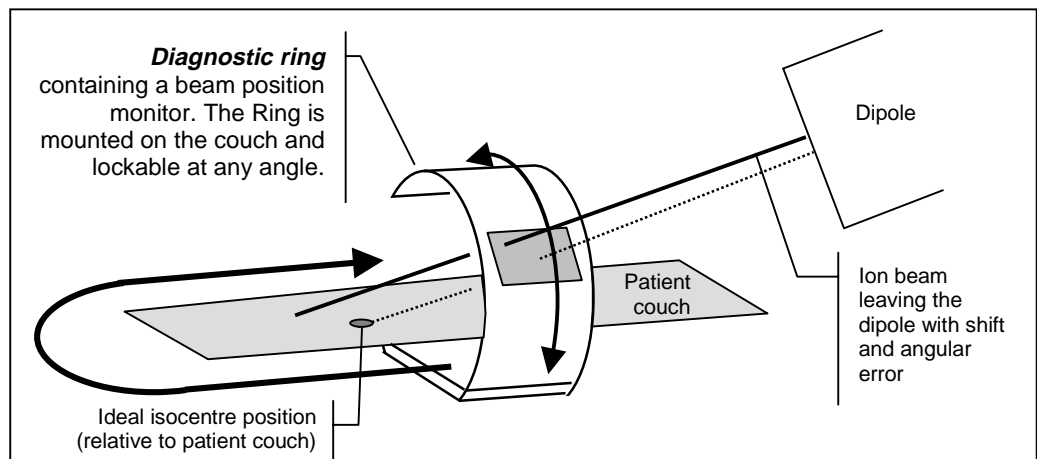


Figure 5-38: Principle of a "diagnostic ring" to permanently measure the actual beam position relative to the patient couch during patient irradiation. A beam position monitor can rotate around the patient on a rigid half-ring. The half-ring itself can be shifted along and rotated around the head of the couch. As the ideal isocentre relative to the patient table is known from the treatment plan, a theoretical beam path can be calculated (depending on the treatment angle and angle of couch rotation) and the centre of the beam monitoring device will be moved to the expected location. From the difference between expected hit and the actual passing point of the beam, a positioning error is calculated.

The CT scanner inside the patient cabin checks the relative position between patient and couch.

Two lasers running along the beam line reveal any accidental position error of the quadrupoles during gantry rotation.

The diagnostic ring gives full information on the beam position relative to the patient couch (hence also controlling the correct functioning of the photogrammetric alignment system). Evidently, any remaining source of uncertainty is related to the position of the tumour relative to the patient couch. Information about this can be . Fortunately, the cabin of the Riesenrad provides adequate space to accommodate this equipment and the same mechanics that hold the patient couch over the beam can reposition the couch in the scanner. It is reasonable to combine the CT with a PET camera (Beyer et al., 2000), offering the possibility to monitor the deposited dose immediately after the treatment in the same convenient way as it was done with the CT scan before irradiation.

In addition to the alignment errors discussed so far, other, let us call them "accidental" errors, may happen during routine gantry operation. They may be caused for instance by the sudden breakage of equipment, impacts on the structure and cameras etc. and would lead to a sudden, and probably large, deviation of the beam from the desired position. Basically, an accidental error can be interpreted as an excessive random misalignment occurring with low probability outside the  $3\sigma$ -region of the random misalignment probability distribution. In order to detect such an accidental error before a treatment starts, an *alignment control system* for the rotator and the gantry is proposed (see Figure 5-40). Two laser beams are running along the line of quadrupoles, whose relative positions towards the laser beams are obtained from retro-reflectors. By turning the quadrupoles, a different set of retro-reflectors becomes visible for the laser beams. Depending on the effort to be invested into this alignment control system, it is certainly capable of detecting misalignments in excess of  $\pm 0.3$  mm ( $3\sigma$ ), however, an even better performance can be expected. Another reason for this system is its ability to identify *the* element responsible for the beam displacement, which is not the case for the beam monitoring system measuring just the final beam position in front of the patient.

Figure 5-39 summarises the procedure for correct gantry alignment, alignment control, error detection and error compensation.

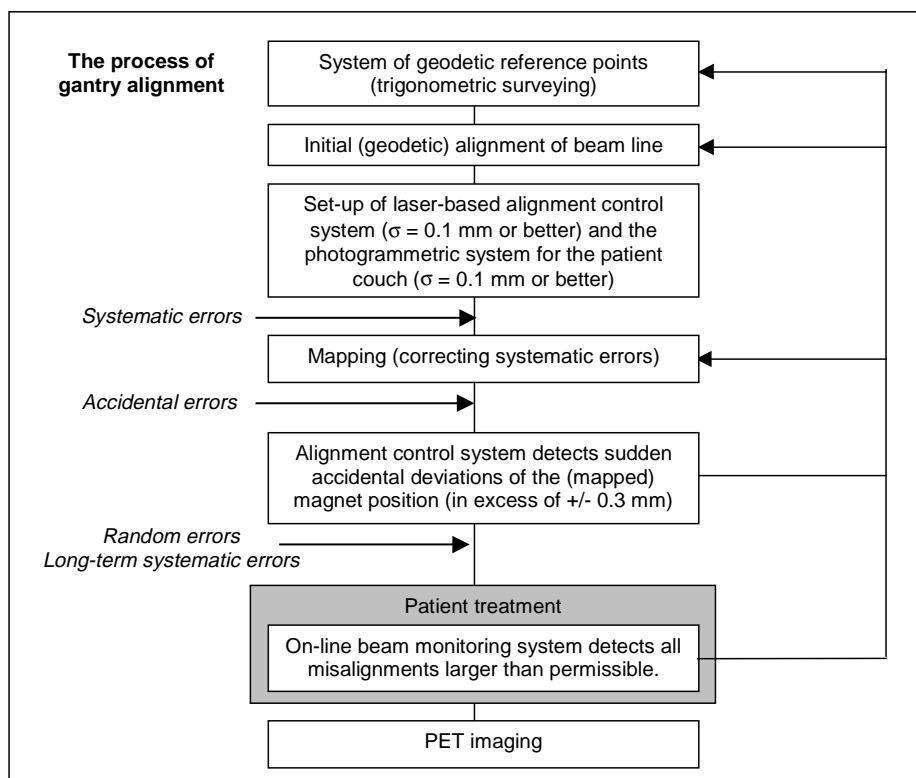


Figure 5-39: Principal steps in the alignment process of the Riesenrad ion gantry.

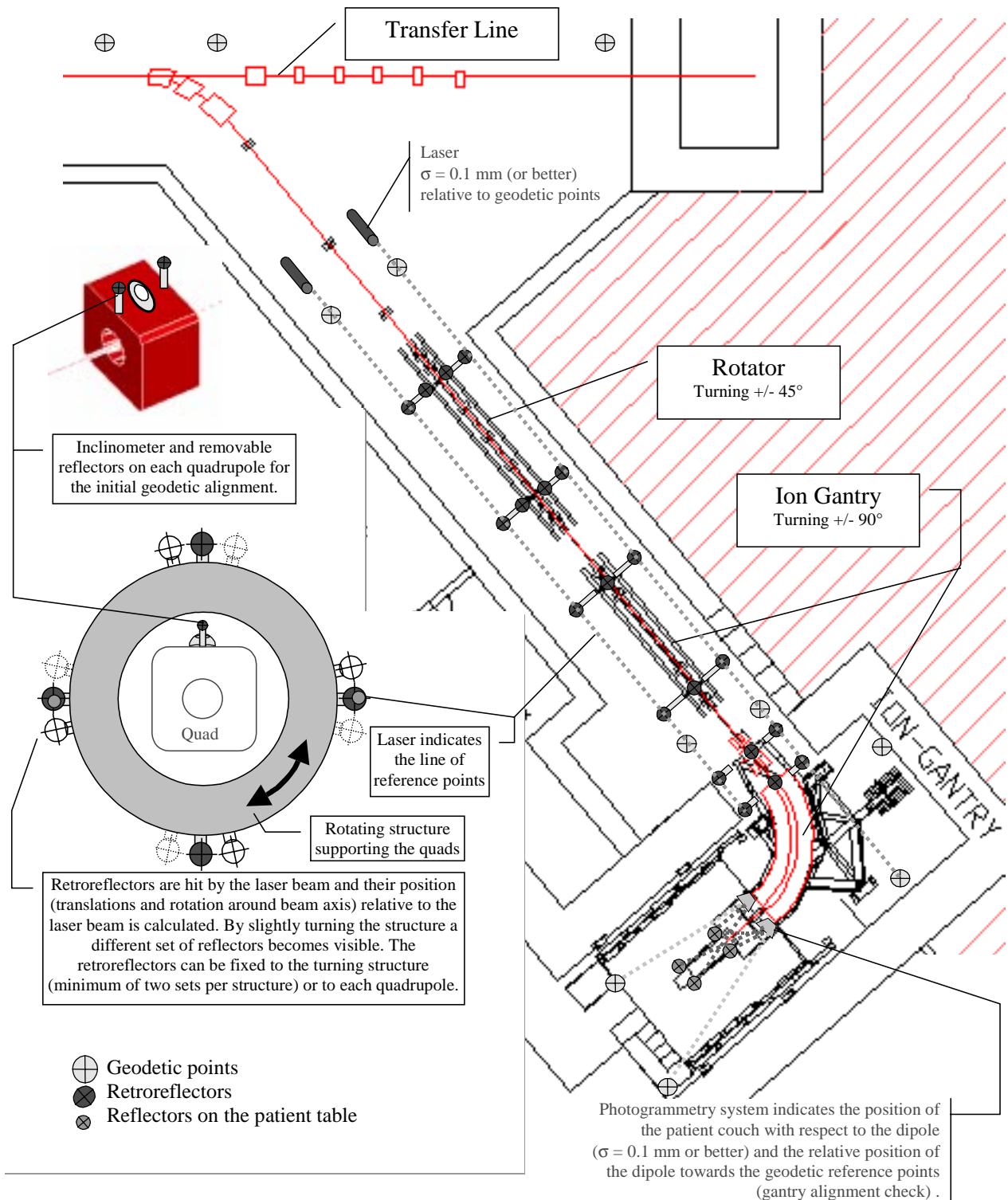


Figure 5-40: Function of the alignment control system and the photogrammetric alignment system in the Riesenrad gantry.



## 5.7 Gantry Hall

The gantry hall is the room housing the rotating gantry (cage) and the patient cabin, as well as additional equipment such as the lift, a maintenance staircase, an emergency staircase and an overhead crane. Principally, no (substantial) storage capacity (for instance for patient moulds) is foreseen inside the - heavily shielded - gantry hall but it could be implemented in the design if desired. It is expected that the horizontal ion beam will enter the gantry hall roughly 1 m above ground level (perhaps a little lower if the accelerator complex were to be partially underground for shielding reasons), therefore, at least half of the gantry hall is underground. The operational access to the hall is via the chicane, while maintenance and emergency access is from the transfer-line building. Each of these access points is at mid-height of the hall and adjacent to a staircase.

### 5.7.1 Geometry

The following conditions govern the geometry of the gantry hall:

- The vertical movement of the patient cabin requires a free space of about 8 m above and below the beam level. Including one extra metre for the overhead crane, the total height of the hall is 17 m.
- In the current design the breadth of the hall is 7.1 m. This parameter is governed, on one hand, by the patient cabin which has to allow a 360° couch rotation and accommodate a CT/PET and, on the other hand, this value also represents the minimum to accommodate the access to the chicane, the lift and the staircase.
- When rotating the cage, the most eccentric point describes a circle with a diameter of 8.6 m. Adding the space needed for the (enlarged) patient cabin (6.8 m), the emergency staircase (1.8 m) and some additional space for the ventilation ducts and the connection bridge on the counterweight side of the hall (0.6 m), gives a total length of the gantry hall of 17.8 m. In the case that the total desired depth of the lift exceeds 1.8 m, the length of the hall can be increased locally.

Although the geometry of the gantry hall could be fitted more tightly to the equipment (in particular on the counterweight side of the room), a cubic geometry is maintained to allow the installation of an overhead crane travelling the whole length of the hall. Thus, one obtains for the floor area and the inner volume of the hall about 126.4 m<sup>2</sup> and 2148.5 m<sup>3</sup> respectively.

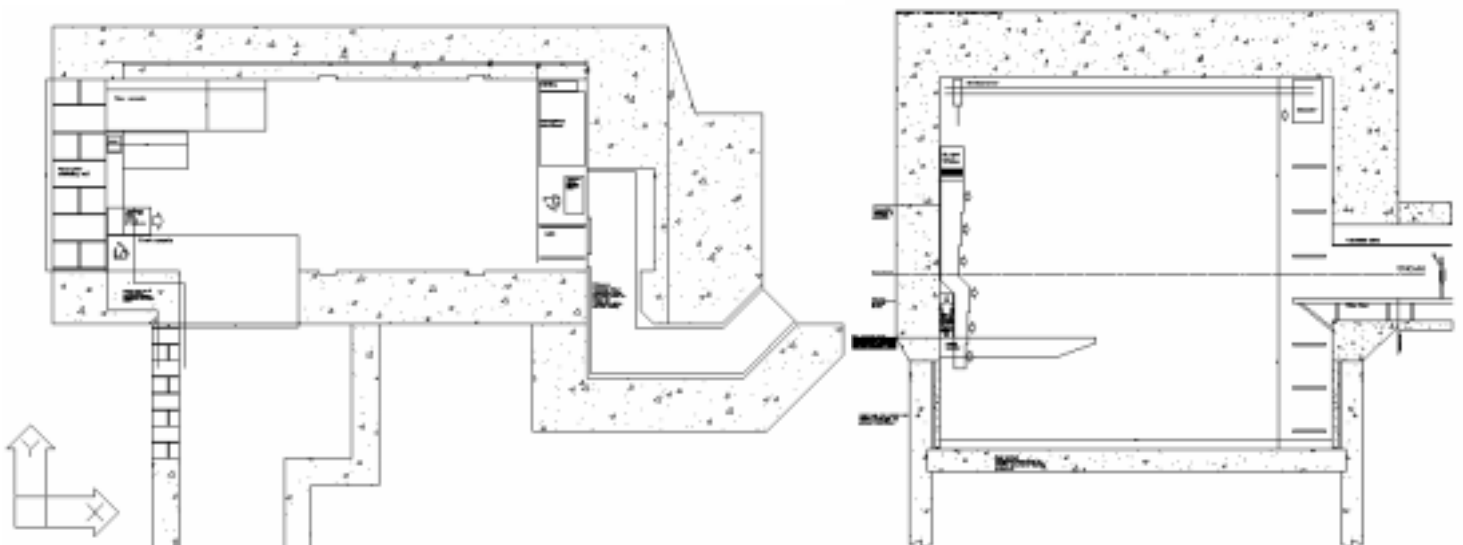


Figure 5-41: Plan and vertical section of the gantry hall

The final design of the chicane depends on the integration of the ion gantry into the facility and the required shielding performance. The minimum corridor breadth is 2 m to allow the transportation of already pre-positioned patients on movable couches. The chicane will be equipped with a false floor and a suspended ceiling to make space for ventilation ducts and cables.

The following access points will have to perforate the shielded enclosure:

- *Access from the chicane.* This is the general access for personnel and patients connecting the chicane with the lift, emergency staircase and patient cabin. At the opening - 3.8 m × 4.4 m - ventilation ducts and cabling will be guided towards the false floor or the suspended ceiling of the chicane.
- *Access from the transfer line.* This is the point at which the transfer line to the gantry "docks" onto the gantry hall. The front structure of the cage (carrying the scanning magnets) cantilevers into this opening and determines its minimum size. However, the actual dimensions of 4.4 m × 5.15 m are considerably larger because this area also houses several secondary functions like the cable drum to roll on and off the heavy conductors and water-cooling pipes of the dipole during gantry rotation, a staircase to bridge the vertical distance between transfer line and the console and - desirably - a small platform to facilitate any work concerning the scanning magnets. Theoretically, the opening could be slightly widened and then act as the main passage to bring in all the heavy equipment during gantry installation. However, this would also require a heavy-load overhead crane in the transfer line. In addition, the "hand-over" from this crane to the one in the hall seems difficult. The solution below is preferred.
- *Temporarily removable sidewall to bring in the heavy equipment (optional!).* The feasibility of this option depends on the final integration of the gantry into the facility. The gantry body, main ring and the rear support unit could be assembled outside of the hall in one piece, which is then shifted as a whole laterally through the opening to its final position. Rails could be fixed to the consoles, hence avoiding the need for a heavy overhead crane. Should this option be impossible (because there has to be for instance another gantry room adjacent) the access for bringing in the major parts of the gantry for assembling has to be via the ceiling or via the access from the transfer line. The former is preferred.
- *Service ducts, in particular for the ventilation system.* The location of ducts depend on the final layout of the facility.

## 5.7.2 Radio-Protection and Shielding

When a beam of high energy particles, such as a carbon-ion beam with 400 MeV/u, interacts with matter or human tissue, secondary ionising radiation (mainly fast neutrons with energies up to the one of the original particle) is emitted, having sufficient energy to damage human DNA. In order to protect the outside - personnel and the public - from this ionising radiation, a suitable shield has to attenuate the radiation to an acceptable limit<sup>26</sup>. In addition, the gantry is a controlled area (radiation zone) and the access to the room must be restricted to monitored personnel only. Before the ion beam is directed into the ion gantry (for testing or treatment), it has to be guaranteed that no person (except from the patient) is inside and that the access to the gantry hall and transfer line is blocked (interlocks!).

Usually, the shielding is achieved by sufficiently thick concrete walls or - for a building underground - by the soil. Generally, attenuation of the dose is proportional to the density of the shielding material and increases exponentially with the thickness of the shield. However, when secondary neutrons enter the shield they produce more particles by interaction than are absorbed, hence this exponential attenuation will only occur after secondary particle equilibrium has been established. For a concrete shield and small emission angles of the secondary neutrons this equilibrium is reached approximately after the first metre of penetration as it can be seen from Figure 5-42. Consequently, a concrete

<sup>26</sup> When the fast neutrons interact with shielding material, additional gamma radiation is emitted which contributes up to about 30% to the dose equivalent behind the shield (Agosteo et al., 1999, Table 1).

thickness in excess of one metre has to be expected throughout the facility. For example, the average wall thickness applied in the existing proton therapy facilities is around 2 m. Openings in the shielded enclosure (access points or service ducts) must not reduce the shielding thickness, which is usually achieved by giving this "duct" the shape of a chicane.

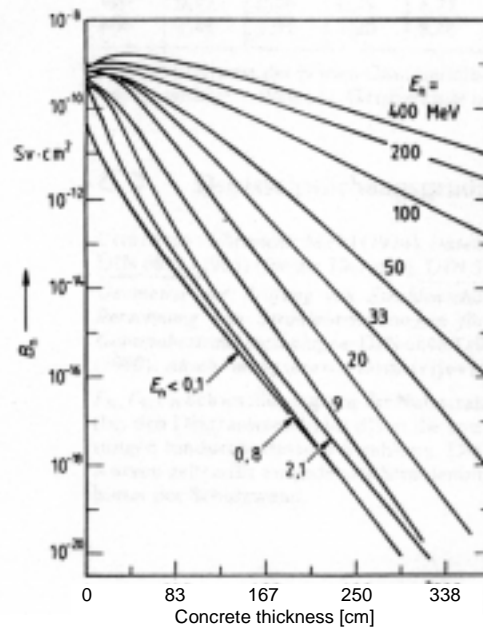


Figure 5-42: Reduction of equivalent dose in concrete ( $\rho = 2.4 \text{ t/m}^3$ ). One can see the dose build-up region within the first metre before the shielding becomes "effective". Source: similar to Reich et al., 1990, p. 362

The determination of the necessary shield requires the estimation of the equivalent dose to be expected outside a given shield for a known beam loss. Whereas there is plenty of data available to estimate the required shielding thickness in proton therapy (see for example the new ICRU Report 63 (entitled "Nuclear Data for Neutron and Proton Radiotherapy and for Radiation Protection"), information concerning the necessary shielding due to ion treatment is rare. There is no general guideline on how to calculate the necessary shielding thickness, nor is there a detailed description available on how to exactly enforce the above principles for radio-protection.

*A maximum shielding thickness of 4 m of concrete can be expected.*

For the planned ion-therapy facility in Germany (Debus et al., 1998) G. H. Hartmann (1998) based his calculation on the assumption that only fast neutrons with an energy higher than 100 MeV will substantially contribute to the dose behind the shielding wall. Given the maximum ion flux of  $3 \times 10^8 \text{ s}^{-1}$  (PIMMS:  $4 \times 10^8 \text{ s}^{-1}$ ) he derived the maximum neutron flux density in the forward direction to be  $8.33 \times 10^3 \text{ s}^{-1} \text{ cm}^{-2}$ . Converted to a maximum equivalent dose rate, this gives 8.55 mSv/h *in front* of the shielding wall. About 4 m of concrete would be necessary to reduce this by a factor of 1000 to the aimed value of  $5 \mu\text{Sv/h}$  for the effective dose per hour behind the shielding wall when the machine is running at *maximum* energy and *maximum* intensity. Assuming an *average* value of  $2 \mu\text{Sv/h}$ , a 10% presence of a reference person and about 4 hours per day beam-on in the gantry, the person would not receive more than the allowable 0.3 mSv/a effective dose specified in the German code for radiation protection (Deutsches Bundesamt f. Strahlenschutz, 1976/1997, §45).

A different approach can be found at the TERA-blue book (1995, pp. 455-462) where the shielding calculation concerning protons was extrapolated to carbon ions. Assumed dose limits for the staff (occupationally exposed workers) were 2 mSv/a. Considering someone working 2000 h/a the authors derived a design dose rate of  $1 \mu\text{Sv/h}$ . The results indicate concrete thicknesses of up to 3.8 m, nevertheless it was stated that for ions the calculated dose rate was "much higher than the design dose rate" (p. 461).

For the final design of the Riesenrad gantry a detailed study on the required shielding has to be made taking into account the actual integration of the gantry into the facility and the foreseen operational procedures. For the preliminary design of the gantry hall 4 m thick concrete walls are assumed for the chicane design, since this is probably the only part

behind which a regular occupancy is to be expected. For those walls on which the beam can be directed, i.e. the upper part of the chicane-wall and the ceiling, 3 m concrete are assumed. The rest is foreseen to have a shielding thickness of 2 m.

### 5.7.3 Civil Engineering

*Diaphragm walls will form an earth retaining perimeter wall.*

Given that the level of the incoming beam is about 1 m above ground, then the lowest part of the gantry hall will be about 10 m below surface level. Construction of the hall will therefore depend on ground conditions, in particular the ground water table. The most likely construction method, however, is to use *diaphragm walls* to form an earth retaining perimeter wall prior to the excavation of the pit.<sup>27</sup> These walls - usually about 80 cm thick - will have to cross the water carrying soil layers until they are well embedded into impermeable soil with a sufficient bearing capacity. If such a layer can not be found at reasonable depth, other methods like underwater-cast slabs with tension piles have to be considered.

Once the diaphragm walls are in place, excavation can start. Each wall becomes a continuous reinforced concrete slab that cantilevers from the bottom, their principal support being the two perpendicular walls at the ends. For the longer walls this might not be sufficient. Instead of adding a row of permanent ground anchors the preferred solution would be to build a cross girder somewhere at the top of the longer diaphragm wall that would function as a simple support for the diaphragm wall on their upper edge. This girder then transfers the loads to the smaller, lateral walls (see Figure 5-41). In addition to their earth retaining function, the diaphragm wall will - and this is its essential feature and makes it well suited in our application - provide the permanent support and foundation for the shielding walls above.

*The gantry hall has to be insulated.*

Once the underground part of the hall is excavated, a 30 cm thick internal facing wall will be added, separated from the diaphragm wall by a thermal insulation (e.g. 8 cm extruded polystyrol) and a watertight lining. A reinforced cap at the top of the diaphragm walls will widen their cross-sections to accommodate the considerably thicker reinforced concrete shielding walls.

Depending on the final integration of the gantry into the clinic one has to foresee zones of removable shielding to bring in the large body of the gantry. As mentioned above, a removable sidewall made out of large, cubic concrete blocks is preferred. However, one could also imagine that parts of the ceiling are made out of pre-cast beams (7.1 m free span) piled up to the required shielding thickness which can be removed by a mobile crane. For insulation purposes the gantry hall will have a 10 cm outside insulation (e.g. expanded polystyrol) covered by a cladding.

Inside the gantry hall, three consoles are foreseen, each of them is built-in the concrete wall and cantilevers into the gantry hall:

- *The front console supporting the rollers of the front ring.* A steel-concrete composite structure is suggested for this critical area since the load is heavy (800 kN to be carried with a lever arm of approx. 1.3 m) and the ratio between the cantilever length and the permitted height is more that of a cantilever than a console. In fact for the inner pair of rollers - inner with respect to the centre of the gantry hall - the height of the console is limited to ~0.55 m, since a larger height would lead to a collision with the telescoping patient cabin.
- *The rear console.* This is a classic unit that is highly loaded (400 kN).
- *The access platform.* This is made out of steel, connecting the chicane with the patient cabin.

<sup>27</sup> A diaphragm wall is constructed by excavation in a trench, which is temporarily supported by a bentonite slurry. On reaching founding level steel reinforcement is lowered into the trench, followed by placing concrete to displace the bentonite (see also the glossary).

*Large settlements have to be expected due to the heavy shielding walls*

Due to their difference in weight, a joint separates the gantry hall from the adjacent buildings (chicane and transfer line building). This joint allows a differential settlement of the buildings in a controlled manner. The 1270 kN of the gantry are entirely taken by the walls of the building (via the consoles) and directed to the foundation. Nevertheless, that weight is negligible compared to the own weight of the shielding walls: for a 3 m thick shielding wall supported by a 1 m thick diaphragm wall, the ground below the base of the diaphragm wall has to withstand a pressure of about 1100 kN/m<sup>2</sup> - a value that is usually presumed for the allowable bearing strength of moderately weak rock. A reasonable estimation of the settlements can only be made once the ground conditions are known. In the worst case, settlements for the gantry hall that are in the cm-region have to be expected. Suitable detection mechanisms and compensation possibilities (at the equipment supports and with the beam control software) have to be foreseen.

*An overhead crane is foreseen in the hall*

The height of the gantry hall foresees the installation of an overhead crane. Depending on the chosen procedure for the installation of the cage and the dipole, the required load capacity varies between 620 kN (dipole weight) and 100 kN.

### 5.7.4 Dipole Cooling and HVAC

Table 5-1 showed the unfavourable effects of temperature fluctuations inside the gantry hall on the beam stability and the recommended maximum for the fluctuations was  $\pm 1$  K. This value is equally true for a uniform temperature rise and a temperature gradient in the gantry hall, as well as for a relative temperature difference between dipole and structure, the latter being at room temperature which was set to 24°C since patients might be dressed very lightly, but should not feel uncomfortable.

*Cooling the 60 t dipole should not affect the room temperature.*

This suggests that cooling the dipole should be done in a way that the surface temperature of the dipole always stays within a region between 23°C and 25°C, hence

- Minimising the heat transfer to the air and therefore the heat load for the air ventilation system of the gantry hall.
- Keeping the average temperature of the dipole and the gantry hall the same, which not only avoids relative deformations between structure and dipole during operation but also when the dipole is switched on for the first time or switched off for a longer pause.
- Requiring the average temperature of the water cooling circuit to be approximately room temperature. Inlet and outlet temperature should be symmetric to that value, but the lower bound for the inlet is the dew-point temperature in the room, i.e. 16°C.

As a result of these considerations, it is envisaged to virtually remove all of this heat directly by the (de-mineralised) water cooling system of the dipole, which - compared to the original dipole design - has to be slightly modified. These changes and the characteristics are outlined in Table 5-2.

<b>Modified parameters of the Riesenrad dipole (to minimise heat released into the air)</b>	
Water hole diameter in the outer coils [mm]	16
Water hole diameter in the inner coils [mm]	13
Available water pressure for a single circuit [Bar]	7
Inlet temperature [°C]	16
Resistance (magnet) [ $\Omega$ ]	0.019
Maximum power dissipation [kW]	369
Current density in the outer coil [A/mm <sup>2</sup> ]	4.95
Current density in the inner coil [A/mm <sup>2</sup> ]	4.60
Temperature rise in a single circuit in an outer coil [°C]	16.96
Temperature rise in a single circuit in an inner coil [°C]	16.10
Water flow (magnet) [l/s]	5.29

All other parameters remain unchanged with respect to the initial design (compare Table 3-2).

Table 5-2: Proposed modifications to the design of the Riesenrad dipole in order to achieve a uniform average temperature of the cooling water, of the dipole and in the gantry hall of 24°C.

The inlet temperature of 16°C can not be directly achieved with cooling towers but needs a water chiller for the dipole cooling circuit (power 385 kW). Since the dipole will not run continuously but will be switched on and ramped for 2 minutes say every 20 minutes, its power dissipation is not at all stationary. In order to keep the dipole at a constant temperature it is foreseen to measure the temperature of the water leaving the dipole and adjusting the flow rate so that a temperature rise from 16°C to 32°C is always maintained.

The above assumptions for the dipole cooling are conservative and there is the option to slightly relax the specifications since the heavy mass of the dipole can "store" some excessive heat when the dipole is switched on<sup>28</sup>. This energy can eventually be extracted by the cooling water during the pauses between the treatments.

### *The air conditioning system*

The main task of the air conditioning (AC) system is to guarantee a temperature stability in the gantry hall of  $\pm 1^\circ\text{C}$  (around a reference room temperature of 24°C). This is of particular importance for the central cage and the dipole. In addition, the AC also has to control the humidity, air changes per hour and fresh air supply (as specified in Table 5-5). Depending on the local safety regulations the gantry hall might have to be under-pressurised with respect to the adjacent rooms.

Heat sources inside the gantry hall are estimated to be around 8 kW. Adding 7 kW for the cooling of the fresh air gives a required air-cooling capacity of about 15 kW, which can be supplied by the water chiller for the dipole cooling. Note that the above concept for the dipole cooling has reduced heat dissipation from the dipole surface to the air via surface convection to a negligible amount, although conservative assumptions were made (see Table 5-5).

Since the cage is the most temperature sensitive piece of equipment, the 21500 m<sup>3</sup>/h of pre-conditioned air are blown at a constant flow rate from the counterweight side over inlets that are distributed vertically over the whole height of the cage (~8 m). Possibly, it will be necessary to direct some air to the cable drum, since the conductor cables dissipate a considerable amount of heat. The extraction will be done via two exhausts on the opposite (chicane) side, one at the top and one at the bottom of the hall. Each of them is capable of extracting the total airflow alone. When the cabin is in reference position ("docked" to the chicane), the horizontal airflow will be separated by the cabin and each of the two exhausts will work at half of the maximum flow rate. When the cabin is moved to more "extreme" angles of gantry rotation, say to -90° (representing a beam pointing upwards), then most of the air will be extracted by the bottom exhaust since the telescoped cabin blocks the air flow to the upper one. For a beam pointing downwards, i.e. the cabin being positioned close to the floor of the hall, only the top exhaust will be fully operational.

Small ventilators fixed to the front walls of the inner cabin will supply the cabin with 2150 m<sup>3</sup>/h of air (equalling a volume 10 times that of the fully telescoped cabin).

The complete HVAC system is outlined in Figure 5-43.

---

<sup>28</sup> Heating the entire dipole by 1°C would require running the magnet at full power without *any* cooling for more than one minute.

# Dipole cooling and HVAC concept for the Riesenrad ion gantry

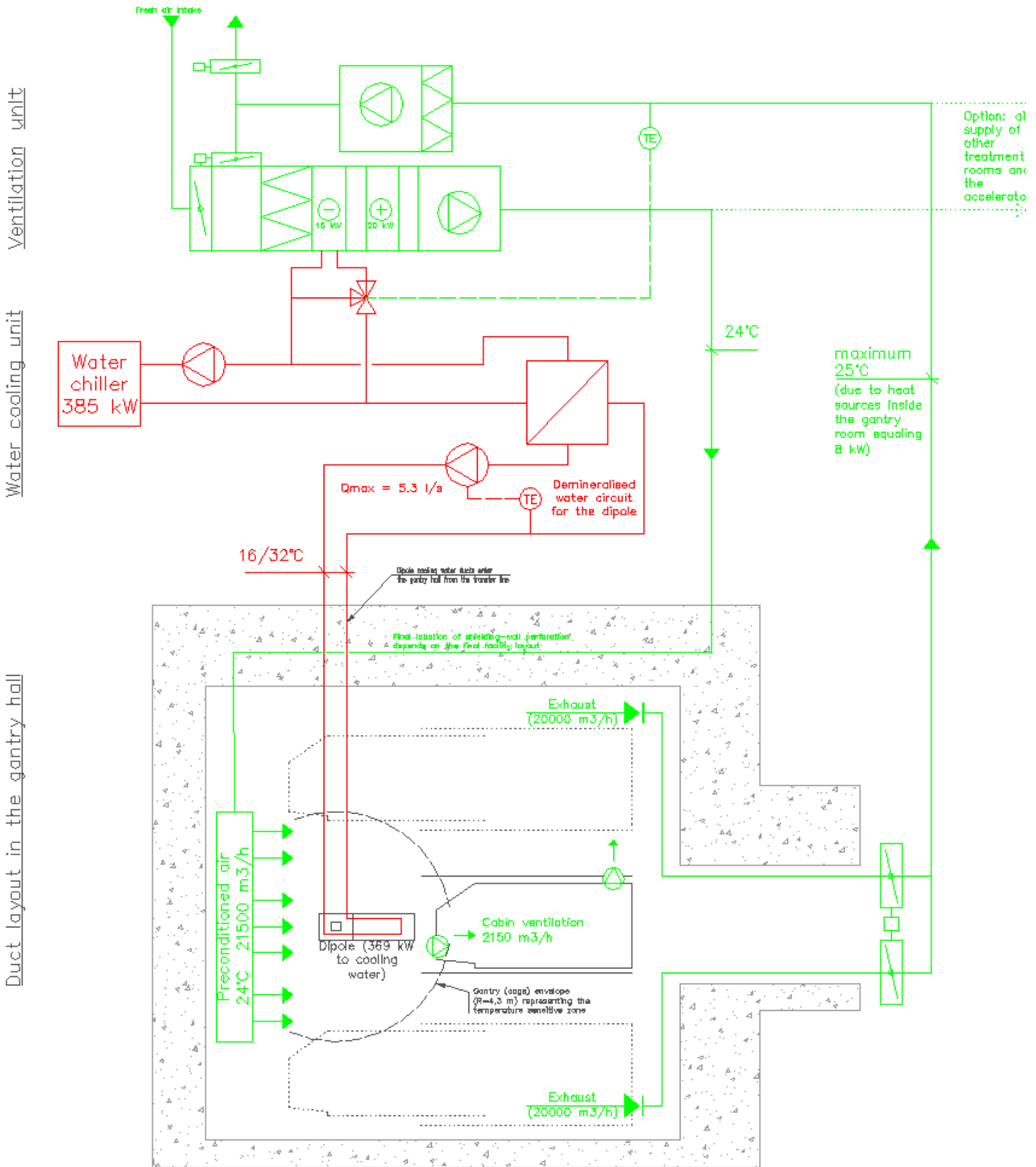


Figure 5-43: The HVAC system of the gantry hall.

### 5.7.5 Integration of the Riesenrad Gantry into a Therapy Facility

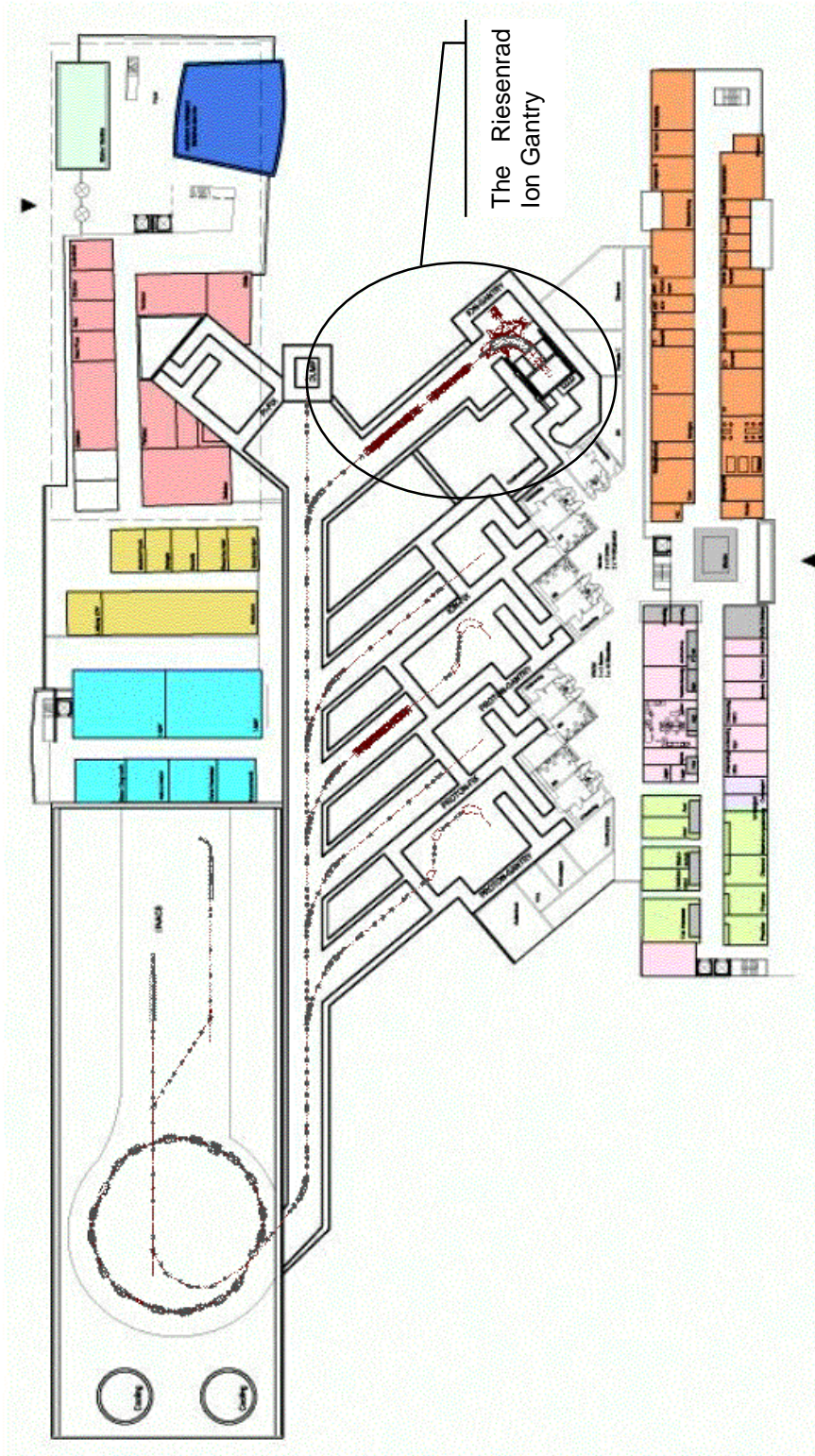


Figure 5-44: The generic facility for proton and ion treatment designed by PIMMS.

Throughout the process of gantry development, attention was paid to the integration of the Riesenrad gantry into a therapy centre for combined ion and proton treatment, which is shown in Figure 5-44. The generic architectural concept - reported in detail in the PIMMS report (Bryant et al., 2000, Chapter II-2) - is based on a modular design (on a green field), which makes it simple to adapt the treatment complex to individual needs. The separation of the main functional areas (science, accelerator and transfer lines, ambulatory, treatment) allows for the further development of any part of the project without disturbing the functionality of the others. All patient-related functions are concentrated on the ground level. Patient preparation and waiting areas are situated adjacent to the treatment rooms.



## 5.8 Cost Estimate

The cost of the Riesenrad ion gantry depends heavily on its procurement method: is the gantry system ordered on the basis of a design & build contract from a potential industrial company or does a client's design and project management team integrate the various participations from industry? The novelty and complexity of the task clearly prefers the latter. Another crucial parameter affecting the cost is the number of gantry systems ordered: does one prototype have to bear all the costs of development and design? This concerns in particular the execution design of the cage, the patient cabin, the patient couch and all the related software for steering.

Table 5-3 gives a rough estimate of the cost to be expected for such a prototype of the Riesenrad ion gantry. However, it should be noted that:

- The Riesenrad gantry is certainly a more cost-effective solution with respect to any other ion gantry variant developed so far
- Business plans for the various projects of therapy facilities clearly identify the running cost of such a centre to be the major cost and not the depreciation of the investment (Hradsky et al., 1998; Debus et al., 1998, pp. 79-90).

<b>Estimated cost of the Riesenrad ion gantry [MCHF]</b>			
Central cage			1,73
structure	40 t x 25 CHF/kg =	1	
counterweight	23 t x 10 CHF/kg =	0,23	
rear support (pair of tapered roller bearings)		0,02	
front support (incl. 4 rollers)		0,03	
drive		0,15	
steering		0,3	
Patient cabin			2,2
structure		1,3	
lift		0,5	
steering		0,4	
Patient couch incl. diagnostic ring			1,9
Rotator and gantry quadrupole cage			0,2
structure	4 t x 25 CHF/kg =	0,1	
steering		0,1	
Alignment system			1
photogrammetry		0,2	
laser-based alignment system		0,3	
beam monitoring equipment		0,5	
Beam line (incl. steering)			2,1
main dipole		1,3	
scanning dipoles (3)		0,1	
quadrupoles (11; taken from a series of 130)		0,1	
design effort	3 manyears	0,3	
vaccum system		0,3	
<b>Total gantry structure</b>			<b>9,1 MCHF ( 5,9 MEuro)</b>
Gantry hall			2,45
civil engineering		1,4	
cooling and ventilation (pro rata)		0,8	
overhead crane		0,2	
staircase (2)		0,05	
Control and safety system (pro rata)			1,6
hardware		0,6	
software	10 manyears	1	
Putting into operation and commissioning	10 manyears		1
Planning & project management			1
Diagnostic (CT/PET)			2
<b>Total Riesenrad gantry</b>			<b>17,2 MCHF ( 11,0 MEuro)</b>

not included: cost of the beam scanning system (software)

Table 5-3: Basic cost estimate for the Riesenrad ion gantry (including rotator, costs for the gantry hall, the combined PET/CT-scanner, and pro rata costs of the HVAC and the control system).

## 5.9 Summary

### Design characteristics of the Riesenrad gantry

#### Cage

Overall dimensions	approx. $\varnothing$ 8.6 m (plane of rotation) $\times$ 7.5 m (depth)
Counterweight	23 t
Weight of the structure	40 t
Dipole weight	62 t
Total weight	127 t
Max. speed of rotation	0.75 rpm
Emergency break within	0.25 s equalling a gantry movement of about 10 cm at the patient
Characteristics of the structure	Balanced steel structure; principal pieces are welded, machined and then bolted together on-site; the design principle is based on shear walls that span between the supports, two truss-like girders assist to hold the dipole on one side and the counterweight on the other; the structure is optimised to reduce deformation as much as possible, parts of the elastic deformation is compensated intrinsically.
Support	Structurally determinate: pair of single-row taper roller bearings at the rear (fixed support), two pairs of self-aligning rollers supporting the front ring
Maximum member stresses	$< 20 \text{ N/mm}^2$ (yield strength is $355 \text{ N/mm}^2$ )
Support reaction forces	Rear support: 400 kN (vertically downwards) Front rollers: 240 kN each (radially)
Elastic deformation (systematic error)	$< 0.1 \text{ mm}$ along the central axis of the beam in all three dimensions
Temperature deformation (random error)	Assuming a temperature control of $\pm 1 \text{ K}$ in the hall and for the dipole, worst case scenarios yield deformations similar to the elastic ones.

#### Patient cabin

Overall dimensions	12.9 m (telescoped length) $\times$ 6.5 m (depth) $\times$ 3.8 m (height)
Total weight	19.5 t
Characteristics of the structure	Telescopic cabin with steel trusses as lateral walls which take the cantilever moment; transfer of forces between inner and outer cabin via small discs, carriages or preferably pinions; simply supported beams span between the walls to transfer the (single) loads; aluminium floor system; maximum telescopic movement 5.6 m; vertical travel $\pm 5.6 \text{ m}$ along 4 masts fixed to the wall; positioning accuracy 2 cm (treatment accuracy guaranteed by the patient couch); 60 s
Max. travel time	60 s
Principal loads	Patient couch 10 kN, combined CT/PET 18 kN
Deformation	Max 2.6 mm at the isocentre (service conditions) and 0.4 mm relative between isocentre and CT/PET
Access	From the rear wall via a rack & pinion lift and a staircase.
Patient couch	4 degrees of freedom (vertical, horizontal and two rotations), re-positioning accuracy $< 0.1 \text{ mm}$ ; carrying diagnostic ring to monitor beam position on-line
Photogrammetric alignment system (PAS)	Guarantees the correct alignment of the patient couch with respect to the dipole face with an accuracy $< 0.1 \text{ mm}$ ( $\sigma$ ). Minimum 4 cameras are attached to the dipole watching reflectors fixed to the patient couch.

#### Flexibility

$4\pi$ -beam access to the patient; large floor area of the cabin facilitates patient handling and the installation of auxiliary equipment; additional equipment loads inside the cabin do not affect the overall alignment; modification of the design in order to house two cabins and thus increase efficiency by over 45% is possible.

#### Treatment procedure



Patient cabin is in its initial reference position, vertically at entrance level, horizontally retracted. The cage is set to the specified treatment angle, meanwhile patient and accompanying personnel enter the patient cabin directly via the chicane. Cabin is set to the actual treatment position using vertical and horizontal translations. Patient lies down on (or is transferred from a transport device onto) a patient couch and positioned with respect to the couch. Patient couch is brought into treatment position and aligned precisely using the photogrammetric system with respect to the exit face of the dipole magnet. The final patient position is verified. Personnel leave the cabin with the lift. Beam is switched on and treatment session starts.

#### Safety

Access	At all times (direct or lift or staircase)
Emergency stop of the cage	Within an angle of $1.2^\circ$ or 0.25 s equalling an over-travel of 10 cm at the isocentre.
Collision prevention	Patient cabin and/or cage can only be moved when the patient couch is in its reference (backward) position. Cage is only rotated when the patient cabin is in the fully retracted position. Cage and the fully retracted patient cabin can be moved independently

### Beam position analysis

Systematic error due to elastic deformation of the structure	< 0.2 mm at the tumour
Random error due to reference misalignments of $3\sigma = 0.1$ mm of the magnets	$3\sigma$ of the beam position probability distribution < 1.4 mm at the tumour
Random error due to photogrammetric alignment system (PAS)	$3\sigma$ of the beam position probability distribution < 0.3 mm at the tumour
Random error due to calculated temperature effects	$3\sigma$ of the beam position probability distribution < 0.5 mm at the tumour
Total random error due to PAS and temp. effects	$3\sigma$ of the beam position probability distribution < 0.6 mm at the tumour

### Alignment control

Check relative position patient to couch	Via CT inside the cabin
Check relative position couch to dipole	PAS (mechanical errors only) and diagnostic ring (mechanical and beam-optical errors)
Check dose deposition after treatment	Via PET inside the cabin
Check mechanical alignment of the magnets	Via laser-based alignment control system (check during gantry rotation)

Table 5-4: Design characteristics of the Riesenrad ion gantry.

### Principal parameters of the gantry hall

Architecture and structure				Comments
Surface area [m <sup>2</sup> ]	126			( = 17,8 m x 7,1 m )
Volume [m <sup>3</sup> ]	2148			( = 17,8 m x 7,1 m x 17 m )
Volume of the patient cabin [m <sup>3</sup> ]	215			when fully telescoped
Adjacency (in order of importance)				control room, sub-waiting area, dressing, storage of immobilisation devices
Special requirements				shielding 2 - 4 m concrete partly removable side wall ( opening of 5 m x 5 m ) restricted use of flammable and burnable material
Equipment				Gantry (127 t) Patient cabin (20 t) Lift 30 t overhead crane
Structure				underground part: 1 m thick diaphragm walls with internal facing wall upper (shielding) walls 2-4 m reinforced concrete heavily loaded consoles partly as composite structure ceiling with prefabricated elements and in-situ casting on top
<b>HVAC</b>				
Reference temperature [°C]	24			
Temperature stability [°C]	+/-1			
Relative humidity [%]	40 - 60			
Highest dew-point [°C]	16			
Relative pressurisation	low or even			depending on national regulations
Fresh air intake [m <sup>3</sup> /(h*person)]	75			
Average occupancy [persons]	3			
Minimum fresh air [m <sup>3</sup> /h]	225			
Air changes per hour in the gantry hall	10			to assure a uniform temperature distribution
Total air flow [m <sup>3</sup> /h]	21480			of which min. 1 % has to be fresh air
Air velocity around the cage [m/s]	0,12			for an assumed cross-section of 50 m <sup>2</sup>
Air changes per hour in the patient cabin	10			
Air flow in the patient cabin [m <sup>3</sup> /h]	2150			when fully telescoped
Heat loads on the ventilation system				
	kW	duty factor	continuous load in kW	
Dipole surface	0,6	0,1	0,1	$\Delta T = 1^{\circ}\text{C}$ (betw. air and dipole surface) surface area = 31,3 m <sup>2</sup> $\alpha = 20 \text{ W}/(\text{m}^2\cdot\text{K})$
Conductors leading to the dipole	1,4	0,1	0,1	$l = 13 \text{ m}$ $A = 3000 \text{ mm}^2$ current density = 1,5 A/mm <sup>2</sup>
Machine drives for cabin, cage and lift	60	0,1	6,0	
Walls to the ground ( 80 cm concrete, 8 cm XPS_035, 30 cm concrete )	-2,9	1	-2,9	$\Delta T = -18^{\circ}\text{C}$ $k = 0,34 \text{ W}/(\text{m}^2\cdot\text{K})$ $A = 475 \text{ m}^2$
Walls to the outside - summer conditions	0,7	1	0,7	$\Delta T = 6^{\circ}\text{C}$
Walls to the outside - winter conditions ( 200 cm concrete, 10 cm EPS_035, air gap, cladding )	-3,9	1	-3,9	$\Delta T = -34^{\circ}\text{C}$ $k = 0,25 \text{ W}/(\text{m}^2\cdot\text{K})$ $A = 455 \text{ m}^2$ i.e. 2/3 of surface above ground
Fresh air cooling in summer	7	1	7,0	Basis: about 4% of total air flow
Fresh air heating in winter	-13,5	1	-13,5	Basis: about 4% of total air flow
Lights	2	1	2,0	
Ventilators for the patient cabin	0,5	1	0,5	
Persons	0,4	1	0,4	
Electronic equipment	1	1	1,0	
CT/PET	0,5	0,2	0,1	
Required cooling power for ventilation system [kW]			15,0	
Required heating power for ventilation system [kW]			-20,3	
<b>Plumbing</b>				
Dipole water cooling [l/s]	5,3			variable; chilled water at 16°C
Pressurised air and vacuum cleaning				in the pit
Floor drain				in the pit
Medical gases				in the patient cabin if required
Automatic fire extinction system (gas)				in the hall and inside the cabin (with automatic delay and cross-control)
<b>Power</b>				
Dipole power supplies				situated in or close to the transfer line
Uninterruptible power supply				for emergency lighting, control system and patient couch
<b>Other</b>				
Communication to the control room				Data / video / voice
Safety interlocks				Manual emergency stops throughout hall and cabin Fire and smoke in hall and cabin Entrance locks Temperature in the hall, on the cage and on the dipole surface Radiation Collision Water in the pit

Table 5-5: Design characteristics of the gantry hall.

## 6 Conclusion

### 6.1 The New Status Quo and Outlook

*Is the objective of the thesis fulfilled?*

In Chapter 1, it was written that the principal objective of this study was to find a viable and competitive solution for a carbon-ion gantry for cancer therapy. To satisfy this objective there was a clear need to break up the conventional mould of gantry design, but the technical complexity and the interdisciplinary nature of this task represented a massive challenge. Once a new gantry concept had been established, focus was put on *integrating* the mechanical and optical designs, the planning of space, the organisation of the complete treatment process and the gantry operation for an *integrated design*.

The current proposal for the Riesenrad gantry shows several examples of integrated, cross-functional planning:

- The gantry forms part of a clinic for cancer therapy and the economic performance of the whole facility is dependent on the speed, reliability and lack of complication of the gantry (integration of safety, quality control and operational efficiency).
- The efficient cohabitation of public areas, medical areas and radiation controlled areas is essential (integration of architecture, shielding and ergonomics)
- The gantry structure and beam-optics are closely coupled and mutually optimised (integration of mechanical design and optics).
- The structural principle of the gantry relies on photogrammetry to virtually couple two mechanical structures: the patient couch and the central cage that is carrying the heavy dipole. The overall result is a lighter construction with a higher rigidity and a higher treatment precision compared to a conventional isocentric design (technological integration).
- The study of the Riesenrad gantry intensively addressed the question on how to assure that the beam actually points to where one wants (integrated alignment concept).
- The Riesenrad gantry design has the flexibility to meet future demands (integration by flexibility). The spacious treatment cabin not only facilitates patient handling, it provides space for the installation of future auxiliary equipment. The building has the long-term possibility of adding a second patient cabin diametrically opposite the first one thus increasing considerably the efficiency of the facility. The construction provides virtually a full  $4\pi$ -irradiation.

*The strength of the Riesenrad is its integrated approach*

All the above issues - in particular the one concerning the alignment concept - have considerable consequences for the organisation, i.e. on the planned process of ion therapy using the Riesenrad gantry. The "status quo" of the planning for that process is shown in Figure 6-1. At the same time, this chart is the basis for further discussion and development *together* with other disciplines, in particular with the medical community. Carrying on with a more detailed technical design only makes sense if there is a general agreement on the process!

*The technical characteristics indicate that the Riesenrad gives the best value for money*

Finally, a few technical characteristics of the Riesenrad ion gantry should be listed in order to demonstrate the advantages of the Riesenrad compared to other ion gantry solutions:

- The Riesenrad is compact and relatively light. The floor area is less than half of what one could expect for an isocentric ion gantry and only about 30% larger than for a conventional proton gantry. This is of particular significance for the cost of the shielded building. The total gantry weight is far less than would be expected for an isocentric design and is in the range of a conventional proton gantry (150 t).
- The Riesenrad design employs the minimum possible bending ( $\pi/2$ ) to obtain the full  $4\pi$  solid angle for treatments. Also, since weight is less of a problem, the single dipole can have a large enough yoke to avoid serious saturation. Consequently, compared to the isocentric design, the power consumption is approximately halved.

- The mechanical structure of the Riesenrad manages with only *one* - comparatively small - support ring of 4.3 m diameter, assisted by a commercially available taper roller bearing unit. The ring is quite rigid since it only has to provide an opening for the dipole and not for a complete patient enclosure as it is usually necessary with isocentric solutions. The load on the ring is low enough to allow its support, in an economic way, by just four rollers.
- The Riesenrad gives the highest possible treatment precision (due to the compact and rigid design). The beam stability analysis indicates that  $3\sigma$  of the beam position probability distribution at the isocentre (caused by expected temperature fluctuations in the treatment hall) are below 0.6 mm. Therefore, the desired sub-millimetre precision ( $3\sigma < 1$  mm) is perfectly feasible with the Riesenrad gantry, since the remaining error budget could accommodate temperature fluctuations twice as high as calculated or another independent random error of the order of  $3\sigma = 0.8$  mm.
- The Riesenrad is both modular and flexible: to a certain degree, patient cabin and dipole-supporting cage can be optimised and adapted to new demands individually, thus guaranteeing optimal efficiency of the facility both now and in the future.

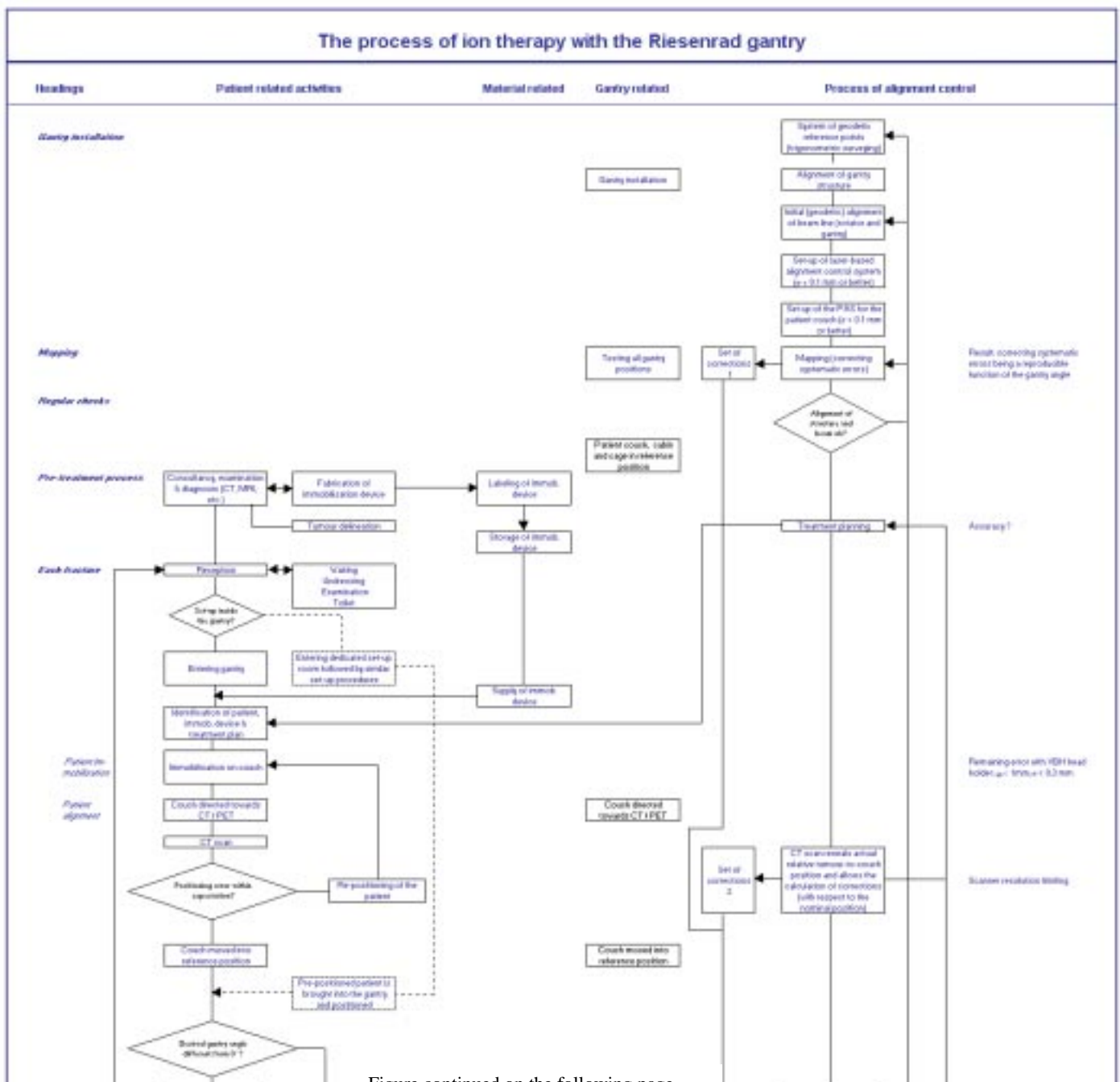


Figure continued on the following page.

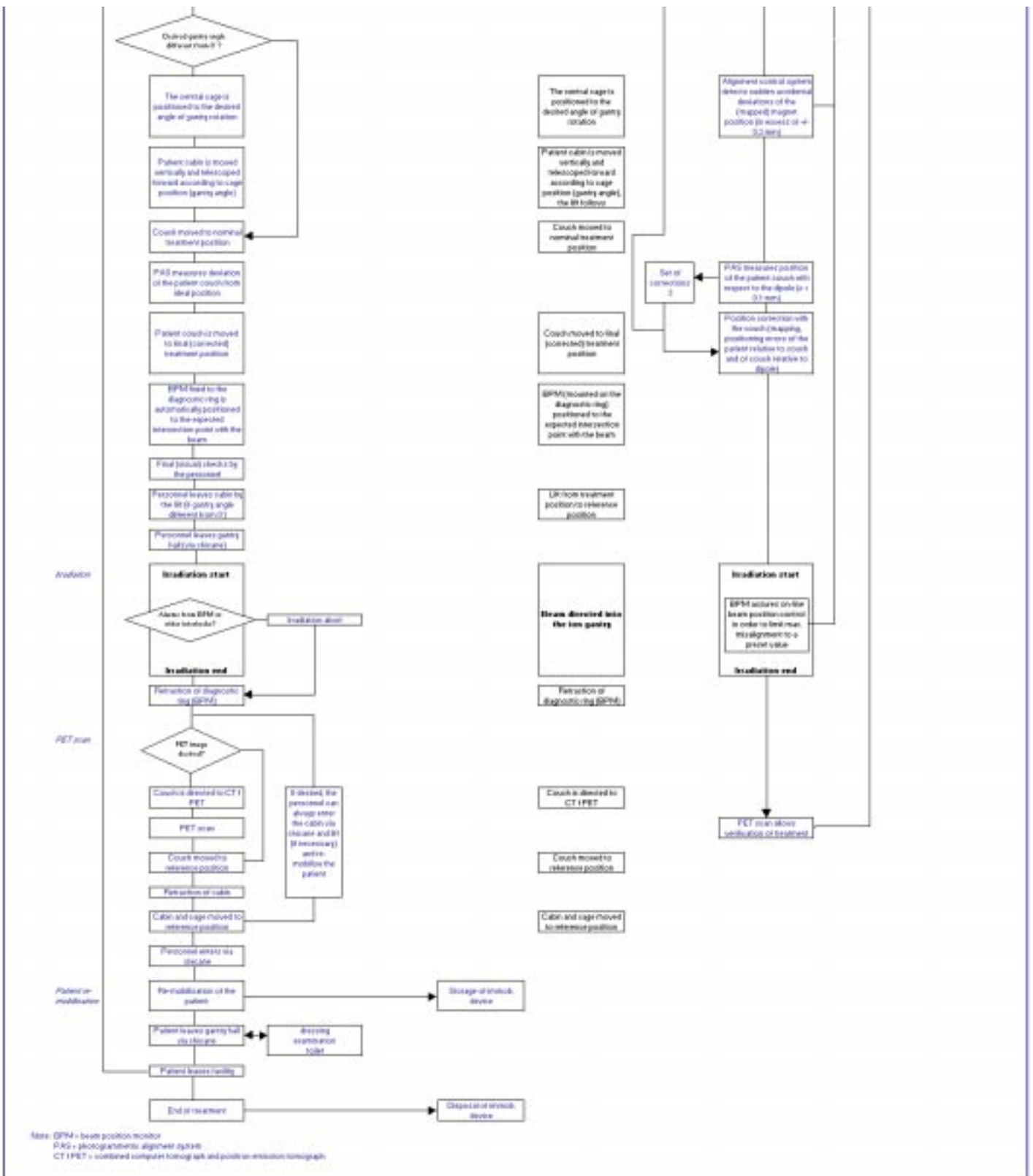


Figure 6-1: Integration of the various aspects of planning in an overall treatment process for the Riesenrad ion gantry. Before design work goes into more detail, all participants should agree on a flow chart similar to this one (or work on its modifications).

*What compromises  
had to be made?*

A widespread argument against exocentric gantry solutions concerns the potentially more difficult access to the patient in case of a technical (e.g. fire) or medical (e.g. heart attack of the patient) emergency. The Riesenrad deals with these concerns by providing two permanent and independent access systems to the patient cabin: a conventional lift for accessing the cabin in about 15 seconds during operation and also in case of a medical emergency, and a staircase, which can be safely used even in the case of a complete breakdown of all mechanical systems. (What remains is the argument of inconvenience for the personnel of having to use a lift for all gantry positions different from a horizontal beam.) This should be discussed constructively among users, designers and investors whether these additional 15 seconds (plus the "inconvenience") can be *tolerated for the sake of a smaller investment resulting in a cheaper treatment* and - if found not acceptable - how the situation could be ameliorated.

*Gantry specifications  
should be constantly  
reviewed: any  
relaxation facilitates  
the feasibility of an  
ion gantry, additional  
demands endanger it.*

A similar optimisation process should be launched concerning other crucial input parameters for the gantry development, like, the required treatment angles. Is it possible to do without some "exotic" angles and what would be the resulting cost saving? In particular, such questions could be re-addressed after experience has been gained with a first prototype of a carbon-ion gantry.

*How to proceed?*

The development of the Riesenrad gantry is now sufficiently elaborate so that the further design could be handed over to an industrial contractor who should be assisted by a client's project team comprising all major disciplines. Issues still requiring full attention by that team are the actual design of the patient couch with its diagnostic ring, the related aspects of alignment control and the general conception of the control system (software) for the facility. More mechanical questions that remain to be addressed in detail concern the fixation of the 90° dipole (perhaps requiring some modifications to the dipole design) and the drive mechanics of the patient cabin.

*What remains to be  
done?*

## 6.2 Other Scenarios

The Riesenrad concept with an independent patient cabin shows its full advantage when the weight and bending radius of the dipole are high, making the restriction of elastic deformations to a certain level a challenge. If the weight and bending radius could be reduced, for example, if a proton design were requested, or if a superconducting dipole could be used, then the advantages of the Riesenrad gantry compared to an isocentric gantry approach become less stringent. However, it can be doubted that the benefit gained by a superconducting dipole will compensate for the inconvenience related to the introduction of this additional technology into the design. The technological problems of feeding superconducting magnets that are rotating and changing field should not be taken lightly.

*Riesenrad and  
downstream scanning?*

The Riesenrad solution would gain efficiency if the cross-section of the large dipole were reduced by considering downstream scanning. The main argument against the latter is the corresponding increase in gantry radius, however, the cabin concept could in principle be adapted to a larger gantry radius. This option should be reconsidered when experience with an ion gantry is available, thus being able to define more closely the process as well as the required *size* and *quality* of the patient cabin.



---

## Acknowledgements

First, I would like to thank Prof. Meinhard Regler from the Institute for High Energy Physics in Vienna for having encouraged and eventually initiated this thesis on the Riesenrad gantry. His energy and optimism is unique.

Of course, thanks to my mentor, Prof. Degenhard Sommer, Head of the Institute for Industrial Building in Vienna, who pushed me into all this... - and who is responsible for a lot of the knowledge, principles and philosophies I have.

I am very grateful to Phil Bryant, study leader of the Proton-Ion Medical Machine Study at CERN, who made the first sketch of a Riesenrad gantry I ever obtained (on a napkin in the CERN restaurant).

Special thanks to Marius Pavlovic for his work on the beam optical calculations and who also showed me how much iteration it takes to produce a NIM-paper.

I am grateful to Maciej Krasinski for his help with the FEM analysis of the rollers and Tadeusz Kurtyka who had to check it afterwards. His predecessor, Claude Arnaud, was one of few believing into the project from the beginning, for which I would like to thank him explicitly.

Thanks to Chris Andrews, who could not restore my files after the CIH-virus has spoiled them, however he made AutoCAD drawing my gantries (nearly) automatically.

It would have been impossible to explain the kinematics of the gantry to other people ("so the patient rotates rapidly during treatment...?") without the help of Silvano and Michele de Gennaro, who animated the gantry model.

I want to thank my division (ST) and my group (CV) at CERN for their support, in particular Alberto Scaramelli and Mats Wilhelmsson, who patiently signed all my "demande de voyage", and my supervisor, Rosario Principe, for all pragmatic advice ("You know Stefan, if you want to survive all this...").

Special thanks also to Williame Coosemans who communicated to me his fascination for lasers, digital cameras and retroreflectors.

Last but not least I want to thank Cornelia for her constant support as well as my parents who were always there when I needed them.

## References

- Agosteo S, Fasso A, Ferrari A, Sala P R, Silari M, Tabarelli de Fatis P, "Attenuation curves in concrete for neutrons produced by 710 MeV  $\alpha$ -particles on steel and water and by 337-390 MeV/u Ne ions on Al, Cu and Pb", Nucl. Instr. and Methods in Physics Research B, Vol. 155, 1999, pp. 102-109
- Alonso J R, "Review of Ion Beam Therapy: Present and Future", invited talk at the European Particle Accelerator Conference (EPAC), Vienna, 26 -30 June 2000, in press, available from: <http://accelconf.web.cern.ch/accelconf/e00/PAPERS/WEXF103.pdf> [accessed 2000-07-28]
- Amaldi U (ed.), The National Centre for Oncological Hadrontherapy at Mirasole, TERA Red Book, 1997
- Amaldi U, "Cancer therapy with particle accelerators", Nuclear Physics, A654, 1999, pp. 375c-399c
- Amaldi U, Larsson B (eds.), Hadrontherapy in Oncology, Proceedings of the First International Symposium on Hadrontherapy, Como, 18-21 October 1993, Elsevier, 1994
- Amaldi U, Larsson B, Lemoigne Y (eds.), Advances in Hadrontherapy, Elsevier, 1997
- Amaldi U, Rossi S (eds.), "The National Centre for Oncological Hadrontherapy at Mirasole - The Synchrotron and the Beam Transport System", Feasibility Study, TERA Group, CERN, January 1998
- Barkhof J, Schut G, Flanz J B, Goitein M, Schippers J M, "Verification of the alignment of a therapeutic radiation beam relative to its patient positioner", Medical Physics, Vol. 26, Number 11, 1999, pp. 2429 - 2437
- Baroni G, Ferrigno G, Pedotti A, Cattaneo P W, Scannicchio D, Corbella F, Gerardi F, Negri P, Ottolenghi A, Redaelli N, Orecchia R, Tosi G, "New methods for patient alignment", in: Amaldi et al., 1997, pp. 278-283
- Benedikt M, Bryant P J, Pullia M, "A New Concept for the Control of a Slow-Extracted Beam in a Line with Rotational Optics: Part II", CERN/PS 99-008 (OP), January 1999, Nucl. Instr. and Meth. A, Vol. 430/2-3, 1999, pp. 523-533
- Beyer Th, Townsend D W, Brun T, Kinahan P E, Charron M, Roddy R, Jerin J, Young J, Byars L, Nutt R, "A Combined PET/CT Scanner for Clinical Oncology", The Journal of Nuclear Medicine, Vol. 41, 2000, pp. 1369-1379
- Böhne D, "Gantry Costs", presentation held at the gantry meeting on March 18th, 1998 at GSI, Darmstadt
- Boice J Jr., Engholm G, Kleinman R A, et al., Radiation dose and second cancer risk in patients treated for cancer of the cervix, Radiation Research, Vol. 116, 1988
- Brady L W, Sheline G E, Suntharalingam N, Sutherland R M, "The Interdisciplinary Program for Radiation Oncology Research: Introduction and Overview", Cancer Treatment Symposia, Vol. 1, 1984, pp. 1-11
- Bryant P J (study leader), Badano L, Benedikt M, Crescenti M, Holy P, Maier A, Pullia M, Reimoser S, Rossi S, Borri G, Knaus P, Gramatica F, Pavlovic M, Weisser L, "Proton-Ion Medical Machine Study (PIMMS)", CERN yellow report, CERN-2000-006 and CERN-PS-2000-007 (DR), Geneva, 2000, available also on CD-rom and on-line from: [http://weplib.cern.ch/format/showfull?uid=2240912\\_6268&base=CERCER&sysnb=2200578](http://weplib.cern.ch/format/showfull?uid=2240912_6268&base=CERCER&sysnb=2200578) (part 2) and [http://weplib.cern.ch/format/showfull?uid=2240912\\_6268&base=CERCER&sysnb=0311417](http://weplib.cern.ch/format/showfull?uid=2240912_6268&base=CERCER&sysnb=0311417) (part 1) [accessed 2000-08-11]
- Bryant P J, "WinAGILE", available from: <http://nicewww.cern.ch/~bryant> [on-line, accessed 2000-06-17].

- Carey D C et al., "Third-Order Transport. A Computer Program for Designing Charged Particle Beam Transport Systems", SLAC-R-95-462, Fermilab-Pub-95/0, UC-414, May 1995
- CUBUS Software, Statik-3 Benutzeranleitung: Berechnung von ebenen und räumlichen Stabtragwerken, Zürich, 1998
- Debus J (spokesman), Gross K D, Pavlovic M (eds.), Proposal for a Dedicated Ion Beam Facility for Cancer Therapy in Heidelberg, Universitätsklinik Heidelberg, German Cancer Research Centre Heidelberg (DKFZ), Gesellschaft für Schwerionenforschung Darmstadt (GSI), Forschungszentrum Rossendorf (FZR), September 1998
- Deutsches Bundesamt für Strahlenschutz, Verordnung über den Schutz vor Schäden durch ionisierende Strahlen (Strahlenschutzverordnung - StrlSchV), 1976 (BGBl. I S. 2905, 1977 S. 184, 269) in the version of 30. June 1989 (BGBl. I S. 1321, ber. S. 1926), last change 18. August 1997 (BGBl. I S. 2113)
- DIN EN 10025, Warmgewalzte Erzeugnisse aus unlegierten Baustählen, Technische Lieferbestimmungen, edition 3.94,
- EC 3, DIN V ENV 1993-1-1, Eurocode 3: Bemessung und Konstruktion von Stahlbauten, part 1-1, edition 4.93 DIN V ENV 1993-1-2, Ausgabe:1997-05
- Eickhoff H, Böhne D, Haberer Th., Schlitt B, Spiller P, Debus J, Dolinskii A, "The Proposed Dedicated Ion Beam Facility for Cancer Therapy at the Clinic in Heidelberg", European Particle Accelerator Conference (EPAC), Vienna, 26 -30 June 2000, in press, available from: <http://accelconf.web.cern.ch/accelconf/e00/PAPERS/WEP3A13.pdf> [accessed 2000-07-31]
- Enghardt W, Haberer Th, Heeg P, Jäkel O, Karger C, Krämer M, "Heavy-Ion Therapy at GSI: Progress Report", GSI Scientific Report 1998, GSI Report 99-01, May 1999, pp. 138-142
- Flanz J B, "Large Medical Gantries", Proceedings 16th Particle Accelerator Conference, Dallas, 1995
- Flanz J B, Bradley S G, Goitein M, Smith A, Jongen Y, Bailey J, Ladeuze M, Schmidt S, Schubert J, VanMeerbeeck A, Hurn T, Junge R, "Initial Equipment Commissioning of the Mortheast Proton Therapy Centre", proceedings Cyclotrons and their Application 98, Caen 14-19 June 1998
- Galle R, Auberger Th, "Zu erwartende Einnahmen", in: Pötter et al., 1998, op. cit.
- Galle R, Pfeiffer K P, "Gesundheitsökonomische Betrachtung eines Hadronentherapie-zentrums in Österreich", Kap. III.11, in: Pötter R et al., 1998, op. cit.
- Goitein M, "The technology of hadrontherapy: the context within which technical choices are made", in: Amaldi U et al., 1997, pp. 141-159, op. cit.
- GSI (Gesellschaft für Schwerionenforschung), "Heavy Ion Radiotherapy @ GSI" [on-line], available from: <http://www-aix.gsi.de/~bio/therapy.html> [accessed 2000-07-31]
- Haberer Th, Becher W, Schardt D, Kraft G, "Magnetic scanning system for heavy ion therapy", Nucl. Instr. and Meth. A, Vol. 330, 1993, pp. 296-305
- Hartmann G H, "Abschätzung der erforderlichen Abschirmmassnahmen für eine geplante Protonen/Schwerionen-Beschleunigeranlage zur Tumorthherapie in Heidelberg", Abt. Medizinische Physik, DKFZ Deutsches Krebsforschungszentrum, 1998
- HIMAC (Heavy-Ion Medical Accelerator in Chiba), Japan, <http://www.nirs.go.jp/ENG/facilt07.htm> [accessed 2000-07-28]
- Hradsky A, Hoffmann D, Schmähel D, Auberger T, Bierleutgeb L, Regler M, Schönauer H, "Kosten", Kap. III.8, in: Pötter R et al., 1998, op. cit
- IBA (Ion Beam Applications), "Proton Therapy System: Technical Description", Rev. 1, Louvain-la-Neuve, July 1997
- IBA (Ion Beam Applications), "Typical Treatment Scenario", 1998
- ICRP (International Commission on Radiological Protection), "Conversion Coefficients for Use in Radiological Protection against External Radiation", Publication 74, can be ordered from: <http://www.icrp.org/ordering.htm>

- ICRU (International Commission on Radiation Units and Measurements), "Nuclear Data for Neutron and Proton Radiotherapy and for Radiation Protection", ICRU Report 63, Bethesda (USA), 2000, can be ordered from: <http://www.icru.org/>
- ICRU (International Commission on Radiation Units and Measurements), "Prescribing, Recording and Reporting Photon Beam Therapy", ICRU Report 62 (supplement to ICRU Report 50), Bethesda (USA), 1999, can be ordered from: <http://www.icru.org/>
- Ion Beam Applications (IBA), Information brochure on "Patient Throughput", Louvain-la-Neuve (Belgium)
- Janik J, Mueller M, "Some Remarks on the Ion Optics Beam Delivery Systems for Tumour Treatment", Nucl. Instr. and Meth. B, Vol. 84, 1994, pp. 117-119
- Kalimov A, Wollnik H, "Wide-aperture magnets for an isocentric gantry for light-ion cancer therapy", Nucl. Instr. A, Vol. 428, 1999, pp. 508-512
- Kataoka S, Tachikawa T, Nonaka H, Koumura I, Manabe N, Sano M, Ochi T, Sakaue T, Sato T, "Gantry Positioning Accuracy at NCC Kashiwa", presentation given at the XXXI PTCOG meeting, Bloomington, Indiana, October 1999
- Koehler A M, Sisterson J M, Gottschalk B, Rabin M S Z, Enge H, "Preliminary Study for a Corkskrew Gantry for Proton Beam Delivery", Harvard Cyclotron Laboratory, Cambridge, 1987, unpublished
- Kraft G, Kraft-Weyrather W, Taucher-Scholz G, Scholz M, "What kind of radiobiology should be done at a hadron therapy center?", Gesellschaft für Schwerionenforschung, GSI-Preprint-97-05, Darmstadt, 1997
- Krämer M, Kraft G, "Heavy Ion Track Structure Calculations", in: Chadwick K H, Moschini G, Varma M N (eds.), Biophysical Modelling of Radiation Effects, Adam Holger, Bristol, 1992
- Leunens G, Menten J, Weltens C, Verstraete J, van-der-Schueren E, "Quality assessment of medical decision making in radiation oncology: variability in target volume delineation for brain tumours", Radiotherapy and Oncology, Vol. 29(2), Elsevier, 1993, pp. 169-175
- Mandrillon P, "High energy medical accelerators", European Particle Accelerator Conference, Proceedings of EPAC 90, Nice, 12-16 June 1990, pp. 263-267
- Martin R M, "The ACCTEC proton medical accelerator and beam delivery system for cancer therapy and radiography", European Particle Accelerator Conference, Proceedings of EPAC 90, Nice, 12-16 June 1990, pp. 1802-1804
- Maughan R L, Yudelev M, Warmelink C, Forman J D, Maruyama Y, Porter A T, Powers W E, Blosser E B, Blosser G, Blosser H G, "Facility for fast neutron therapy at the Harper hospital", in: Amaldi U et al., 1994, pp. 377-385, op. cit.
- Negri P, "Outline of a mobile-cabin gantry for an ion beam", Dipartimento di Fisica dell'Università degli Studi di Milano and INFN Sezione di Milano, 3/1998, unpublished
- Optivus Technology, public relations department, 1998, <http://www.optivus.com>
- Pavlovic M, "A design of a rotating gantry for non-symmetric ion-therapy beams", Nucl. Instr. and Meth. A, Vol. 438, 1999, pp. 548-559
- Pavlovic M, "Oblique gantry - an alternative solution for a beam delivery system for heavy-ion cancer therapy", Nucl. Instr. and Meth. A, Vol. 434, 1999, pp. 454-466
- Pedroni E, "Beam Delivery", in: Amaldi U, Larsson B, 1994, pp. 434-452, op. cit.
- Pedroni E, "Latest Developments in Proton Therapy", invited talk at the European Particle Accelerator Conference (EPAC), Vienna, 26 -30 June 2000, in press, available on-line from: <http://accelconf.web.cern.ch/accelconf/e00/PAPERS/WEXF102.pdf> [accessed 2000-07-28]
- PIMMS, see: Bryant et al., 2000
- Pötter R, Auberger Th, Regler M (eds.), Med-AUSTRON - Ein Österreichisches Krebsforschungs- und Behandlungszentrum zur Hadronentherapie in Europa, feasibility study, Verein zur Förderung einerer Grossforschungsanlage in Österreich - "Verein AUSTRON", Wiener Neustadt, 1998

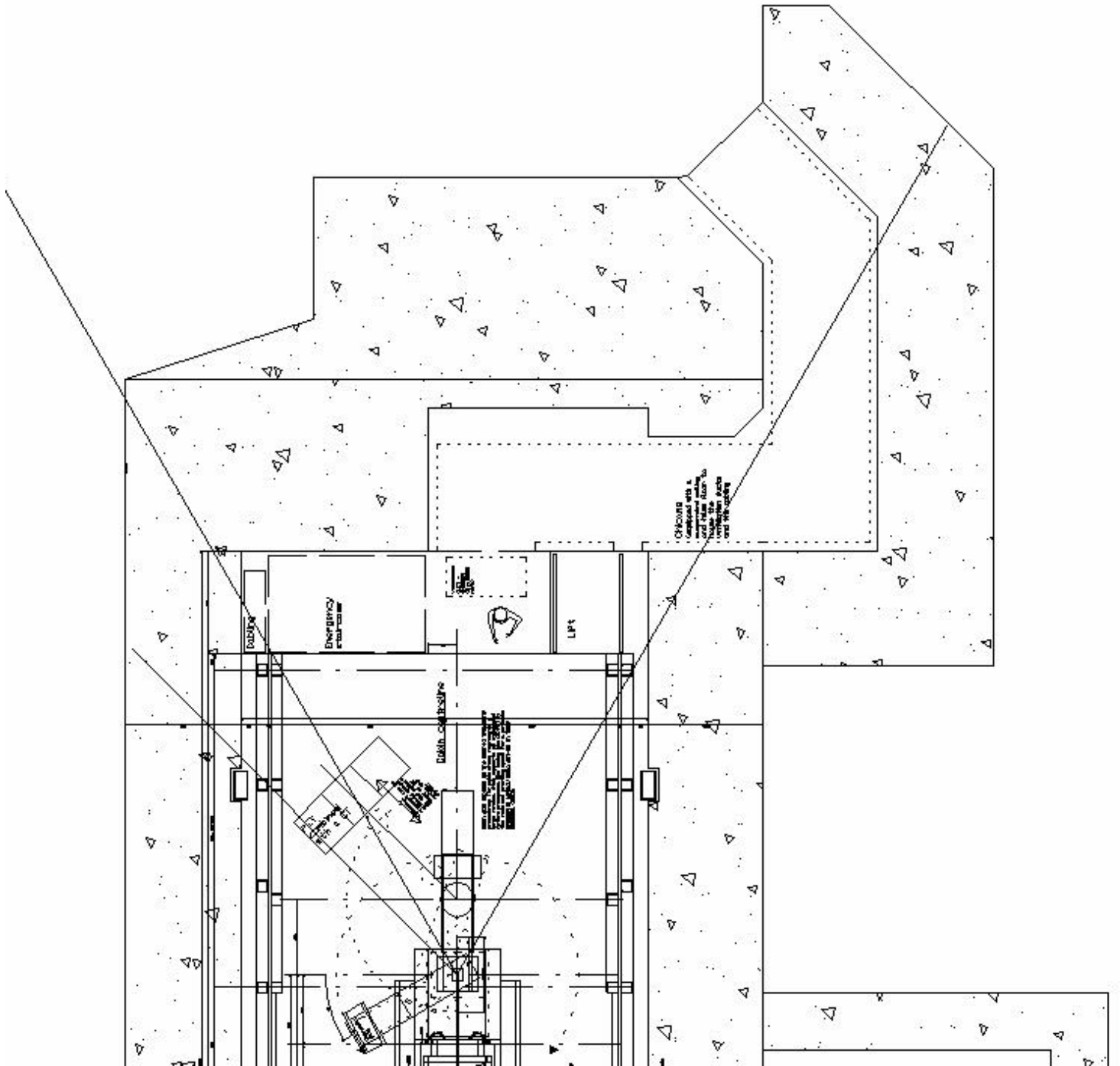
- PSI (Paul Scherrer Institut), "The PSI Proton Therapy Facility" [on-line], available from: [http://www1.psi.ch/www\\_asm\\_hn/gantry/gantry\\_master.html](http://www1.psi.ch/www_asm_hn/gantry/gantry_master.html) [accessed 2000-07-28].
- Regler M, Rabitsch H, Maier A, "Physikalische Grundlagen ionisierender Strahlung", in: Pötter et al., 1998, Vol. II, Chapter 1, op. cit.
- Reich H (ed.), Burmester U, Dosimetrie ionisierender Strahlung - Grundlagen und Anwendungen, Teubner Verlag, Stuttgart, 1990
- Rocher Ch, Fietier N, "Mechanical Design of the Gantry", EULIMA feasibility study group, CERN, PS Div., Geneva, 1991, unpublished, can be obtained from: Mandrillon P, Laboratoire du Cyclotron, Centre Antoine Lacasagne, Nice
- Rossi S, "Medical applications of accelerators", lecture, CERN, Geneva, 8 - 9 Jun 1998
- Schär Engineering AG, Information brochure on the "Proton Therapy Facility", Lachen 7, CH-8416 Flaach
- Selzer E, Weyrather W, Hackl A, Tritthart H, Pötter R, "Strahlenbiologische Grundlagen", in: Pötter R et al., 1998, Vol. 1, pp. 65-88, op. cit.
- Sisteron J M, Enge H, Gottschalk B, Koehler A M, Verhey L, Goitein M, "Design considerations for a proton beam gantry", Harvard Cyclotron Laboratory, Cambridge, 1987, unpublished
- Spiller P, Böhne D, Dolinski A, Eickhoff H, Franczak B, Langenbeck B, Haberer Th, Malwitz E, Pavlovic M, "Gantry Studies for the Proposed Heavy Ion Cancer Therapy Facility in Heidelberg", European Particle Accelerator Conference (EPAC), Vienna, 26-30 June 2000, in press, available on-line from: <http://accelconf.web.cern.ch/accelconf/e00/PAPERS/WEP3A15.pdf> [accessed 2000-07-31]
- Spiller P, Dolinski A, Eickhoff H, Franczak B, Langenbeck B, Haberer Th, Kalimov A, Malwitz E, Pavlovic M, "Gantry Studies for the German Heavy Ion Medical Accelerator Project", presentation given at XXXI PTCOG meeting, Bloomington, Indiana, October 11 - 13, 1999
- Sweeney R, Bale R, Voge M, Nevinny-Stickel M, Bluhm A, Auer Th, Hessenberger G, Lukas P, "Repositioning accuracy: comparison of a noninvasive head holder with thermoplastic mask for fractionated radiotherapy and a case report", Int. Journal Radiation Oncology Biol. Phys., Vol 41, No. 2, 1998, pp. 475-483
- Takada E and 15 other authors, "Present Status of HIMAC", European Particle Accelerator Conference (EPAC), Vienna, 26 -30 June 2000, in press, available on-line from: <http://accelconf.web.cern.ch/accelconf/e00/PAPERS/WEP5A02.pdf> [accessed 2000-07-28]
- Tosi G, Arduini G, Canzi C, Casamassima F, Cionini L, Geradi F, Leone R, Lombardi F, Sangaletti L, Silari M, Tessa M, Vasario E, Vitale V, "Clinical requirements and physical specifications of therapeutical proton beams", TERA 94/10 TRA 13, 1994, in: Amaldi, U., Silari, M., (ed.), The National Centre for Oncological Hadrontherapy, Vol. II, 2<sup>nd</sup> edition, "TERA Blue Book", 1995
- University of Pittsburgh Medical Center and CTI PET Systems Inc., "The PET/CT tomograph project", [http://www.pet.upmc.edu/~tbeyer/pet\\_ct/PETCT.html#functional](http://www.pet.upmc.edu/~tbeyer/pet_ct/PETCT.html#functional).
- Vermoken A J, Schermer F A (eds.), "Towards Coordination of Cancer Research in Europe", Vol. 5 in Biomedical and Health Research, IOS Press, 1994, 206 pp
- Vorobiev L G, Pavlovic M, Weik H, Wollnik H, "Conceptual and Ion-Optical Designs of an Isocentric Gantry for Light-Ion Cancer Therapy", GSI Report 98-02, Darmstadt, 1998
- Vorobiev L G, Wollnik H, Winkler M, "Ion Optical Design for a Gantry for Heavy Ion Tumour Treatment", GSI Report 97-06, April 1997
- Vorobiev L G, Wollnik H, Winkler M, "Ion Optical Design for a Gantry for Heavy Ion Tumour Treatment", GSI Report 97-06, Darmstadt, April 1997

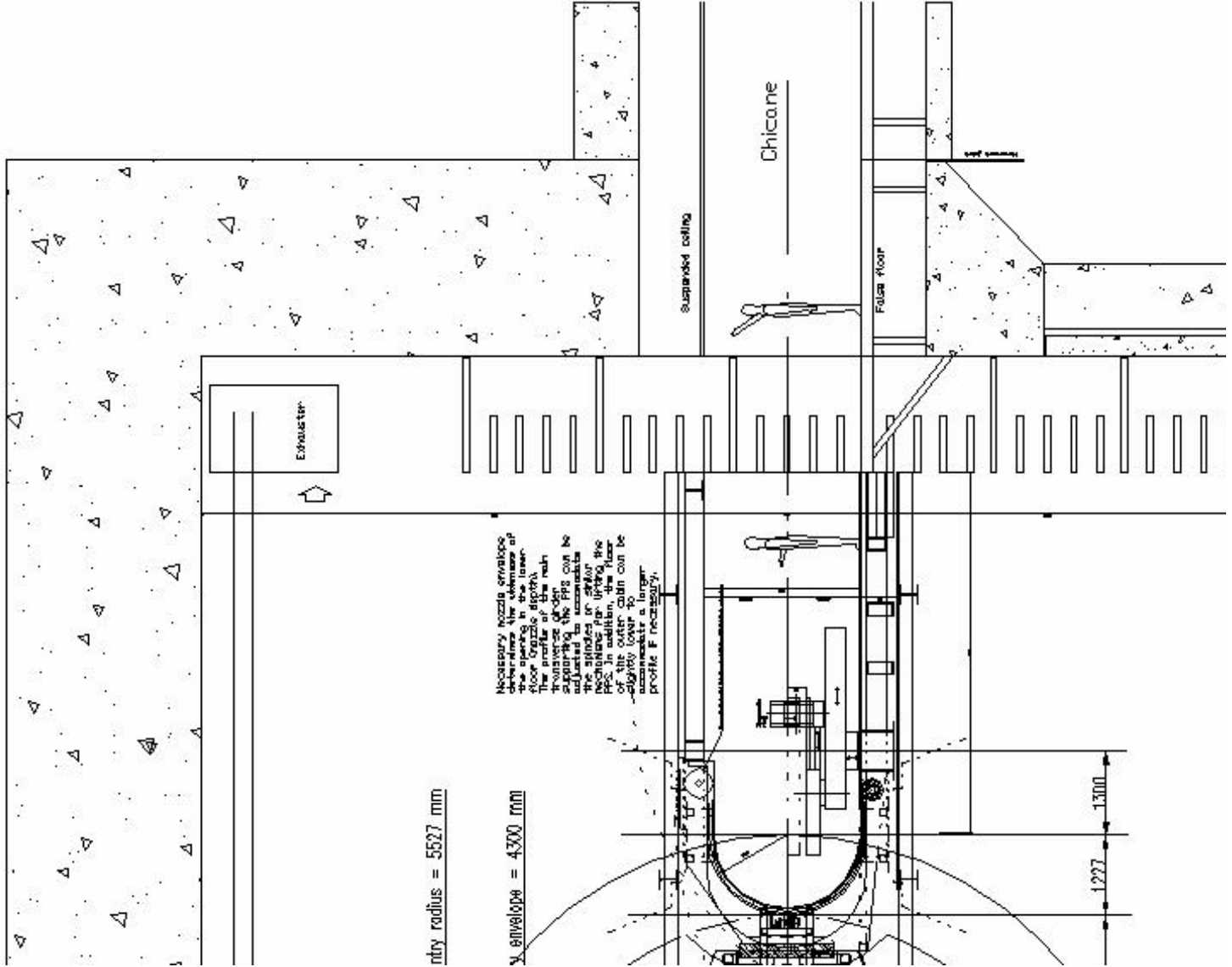
---

## Annex A: Design Drawings

The following pages contain 9 design drawings of the Riesenrad ion gantry, namely:

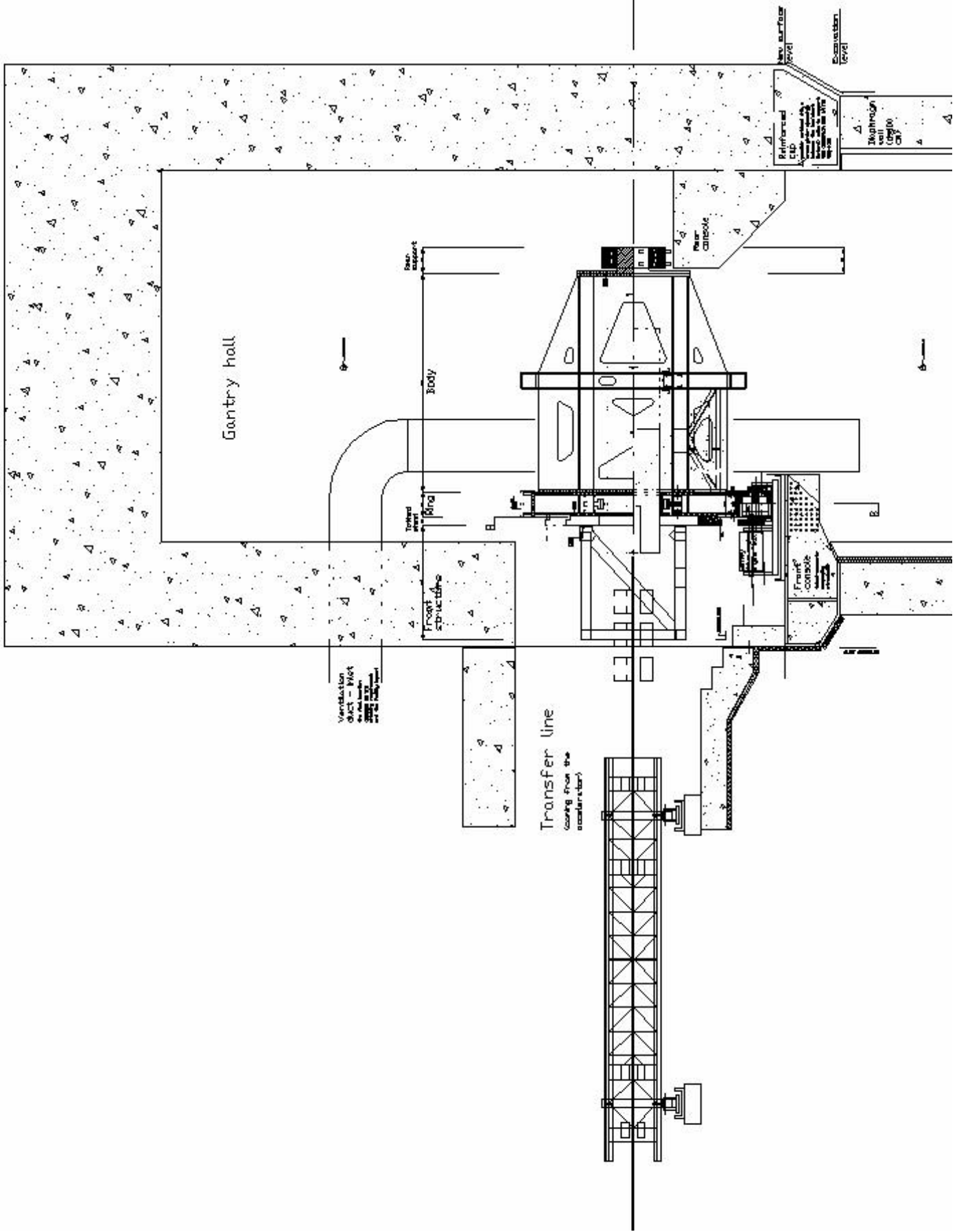
- Horizontal section (plan 1:100)
- Vertical section (front view 1:100)
- Vertical section (side view 1:100)
- Horizontal section (plan 1:50)
- Vertical section (front view) through the cabin and the tongs (1:50)
- Vertical section (front view) showing the kinematics of the patient cabin (1:50)
- Vertical section (side view 1:50)
- Vertical section through the front ring showing the drive mechanism (1:20)
- Vertical section through the front structure showing the cable drum (1:20)

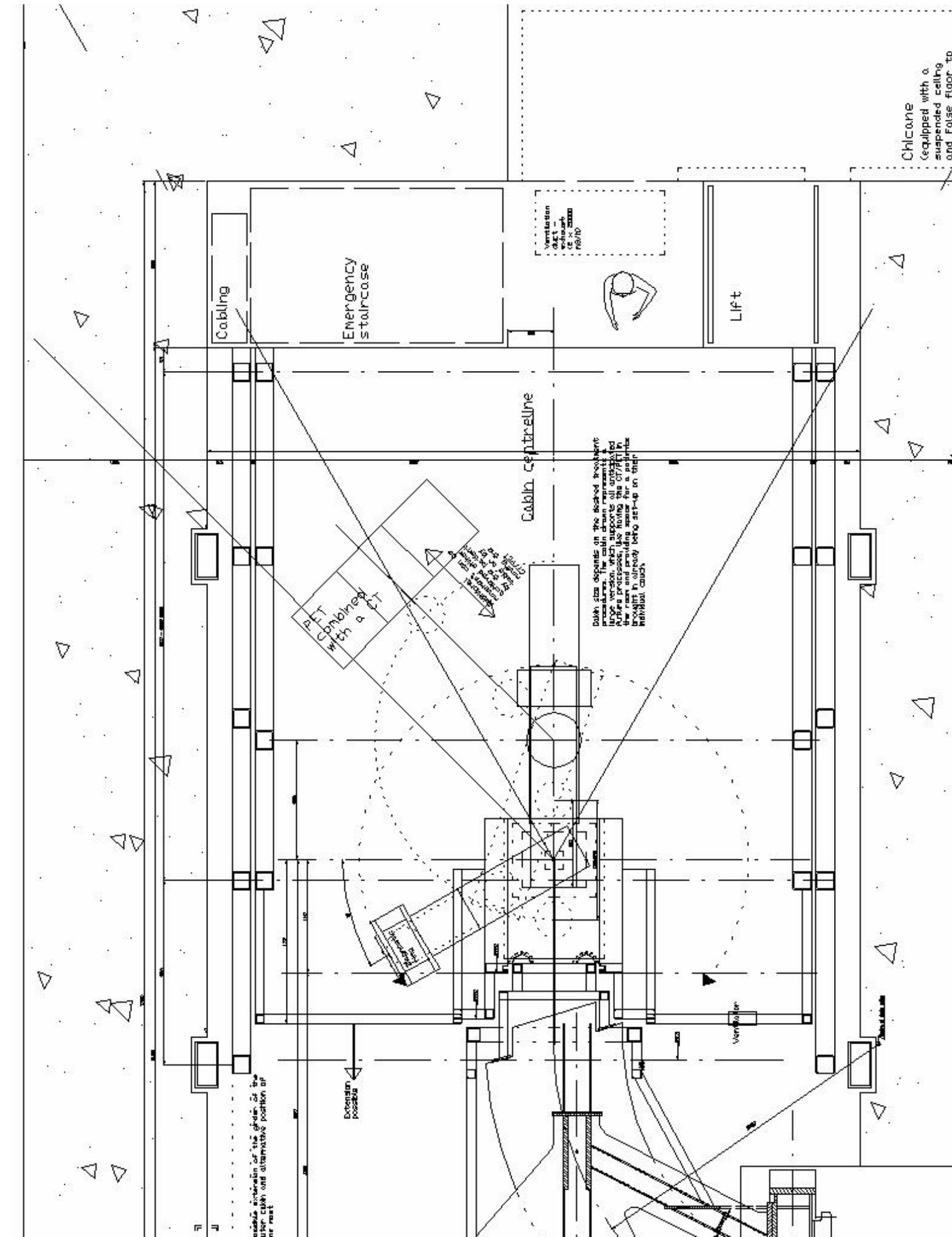




Necessary nozzle envelope determines the clearance of the opening in the outer profile of the main transverse duct. Depending on the PPS can be adjusted to accommodate the necessary clearance for lifting the PPS. In addition, the floor of the outer duct can be adjusted lower to larger profile if necessary.







Cabling

Emergency staircase

Ventilation duct  
0.25 x 0.25 m  
RS/10

LIFT

Cabin central line

LET  
A  
C  
combined  
with a CT

Cabin size depends on the desired procedure. The cabin door represents the area procedure, like moving the CT in the room and providing space for a person brought in already being set-up in their individual cabin.

Chicane  
equipped with a  
suspended ceiling  
and false floor. TO

max. extension of the order of the  
lift cabin and alternative position of  
it next

Extension  
possible

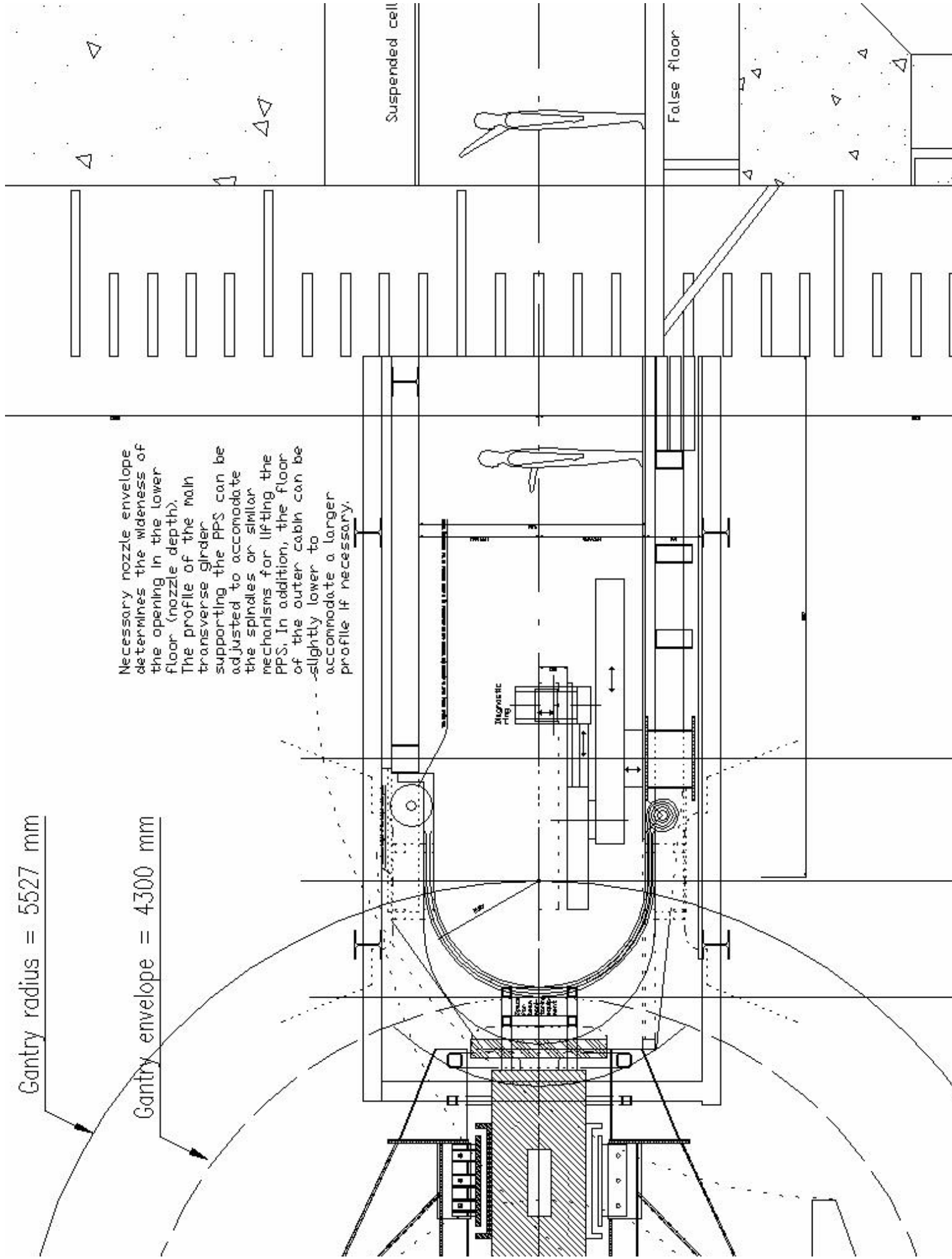
Ventilator

Door

Gantry radius = 5527 mm

Gantry envelope = 4300 mm

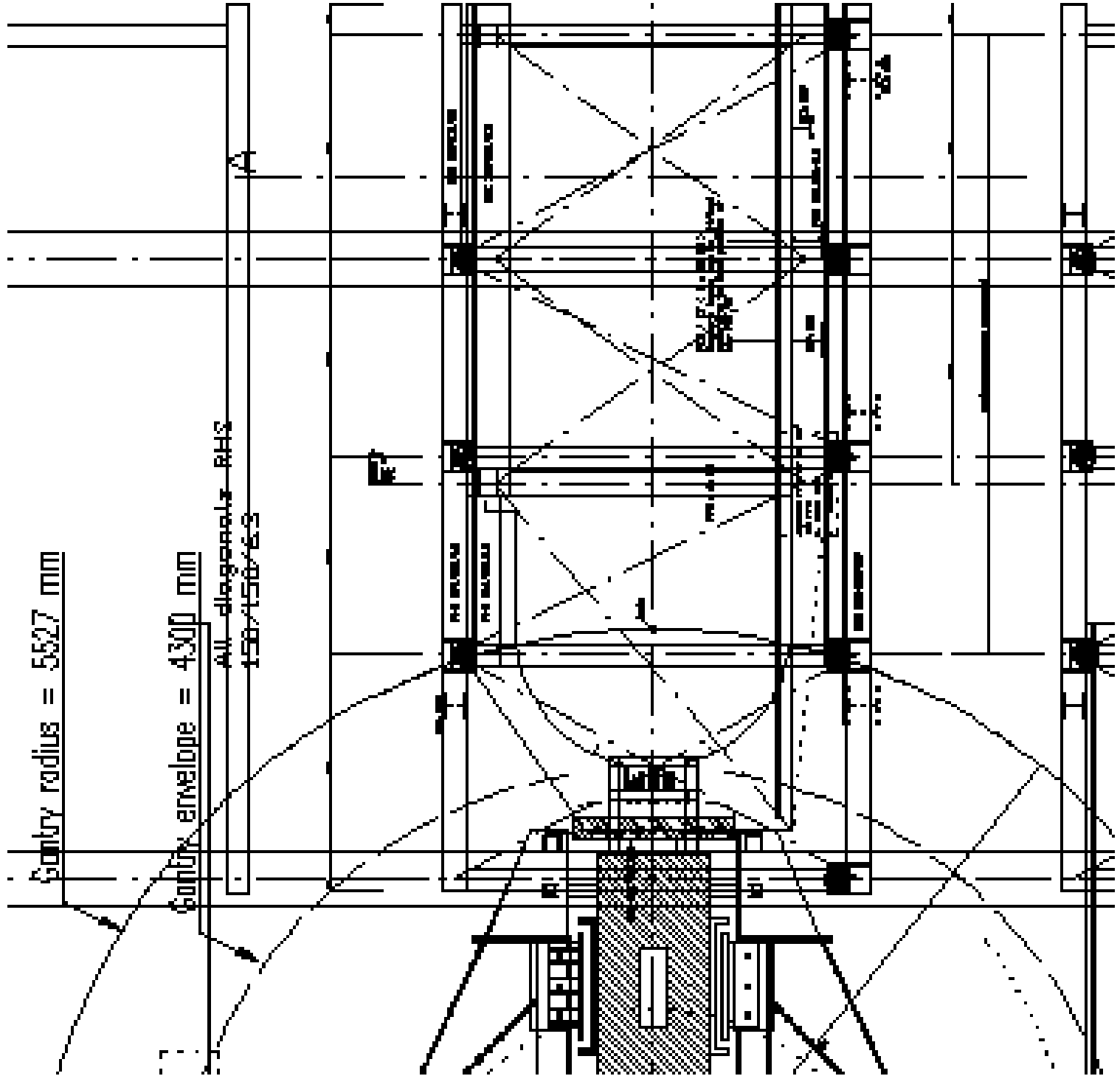
Necessary nozzle envelope determines the wideness of the opening in the lower floor (nozzle depth). The profile of the main transverse girder supporting the PPS can be adjusted to accommodate the spindles or similar mechanisms for lifting the PPS. In addition, the floor of the outer cabin can be slightly lower to accommodate a larger profile if necessary.



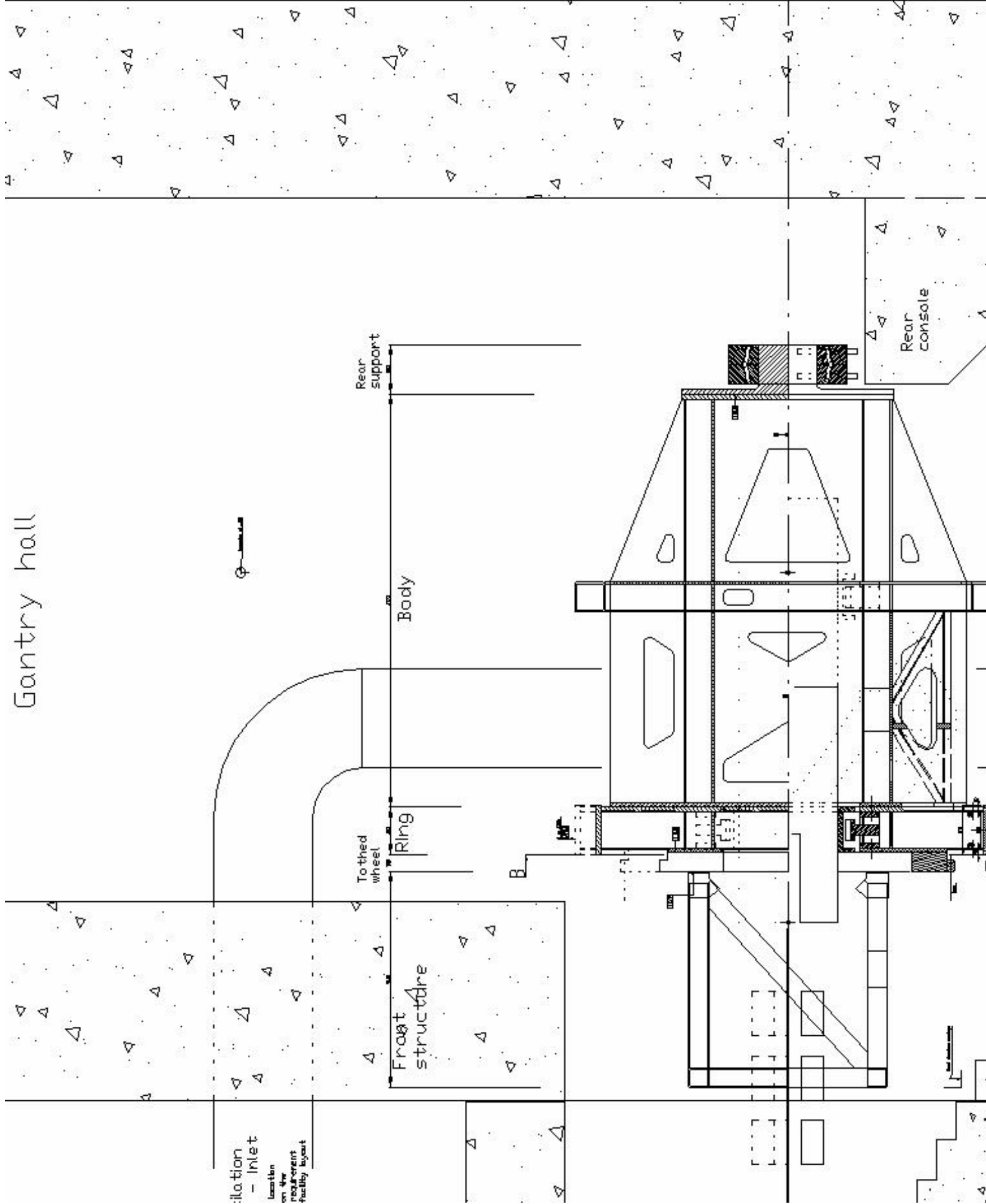
Gantry radius = 5527 mm

Gantry envelope = 4300 mm

All diagonals RHS  
150x150x6.3

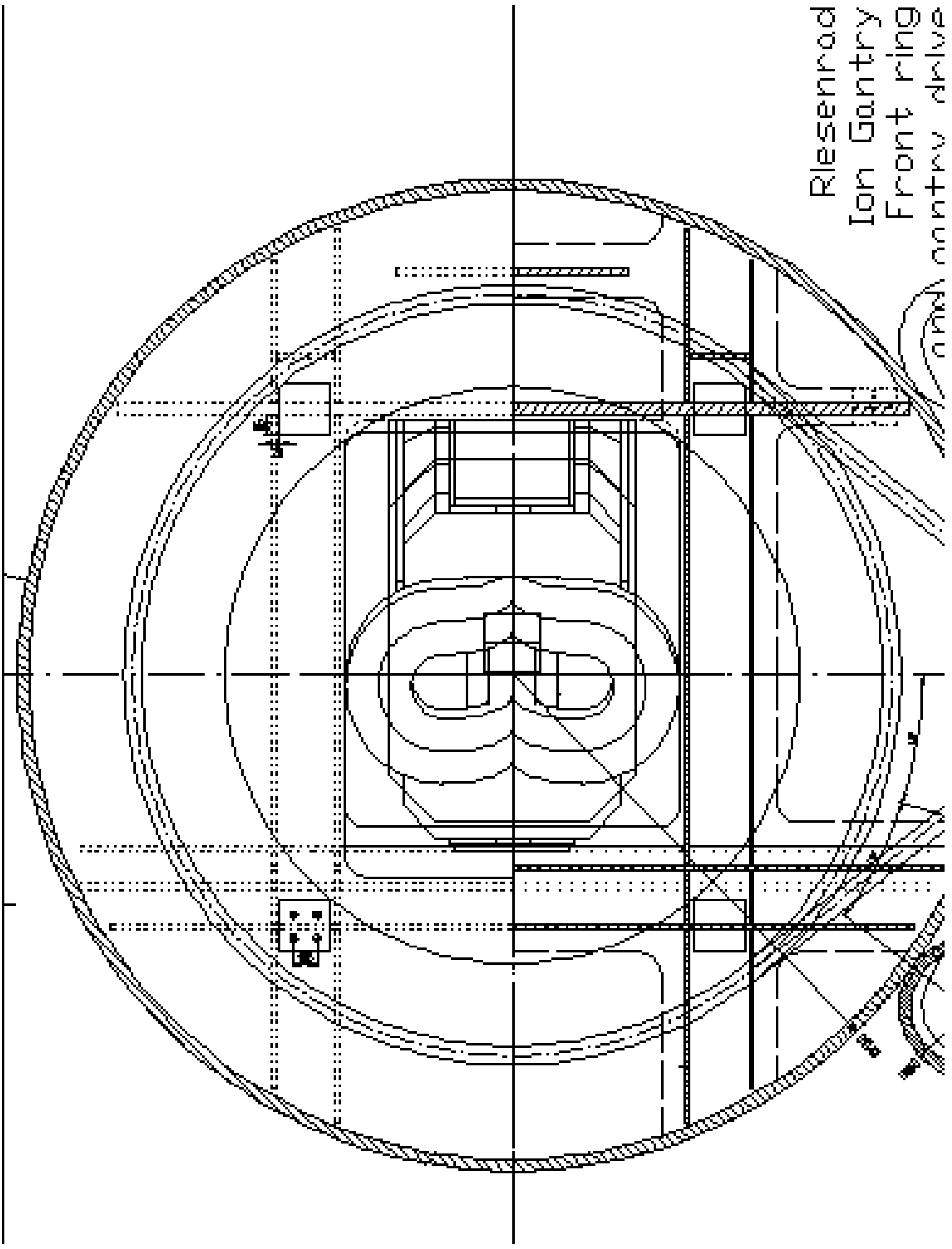


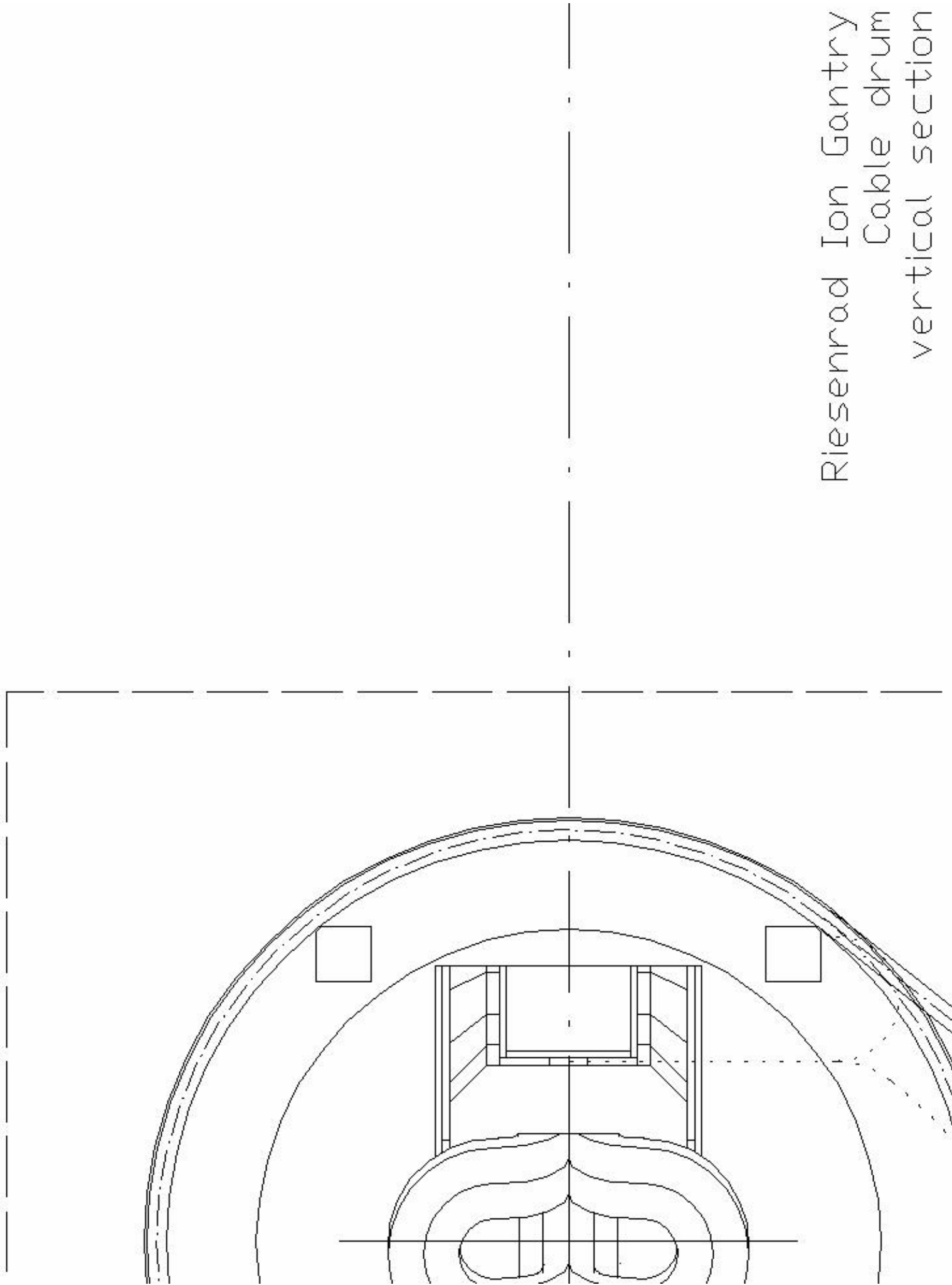
# Gantry hall



Location - Inlet  
Location on the requirement facility layout

Rieserrod  
Ion Gantry  
Front ring drive





Riesenrad Ion Gantry  
Cable drum  
vertical section

---

## **Annex B: Design Calculations**

A floppy disk containing all input and output data for the structural analysis of the cage, the patient cabin and the dipole is attached to the last page of the thesis (cover). Should this disk be missing a copy can always be obtained from the author.



## Annex C: The Roller Supports (FEM-Study)

### C.1 Introduction

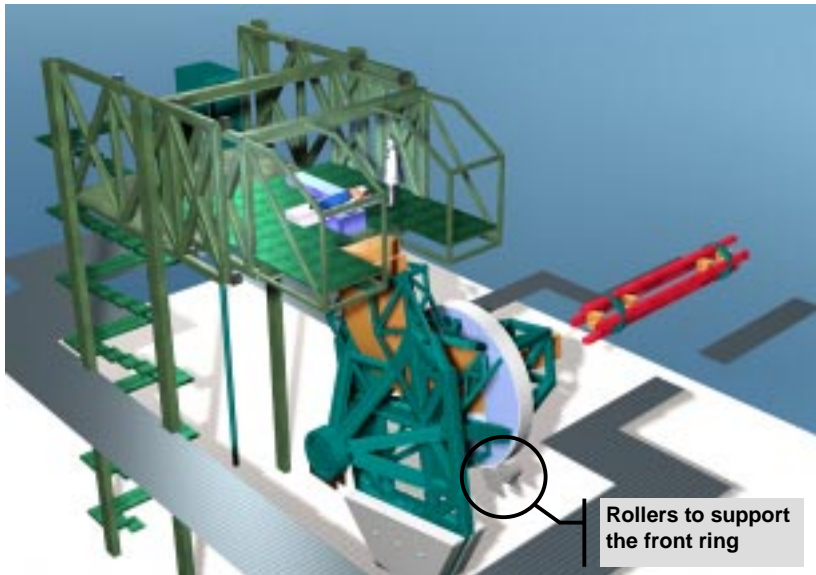


Figure C-1: Perspective view of the Riesenrad ion gantry. The large front ring is supported by two pendular bearing units equipped with two rollers each (statically determinate support), which are indicated.

This Annex deals with the design and optimisation of the four, highly loaded, cylindrical rollers used in the pendular bearings, which support the front ring. Each of them has to withstand a radial force of 250 kN (service condition). However, plastic deformation in the contact area between roller and large ring should be strictly avoided since such plastic deformations would possibly:

- modify the geometry of the gantry in an unknown way and by that affect adversely the gantry alignment precision,
- in the long term deteriorate the surface of the large ring.

Consequently, the objectives of this study were:

- First, to check *analytically* for a section perpendicular to the axis of roller rotation that the equivalent stresses in the (perfectly supported) contact zone do not exceed the yield strength of the steel.
- Second, to establish the geometry necessary in the third dimension, namely the radius of the crown roll (camber), in order to achieve a smooth stress distribution (if possible) over the whole length of the roller.

If the FEM study indicated non-satisfying bearing capacity of the roller the possible mitigation strategies would be:

- Increase the diameter of the rollers, which would lead to strong geometrical inconveniences in the gantry design.
- Surface hardening of the rollers and the large ring. However, for the latter this seems difficult and expensive. Additionally, the ring should have a slightly better surface quality than the rollers in order to restrict any potential damage to the (more easily replaceable) rollers.
- Increase the number of rollers. Again, space for additional rollers is scarce. A self-aligning pendular bearing unit with more than two rollers becomes inconveniently large in height (compare for example the impressive "wiffle trees" for the proton gantries installed at the NPTC in Boston [2]).



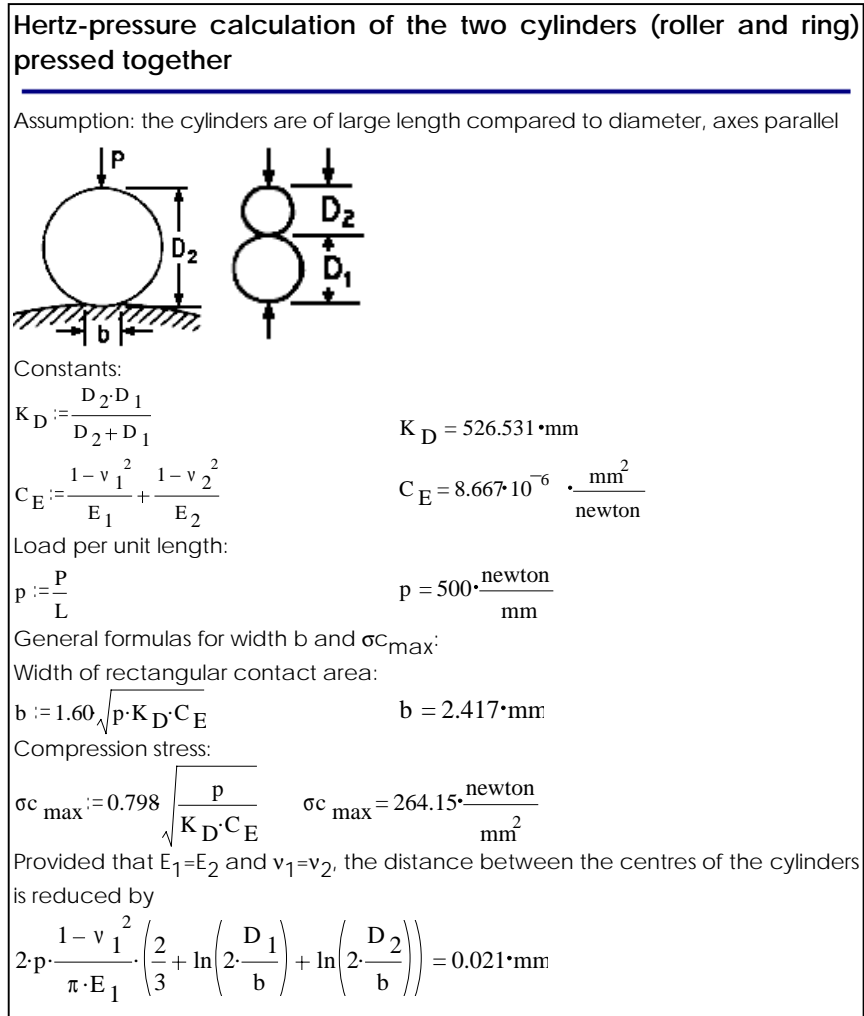


Figure C-3: Analytical calculation of Hertz stresses and local deformations in the contact zone of roller and ring for the section through the central plane. Ring and roller were assumed to be solid. Formulas according to [4].

For brittle materials, tensile stresses that occur on the surface layer of compressed bodies, close to the area of contact, are responsible for fatigue failure [6]. Ductile materials, however, are likely to fail due to excessive shear stress causing plastification at a depth of  $x \approx 0.39 b$  (in our case about 1 mm below the surface) its value being  $\tau_{45} = 0.3 p_{max}$  (see Figure C-4). The comparatively high hydrostatic part of the stress tensor in that point for plain-strain conditions yields comparatively low values for the relevant equivalent (Mises) stress  $\sigma_{Mises,max} = 0.55 p_{max}$  [7]. In the present case this value turns out to be  $\sigma_{Mises,max} = 145 \text{ N/mm}^2$ , i.e. less than half of the yield strength. However, when approaching the edges of the rollers, the plain strain conditions would successively be turned into plain stress conditions and the maximum equivalent stress would rise and eventually become equal to the maximum surface pressure  $p_{max}$ .

The results suggest that stresses in the highly loaded contact zone can be kept within the elastic range provided that the 2D situation analysed above can be achieved uniformly along the entire length of the roller. However, the assumption that maximum stresses rest unchanged when moving along the ( $z$ -) axis of rotation seems doubtful since the rigidity of the roller rim alters considerably when focus is shifted from the comparatively flexible central part towards the more rigid regions close to the webs. In fact the situation resembles - for the ring as well as for the roller - a simply supported girder (with a height equalling the rim thickness) that is resting on the two webs and spanning 380 mm. One would expect that the radial force transferred from the web of the ring towards the one of the roller would

cause high contact stresses in the vicinity of the webs only, hence leaving the rest of the roller surface more or less unloaded.

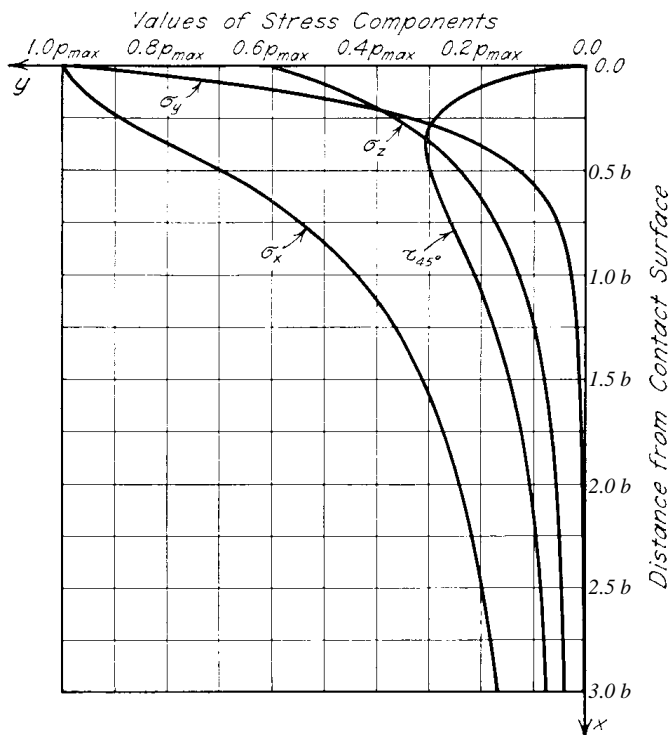


Figure C-4: Distribution of stresses in the contact zone along the line of symmetry for the two cylinders pressed together having parallel axes (similar to [5]), where  $p_{max}$  is the maximum contact pressure and  $b$  is the (total) width of the contact strip.

The theoretical approach to achieve a smooth stress distribution would be to give one of the contact surfaces - reasonably the roller one - a shape that corresponds negatively to its calculated deformed shape. In practice, it is sensible to give the cylindrical rollers a slightly spherical surface, i.e. to manufacture them with a crown roll defined by a camber radius, the result is a convex contour or "barrel" roller (see Figure C-5). In addition to the smoothed surface-stress distribution one also benefits from an increased ability of the bearing to cope with small misalignments - in particular an expected sagging - of the axis of gantry rotation.

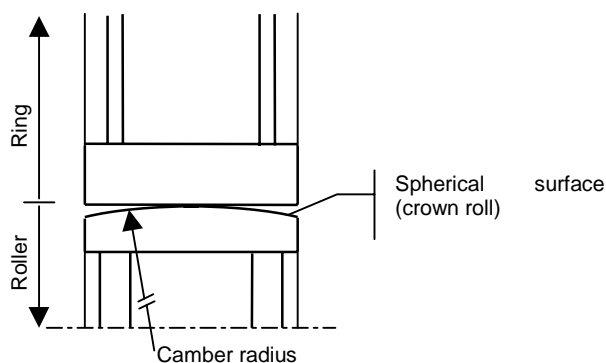


Figure C-5: Ring-roller interface showing schematically the spherical surface of the former cylindrical roller now having a convex contour or "barrel" shape. The "intensity" of this crown roll is defined by a camber radius.

As a consequence, analytical Hertz-stress calculations would have to be performed for the more general case of two arbitrarily shaped bodies pressed together (formulas can be found for example in Ref. 4) where each of the two contact surfaces is geometrically modelled by two (mutually perpendicular) principle curvatures. Unfortunately, the formulas do not work when the ratio between the two principal curvatures becomes too large which is the case

here.<sup>29</sup> Therefore, it was decided to model and analyse the problem using the finite element method (FEM).

## C.4 3D Modelling With Finite Elements

Due to the high complexity of the task a coarse model was created first with subsequent sub-modelling of the area of interest. The model was built and analysed with the finite element package ANSYS v. 5.5 [8].

### Finite element model

- *3D coarse model using shell elements suited for subsequent sub-modelling.* The model is presented in Figure C-6. It consists of the roller and a fragment of the ring modelled by shell elements (type SHELL63). Only half of the real object is modelled due to symmetry. There are contact (interface) elements (CONTAC49) between the rims of the roller and the ring. The number of elements is about 35000. Boundary conditions are either according to symmetry or totally restrained. A radial force of 125 kN is applied as a distributed load along the inner radius of the roller. The model allows the preliminary estimation of nodal forces and equivalent stresses on the contact surface.
- *3D sub-model to obtain more accurate results.* The sub-model shown in Figure C-7 is a fragment of the 3D coarse model but consists of 4-nodes volume elements (SOLID45). Contact elements (CONTAC49) are applied between the surfaces of the rims. The model has around 55000 elements and 61000 nodes. Boundary conditions (including loading) for the sub-model are directly created from the coarse model by the ANSYS program. The 3D sub-model gives full information about stress and strain states in the region of interest.

Friction in the contact elements (CONTAC49) is neglected, which decreases the time of calculation without significant influence on the accuracy of the results.

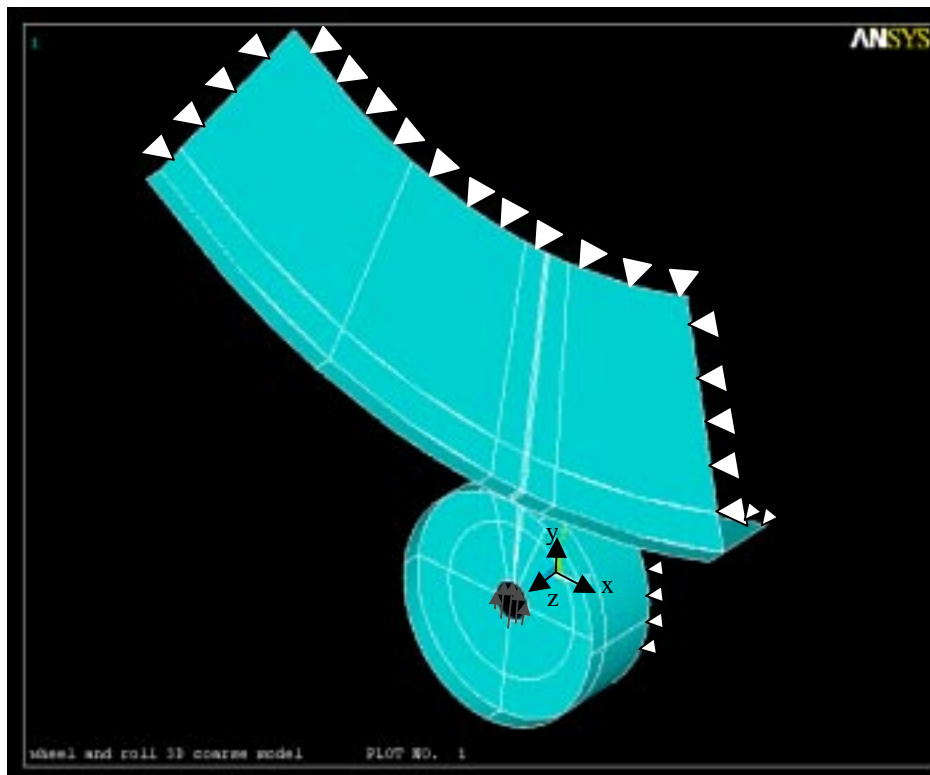


Figure C-6: Coarse model made out of shell elements. Contact elements were put in the interface zone. Boundary conditions (white), loads (red) and the coordinate system are indicated.

<sup>29</sup> The major semi-axis of the contact ellipse approaches a maximum value of about 90 mm even when the larger radii of curvature of the two bodies approach infinity (modelling two cylinders).

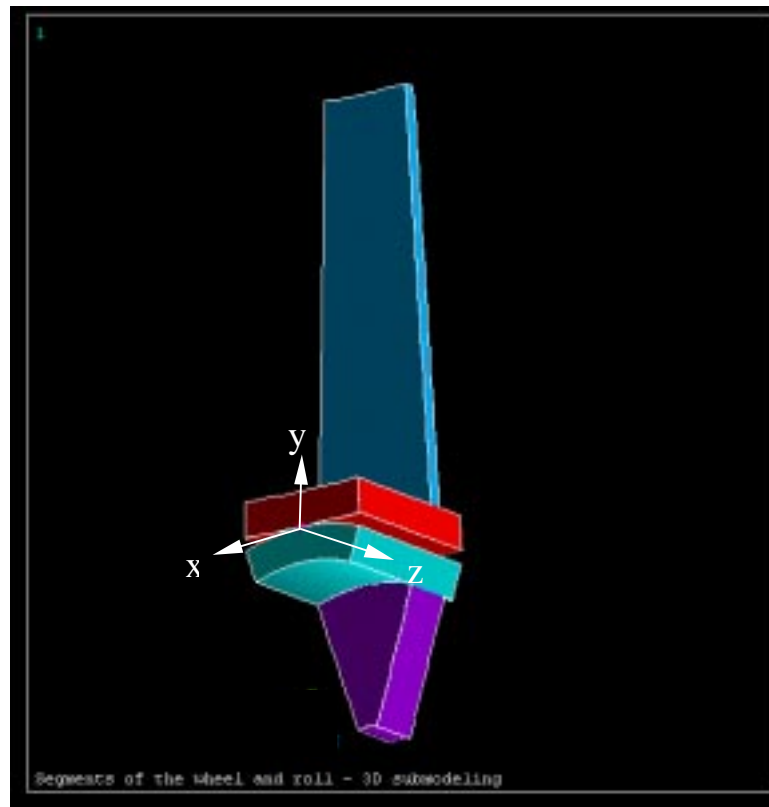


Figure 7: The sub-model including loads and the coordinate system

### Results of computation

Figure C-8 gives a *qualitative* idea of how the contact area and the surface pressure vary with different radii of the camber radius ( $r = 30, 45, 60$  m), calculated with the coarse model. Because shell elements were used, the vertical axis indicates *nodal* forces (and not stresses) perpendicular to the contact surface. The horizontal axis ( $Z$ ) indicates the major semi-axis of the contact ellipse. As expected, the maximum normal nodal force decreases with increasing camber radius, showing a corresponding increase in length of the contact area. A small camber radius, i.e. a compact barrel roller, gives a spot-like contact zone in the middle of the roller surface. With increasing radius, the contact pressure becomes more uniformly distributed over a larger area. However, one immediately recognises a growing influence of the webs on the stress distribution in the contact area, leading to considerably higher stress levels at the edges of the contact zone than they are in the centre. Eventually, this contact zone would become separated into two zones where the forces are transferred directly from one web into the other. As can be seen from Figure 8 a camber radius of about 60 m seems to be a good compromise.

		Axial curvature radius of the roller in [m]		
		30	45	60
Semi-axes of the contact ellipse [mm]	X-axis	4.0	4.0	3.9
	Z-axis	93	122	150
Maximum contact pressure $p_{max}$ between ring and roller rims in [N/mm <sup>2</sup> ]		-398	-322	-278
Maximum equivalent (Mises) stress in the rim and the webs of roller and ring in [N/mm <sup>2</sup> ]	Roller rim	218	163	156
	Roller web	48	50	52
	Ring rim	193	142	132
	Ring web	45	45	45

Table C-2: Principle results of the FEM-analysis of the sub-model.

Table C-2 presents the major results of computation for the 3D sub-model for the different camber radii of 30, 45 and 60 m respectively. Note the modified co-ordinate system in the sub-model as indicated in Figure 7 (compared to the analytical calculations): now the  $y$ -axis is perpendicular to the contact area and  $[x-z]$  form a plane parallel to the contact area. Due to the size of the elements used in the web modelling, the calculated stresses in the webs are only valid if the fillet radius between the web and the rim is larger than about 5 mm.

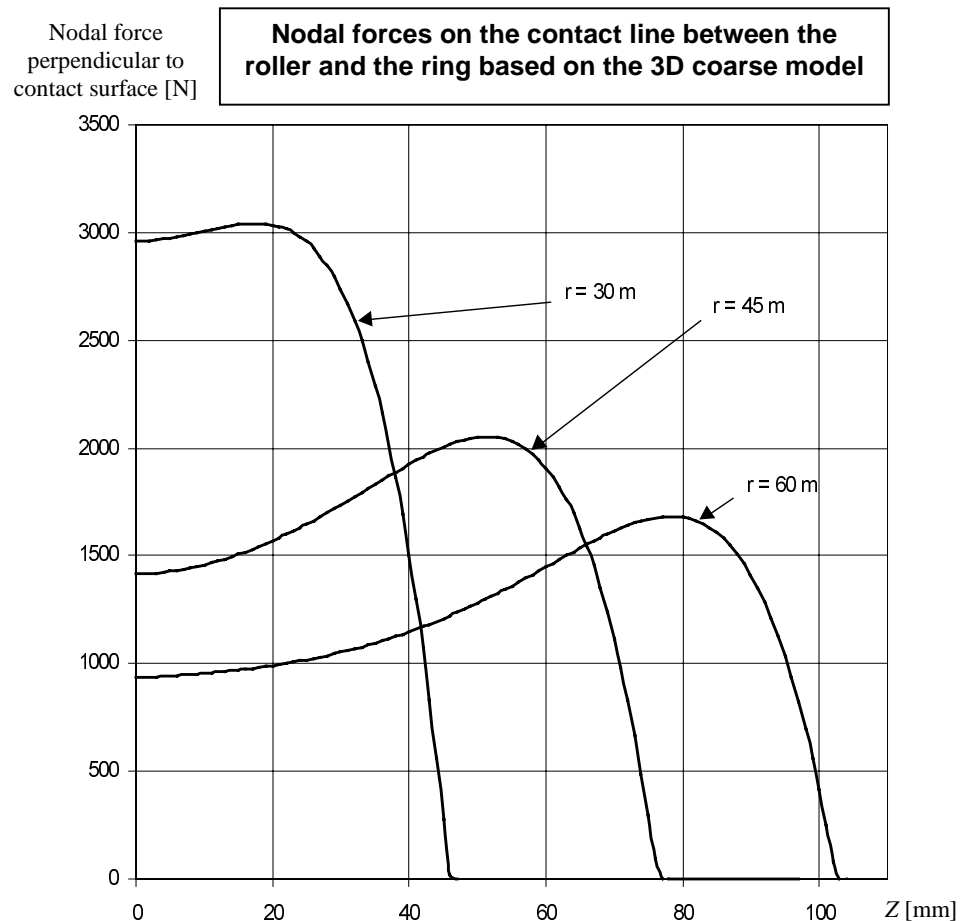


Figure C-8: Nodal forces on the contact line between the roller and the ring calculated from the 3D coarse model.  $Z$  is parallel to the axis of roller and ring rotation.

The following issues - all with respect to the 60 m camber radius - merit further attention:

- The major axis of the contact ellipse is about 50% larger than calculated for the coarse model. This is due to the fact that the shell elements used in the coarse model obey the Bernoulli-Euler hypothesis and hence the model is more rigid than the 3D sub-model using brick elements, which are, however, more adequate for evaluating contact problems. The contact area is 300 mm long which is exactly the free span between the two roller webs.
- The minor axis of the contact area turns out to be much longer than predicted by the analytical Hertz pressure calculations, 7.8 mm (!) compared to 2.4 mm respectively, while undergoing similar maximum contact pressures. Consequently, the general stress situation is far less critical than expected and in fact it is due to this broadened contact area that maximum contact stresses are not exceeding the yield stress of the material although not all the 500 mm of the roller breadth are in contact. One reason for this dramatic increase of the contact breadth is that the FEM analysis takes into account *global* deformations (due to the elasticity of the *structures*) whereas the Hertz calculations are based on the Saint-Venant's principle, i.e. only the *local* deformations are considered. However, it should be mentioned that the computed contact breadth

comprises only 4 to 6 elements of the FE model (see Figure C-9), perhaps indicating that the finite elements are still a bit too coarse at that critical region.

- The contact area forms an ellipse of  $150 \text{ mm} \times 3.9 \text{ mm} \times \pi = 1838 \text{ mm}^2$ , giving an average contact pressure of  $136 \text{ N/mm}^2$ .
- The maximum surface pressure  $p_{\max} (= \sigma_{y, \max})$  is  $278 \text{ N/mm}^2$  i.e. about twice the average value. The pressure distribution on a radial half-slice of the roller rim (cut through the centre point of the contact area) is illustrated in Figure C-10. The same values were observed on the contact surface of the ring rim.
- The equivalent (Mises) stresses for the crucial slice in the rims are presented in Figure C-11. They show a similar distribution as for the surface pressure. The maximum equivalent stress occurs already close to the webs and *on* the surface. Obviously, the model does not behave in a classical Hertz-pressure manner anymore (whereas for the 30 m camber radius the maximum Mises stress was observed at the centre and slightly *below* surface.)
- Equivalent (Mises) stresses in the webs are non-critical. The maximum value for the 20 mm web of the ring is about  $45 \text{ N/mm}^2$ .
- According to analytical Hertz-pressure assumptions,  $\sigma_y$  and  $\sigma_x$  should be equal, but they are  $278 \text{ N/mm}^2$  and  $188 \text{ N/mm}^2$  respectively. Again the probable reason is that the Hertz-pressure calculations refer to the contact of two infinite elastic bodies, which are more rigid in circumferential direction than the rims of the roller and the wheel.  $\sigma_z$  almost exactly has the value predicted in the analytical section, i.e.  $0.6 \times \sigma_y = 166 \text{ N/mm}^2$ .

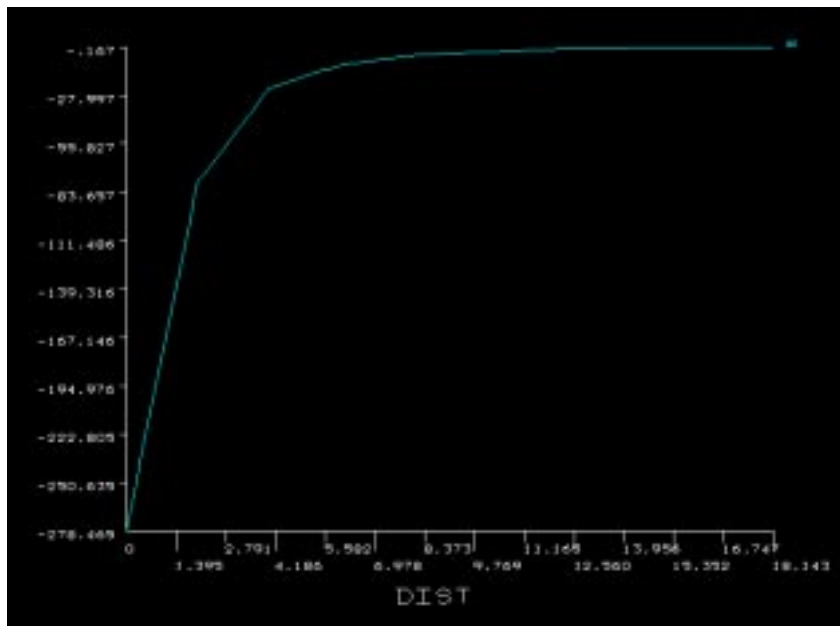


Figure 9: Contact pressure  $\sigma_y$  [ $\text{N/mm}^2$ ] plotted along the circumferential direction of the roller ( $x$ -direction in the sub-model [mm]) starting from the centre of the contact area. Every bend in the graph marks the border between two elements, hence the total length of the minor semi-axis of the contact ellipse comprises only two to three elements approximately.



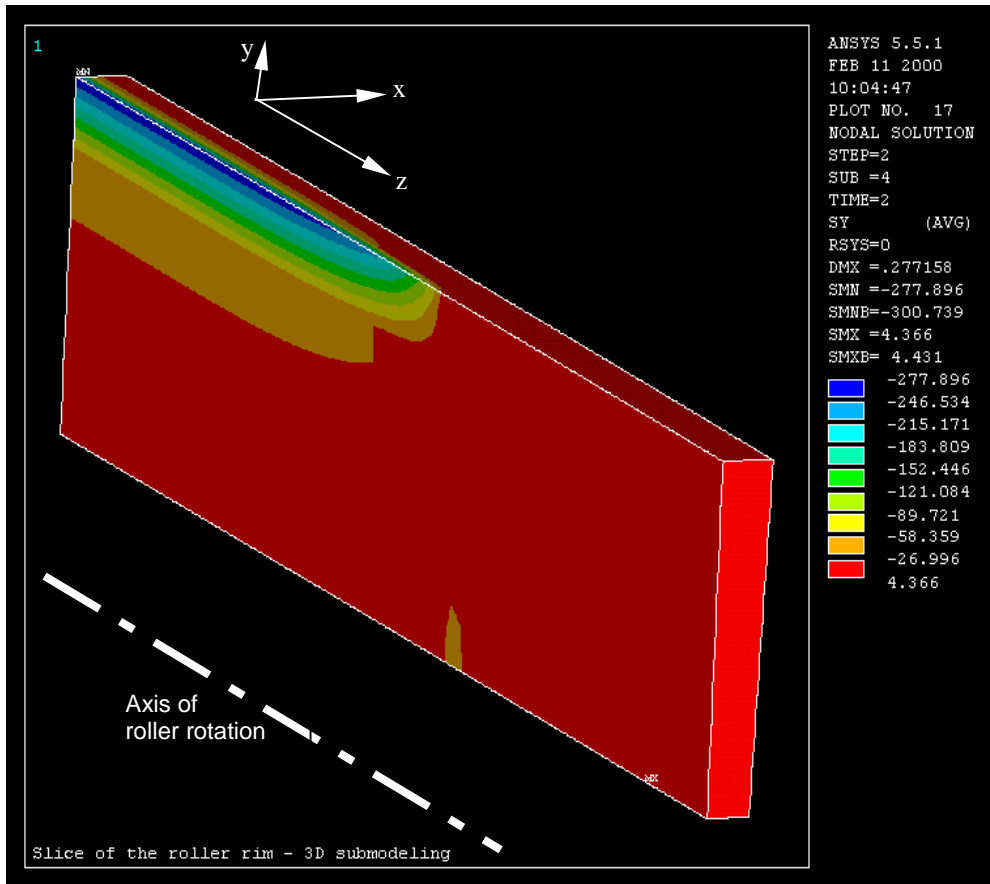


Figure C-10: Distribution of the contact pressure ( $\sigma_y$  in the sub-model) on a radial half-slice of the roller rim which was cut through the centre point of the contact area.

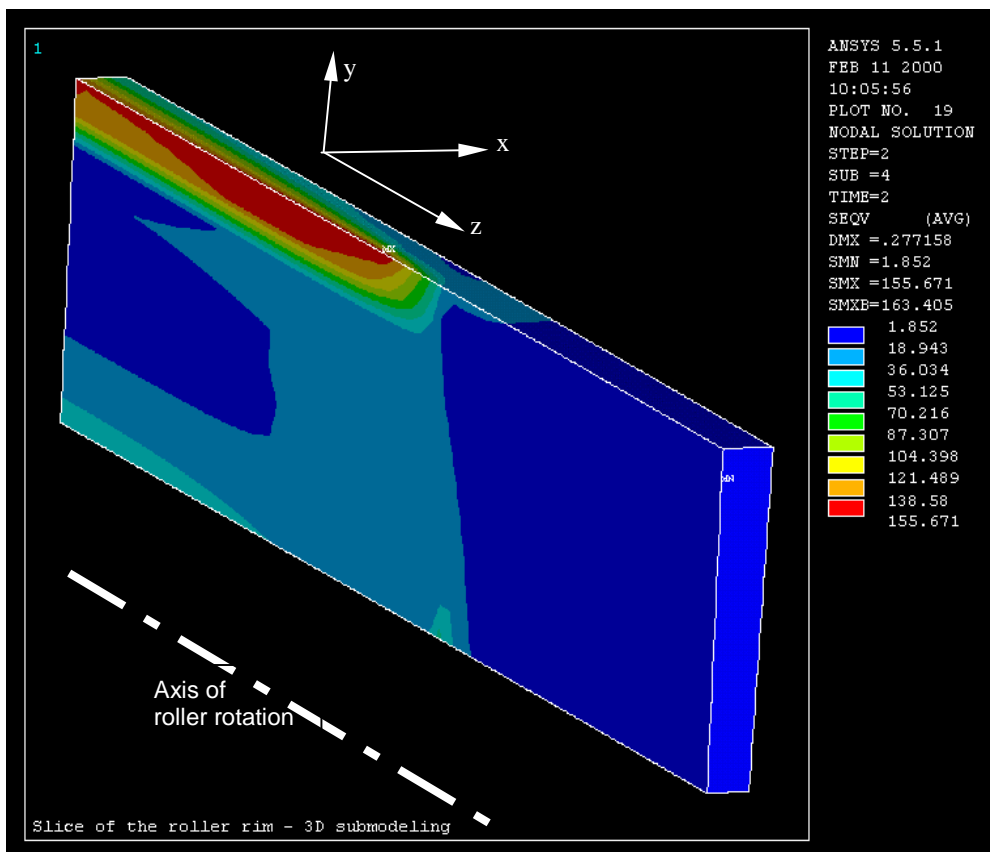


Figure C-11: Distribution of  $\sigma_{Mises}$  (equivalent stress) along a radial half-slice of the roller rim that was cut through the centre point of the contact area. The maximum value occurs close to the web and on the surface. At the bottom, the influence (and hence the position) of the roller web is visible.

## C.5 Conclusions

On the basis of the results obtained by means of FEM, the following conclusions can be made:

- To give the rollers a slightly spherical shape (i.e. to manufacture them applying a camber radius to achieve a barrel type shape) is a useful measure to smooth the stress distribution in the roller-ring interface. It also helps to avoid stress concentration on the roller edges in case of a slight misalignment of the axis of rotation.
- A camber radius of around 60 m - perhaps slightly higher - seems to give a maximised contact area while still keeping contact stresses comparatively uniform.
- Provided that a contact breadth as computed in the FEM analysis can be achieved, maximum equivalent stresses calculated are  $155 \text{ N/mm}^2$ , i.e. well below the value of the yield point of  $355 \text{ N/mm}^2$  hence suggesting a considerable bearing reserve for the contact zone.
- The maximum surface pressure calculated is  $280 \text{ N/mm}^2$  (camber radius 60 m). If this value is interpreted as a Hertz pressure, it is acceptable and far away from the allowable maximum quoted in Table C-1 ( $1000 \text{ N/mm}^2$ ). Obviously, such a high allowable surface pressure refers to classical Hertz pressure calculations and do already take into account several beneficial effects occurring in real situations like increased contact breadth due to global deformations, surface hardening and plain strain conditions in the contact area.
- The influence of the camber radius on the equivalent stresses in the webs can be neglected.
- In a revised design the following changes in geometry should be discussed: the thickness of the roller webs could be decreased and, as a consequence, one could reduce the length of rollers. In particular, the distance between web and outer edge should be minimised since this outer part of the rim does not contribute to the transfer of forces. If there is a severe lack of space in the bearing unit, the diameter of the roller could be slightly decreased without running into major problems. In contrast, an increase in rim thickness of roller and ring is strongly recommended in order to enhance the smoothing of the surface stress.

## References

- [1] Bryant P J (study leader), Badano L, Benedikt M, Crescenti M, Holy P, Maier A, Pullia M, Reimoser S, Rossi S, Borri G, Knaus P, Gramatica F, Pavlovic M, Weisser L, "Proton-Ion Medical Machine Study (PIMMS)", CERN yellow report, CERN-2000-006 and CERN-PS-2000-007 (DR), Geneva, 2000, available also on CD-rom, Part II, Chapter 6
- [2] Reimoser S, "Protonengantries" in: Pötter R, Auberger T, Regler M, (eds.), "Med-AUSTRON Feasibility Study", Med-AUSTRON Planning Office, c/o RIZ, Stephan-Koren-Strasse 10, A-2700 Wiener Neustadt, December 1998, Section II.3.1.
- [3] Schneider K J (ed.), *Bautabellen für Ingenieure*, Werner Verlag, 12<sup>th</sup> edition, 1996, p. 8.113
- [4] Roark's Formulas for Stress & Strain, Vol. I, McGraw-Hill, 6<sup>th</sup> edition, 1989, in the version of: Electronic Book in MathCAD, Warren C Young, MathSoft Inc.
- [5] Radzimovsky E I, "Stress Distribution and Strength Conditions of Two Rolling Cylinders Pressed Together", Eng. Experiment Station, Univ. of Illinois, Bull. 408, 1953, p. 13
- [6] Czichos H (ed.), *Hütte: Die Grundlagen der Ingenieurwissenschaften*, 29<sup>th</sup> edition, 1989, p. E100
- [7] Radzimovsky E I, op. cit., p. 16
- [8] ANSYS Analysis Guides version 5.5, 001083, 2<sup>nd</sup> Edition, SAS IP Inc.

## Glossary

Since the development of a novel solution for an ion gantry brings together people with different scientific background, readers of the present study might find it practical to look up in a glossary specific vocabulary common in other disciplines. The glossary also acts as a list of terms and their definitions, which were used throughout the work. Expressions used synonymous are always listed in the first line of the paragraph.

### $\sigma$ (Sigma)

Standard deviation of the gaussian (normal) probability distribution.

### $3\sigma$ (tolerance) region for random misalignments

Specifying  $3\sigma$  values for misalignment tolerances indicates that the elements are expected to be found within a  $-3\sigma$  to  $+3\sigma$  tolerance region with a probability of 99.73 %, i.e. practically always. Therefore, in the present study, maximum values were frequently interpreted as  $3\sigma$  of a random distribution and vice versa.

### $4\pi$ -beam access to the patient

see *Treatment angle*

### $90^\circ$ dipole magnet

see *Main bending magnet*

### Absorbed dose

see *Dose*

### Accelerator

see *Particle accelerator*

### Accidental errors

In the present study, an accidental error refers to a relatively large misalignments of one or more beam transport elements caused for instance by the sudden breakage of equipment, impacts on the structure and cameras etc. Such errors lead to a sudden, and probably large, deviation of the beam from the desired position. They have to be detected and corrected before irradiation of the patient starts.

### Achromatic

The quality of a beam transport line or optical system where particle momentum has no effect on its trajectory through the system. An achromatic device or system is that in which the output beam displacement or divergence (or both) is independent of the input beam's momentum.

### Active beam scanning

see *Beam delivery system*

### Alignment control system

Proposed for the Riesenrad gantry to detect (during gantry rotation) accidental errors in excess of  $\pm 0.3$  mm ( $3\sigma$  or better). Two laser beams are running along the line of quadrupoles, whose relative positions towards the laser beams are obtained from retro-reflectors. By turning the quadrupoles, a different set of retro-reflectors becomes visible for the laser beams. Thus the system identifies directly the element responsible for the beam position error.

### Alpha particle

Positively charged particle, identical to the *nucleus* of the helium-4 atom, spontaneously emitted by some radioactive substances, consisting of two *protons* and two *neutrons* bound together, thus having a mass of four units and a positive charge of two.

### Angle of gantry rotation / gantry angle

The angle with which a gantry can direct a beam onto the patient with respect to a reference plane. For the Riesenrad gantry the range is between  $+90^\circ$  and  $-90^\circ$  from the horizontal position.

### Aperture

A measure of the physical space available for the beam to occupy in a device, e.g. the *vacuum chamber* (tube).

### Atomic mass

The quantity of matter contained in an atom of an element, expressed as a multiple of one-twelfth the mass of the carbon-12 atom,  $1.9924 \times 10^{-23}$  g, which is assigned an atomic mass of 12 units.

### *Beam delivery system*

Necessary to adjust a therapy beam to the size and shape of the tumour targeted by spreading it transversally and modulating it in energy (longitudinal spread). In passive beam delivery systems this task is achieved by scatterers and range shifters respectively (*passive beam spreading*). The latter create a so-called spread-out *Bragg peak* (SOBP). Afterwards, patient specific or adjustable laminated collimators (*multi leaf collimator*) limit the beam to the actual tumour size and a compensator or bolus adjusts the beam to the shape of the back of the tumour. Usually, these devices are located in the *nozzle* between gantry exit and patient. This procedure is the standard technique in radiation therapy with photons, electrons and protons. Contrarily, in an *active scanning system* (like *pencil-beam scanning* or *raster scanning*), the beam is scanned in one or two transversal dimensions over the tumour by fast scanning magnets (*dipoles*). The energy or depth adjustment can be done also with a range shifter or by varying the energy of the accelerator itself pulse-to-pulse in the case of a synchrotron. In the latter case, the dose can be delivered 3D target conform in a tumour specific voxel plan. Sensitive parts in the area or vicinity of the tumour can be treated with a reduced dose, i.e. spot by spot *intensity modulation* is possible in this case. A hybrid system is the so-called beam *wobbling*, where the beam scatterer is used together with scanning magnets to form a (very) large uniform field, individually shaped with a multi-leaf collimator.

### *Beam intensity*

The average number of particles in a *beam* passing a given point during a certain time interval, given, for example, as the number of protons per pulse or protons per second.

### *Beam line*

Beam line is a collective term referring to all the devices used to control, monitor, and produce a beam having particular characteristics. The common elements of a beam line are (*electro*)magnets, *intensity* monitors, beam position monitors, and *collimators*.

### *Beam position accuracy*

In the present study, the beam position accuracy indicates how precise the centre of the non-scanned beam can hit the ideal gantry isocentre. An incorrect beam position can be caused by *systematic* or *random misalignments* of a *beam transport element*. More precise is the term *beam position probability distribution*.

### *Beam position probability distribution*

Indicates the isocentre response to various misalignments of the beam transport elements. Systematic misalignments (errors) are responsible for the mean value, random misalignments for the standard deviation (i.e. the beam position uncertainty) of the beam position probability distribution.

### *Beam rigidity*

In particle physics the (magnetic) beam rigidity refers to the "stiffness" of a beam that is subjected to a deflection due to a magnetic field; unit: Teslametre [Tm]

### *Beam transport element*

An *electromagnet* that bends (dipole) or focuses (quadrupole) the particle beam.  
See also *Electromagnet*

### *Beam*

In particle physics: a slender unidirectional stream of particles or radiation.  
In building construction: a horizontal member spanning an opening and carrying a load (e.g. a wall or a floor)

### *Beta particle*

An *electron* emitted by the nucleus of a radionuclide. The electric charge may be positive, in which case the beta particle is called a positron.

### *Boron Neutron Capture Therapy (BNCT)*

BNCT is based on the fact that some boron compounds may accumulate in certain tumours, particularly in brain tumours, and enhance their sensitivity to (external) irradiation with *thermal neutrons*. Boron atoms capture the neutrons and give rise to *alpha* and lithium particles. These have a high energy density and their track is less than a millimetre in tissue, so that they do not leave the tumour and can control the developments of the cancerous tissues in which the boron is fixed.  
see also *Radiation therapy*

### *Brachytherapy*

Interstitial brachytherapy is a type of internal radiation therapy. Radioactive "seeds" are planted directly into the tumour where they can remain for a period of time. This technique is useful for treating small tumours that cannot be removed surgically.

### *Bragg peak*

When protons and ions traverse matter they deposit most of their energy near the end of their path in what is called the Bragg peak. This property makes them particularly suited for conformal radiation therapy.

### *Bremsstrahlung*

Electromagnetic radiation (*photons*) produced by a sudden slowing down or deflection of charged particles (especially electrons) passing through matter in the vicinity of the strong electric fields of atomic *nuclei*.

### *Cancer*

Any of a group of more than 100 related diseases characterised by the uncontrolled multiplication of abnormal cells in the body. If this multiplication of cells occurs within a vital organ or tissue, normal function will be impaired or halted, with possible fatal results.

### *Cantilever*

A cantilever is a beam, which on one end can be considered as "built-in" ("encasté") to some rigid support. The other end of the cantilever sticks out and supports the load.

### *Carbon-11 (<sup>11</sup>C)*

Positron-emitting isotope of carbon. In *ion therapy*, carbon-11 (and also carbon 10) is produced directly by fragmentation of parts of the carbon-12 beam with the human tissue. Its spatial distribution can be monitored with a PET camera.  
see also *Positron emission tomography*

### *Chicane / maze / labyrinth*

All shielded areas require holes or openings for cables, ventilation ducts and personnel access. By giving these "perforations" of the shielded enclosure the shape of a chicane, the overall efficiency of the shield is not severely undermined. In the Riesenrad gantry "chicane" usually refers to the personnel access.

### *Collimator*

A movable, solid block of material which can be used to limit the beam size or to stop it altogether.

### *Computer tomography (CT)*

Radiologic medical imaging technique for obtaining clear X-ray images of deep internal structures. In this procedure a narrow beam of X-rays sweeps across an area of the body and is recorded not on film but by a radiation detector as a pattern of electrical impulses. Data from many such sweeps are integrated by a computer, which uses the radiation absorption figures to assess the density of tissues at thousands of points. The density values appear on a screen as points of varying brightness to produce a detailed cross-sectional image of the internal structure under scrutiny.

### *Cross-section*

In particle physics the cross-section is a measure of the probability of the occurrence of a specified interaction between a particular incident particle and a specified target particle or system of particles. Unless otherwise specified, the cross-section is given by the reaction rate per target particle for a specified process (e.g. capture), divided by the flux of the incident.

### *Cryogenics*

Cryogenics is the technology of the production and effects of very low temperatures. The adjective "cryogenic" is frequently used when describing the phenomena of superconductivity.  
see also *Superconductivity*

### *CT*

see *Computer tomography*

### *Current density*

Electric current or flow of electric charge through a conducting medium per unit cross-sectional area. Unit ampere per square metre, symbol  $A\ m^{-2}$ .

### *Cyclotron*

The cyclotron, was the first cyclic *particle accelerator* that produced particles energetic enough to be useful for nuclear research. In classical cyclotrons, the accelerating electric field oscillates at a fixed frequency and the guiding magnetic field has a fixed intensity. The path of the accelerated particle is thus a spiral-like series of semicircles of continually increasing radius.  
see also *Synchrotron*

### *Deformations / displacement / deflection / excursion*

Movement of a specified point, element or the beam caused by some structural or ion-optical effect recognisable from the context. In the present work, usually, calculated deformations and

deflections are the result of a *structural analysis*, beam displacements or excursions are the result of the *ion-optical analysis*.

#### *Diaphragm wall*

The diaphragm wall technique is one principal method to construct large and in particular deep basements. A diaphragm wall is constructed in advance of the main excavation and it forms part of the permanent substructure. The embedded wall is designed to be virtually watertight, sometimes an internal facing wall is added. Its construction is based on the use of bentonite mud as a means of stabilising the walls of a trench whilst it is being excavated. The construction sequence of a diaphragm wall is the following: 1. Construction of a guide trench that establishes the line and level of the wall, and acts as a bentonite reservoir during panel excavation. The guide trench also supports reinforcement cages and concreting activity. 2. Excavation of the trench in panel lengths (usually 2 - 6 m). Bentonite mud is pumped into the trench as the excavation proceeds. 3. When the panel excavation is completed to the required depth, stop ends are placed in position at both ends of the trench and a reinforcement cage is lowered into position through the bentonite mud. 4. Concrete is then placed through tremie tubes so that the bentonite mud is displaced upwards by the concrete rising from the bottom of the trench. 5. The stop ends are withdrawn prior to the setting of the concrete thus leaving recesses, which form keys for the adjacent panels. 6. Adjacent panels are then constructed repeating the processes above.

#### *Dipole*

A magnet with two pole faces, used to bend a *beam* either horizontally or vertically.  
see also *Electromagnet*

#### *Dispersion*

Quality of a beam transport system at a given point that defines the variation of the transverse position of the beam with variations in beam momentum. Usually expressed in metres. Dispersion of the momentum variety can be looked at as the size of a beam as a function of the momentum spread. Dipoles can create dispersion or take it away (particles of different momenta will be bent at different angles by a dipole with uniform field), as can quadrupoles.

#### *Divergence*

*The angle that the trajectory of each particle makes with the beam axis.*

#### *DNA*

Deoxyribonucleic acid. The compound that controls the structure and function of cells and is the material of inheritance.

#### *Dose*

General term for quantity of ionising radiation. The *absorbed dose* (frequently called *dose* in radiation therapy) is the radiation energy imparted *per unit mass* of an irradiated body. It is measured in joule per kilogram, a unit which is also called the Gray (Gy). Multiplying the absorbed dose by appropriate weighting factors depending on the type of radiation, creates the *equivalent dose* in the relevant organ or tissue. By weighting the equivalent dose in each organ in proportion to the probability and severity of the harm done by radiation, and adding the weighted contributions from each organ to a total body dose, a third term, the *effective dose* is obtained. In radiation protection it is usually the effective dose that is determined for comparison with dose limits or for assessments of risks. Both the equivalent dose and the effective dose are also measured in joule per kilogram, but in these cases the unit is called the Sievert (Sv). For X-rays and gamma rays the absorbed and equivalent doses in Gray and Sievert are numerically equal.  
see also *Ionising radiation*

#### *Dose-to-target conformity*

see *Bragg Peak*

#### *Effective dose*

see *dose*

#### *Electromagnet*

A device consisting of a core of magnetic material surrounded by a coil through which an electric current is passed to magnetise the core. An electromagnet is used wherever controllable magnets are required, as for example in particle accelerators (including its medical applications): a moving particle that carries a charge, such as an electron, can be regarded as an electric current and, like a current-carrying wire, experiences a force in a magnetic field. The direction of the force is perpendicular both to the direction of motion of the particle and to the magnetic field, so that the particle is deflected from its original path. This principle can be used to focus a stream of charged particles like electrons, protons or ions into a narrow beam and to deflect the beam by creating suitable magnetic fields, with the help of quadrupoles and dipoles respectively.

#### *Electromagnetic radiation*

Radiation that can be considered as a wave of electric and magnetic energy travelling through a

vacuum or a material. Examples are *gamma rays*, *X-rays*, ultraviolet radiation, light, infrared radiation and radiofrequency radiation.

*Electron LINAC*

see *Linear accelerator*

*Electron volt*

Unit of energy used in atomic and nuclear physics. Equal to the energy gained by an electron (carrying unit electronic charge) in passing through a potential difference of 1 volt. Symbol eV.  $1 \text{ eV} = 1.6 \times 10^{-19}$  joule approximately. In radiation therapy the energy of a particle beam is frequently specified in MeV (millions of electron volts). For an ion beam the energy is given in MeV/u (millions of electron volts per nucleon).

*Electron*

An elementary particle with low mass, 1/1836 that of a proton, and unit negative electric charge. Positively charged electrons, called positrons, also exist.

*Epidemiology*

is the study of the distribution of disease in populations and of the factors that affect this distribution. In contrast to clinical medicine where the emphasis is on the individual, epidemiology involves the examination of patterns of disease in groups of individuals. While epidemiology originated from investigations of epidemics of infectious diseases in the 19<sup>th</sup> century, epidemiological research in western countries is now directed largely at chronic diseases, such as heart disease and *cancer*.

*Equivalent dose*

see *dose*

*Exocentric gantry / eccentric gantry*

In an exocentric gantry - contrarily to an *isocentric gantry* - the patient is placed eccentrically to the axis of gantry rotation that coincides with the axis of the incoming beam. A 90° bending magnet terminating the transfer line is placed on the axis. The magnet can be rotated around the beam axis and set to any angle. The beam deflection will correspond to the magnet angle. The patient must in this case be placed in a cabin that follows the magnet rotation. Exocentric gantries are frequently referred to as *Riesenrad* gantries.

*External radiotherapy*

see *Radiation therapy*

*Extraction*

The controlled removal of the *beam* from an accelerator.

*Fast neutrons*

Neutrons with energies in excess of 0.1 MeV. Corresponding velocity of about  $4 \times 10^6 \text{ m s}^{-1}$ .

*Fixed beam line*

Contrarily to a (rotating) *gantry*, a fixed beam line is able to deliver a therapy beam towards the patient from one single direction only (usually horizontal). In combination with a rotatable patient couch, several beam entrance channels in a single plane can be achieved.

*Fraction*

Treatment session in radiation therapy. A fractionated treatment benefits from the inferior repair characteristic of cancerous cells compared to healthy tissue.

*Gamma Knife*

see *Stereotactic radiosurgery*

*Gamma ray*

A discrete quantity of electromagnetic energy without mass or charge, emitted by a radionuclide.

*Gantry hall / gantry room*

The shielded enclosure housing a gantry.

*Gantry quadrupoles support structure*

see *Rotator*

*Gantry radius*

Refers to the radial distance between the axis of rotation and the most eccentric beam transport element (*isocentric gantry*) or the patient (*exocentric gantry*), whichever is larger.

*Gantry*

Mechanical structure capable of delivering a therapy beam for cancer treatment from any direction to the patient (medical gantry). Typically, a gantry rotates around the patient who is kept

in the supine position (rotating gantries, *isocentric gantry*), however, the geometry can also be inverted leading to a an *exocentric (Riesenrad gantry)*. The original meaning of the word gantry refers to any of a diverse group of machines that not only lift heavy objects but also shift them horizontally (moveable platforms or cranes).

#### *Girder*

In construction engineering usually a large *beam* carrying the ends of other beams perpendicular to them.

#### *Hadron*

Any of the subatomic particles that are built from quarks and thus react through the agency of the strong nuclear force. In *radiation therapy* hadrons (hadron therapy) usually refer to the use of *protons* and *ions* (proton or ion therapy) and not to *neutrons*, although the latter are also hadrons.

#### *Immobilisation*

see *Patient couch*

#### *Intensity modulated radiotherapy (IMRT)*

Irradiation technique that makes use of several multiple *photon* beam entry ports (*gantry* required!) where the intensity of each beam is varied across the irradiation field with the help of individualised absorbers. In addition, computer-controlled *multi-leaf collimators* can be used to shape the fields to the contours of the tumour. The procedure is then called *conformal intensity modulated radiotherapy* or *intensity modulated 3D photon therapy*.

see also *Beam delivery system*

#### *Intensity*

see *Beam intensity*

#### *Interlock*

Something which constrains or inhibits a device, generally for the purpose of safety, e.g. temperature interlocks, electrical interlocks, radiation interlocks, etc.

#### *Internal radiation therapy*

see *Brachytherapy, radiation therapy*

#### *Ion therapy*

Beams of light ions like carbon (called "heavy ions" in the medical community) represent the most advanced tool for *radiation therapy* of deep seated tumours. They combine an excellent physical depth-dose profile (*Bragg peak*) with an increased *relative biological efficiency* (RBE) in the target volume. With the help of an active *beam delivery system* (beam scanning) one can deliver the dose to arbitrarily shaped target volumes with considerably reduced damage in the healthy tissue. There are two facilities today offering carbon-ion treatment, the HIMAC in Chiba, Japan, and a test facility at the GSI in Darmstadt. The promising clinical results have triggered the planning of several dedicated clinical centres for carbon-ion therapy, for instance in Austria (Med-AUSTRON), Germany (Heidelberg) and Italy (TERA - CNAO).

see also *Radiation therapy*

#### *Ion*

Electrically charged atom or grouping of atoms.

#### *Ionisation Chamber*

A particle passing through the gas in a small chamber forms ions. A voltage will cause the ions to be attracted to the collection plate, depending on their charge. As a result a pulse of current will flow for each particle that forms ions. Each pulse is proportional to the ionisation energy delivered by the particle.

#### *Ionisation*

The process by which a neutral atom or molecule acquires or loses an electric charge. The production of ions.

see also *Ionising radiation*

#### *Ionising radiation*

Radiation that produces ionisation in matter. Ionising radiation is radiation that produces ions in matter during interaction with atoms in the matter. The toxic effect of ionising radiation is related to the ionisation. It is believed that ionisation of tissues, composed mainly of water, generates  $\text{H}_2\text{O}^+$  and  $\text{H}_2\text{O}^-$  ions, which in turn form H and OH radicals. Because radicals are very reactive chemically, biological damage, such as attacks on DNA and proteins, results. There are two classes of ionising radiation: particulate and electromagnetic. *Alpha particles, beta particles, neutrons* as well as *protons* and *ions* are examples of particulate ionising radiation. *Gamma rays* and *X-rays* are electromagnetic ionising radiation. Biological damage is related to the degree of tissue ionisation produced by radiation. Thus, a physical (absorbed) dose of alpha particles or



carbon ions does not produce the same amount of damage as that produced by the same dose of beta particles, gamma rays or X rays.

See also *Dose, Non-ionising radiation*

#### *Ion-optical analysis*

In the present study the *structural analysis* was followed by an ion-optical one in order to establish the response of the ion beam to the misalignments of the *beam transport elements* caused by elastic deformations and temperature fluctuations of the support structure.

#### *Isocentre*

Generally, the isocentre represents the spot, where the beam is meant to deposit its energy. Originally, the term only referred to the geometrical (iso-)centre of an *isocentric gantry*, however, as *exocentric gantry* concepts were developed, the expression is now also used to name their point of interaction, preferably called "local" isocentre. One could justify this name in the context of exocentric gantries by taking the patient's point of view as a reference.

#### *Isocentric gantry / conventional gantry / classic gantry*

Generic term for a gantry where the patient is placed on-axis of the incoming beam line, i.e. in the *isocentre*. Therefore, to achieve different treatment angles, the beam has to be bent out of axis somewhere upstream and eventually be bent back towards the central patient. The isocentric approach is the classic gantry concept in *radiation therapy*.

See also *exocentric gantry*

#### *Isotope*

Any member of a set of *nuclides* having the same number of protons but different numbers of neutrons.

#### *Laser*

Device which amplifies light and usually produces an extremely narrow intense beam of a single wavelength.

#### *Lattice*

The arrangement of *beam transport elements* and drift spaces in a *particle accelerator*.

#### *Linear accelerator (LINAC)*

type of *particle accelerator* that imparts a series of relatively small increases in energy to subatomic particles as they pass through a sequence of alternating electric fields set up in a linear structure. The small accelerations add together to give the particles a greater energy than could be achieved by the voltage used in one section alone. Classical *radiation therapy* uses compact linear electron accelerators as a (primary) source of radiation for cancer treatment. Usually, such LINACS are mounted directly on a *gantry*.

#### *Magnetic flux density, magnetic induction*

A measure of the magnetic effect induced in a medium by an external field. Unit Tesla, symbol T.

#### *Magnetic resonance imaging (MRI)*

Magnetic resonance imaging (MRI) relies on the response of magnetic fields to short bursts of radio-frequency waves to produce computer images that provide structural and biochemical information about tissue. The process uses radio waves and is thus much safer than imaging using X rays or gamma rays. This totally non-invasive procedure is particularly useful in detecting early-stage cancer. Because patients must lie quietly inside a narrow tube, MRI may raise anxiety levels in the patients, especially those with claustrophobia. Another disadvantage of MRI is that it has a longer scanning time than *computer tomography* (CT), which makes it more sensitive to motion and thus of less value in scanning the chest or abdomen. Because of the strong magnetic field, MRI cannot be used if a pacemaker is present or if metal is present in critical areas such as the eye or brain.

#### *Main bending magnet / 90° bending magnet / main dipole / Riesenrad dipole*

In the *Riesenrad gantry* a large 62 t dipole magnet - placed on the axis of gantry rotation - is terminating the transfer line and supported by a central structure (the "cage"). The magnet is rotated around the incoming beam axis and can be set to any angle. The beam deflection will correspond to the magnet angle.

#### *Mapping / correction map*

In the *Riesenrad gantry*, and partly also in existing proton gantries, a correction map is generated to compensate for an incorrect beam position at the gantry isocentre due to *systematic misalignments* of the *beam transport elements*, for instance due to elastic deformations of the support structures. The correcting action, which is a feed-forward correction, can be performed by the patient couch, by the scanning magnets or by dedicated corrector magnets inserted preferably upstream of the scanning system. Long-term systematic effects like differential settlement of the building or wear of the mechanics will call for a regular "re-mapping".

*MeV*

Abbreviation indicating  $10^6$  electron volts.  
see *Electron volt*

*Misalignment tolerances*

Precision with which the beam transport elements have to be aligned. Two components for the tolerances have to be distinguished: absolute misalignment tolerances (to be met during assembling and alignment of the gantry) and non-reproducible, random misalignments, i.e. the stability of the element position.  
see also *Random misalignment study*

*MRI*

see *Magnetic resonance imaging*

*Multi-leaf collimator*

see *Beam delivery system*

*Neutron*

An elementary particle with unit *atomic mass* approximately and no electric charge.

*Non-ionising radiation*

Radiation that does not produce ionisation in matter. Examples are ultraviolet radiation, light, infra-red radiation and radiofrequency radiation. When these radiations pass through the tissues of the body they do not have sufficient energy to damage DNA directly.  
see also *Ionising radiation*

*Nozzle*

It is current practice in radiation therapy to mount the beam shaping devices and some monitoring equipment in the so-called nozzle that is situated between the last beam transport element and the patient. In case of a gantry, this nozzle is usually fixed to the support structure, cantilevering towards the patient.  
see also *Beam delivery system*

*Nuclear medicine*

Term usually applied to the use of *radionuclides* (radioisotopes) for diagnosing or treating disease in patients. In difference to an examination using X-rays or treating tumours with radiotherapy, where the patient is exposed to a well-defined beam which passes through the body, nuclear medicine examinations involve introducing a radioactively-labelled drug into the body, usually by intravenous injection, which is preferentially taken up by the particular organ under investigation. The radioactive material emits gamma rays which pass out of the body to a gamma camera (scintillation counter) positioned near the organ concerned. This data can then be electronically recorded and studied by clinicians. The radioisotope usually has a short half-life and thus decays completely before its radioactivity can cause any damage to the patient's body.  
see also *Positron Emission Tomography*

*Nucleon*

Either of the subatomic particles, the *proton* and the *neutron*, constituting atomic nuclei. Unstable subatomic particles heavier than nucleons have a nucleon among their final decay products.

*Nucleus of a cell*

The controlling centre of the basic unit of tissue. Contains the important material *DNA*.

*Nucleus*

The core of an atom, occupying little of the volume, containing most of the mass, and bearing positive electric charge.

*Nuclide*

A species of atom characterised by the number of protons and neutrons and, in some cases, by the energy state of the nucleus.

*Particle accelerator*

Any device that produces a beam of fast-moving, electrically charged atomic or subatomic particles. Physicists use accelerators in fundamental research on the structure of nuclei, and the nature of nuclear forces. Accelerators are also used for industrial radiography, sterilisation of biological materials, polymerisation of plastics, a certain form of radiocarbon dating and - concerning the majority of accelerators - radiation therapy and medical imaging.  
See also *Linear accelerator, Cyclotron, Synchrotron*

*Particle energy*

see *Electron volt*

*Passive beam spreading*

see *Beam delivery system*

*Patient cabin / treatment cabin / treatment platform*

In a medical *gantry* this names the enclosure where the patient is positioned and the actual treatment takes place. The patient cabin of the Riesenrad gantry is an independent structure (with no mechanical connection to the central cage) that permits the positioning of the patient on a half-circular path (radius 5.6 m) around the incoming beam axis. Technically, it is a lift structure with a telescopic floor and moderate precision requirements. It has continuous contact with the lateral wall of the gantry hall and, by virtue of this, provides permanent emergency access to the patient via a staircase. The cabin supports the *patient couch* and auxiliary medical equipment, possibly even a *CT* combined with a *PET*.

*Patient couch / patient table / patient positioning system (PPS)*

In order to minimise organ movements during irradiation, the patient is usually immobilised in a supine position lying on a patient couch. Depending on the part of the body to be irradiated, this immobilisation can be done with the help of individually prepared masks or head holders (head treatment) or whole-body moulds. The couch forms part of the patient positioning system (PPS), which is a general expression, and the two are often mentioned in a synonymous context. Usually, the patient couch can be shifted in all 3 dimensions and rotated around the vertical axis to achieve arbitrary positions with respect to the beam. Some versions also have pitch and roll mechanisms to counterbalance deformations. In the Riesenrad gantry the patient couch is brought into the treatment position and aligned precisely with respect to the exit face of the *main dipole magnet* using a *photogrammetric alignment system (PAS)*.

*Patient positioning system (PPS)*

see *Patient couch*

*Pencil-beam scanning*

see *Beam delivery system*

*Pencil-beam scanning*

see *Beam delivery system*

*Pendular bearing*

see *Statically determinate support*

*PET*

see *Positron Emission Tomography*

*Phase space*

A six-dimensional space consisting of a particle's position (x, y and z) and divergence (x-prime, y-prime, and z-prime). The phase space is generally represented in two dimensions by plotting position on the horizontal axis and the corresponding *divergence* on the vertical axis.

*Photogrammetric alignment system (PAS)*

In the Riesenrad gantry the precise alignment of the patient couch is done photogrammetrically with respect to the *90°-bending magnet*. For this purpose, reflectors on the patient couch are monitored by at least four cameras attached to the exit face of the dipole. By measuring the relative couch-to-magnet position the system automatically directs the couch to the desired treatment position with an accuracy better than 0.1 mm ( $1\sigma$ ).

see also *Patient couch*.

*Photon therapy, conventional radiotherapy*

see *Radiation therapy*

*Photon*

Quantum of electromagnetic radiation.

see also *Bremsstrahlung*

*PIMMS*

see *Proton-Ion Medical Machine Study*

*Positron Emission Tomography (PET)*

PET is an imaging technique in *nuclear medicine* used in diagnosis and biomedical research. It has proved particularly useful for studying brain and heart functions and certain biochemical processes involving these organs. In PET, a radiopharmaceutical - i.e. a chemical compound specifically designed to be taken up by the area of interest and "labelled" with a short-lived, positron-emitting *radionuclide* of carbon, oxygen, nitrogen, or fluorine - is injected into the body. As the radionuclide decays, positrons ( $\beta^+$ ) are annihilated by electrons, giving rise to gamma rays that are detected simultaneously by the photomultiplier-scintillator combinations positioned on opposite sides of the patient. The data from the detectors are analysed, integrated, and

reconstructed by means of a computer to produce images of the organs being scanned. It is a major advantage of carbon-ion therapy that such a positron emitter ( $^{11}\text{C}$ ) is directly produced by fragmentation of the  $^{12}\text{C}$  treatment beam as it passes through tissue on its way to the treatment point. The  $^{11}\text{C}$  has essentially the same range as the  $^{12}\text{C}$ , therefore, imaging the positron annihilation radiation gives a direct measure of the stopping point of the beam. On one hand, PET can verify that the beam has actually reached the target volume, and on the other hand it acts as an important tool to eliminate uncertainties in the treatment planning caused by density variation of the various tissues.

*Positron*

See beta particle.

*PPS (patient positioning system)*

see *Patient couch*

*Probability*

The mathematical chance that a given event will occur.

*Proton therapy*

see *Radiation therapy*

*Proton*

An elementary particle with unit atomic mass approximately and unit positive electric charge.

*Proton-Ion Medical Machine Study (PIMMS)*

PIMMS was set up following an agreement between Med-AUSTRON (Austria) and the TERA Foundation (Italy) to join their resources in the design of a generic facility, in particular the medical synchrotron and the carbon-ion gantry, that could later be adapted to individual national needs. CERN agreed to host this collaboration inside its PS Division and to contribute to the study. The group has worked in contact with GSI (Germany) and was later joined by Onkologie 2000 (Czech Republic).

*Quadrupole*

A magnet consisting of four poles ("quadrupole") used for focusing beams of particles.

see also *Electromagnet*

*Radiation therapy / Radiotherapy*

Term applied to the use of ionising radiation for treating disease, usually *cancers*, in patients. The radiation may be administered to the body by implanting radioactive substances into the tumours (e.g. *brachytherapy*) or by exposing the body to external sources of high-energy rays such as *X-rays* and *gamma rays (photons)* or streams of particles such as *neutrons, protons* and *ions* that penetrate internally. The purpose of such radiation therapy is to destroy cancerous cells with minimal damage to normal healthy tissue or systemic involvement. Ionising radiation bombards the cells exposed to it and breaks the molecular bonds essential to cell growth. There is always the accompanying destruction of some normal tissue along with the tumour.

*Radiation*

The process of emitting energy as waves or particles. The energy thus radiated. Frequently used for *ionising radiation* except when it is necessary to avoid confusion with *non-ionising radiation*.

*Radio biological efficiency (RBE)*

Is defined as the ratio of the *photon dose* to the particle (*ion, proton, etc.*) *dose* leading to the same biological effect, i.e. survival rate of cells. The RBE depends on the *particle energy*, the delivered dose and the type of cells and tissue that is irradiated. Generally, protons show a RBE close to one, while this value increases for (heavier) ions. Very roughly, carbon ions show a RBE of slightly above one in the entrance channel rising to about three in the region of the *Bragg peak*.

*Radioactivity*

The property of radionuclides of spontaneously emitting ionising radiation.

*Radiobiology*

The study of the effects of ionising radiation on living organisms.

*Radionuclide*

An unstable nuclide that emits ionising radiation.

*Radiotherapy*

see *Radiation therapy*

*Random error / Random misalignment*

In a medical *gantry*, random errors represent all possible misalignments with no reproducibility as a function of the gantry angle, hence they can be interpreted as an uncertainty of the position of a *beam transport element*. These misalignments are assumed to have a gaussian distribution

(*random misalignment probability distribution*) and their individual contributions to the beam displacement are added quadratically. Temperature effects are expected to be the main and typical random error contributor, other sources might be backlash of drive mechanics, free-play in bearings etc. The practical effect of random misalignments is that for different *fractions* the position of the (non-scanned) *beam* will vary around the ideal position (*isocentre*) according to a gaussian distribution. Random errors have to be either kept below a certain limit or their effects have to be measured and compensated on-line.

*Random misalignment probability distribution*  
see *Random error*

*Random misalignment study*

It was of major interest for the *Riesenrad gantry* to investigate the sensitivity of the beam position in the isocentre to random misalignments of the beam transport elements, thus giving the possibility to specify "backwards" the permissible random *misalignment tolerances* of the beam transport elements. This was done individual components, namely the quadrupole shift, quadrupole-tilt, dipole-shift and dipole-tilt.

*Raster scanning*  
see *Beam delivery system*

*Riesenrad dipole*  
see *Main bending magnet*

*Riesenrad gantry*

Originally, the word "Riesenrad" refers to the large Ferris wheel in Vienna. In *gantry* technology, however, the name became a metaphoric synonym for large *exocentric gantry* concepts and recently in particular for the novel carbon-ion gantry presented in this study.

*Risk factor*

The probability of *cancer* and leukaemia or hereditary damage per unit *equivalent dose*. Usually refers to fatal malignant diseases and serious hereditary damage. Unit  $\text{Sv}^{-1}$ .

*Rotating gantry*  
see *Gantry*

*Rotator*

In the *Riesenrad gantry*, the rotator is a beam-optics module that is needed to match an incoming *dispersion* vector to the gantry in order to have an *achromatic* beam at the patient. It is a rotatable structure that gives support to seven quadrupoles and that turns with half the angle of the gantry.

*SAD*  
see *Source-to-axis distance*

*Scanning magnets*  
see *Beam delivery system*

*Scintillator*

In certain types of transparent materials, the energy deposited by an energetic particle can create excited atomic or molecular states that quickly decay through the emission of visible or ultraviolet light. Such materials are known as scintillators and are commonly exploited in scintillation detectors. The amount of light generated from a single charged particle of a few *MeV* kinetic energy is very weak and cannot be seen with the unaided eye. Modern scintillation detectors eliminate the need for manual counting by converting the light into an electrical pulse in a photomultiplier tube or photodiode.

*Shear modulus*

The shear modulus is a measure of the ability of a material to resist transverse deformations such as arise, for example, in torsion, as in twisting a metal pipe about its longitudinal axis. Mathematically the shear modulus is equal to the quotient of the shear stress divided by the shear strain.

*Shear wall structure, shell structure, monocoque*  
see *Space truss*

*Source-to-axis distance (SAD) / Source-to-isocentre distance (SID) / Source-to-skin distance (SSD)*

The source to axis distance (or source-to-isocentre distance) is qualitatively similar to the source to surface distance (SSD). The terminus SAD refers originally to isocentric proton *gantries* and specifies the distance between the first beam scatterer ("source") and the isocentre. In the context of other gantry principles one should use the expression "effective SAD", which can be defined more generally as the distance between the (possibly virtual) point source of the beam and the "local" isocentre where the *Bragg peak* occurs.

### *Space truss, space frame*

When it comes to the design of a structure, the engineer is frequently faced with the principal choice between a lattice structure built up, Meccano-fashion, from separate struts and tension rods - which is called space frame or space truss - and a shell structure ("monocoque") in which the load is carried in more or less continuous panels (shear walls). Sometimes the distinction between the two forms of construction is obscured by the fact that space frames are covered by some sort of continuous cladding which does not really carry much load (e.g. timbered cottages). The decision which structural principle to follow with the design is not straightforward and sometimes depends on requirements which are not strictly structural.

### *Spread-out Bragg peak (SOBP)*

see *Beam delivery system*

### *Statically determinate support*

A structure is supported in a statically determinate way if the external support reactions can be calculated from the conditions of equilibrium alone (independent from the stiffness properties of the structure itself). A pendular bearing unit, for example, provides a statically determinate support for a ring, which guarantees an equal load distribution on all rollers, independent of the ring deformation.

### *Stereotactic radiation therapy*

Stereotactic radiation therapy is a refinement of conventional *radiation therapy* techniques based upon multiple fields of radiation entering the body from different locations to maximise radiation dose at the target while minimising normal tissue irradiation. Both fractionated and unfractionated schedules have been devised to maximise benefit while minimising toxicity. The earliest radiosurgical instrument was the Gamma Knife, which uses over 200 radioactive cobalt sources to produce a precise, small volume of concentrated radiation.

### *Structural analysis*

The calculation of internal forces, support reactions, member stresses and deformations for a given model, that has been abstracted from reality. Boundary conditions, material properties and loads have to be defined first. The latter can be gravity, external forces (loads), temperature changes, dynamic impacts, etc. Usually, the loads are applied with a certain safety factor greater than one. Eventually, the results (forces, stresses) are checked with respect to the member resistances and the allowable deformations of the structure.

### *Structural efficiency*

Efficiency in terms of structural weight to supported load.

### *Sub-millimetre precision*

In the present study the sub-millimetre precision is defined as the  $3\sigma$  value of the *beam position probability distribution* in the isocentre being lower than 1 mm in the horizontal and vertical plane ( $3\sigma_{\text{total}} < 1 \text{ mm}$ ).

See also  $3\sigma$  (tolerance) region for random misalignments

### *Superconducting magnet*

A magnet whose coils are made from superconducting material. Superconducting magnets reach much higher magnetic fields than conventional iron/copper magnets at a much lower electrical power cost. They must be cooled to a few Kelvin (depending on the superconducting material), which is usually achieved by a continuous flow of liquid helium through the magnets.

### *Superconductivity*

This is a state of matter that many metals and alloys reach at sufficiently low temperatures (i.e. a few Kelvin). This state is characterised by the total absence of electrical resistance thus making possible the conduction of electrical currents without any measurable loss.

### *Switchyard*

Collector-like building to accommodate the extraction and transfer line  
see also *Gantry hall*

### *Synchrotron*

As the particles in a synchrotron are accelerated, the strength of the magnetic field is increased to keep the radius of the orbit approximately constant. This technique for a *particle accelerator* has the advantage that the magnet required to form the particle orbits is much smaller than that needed in a *cyclotron* to produce the same particle energies. The acceleration is effected by radio-frequency voltages, while the synchronism is maintained by the principle of phase stability. Particles can be stably accelerated with a range of energies and phases with respect to the accelerating voltage, and very intense beams can be produced.

### *Systematic error / systematic misalignment*

Systematic errors are characterised by their short-term reproducibility as a function of the *angle of*

*gantry rotation*. They are assumed to be constant over time and individual contributions have to be added arithmetically. This category covers misalignments of the *beam transport elements* due to elastic deformations of the gantry and rotator support structures, non-ideal initial magnet alignment, manufacturing errors etc.

#### *Taper roller bearing*

Taper roller bearings have tapered inner and outer ring raceways between which tapered rollers are arranged. Their design makes taper roller bearings particularly suitable for the accommodation of combined (radial and axial) loads.

#### *Temperature fluctuations*

Inside the *gantry hall*, the temperature distribution will undergo certain variations (uniform and gradual). Additionally, relative heating of the *Riesenrad dipole* may occur. These effects are summarised as temperature fluctuations and presumably they represent the major contribution to random misalignments of the *beam transport elements*.

#### *Thermal neutrons*

Neutrons that have been slowed to the degree that they have the same average thermal energy as the atoms or molecules through which they are passing. The average energy of neutrons at ordinary temperatures is about 0.025 eV, corresponding to an average velocity of  $2.2 \times 10^3 \text{ m s}^{-1}$ .

#### *Treatment angle*

In classical radiotherapy the treatment angle usually refers to the angle of the beam entering the patient with respect to the horizontal plane. In combination with a *patient couch* rotation gantry designers try to achieve virtually  $4\pi$ -*beam access to the patient* which allows the maximisation of the *dose-to-tumour conformity*. Depending of the gantry concept this is limited by the need to avoid collisions between the *nozzle* and the patient couch.

#### *Treatment cabin*

see *Patient cabin*

#### *Treatment field*

The area exposed to a single radiation beam.

#### *Treatment plan*

Final description of the treatment technique applied to a patient, including methods for planning, dose calculation and for control. A major purpose is reporting.

#### *Vacuum chamber*

In order to minimise losses of particles in the *beam line* due to collisions with air molecules, the *beam* is usually running in a vacuum chamber, i.e. a thin walled tube with extreme low pressure inside.

#### *Vacuum window*

A thin piece of metal in the path of the beam which separates one portion of the beam tube vacuum from another.

#### *Vertical plane*

see *Horizontal plane*

#### *Wobbling*

see *Beam delivery system*

#### *X-ray*

A discrete quantity of electromagnetic energy without mass or charge (*photons*), emitted by an X-ray machine.

#### *Young's modulus*

Young's modulus is a measure of the ability of a material to withstand changes in length when under lengthwise tension or compression. Sometimes referred to as the modulus of elasticity, Young's modulus is equal to the longitudinal stress divided by the strain.

## The Author

### CURRICULUM VITAE

STEFAN REIMOSER, *DIPL.-ING.*

#### Personal Data

<i>Date of birth</i>	May 27 <sup>th</sup> , 1972
<i>Place of birth</i>	Vienna
<i>Nationality</i>	Austria
<i>Family status</i>	married, one daughter
<i>Address</i>	CERN, Div. ST, A 21010 CH-1211 Geneva 23
<i>Telephone</i>	+41 (0)22 7679790
<i>E-mail</i>	Stefan.Reimoser@cern.ch



#### Personal Profile

- Strong points*
- International organisation as work environment
  - Studies in Austria and Great Britain
  - Process-orientated industrial building and planning
  - Interdisciplinary project development
  - Architectural Programming
  - Cost-benefit analysis of transport projects
  - Design & Build, BOT, PPP
  - MS-Office, AutoCAD, CUBUS, Internet
  - English, German and French fluently

#### Education

- Doctoral Thesis (PhD)** **February 1998 - August 2000**  
 Faculty for Civil Engineering, Vienna University of Technology, Inst. f. Industrial building and planning, prepared under the framework of the Doctoral Student Program at CERN, ST Division.  
 Title: *Development and Engineering Design of a Novel Exocentric Carbon-Ion Gantry for Cancer Therapy*
- Diplomingenieur (Master of Science)** **December 1997**  
 First-class honours degree awarded from the Faculty of Civil Engineering, Vienna University of Technology, Diploma thesis: *The Fractal Factory*
- Heriot-Watt University Edinburgh** **Sept. 1995 - June 1996**  
 4<sup>th</sup> (final) Year Study Programme at the Department of Civil Engineering.  
 Thesis project: *Cost-Benefit Analysis of the Second Severn Crossing*  
 (1<sup>st</sup> class honours mark)
- Matura** (Bundesgymnasium Vienna XIII, Fichtnergasse) **May 1990**

#### Interests

Family, volleyball, squash, railways and infrastructure policy



## Practical Experience

- Since February 1998 **CERN (European Laboratory for Particle Physics)**  
Development of a medical gantry for ion therapy.  
Definition of the (cross-functional) program in order to integrate radiological, organisational, beam-optical and engineering aspects.  
Generation of variants and resolution. Structural design and analysis. FE-calculations. Error budget calculations. Design. Safety concept and risk analysis. Project management, presentation and promotion.  
Supervisors: Prof. D. Sommer (Vienna Univ. of Technology), Prof. M. Regler (Austrian Academy of Science)  
CERN ST-CV, CH-1211 Geneva 23
- 1993 - 1997  
June 1996 - June 1997 Student Union at the Vienna Univ. of Technology  
**Head of the Student Union** of the Faculty of Civil Eng., Vienna  
Representation of students in various boards of the university. Organisation of the student services. Editing and publication of the student's journal. Organisation of seminars and workshops.
- July, August 1996 **Vasko & Partner Engineers**  
Studies on thermal building insulation and acoustics.  
Grinzinger Allee 3, 1190 Vienna
- July, August 1995 **PORR AG planning office**  
Pre-cast element construction design.  
Kelsenstr 5-7, 1030 Vienna
- July - Sept. 1994 **Architects Rollwagen-Eisterer**  
Renovation of the Gloriette (Schloß Schönbrunn). Housing design.  
Serravagasse 13, 1140 Vienna
- Oct. 1990 - March 1991 Military service

## Publications

- S. Reimoser, *Cost Benefit Analysis of the Second Severn Crossing*, Department of Civil and Offshore Engineering, Heriot-Watt University, Edinburgh, 1996
- S. Reimoser, C. Gugler, D. Sommer (ed.), *Programming the Fractal Factory: Bewegliche Planung im chaotischen Umfeld*, Institute for Industrial Building and Planning, Vienna University of Technology, 1998
- S. Reimoser, *Program for a novel ion gantry*, CERN-ST-98-036, Geneva, 1998
- S. Reimoser, *Planungsorganisation im Industriebau: Dynamische Partnerschaften als Strategie im chaotischen Umfeld*, in: D. Sommer (ed.), *Industriebau - Praxisreport 98*, Österreichische Studiengemeinschaft für Industriebau, Vienna, 1998
- S. Reimoser, "Protonengantries" sowie "Die Ionengantry", in: *Med-AUSTRON - Ein Österreichisches Krebsforschungs- und Behandlungszentrum zur Hadronentherapie in Europa, Feasibility Study, Vol. II*, eds.: R. Pötter, T. Auberger, M. Regler, Wiener Neustadt, 1998
- S. Reimoser, *Variants for a Riesenrad Ion Gantry*, CERN-ST-99-002, Geneva, 1999
- S. Reimoser, M. Pavlovic, *Engineering Design and Study of the Beam Position Accuracy in the "Riesenrad" Ion Gantry*, *Journal of Nuclear Instruments and Methods in Physics (NIM-A)*, in press
- L. Badano, M. Benedikt, P. J. Bryant (study leader), M. Crescenti, P. Holy, A. Maier, M. Pullia, S. Reimoser, S. Rossi, G. Borri, P. Knaus, *Proton-Ion Medical Machine Study (PIMMS)*, CERN yellow report CERN-2000-006 and CERN-PS-2000-007
- S. Reimoser, L. Weisser, "Vom Kopf zum Industriebau am Beispiel der Hadronentherapie" in: D. Sommer (ed.), *Industriebau - Praxisreport 2000*, Österreichische Studiengemeinschaft für Industriebau, Vienna, 2000, in press

